The self-sensing, electrical and mechanical properties of the epoxy composites reinforced with carbon nanotubes-micro reinforcement nano/micro hybrids

Weikang Li

ÉCOLE CENTRALE DES ARTS
ET MANUFACTURES

《ÉCOLE CENTRALE PARIS》

THÈSE

Présentée par

WEIKANG LI

Pour l'obtention du

GRADE DE DOCTEUR

Spécialité : Science des matériaux
Laboratoire d'accueil : Laboratoire de Mécanique des Sols, Structures et Matériaux
CNRS UMR 8579

Propriété mécaniques, electriques, et de détection des composites comportant des renforts hybrids nano/micro nanotube de carbone/microrenforts

Soutenue publiquement le 10 Septembre 2013

Devant le jury compose de:

M.	**Said Ahzi**	Professeur, IMFS,UStrasbourg	**Rapporteur**
M.	**Marco Gigliotti**	Mdc HdR, ENSMA, Poitiers	**Rapporteur**
M.	**Philippe Poulin**	DR CNRS, CRPP, Bordeaux	**Examinateur**
M.	**Philippe Leclère**	Chercheur Qualifié, UMONS, Belgique	**Examinateur**
M.	**Jacques Cinquin**	Senir Expert Composite Materials, EADS	**Examinateur**
M.	**Philippe Bompard**	Professeur, ECP	**Examinateur**
M.	**Jinbo Bai**	DR CNRS, ECP	**Directeur de thèse**

Acknowledgements

Most of all, I would like to express my most sincere appreciation to my supervisor Mr Jinbo BAI. During the three years, he gave patient guidance, many encouragement and valuable opinions for my thesis.

I very appreciate China Scholarsip Council (CSC) which is the financial support for this research. I also thank the Service de l'Education Ambassade de la République Populaire de Chine en République Française for their many help.

I am very grateful for Said Ahzi and Marco Gigliotti as the rapporteurs and Philippe Poulin, Philippe Leclère, Jacques Cinquin and Philippe Bompard as the examinateurs in the jury of this thesis. I also sincerely thank all the committee members for their evaluations and suggestions.

My thanks are given to the staff of Laboratoire MSSMat and my colleagues who help me a lot during my three years study: Delong He, Anthony Dichiara, Jinkai Yuan, Youqin Lin, Jing Zhang, Hassan Harris, Farida Djebbari, Sokona Konaté, Philippe Bompard for the discussion and his suggestions in the three years, Sylviane Bourgeois for her help in the measurement system and françoise Garnier for SEM observation.

Finally, I would like to my family, especially my parents for their love and care over the past years.

Résumé

Hybrides nano /micrométriques de nanotubes de carbone (NTC) greffés sur microparticules d'alumina, microplaques de SiC ou nanoplaquettes de graphène (NPG) ont été utilisés comme renforts multifonctionnelles dans les composites à matrice polymère. Le NTCs utilisés étaient généralement sous forme de six branches symétriques et orthogonales sur microparticules sphériques d'Al_2O_3, mais d'une ou deux branches alignées verticalement sur les deux cotés de microplaques de SiC et de NPG.

L'introudction des structures hybrides dans une matrice époxy permet d'améliorer la dispersion des NTC et l'interaction interfaciale entre les renforts et la matrice. Les propriétés mécaniques des composites ont été fortement améliorées avec une faible concentration de hybrides. La résistance électrique *in situ* des composites a affeint d'abord à sa valeur maximale et puis diminue avec la presence d'une déformation irréversible. Ce phenomena servé est complètement différent par rapport à ce des composites renforcé par NTC, c'est-à-dire, une augmentation monotone de la résistance jusqu'à leur rupture final. Les propriétés mécaniques et les comportements de self-sensing des composites dependent fortement de l'élancement de NTC de leur organisation et aussi des substrats.

L'introduction des hybrides dans les composites renforcés par des fibres longues (verre) a demontré un grand potentiel pour développer des composites multi-échelles. Les études réalisées sur la matrice époxy renforcée par les hybrides bien dispersés avec une faible fraction ont montré des améliorations importantes des propriétés de flexion à 3 points et des propriétés thermo-mécaniques. Les réseaux conducteurs formés par hybrides nano/micrométriques permettent de suivre in situ l'évolution de l'état de dégradation des composites à matrice époxy renforcés par des tissus de verre sous contrainte appliquée.

Mots clés: Composites Polymère; Hybrides; Propriétés mécaniques; Propriétés électriques; Piézorésistivité

Abstract

Nano/micro multiscale hybrids with carbon nanotubes (CNTs) grown on the Al_2O_3 microparticles, SiC microplates or graphene nanoplatelets (GNPs) could serve as multifunctional reinforcements in the composites. The CNTs generally form into symmetric six-orthogonal branches on the spherical Al_2O_3, but vertically align on the flat surfaces of the SiC and GNP.

The introduction of hybrids into the epoxy matrix endows uniform dispersion of CNTs as well as improved interfacial interaction between the reinforcements and matrix. Significantly enhanced mechanical properties of the composites were achieved at low hybrid concentration. The *in situ* electrical resistance of the composites initially increases to its maximum value and then begins to decrease with the appearance of irreversible deformation, which is different from the pristine CNTs filled composites only with monotonic increase of the resistance until the catastrophic fracture. The mechanical and self-sensing behaviors of the composites are found to be highly dependent on CNT aspect ratio, organization and the substrates.

Besides, the introduction of hybrids into the traditional fiber-reinforced composites shows great promise in development of the high-performance multiscale composites. The epoxy matrix is toughed by the well dispersed hybrids at low fraction, resulting in improved flexural and thermomechancial properties. Besides, the conductive network provided by the hybrids could be utilized as *in situ* damage sensors to monitor the damage evolution in the glass fabric/epoxy composite laminates under tensile loading.

Keywords: Polymer composites; Hybrids; Mechanical properties; Electrical properteis; Piezoresistive

Table of Contents

Acronyms and Symbols

Acronyms

ABS	acrylonitrile butadiene styrene
AR	aspect ratio
CB	carbon black
CF	carbon fiber
CNT	carbon nanotube
CVD	chemical vapor deposition
DMA	dynamic mechanical analysis
EMI	electromagnetic interference
FRPs	fiber-reinforced polymer composites
GF	glass fiber
GNP	graphene platelet
IFSS	interfacial shear strength
ILSS	inter-laminar shear strength
MWNT	multi-walled nanotube
PANI	polyaniline
PE	polyethylene
PEO	poly(ethylene oxide)
PF	phenol formaldehyde
PI	polyimide
PMMA	polymethyl methacrylate
PP	polypropylene
PS	polystyrene
PU	polyurethane
PVA	polyvinyl alcohol
PVDF	polyvinylidene fluoride
UHMWPE	ultrahigh molecular weight polyethylene
VMQ	methylvinyl silicone rubber
RTM	resin transfer molding
SEM	scanning electron micrograph
SWNT	single-walled nanotube

TEM	transmission electron micrograph
TGA	thermogravimetric analysis
TPE	thermoplastic elastomer

Symbols

E	tensile modulus
E'	storage modulus
E''	loss modulus
f_c	percolation threshold
f_{CNT}	carbon nanotube concentration
f_{hybrid}	hybrid concentration
$\tan \delta$	loss factor
T_g	glass transition temperature
UTS	ultimate tensile strength
vol.%	volume fraction
wt.%	weight fraction
ε	strain
σ	tensile strength
ρ	density

General introduction

More recently, the multifunctional materials have been increasingly paid attention, which are tailored to achieve superior mechanical performance and specific functional requirements. The future multifunctional materials are desired to possess combined the sensing, actuation, energy storage, and healing capabilities, etc. It has been found that the nanocomposites with polymer modified by nanoscale reinforcements could open up a wide range of opportunities for the multifunctional materials. Carbon nanotubes (CNTs) have drawn specific interest towards the development of new multifunctional materials due to their extraordinary intrinsic mechanical, thermal, electrical properties and high aspect ratios, which have wide applications from aerospace to electronics. Introducing a small amount of CNTs into the polymer matrix can improve the mechanical properties and enable the formation of electrical conductive networks in the composite, which make them to serve as structural reinforcement, conductive and piezosensitive materials, etc.

Besides, nanotubes have shown great promise for use in development of multifunctional multiscale laminated composites. It is known that the traditional fiber-reinforced polymer composites (FRPs) with excellent in-plane properties, such as, high tensile modulus and strength are important structural materials. However, their relatively weak out of-plane properties (matrix-dominated) still remain major obstacles. It has been demonstrated that the poor properties of the FRPs can be tailored at nanoscale by introduction of the CNTs. Due to their extremely small sizes, it is possible for CNTs to penetrate into the matrix-rich regions between the individual fibers and between the plies of the composites. The CNTs could be dispersed uniformly throughout the whole polymer matrix or directly deposited on the fiber surfaces. The multiscale hybrids with nanoscale CNTs as well as continuous microscale fiber have drawn significant interest in the field of advanced, high-performance materials. Besides, due to their exceptionally electrical properties, the formed conductive networks in the matrix enable CNTs to be utilized as sensors for *in situ* monitoring the deformation and damage of composites during loading.

However, the critical issues for preparing the multifunctional CNT-based polymer nanocomposites include the uniform dispersion of CNTs, control of CNT alignment, and strong CNT/matrix interfacial bonding for good load transfer, etc, which need to be solved. Moreover, with regard to the CNT and fiber multiscale reinforcements reinforced composites, the dispersion of CNTs in the matrix are still urgent issues. Inadequate dispersion of CNTs in the matrix will introduce entangled aggregates, resulting in non-uniform infiltration of the fiber bundles and decreased mechanical properties. In addition, the nanotubes can result in substantially increased viscosity of the nanotube/polymer suspension, creating challenges for the infusion and wetting of the fibers. It is desirable that very low concentration of well dispersed CNTs could realize structural reinforcements and be used as damage sensor.

Based on the main problems of pristine CNTs, this thesis is focus on the multi-scale hybrid structures to be utilized as superior multifunctional reinforcements in the composites. The hybrid structures with CNTs grown on microsized ceramic particles or two dimensional graphene were *in situ* synthesized by a simple one-step chemical vapor deposition (CVD) method, without any pre-patterned catalyst treatment. These hybrids could endow uniform CNT distribution and controllable CNT orientation and organization as well as the improved interfacial connection and load transfer between CNTs and matrix.

Firstly, three kinds of hybrids with CNTs grown on SiC microplates (CNT-SiC), Al_2O_3 microparticles (CNT-Al_2O_3) and graphene platelets (CNT-GNP) synthesized by CVD were used. The different CNT aspect ratios and organizations on the substrates were adjusted by the CVD conditions, such as growth temperature, time and hydrogen ratio, etc. The CNT-SiC, CNT-GNP and CNT-Al_2O_3 reinforced epoxy nanocomposites were respectively fabricated using calendaring method. Compared to the randomly distributed CNTs, the more improved mechanical and electrical properties of the multiscale hybrids filled nanocomposites were studied in detail. Such as, with respect to neat epoxy, significantly enhanced mechanical properties in the CNT-GNP filled composites were achieved at ultralow hybrid loading (0.5 *wt.%*). The tensile modulus showed ~40% increase and the tensile strength was improved by ~36%. The value of percolation threshold (f_c) of the hybrids filled systems is much lower, for example, $f_c \sim 0.2$ *vol.%* in the CNT-SiC composites. Besides, the epoxy composites with the hybrids could exhibit distinctive self-sensing behavior for *in situ* monitoring the onset of

irreversibly permanent deformation. The *in situ* electrical resistance initially increases to its maximum value and then begins to decrease with the appearance of the residual strain and irreversible deformation, which is remarkably different from the randomly distributed CNTs filled composites only with monotonic increase of the resistance until catastrophic fracture. In addition, the relationship between the hybrid structure (CNT aspect ratio, organization and substrate morphology) and composite mechanical and self-sensing properties has been well established. For the underlying mechanisms of the self-sensing properties, it is found that the evolution of conductive networks resulted from the rotation of the substrates and hybrids as well as the reorientation of CNTs during loading plays an important role on the self-sensing behavior of the composites.

Secondly, the CNT-Al_2O_3 hybrids which replace the pristine CNTs were used for matrix modification and *in situ* damage sensor in the glass fiber reinforced composites. The woven glass fabric/epoxy with CNT-Al_2O_3 hybrids multiscale composite laminates were fabricated. The composites incorporated with 0.5 *wt*.% CNT-Al_2O_3 hybrids showed increment in the flexural modulus ~ 19% and flexural strength ~ 13% over that of the reference sample. Similar, from the results of dynamic mechanical analysis, the samples exhibited considerable improvement of ~ 20% in the storage modulus at 50 ^oC and an increase of 15 ^oC in glass transition temperature compared to the control samples. As multifunctional reinforcements, the CNT-Al_2O_3 hybrids could be utilized as *in situ* damage sensor to monitor the damage evolution of the glass fabric reinforced epoxy composites when subjected to uniaxial tensile loading. From the change of the *in situ* electrical resistances, the damage mechanisms in the composites were analyzed.

Chapter I
CNTs for Multifunctional Reinforcements

1.1. Carbon nanotubes

Carbon nanotubes (CNTs) have attracted considerable attention in a wide range of scientific research fields since their discovery [1], which open the possibility for a new class of materials. Their intriguing nanostructure as well as combination of the extraordinary mechanical and electrical properties has aroused extensive interest to understand their fundamental nature and explore their potential applications.

1.1.1. CNT morphology

Carbon nanotubes could be visualized as a sheet of graphite that has been rolled into a cylinder [2]. The graphite layer could be formed as a 2-D sheet of carbon atoms arranged in a hexagonal array and each carbon atom has three nearest neighbors in this case. According to their arrangement, nanotubes can exist as either single-walled or multi-walled structures. A single-walled nanotube (SWNT) can be seen as a seamless cylinder by rolling up a single such sheet with a typical diameter of 1-1.5 nm [3], whereas multi-walled nanotube (MWNT) is generally made of multiple layers of graphene sheets with inner diameters as small as those of the SWNTs rolled into a hollow core. But their outer diameters can vary from a few nanometers to tens of nanometers [4]. In general, the van der Waals interactions between sidewalls of the SWNTs result in close-packed bundles. MWNTs have an interlayer spacing of approximately 0.34 nm where the interaction between the individual shells is van der Waals bonding. Fig. 1-1a and b show the transmission electron micrograph (TEM) images of SWNT and MWNT, respectively.

The atomic structure of nanotubes is usually described in terms of the tube chirality, or helicity, which is assigned by a chiral angle $\boldsymbol{\theta}$, and the roll-up or chiral vector $\boldsymbol{C}$ ($\boldsymbol{C}=n\boldsymbol{a_1} + m\boldsymbol{a_2}$) from a point of origin on a graphene sheet [5], as illustrated in Fig. 2. Here, n and m are the number of steps along the ziz-zag carbon bonds of the hexagonal lattice; a_1 and a_2 are

unit vectors; and θ is the angle between the zigzag axis and roll-up vector, which determines

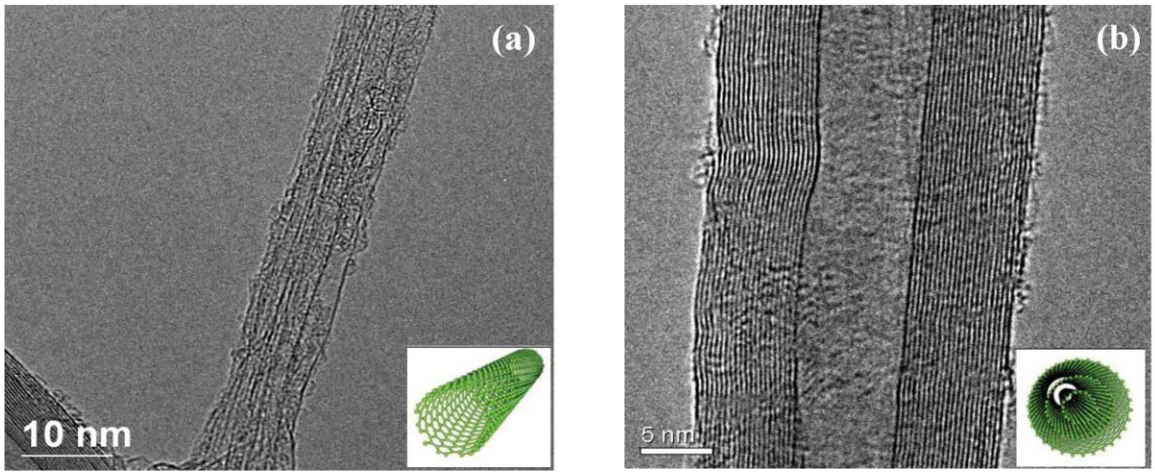

Fig. 1-1 *TEM images of (a) SWNT and (b) MWNT.*

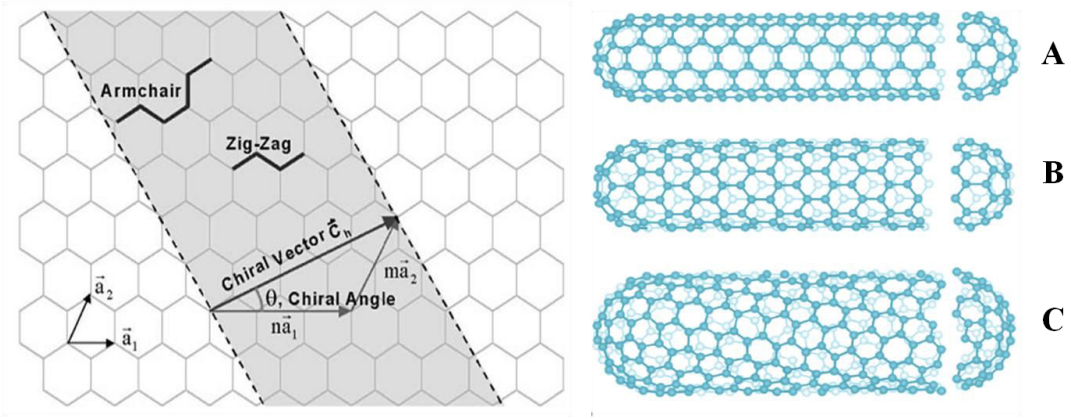

Fig. 1-2 *Schematic diagram showing how a hexagonal sheet of graphite is 'rolled' to form a carbon nanotube and illustrations of the three chiralities, A: 'armchair', B: 'zigzag' and C: 'chiral'.*

the amount of 'twist' of the tube. We can visualize cutting the graphite sheet along the dotted lines and rolling the tube so that the tip of the chiral vector touches its tail. The rolling direction of graphene sheet and the nanotube diameter will determine the nanotube chiralities which denote its type. According to the geometry of carbon bonds around the circumference of the nanotube, three types of microstructure can be realized, as shown in Fig. 1-2. If n=m and θ=30°, the nanotube is known as "armchair." In the case of m=0 and θ=0°, the tube is

called “zigzag”. Othervise, for $0^o < \theta < 30^o$, the nanotube is called “chiral” [5]. Depending on their chirality, nanotubes can either be conducting or semiconducting [2]. All armchair nanotubes are generally metallic. For all other nanotubes, there are two possibilities. If n-m=3k (k is an integer), the tubes are expected to be metallic; otherwise, the tubes are semiconducting [5]. The properties of nanotubes depend on their diameter, nanostructure and atomic arrangement, i.e., the rolling form of the graphite sheets. [6-8].

1.1.2. CNT properties

Due to their perfect sp^2-hybridized in-plane bonds (σ bonds) between adjacent carbon atoms and the regular crystal lattice, nanotubes possess remarkable mechanical properties i.e., high modulus, strength and flexibility, exceeding those of any existing materials. Numerous experimental and theoretical research been made to determine the mechanical properties of nanotubes. Salvetat *et al.* reported the CNT mechanical properties are largely independent on their chirality [9]. Though there is no consensus on the exact value of mechanical properties of CNTs, the theoretical and experimental results have shown unusual mechanical properties of CNTs with Young’s modulus as high as about 1-1.2 TPa and tensile strength of 50-200 GPa [10].

Besides, nanotubes also exhibit excellent electrical properties ranging from metallic to semiconducting in a large band gap [11], which are considered to depend the diameter and chirality of carbon atoms in the surface of nanotubes. The nanotubes have extraordinarily high current carrying capacity and can carry the highest current density as high as 10^9 A/cm^2 or more [12, 13], which is almost one hundred times larger than typical metals. In addition, the superconductive behavior has also been found in SWNTs with carbon atoms arranged in certain way [14]. These superior electrical properties have generated substantial interest in utilizing CNTs in nanoelectronics, as shown in Fig. 1-3.

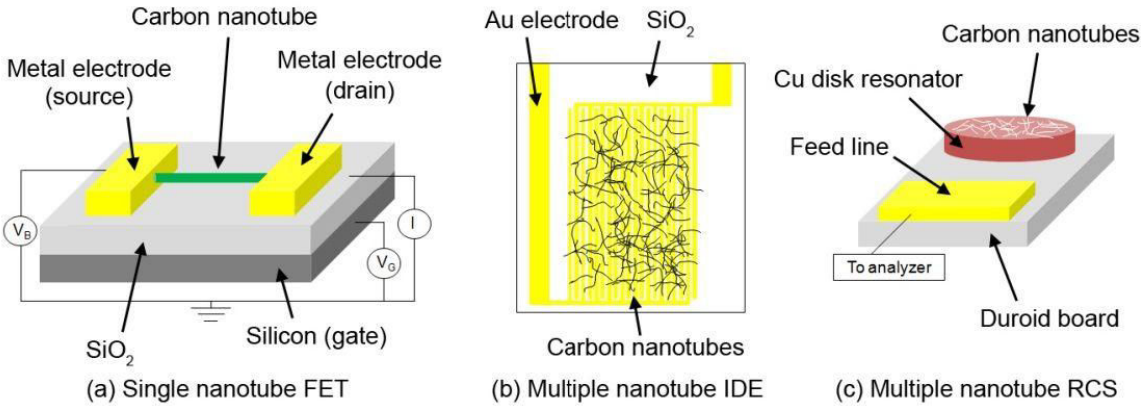

Fig. 1-3 *Schematic diagrams for nanotube sensors. (a) A single nanotube field-effect transistor; (b) A multiple nanotube interdigitated electrode device; (c) A multiple nanotube resonant-circuit sensor.*

Each atom on the surface of nanotubes is exposed to the environment, thus, any small changes from the chemical, thermal or mechanical environment could cause drastic changes in their electrical properties. As reported [15-18], the band structure of a nanotube is dramatically altered by mechanical strain and that the conductance of the CNTs can increase or decrease depending on the chirality of the nanotubes. Besides, nanotubes show extreme sensitivity towards changes of local chemical environment that stems from the susceptibility of their electronic structure to the interacting molecules [19-24]. Unlike the conventional piezoelectric materials, electromechanical coupling of carbon nanotubes results from phonon frequency shifts as a consequence of charge injection. This electromechanical property of nanotubes has attracted wide attention in their potential applications for gas, temperature and strain sensors.

1.1.3. Controlled synthesis of CNTs

The CNT morphology can be controlled by the process for CNT fabrication. There are three most common techniques for CNT synthesis, i.e., carbon arc-discharge, laser ablation and chemical vapor deposition (CVD).

Since MWNTs was discovered in the soot of the arc-discharge method by Iijima in 1991, this technique became a relatively simple method for preparing CNTs [1]. After that, Iijima *et al.* [25], and Bethune *et al.* [26] also synthesized SWNTs using this method with an

assistance of a metal catalyst in 1993. This method involves passing a direct current between two carbon electrodes in order to create an arc discharge at high temperature. Then, this high temperature arc discharge would melt and vaporize one of the carbon rods and the nanotubes would be collected on the other rod. Chemical refinement is necessary to obtain the pure CNTs by this method because there is soot and other forms of carbon apart from CNTs. The disadvantages of the arc discharge method lie in low purity of the resulting products and difficulty in controlling over arrangement relative to other methods.

In order to obtain pure CNTs with small diameter distribution, laser ablation technique was developed. Using this method, a significant progress was achieved on synthesis of bundles of aligned SWNTs with small diameter distribution by Smalley *et al.* in 1996 [27]. A horizontal tube furnace with a target inside is pre-heated around 1200 ^{o}C under a controlled pressure using a flow of inert gas (Helium or Argon). This target consists of a composite, which is a mixture of graphite and metal catalysts such as Co or Ni. A laser is introduced onto the target for its vaporization. Then the plume from vaporization is collected at the cooler downstream end of the horizontal tube. However, this synthesis also produces soot and other carbon compounds apart from CNTs. The amount and type of catalysts, laser parameters (power and wavelength) and the environment parameters (temperature and pressure) will have influence on the quantity and quality of the products. Compared to the arc-discharge, this method has advantages in achieving high purity of CNTs and controlling the uniformity of CNT dimension, however, this technique is more expensive.

CVD is a more recent method for industrial synthesis of both MWNTs and SWNTs, which could easily control the dimension of resulting CNTs, such as diameter, length, aspect ratio, etc. Besides, the achieved products are high-yield and nearly completely graphitized without amorphous carbon. Catalytic growth of nanotubes using CVD method was first used by Yacaman *et al.* [28]. The CVD process used for CNT growth is actually catalyst-assisted decomposition of hydrocarbons. A number of CVD reactor configurations such as horizontal, vertical and barrel have been reported to synthesize CNTs [29]. The horizontal quartz tube reactor is a relatively simple system which is widely used in floating catalytic CVD. This process usually happens in a horizontal quartz tube, which is heated to a temperature ranging 500 to 1000 ^{o}C in inert carrier gases (argon and nitrogen). Gaseous or liquid carbon sources,

such as methane, acetylene, ethylene, benzene, toluene and xylene, etc., are thermally decomposed, then the separated carbon molecules are attached on the surface of a metal catalyst (Fe, Ni, or Co, etc). The common combination of substrates and catalysts is silica and Fe catalysts for MWNTs, and silicon wafer and Fe/Mo catalysts for SWNTs. High temperature is especially needed for the SWNT production.

Recently, it is necessary to synthesize CNTs on a significant scale in order to improve their availability for the still growing number of potential applications, and to see their prices decrease on the market place. Among the three synthesis processes discussed above, both the arc discharge and laser ablation methods are demonstrated to rely on the evaporation of carbon atoms from solid graphite targets at temperature >3000 ^{o}C. Besides, the nanotubes are always tangled, which makes their purification difficult and greatly hinders their large scale applications. However, CVD is the mostly used method for CNT synthesis at moderate temperatures (500-900°C) [29]. CVD synthesis appears to be the most promising route because of its cheapness, flexibility, high yield, homogeneity and selectivity. Especially, the vertically fluidized bed CVD is widely used for large-scale production of CNTs [30, 31].

Today, bottlenecks are still remaining like the control of CNT morphology (orientation and organization) and the improvement of CNT distribution in different media, which are two urgent issues and need to be solved. As far as the CNT dispersion is concerned, the large scale controlled growth of vertically aligned CNTs may contribute to solve the problems encountered in this area. The growth of aligned MWNTs was first reported in 1996 [32] on a flat substrate. Since then, the investigation in this field has been of great interest. More recently, the floating catalytic CVD as a simple one-step method has been successfully used to construct various nano/micrometer hybrid structures with CNTs selectively grown on the fibers or micrometer particles including nanosized metal or oxide particles, microsized ceramic particles, fullerenes and two dimensional graphene, such as, CNTs/SiO_2 [33], CNTs/Al_2O_3 [27], CNTs/large ceramic spheres [34] (Fig. 1-4), CNTs/carbon fiber [35-38] (Fig. 1-5), CNTs/alumina fabric [39] (Fig. 1-6) and vertically aligned CNT arrays grown on the carbon fiber fabric [40] (Fig. 1-7).

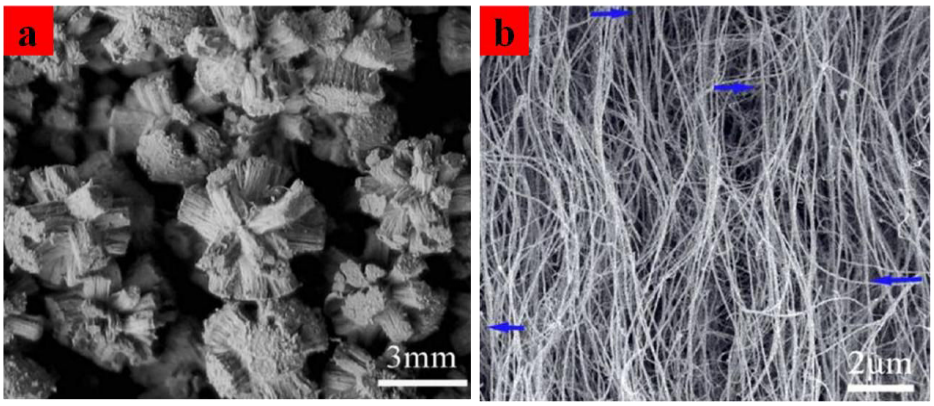

Fig. 1-4 *Large amounts of VACNT array grown at 800°C on spheres with ethylene as carbon source for 2 h; (b) SEM of the VACNTs in (a).[34]*

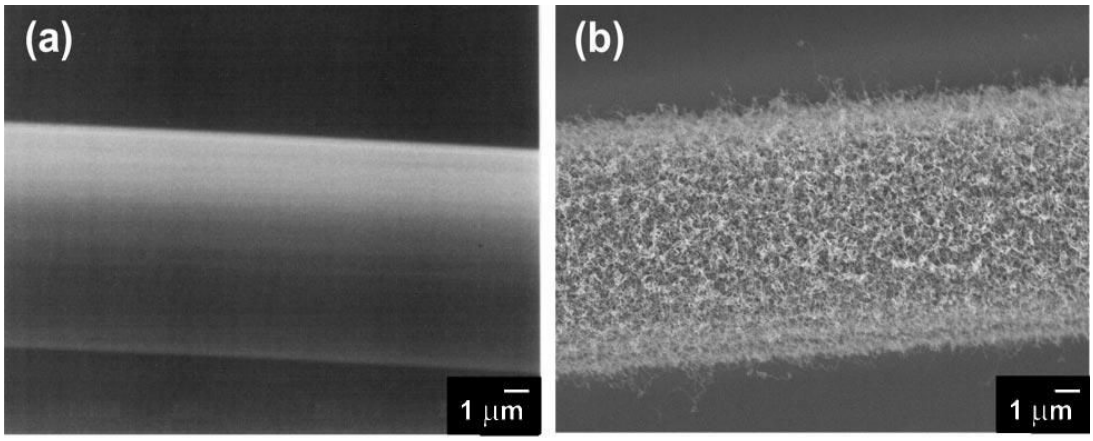

Fig. 1-5 *SEM micrographs of carbon fibers, (a) before and (b) after nanotube growth.[36]*

It is worth noting that the CVD method could allow selective growth of CNTs on the given substrate in controllable ways, resulting in desirable CNT architectures with controlled orientation for various potential applications [41, 27]. The widely reported CNT structures include the forms of arrays of CNT carpets, pillars, forests, etc [42-44, 33, 45, 46]. However, owing to the catalyst particles, such as iron (Fe), may be easily diffused into the carbon substrate at high temperature (over 850 °C) to lose activity [47], direct growth of CNTs onto carbon fiber commonly results in low density and inhomogeneity of CNTs with no orientation on the carbon fibers using CCVD [38]. An alumina [48], silicon [49] or silica [50] buffer layer may prevent the Fe catalyst diffusing into the carbon substrate and obtain

vertically aligned CNT arrays grown onto the carbon fiber surface.

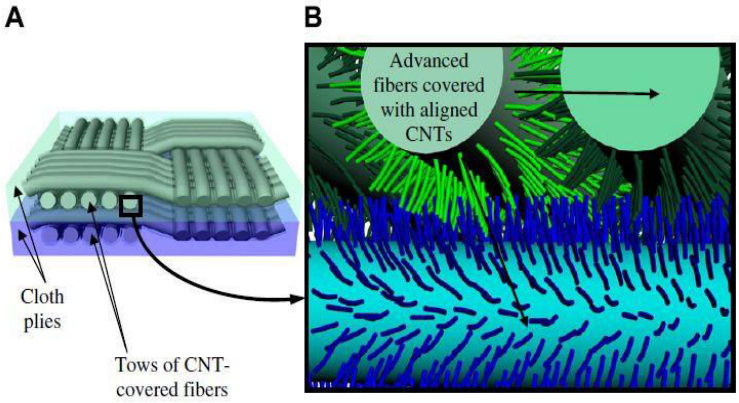

Fig. 1-6 *Illustration of the hybrid composite (A) Schematic illustration of the architecture composed of a cloth containing fiber tows, covered by CNTs. The two different plies are shown in two different colors; (B) Closer view of the interface cross-section between the two composite plies. The CNTs grown on the surface of each individual fiber. [39]*

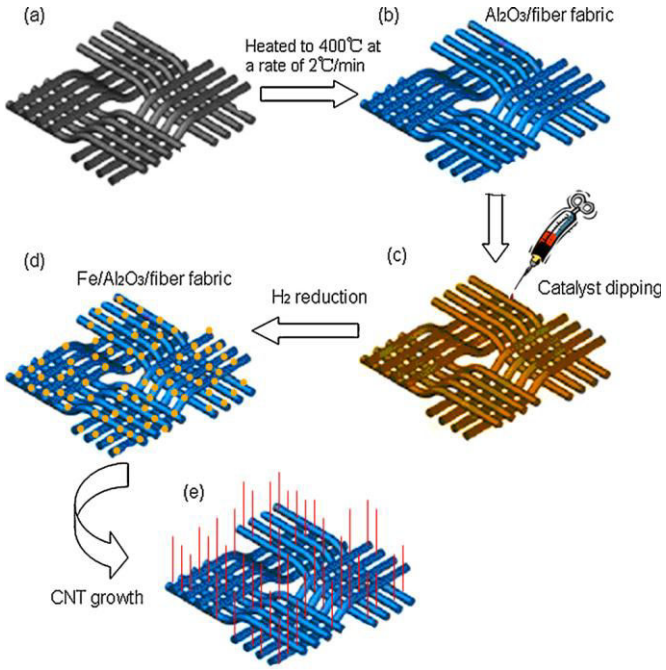

Fig. 1-7 *Overview of preparing CNTs grown onto carbon fiber fabric.[40]*

As largely reported about the CNT growth on flat substrate, the diameter, length, area number density and organization of CNTs depend on both substrate properties, including their size, morphology, and the CVD synthesis parameters, such as carbon source, catalyst precursor, gas atmosphere, hydrogen ratio, temperature, growth time (see Fig. 1-8), gas flow, etc. However, many related research were generally obtained by exploring pre-patterned substrate or predefining catalyst particles into certain morphologies on the corresponding substrate. It is worth noting that the pattern procedures are generally limited to be applicable to the large flat surfaces. Obviously, these complex pretreatment techniques and strict application conditions greatly increase the difficulty and costs of elaborating aligned CNTs. Besides, it is desirable to control CNT arrangements in the hybrid structures for achieving advanced multifunctional composite properties.

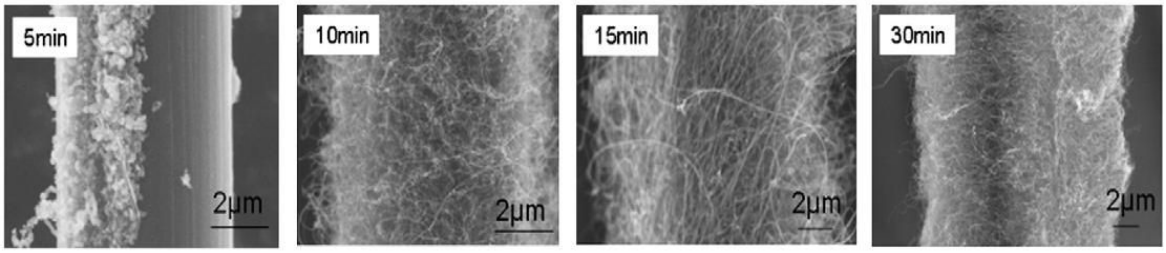

Fig. 1-8 *CNT morphology grown on the surface of carbon fiber (T650-35, unsized) as a function of growth time.[38]*

In our recent research, the well-organized nano/micro hybrid structures achieved by directly growing CNTs on micro SiC, micro-spherical Al_2O_3 and graphene nanosheet during CVD synthesis process, without any pretreatment [51-55]. The schematic image in Fig. 1-9 illustrates the synthesis procedure of the hybrid structures. Most importantly, the control of CNT organization and orientation on the Al_2O_3 particles has been deeply investigated as shown in Fig. 1-10, especially in the case of the particle substrate without any pretreatment. The selective decomposition of carbon sources resulted in different CNT patterns. It was found that the CNT organization on Al_2O_3 is strongly dependent on their diameter, length and area number density. Three hybrid structures with different distribution CNT patterns have demonstrated by changing CNT growth temperature, time and hydrogen ratio.

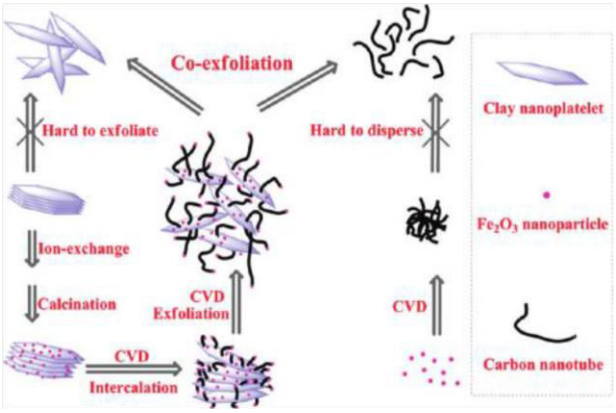

(A)

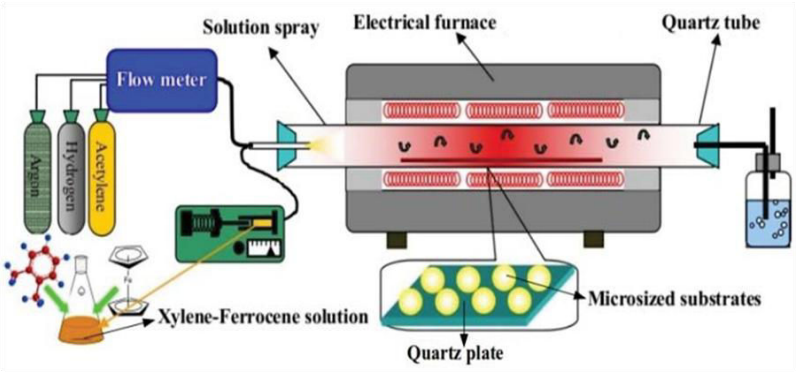

(B)

Fig. 1-9 *(A) Schematic of the procedure for the preparation of CNT-clay hybrids; [56] (B) Schematic of the CNT growth by liquid injection CVD.*

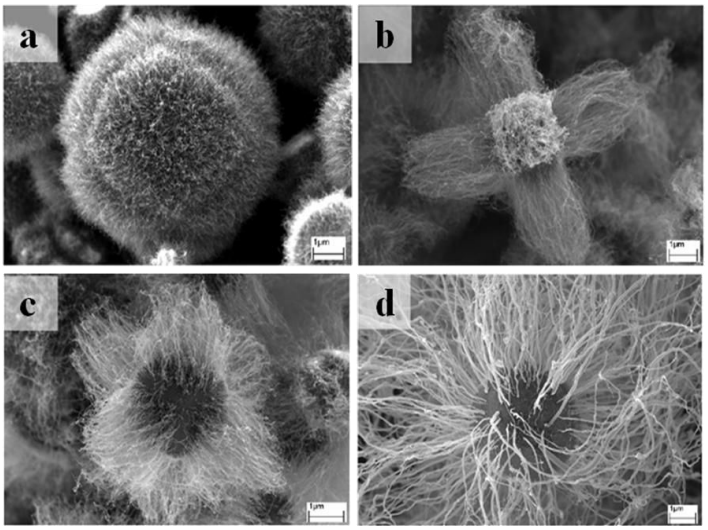

Fig. 1-10 *SEM images of self-organized CNT patterns on Al_2O_3 with different aspect ratios and organizations.[53]*

1.2. Critical issues in CNT/Polymer nanocomposites

According to the different applications purposes, polymer composites can be classified as structural and functional composites. More recently, the multifunctional composites with excellent mechanical properties as well as specific functional requirements have attracted keen interest [57]. Future multifunctional materials may possess integrated sensing, actuation, energy storage, and healing capabilities, much like biological systems. The extraordinary mechanical, electrical and thermal properties of carbon nanotubes make them candidates for the multifunctional fillers in the composites and endow them with many scientific and technological opportunities [58, 59]. The modification of composite properties by integrating small amount of nanotubes is an enabling technology towards the development of new multifunctional material systems [60]. To date, more and more effort has been made to incorporate both SWNTs and MWNTs into the thermosetting polymers, such as, epoxy, polyimide (PI), polyurethane (PU), and phenol formaldehyde (PF) resins as well as the thermoplastic polymers, including polyethylene (PE), polypropylene (PP), polystyrene (PS), polyvinyl alcohol (PVA), polymethyl methacrylate (PMMA), polyvinylidene fluoride (PVDF), nylon, and so on for the improved strength and conductivity. The mechanical properties combining with electrical, thermal, and many other properties have been widely investigated for a wide range of applications. However, in order to develop high performance CNT/polymer composites, the main problems and challenging tasks are in selecting CNT aspect ratio, controlling CNT alignment, creating a good dispersion and strong interface bonding of CNTs in the polymer matrix, forming a structural frame and electrical conducting path, attaining good load transfer from the matrix to the CNTs during loading, and increasing the electrical conductivity. In this part, these critical issues closely related to the composite properties will be introduced one by one.

1.2.1. CNT aspect ratio

A large amount of CNTs could be prepared by the arc discharge, laser ablation and CVD methods. But the obtained CNTs are not consistent in their intrinsic characteristics. Aspect ratio ($AR=l/d$) as one of the most inherent properties is strongly dependent on the

synthesis method used and other parameters involved. It is an important parameter that greatly influences the composite properties. The aspect ratio should be sufficiently large to maximize the load transfer between the nanotubes and matrix, thus achieving enhanced mechanical properties. The effect of CNT aspect ratio on the electrical and mechanical properties of the composites has been investigated. The composites with high MWNT aspect ratio demonstrate higher modulus and tensile strength than those with low aspect ratio MWNTs at the same filler concentration [61, 62]. Zhang *et al.* [63, 64] reported that the MWNTs with larger aspect ratio were more suited for the reduction of fatigue crack growth rate and exhibited higher toughening efficiency than the shorter ones. Sandler *et al.* [65] concluded that it was easier for CNTs with extremely high aspect ratio to form electrically percolative networks along the tangled CNTs in the insulating polymer matrix, resulting in the ultra-low percolation thresholds as low as 0.0025 *wt.%*. Li *et al.* [66] reported that there is a critical aspect ratio and with increasing the aspect ratio below a critical value, the percolation threshold of the composites decreased. Tucker and Liang [67] summarized five different physical models, including Halpin-Tsai, and suggested that under strictly idealizing assumptions, the overall mechanical properties of composite materials significantly vary with the aspect ratio of the reinforced CNTs. However, these assumptions are difficult to experimentally achieve because CNTs coil and agglomerate to form bundles.

1.2.2. CNT dispersion

The potential of employing CNTs as reinforcements has been severely limited mainly because of the difficulties associated with dispersion of entangled CNTs during processing. CNT dispersion is the foremost important issue in producing CNT/polymer nanocomposites. Better dispersion not only makes more filler surface area available for bonding with polymer matrix, but also prevents the aggregated filler from acting as stress concentrator, which are detrimental to the composite performance. However, some challenges, such as CNT content in the composites, length and entanglement of CNTs as well as viscosity of matrix have to be overcome to obtain uniform CNT dispersion in nanocomposites. There were many reports [68, 69] showing that there is a critical CNT content below which the strengthening effect for the composites increases with increasing CNT content. However, above this critical

content, the mechanical properties of the composites decrease. These observations can be attributed to (i) the difficulties associated with uniform dispersion of CNTs at high CNT contents; (ii) lack of polymerization reactions that are adversely affected by the high CNT content. The latter effect becomes more pronounced when the functionalized CNTs are employed.

For CNT/polymer nanocomposites, dispersion has two aspects: (I) disentanglement of CNT bundles or agglomerates, which is nanoscopic dispersion and (II) uniform distribution of individual CNTs or their agglomerates throughout the nanocomposites, which is more of a micro- and macroscopic dispersion. In general, several factors that influence the dispersion of CNTs in polymer matrix have to be considered in the preparation process. The nanometer scale of CNTs with large aspect ratio, surface area combined with high flexibility increase the more difficulty of their dispersion. Besides, the CNT entangling during growth process and the attraction between CNTs by van der Waals force make CNTs themselves tend to aggregate. These factors will prevent CNTs from being well dispersed within polymers.

Usually, in order to achieve a homogenous dispersion of CNTs in the matrix, many different methods have been focused on. Many mechanical techniques have been employed including sonication, ball milling, calendering, stir, etc. Besides, there are two main kinds of surface treatment for CNTs to achieve well dispersed CNTs. One is surface functionalization: Some functional groups (amino, alkyl or hydroxyl, etc.), which can improve the interaction between CNTs and polymer matrix, are covalently bonded directly to the surface of CNTs [70]. The composite with a low CNT loading is fabricated by solution casting method or in situ polymerization method [71, 72]. Sometimes, the surfactant is also used to promote the dispersion of CNTs in the matrix [73, 71]. However, this method may disrupt the bonding between graphene sheets, and thus reduce the properties of functionalized CNTs in the final composites. Another method is to have CNTs physically coated by some surfactants, which is a non-covalent approach and may be a more facile and practical processing technique. In general, proper functionalization facilitates the CNT dispersion in the composites. However, the addition of functional groups resulted in disturbance of the graphitic layer and reduced the conductivity of the nanotubes. The reaction of the polymer chains with the surface groups of CNTs formed an electrically insulting polymer layer, which increased the contact

resistance between individual CNTs, making the tunneling of electrons between nanotubes harder.

The technique employed for CNT dispersion can influence on the mechanical properties of CNT/polymer composites. Table 1-1 summarizes the flexural properties of CNT/epoxy composites fabricated from the same CNT type and content and the same epoxy matrix using different techniques for CNT dispersion. It is worth noting that the multi-scale hybrids with CNTs grown on carbon fibers or on different ceramic particles, as discussed in the previous section. In this case, CNTs can be homogeneously dispersed at microscale in the matrix with the help of these microscale carbon fibers or ceramic 'vehicle' because the microscale reinforcements can be much easily handled.

Table 1-1

Effect of CNT dispersion on the flexural properties of CNT/epoxy nanocomposites.[74]

CNT dispersion technique	Flexural modulus (GPa)	Flexural strength (MPa)
Neat epoxy	3.43 ± 0.01 (+0.00%)	140.0 ± 2.3 (+0.00%)
Sonication in water bath	3.41 ± 0.04 (-0.58%)	144.1 ± 1.8 (+2.93%)
Shear mixing	3.36 ± 0.09 (-2.08%)	140.4 ± 2.4 (+0.29%)
Probe sonication	3.47 ± 0.06 (+1.17%)	142.7 ± 1.7 (+1.93%)
Calendering	3.65 ± 0.02 (+6.41%)	145.2 ± 0.82 (+3.71%)

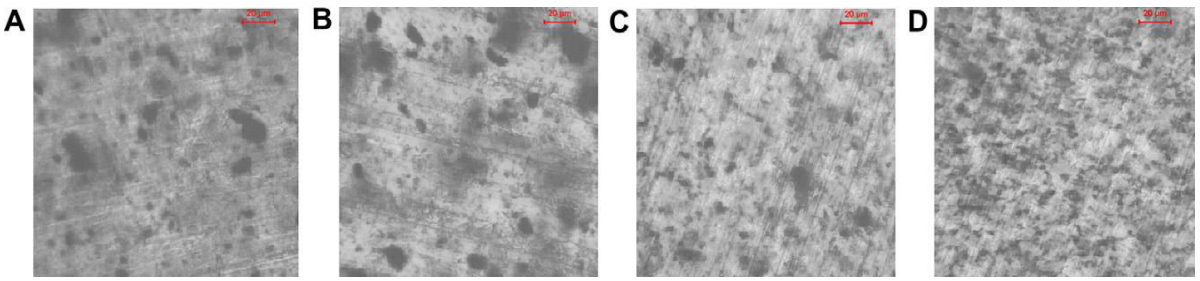

Fig.1-11 *Dispersion of CNTs in nanocomposites fabricated using different dispersion techniques (A: sonication in water bath; B: shear mixing; C: probe sonicator; D: Calendering).*

1.2.3. CNT orientation

Besides the dispersion of CNTs, their high orientation in matrix is another key issue for developing the CNT/polymer composites. It is desirable to align the nanotubes in a primary direction to take advantage of their anisotropic properties. With the limitations of randomly oriented CNTs based composites and the advance of the composite processing techniques, this topic has drawn much attention.

From geometric consideration, the difference between aligned and randomly orientated CNTs can result in significant changes in various properties of composites [75]. The storage modulus of the polystyrene composite films containing random and oriented CNTs were 10% and 49% higher than the unreinforced bulk polymer, respectively [76]. The alignment can be regarded as a special CNT dispersion. However, it is very difficult to align the SWNT in matrix homogeneously. Some methods such as electrospinning [77-79], magnetic field inducing [80, 81], liquid crystal inducing [82, 83], shear flow [84, 85], extrusion or injecting [85], melt spun [86-88], mechanical stretching methods [89, 72] and so on are used to align SWNT in the composite. The degree of CNT alignment in the composite can be governed by two factors: (i) CNT diameter and (ii) CNT content. A smaller diameter of CNT can enhance the degree of CNT alignment due to the greater extensional flow; and a higher CNT content decreases their alignment because of the CNT agglomeration and restrictions in motion from neighboring CNTs. While alignment is necessary to maximize the strength and modulus, it is not always beneficial because the aligned composites have very anisotropic mechanical properties, i.e., the mechanical properties along the alignment direction can be enhanced, whereas these properties are sacrificed along the direction perpendicular to this orientation. Dai *et al.* [90] reported the SWNT/epoxy composite with good uniformity and alignment of SWNTs produced by solution casting and repeated stretching technique in semidried matrix. Composite showed higher electrical conductivities and mechanical properties along the stretched direction than perpendicular to it, as shown in Fig. 1-12. In addition, the value of percolation threshold along the stretching direction is lower than that perpendicular to the SWNT orientation. Nanni *et al.* [91] investigated the self-monitoring aligned MWNT loaded polyethylene terephthalate (PET) composites prepared via the twin-screw extrusion from a

PET/MWCNT masterbatch. It was found that both the self-monitoring and mechanical performances are directly related to the direction of applied stress with respect to CNT orientation. Alignment is necessary to maximize the strength and modulus. However, it is not always beneficial because the aligned composites have very anisotropic mechanical properties. The mechanical properties along the alignment direction can be enhanced, whereas these properties are sacrificed along the direction perpendicular to this orientation.

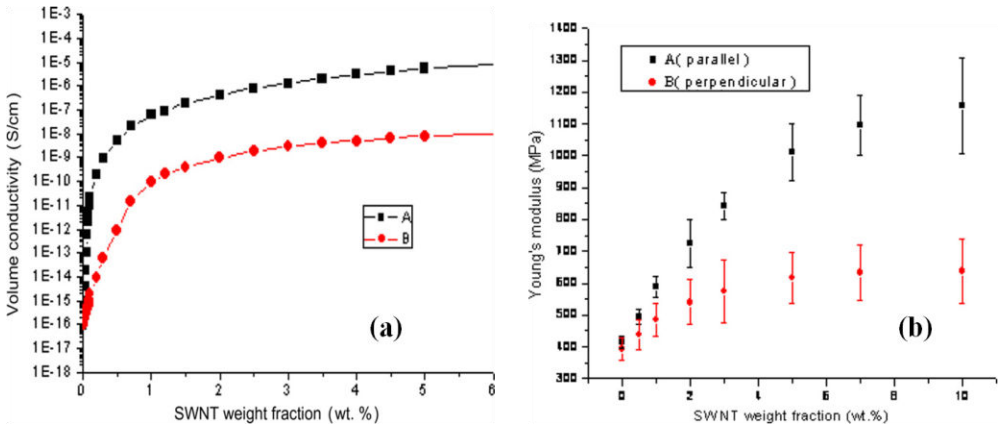

Fig. 1-12 *(a) DC volume conductivity vs. SWNT weight fraction of epoxy/SWNT composite; (b) Young's modulus vs. SWNT weight fraction of epoxy/SWNT composite. (A) Along the alignment of SWNT and (B) perpendicular to the alignment of SWNT. [90]*

1.2.4. Interfacial interaction between CNTs and matrix

Achieving strong CNT/polymer interfacial bonding which could provide effective load transfer is another critical challenge, especially for the CNT/polymer structural composites. There are three main mechanisms of load transfer from the reinforcement to the matrix. The first is the weak van der Waals bonding between CNTs and the matrix, which is the main load transfer mechanism for the CNT/polymer composites. The second is micromechanical interlocking, which may be marginal in the CNT/polymer composites if the nanotubes have smooth surface. The third is chemical bonding between CNTs and matrix, which is not guaranteed in many cases.

Based on the above mechanisms, it is possible to enhance the load transfer from CNTs to the matrix by different treatments. Chemical and physical functionalization of CNTs has

proven to enhance the interfacial adhesion. The van der Waals bonding can be increased by using CNTs with small size and close contact at the interface. From this point of view, individual SWNT well dispersed in a matrix is helpful. In the case of the micromechanical interlocking between CNTs and the molecular chains of matrix, we hope that CNTs are strong enough and inter-connected or long enough to block the movement of the polymer chains [34, 134]. The contribution of this mechanism may reach saturation at a relatively low CNT content [134]. It is unclear at this stage whether or not this critical content depends on the CNT orientation in the matrix. The chemical bonding between CNTs and matrices can be enhanced or created by surface treatments such as chemical and physical functionalization of CNTs. In order to achieve a strong interfacial bonding of CNTS and polymer, the CNTs are usually functionalized with some radical group chemically. It is well known that they can be functionalized easily with some radical groups such as alkyl, carboxyl and carbonyl in the purification process of pristine CNTs product using condensed sulfuric acid and nitric acid [1,2,6]. This covalent method can provide useful functional groups onto the CNT surface. Non-covalent functionalization is an alternative method for tuning the interfacial properties of nanotubes. The suspension of CNTs in the presence of polymers leads to the wrapping of polymer around the CNTs to form supermolecular complexes of CNTs (Fig. 1-13a). Besides polymers, surfactants have also been employed to functionalize CNTs (Fig. 1-13b).

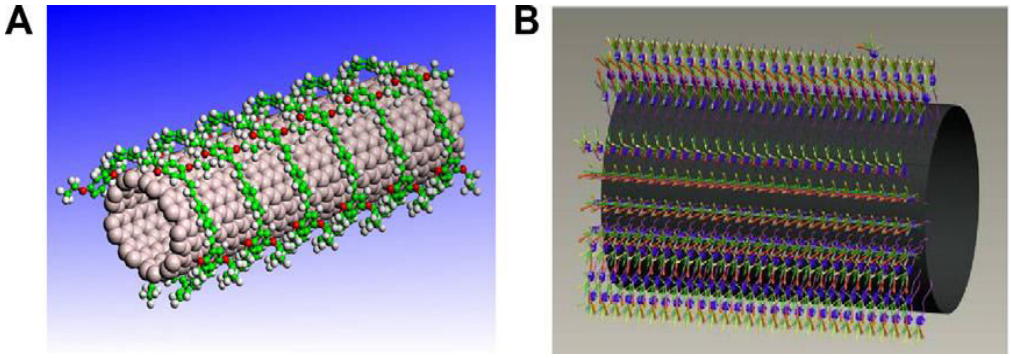

Fig. 1-13 *Schematics of CNT functionalization using non-covalent methods (A) polymer wrapping; (B) surfactant adsorption.[92]*

The physical adsorption of surfactant on the CNT surface lowered the surface tension of CNT, effectively preventing the formation of aggregates. Furthermore, the surfactant-treated

CNTs overcome the van der Waals attraction by electrostatic/steric repulsive forces. It was shown that CNT functionalization can enhance the modulus, strength as well as fracture resistance of the composites [93-96]. Besides, proper functionalization facilitates the CNT dispersion and the formation of conducting networks in the composites, resulting in lowered percolation threshold [97]. However, some research reported that functionalized CNTs are detrimental to the composite electrical properties [98]. The addition of functional groups resulted in disturbance of the graphitic layer and reduced the conductivity of the nanotubes. The functionalization significantly improved the affinity between the polymer and CNTs. The reaction of the polymer with the CNT surface groups formed an electrically insulting polymer layer, which increased the contact resistance between individual nanotubes, making the tunneling of electrons between nanotubes harder. In addition, functionalizations using acids of a high concentration can severely damage and fragment CNTs into smaller pieces with decreased aspect ratios.

It needs to be emphasized that the introduction of the multiscale hybrid nanofillers with the hybridization of CNTs and 2D lamellar flakes is helpful for improving the interfacial interaction within the polymer matrix. Without any purification, the CNT-clay hybrids were directly used to fabricate nylon-6 composites via simple melt-compounding. The composites showed remarkably enhanced mechanical properties due to the homogeneous dispersion of nanohybrids and their strong interfacial interaction with the nylon matrix [56] (Fig. 1-14).

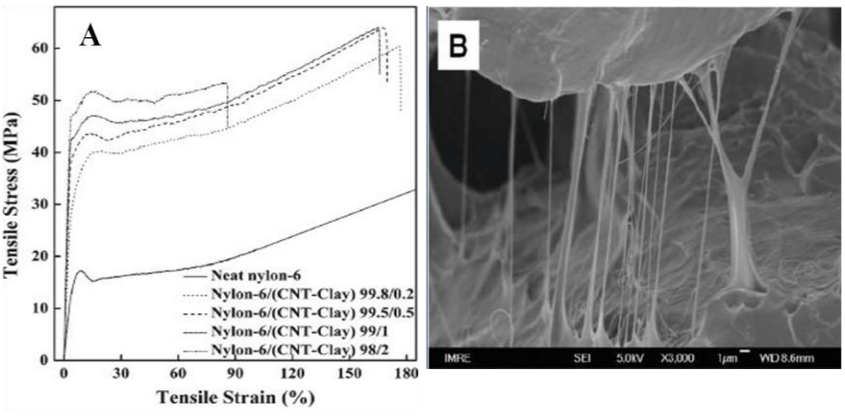

Fig. 1-14 *(A) Typical stress-strain curves of neat nylon-6 and CNT-clay hybrid composites (B) The microcrack linked by MWNTs sheathed with polymer showing the strong interfacial interaction between fillers and matrix. [56]*

1.2.5. Other problems

For the electrically and thermally conductive CNT/polymer composites, good contact between individual CNTs is very important. Only when excellent contacts are established between the individual CNTs, the electrical and thermal signals could be well transmitted. Simulation results indicated that the contact resistance of CNTs in composites played an important role in enhancing the conductivity of composites [99, 100]. This was confirmed by a recent study [68] in which when silver decorated CNTs were employed as conducting filler, the composites exhibited a significantly higher conductivity above the percolation threshold than those containing pristine CNTs. If the contact resistance between the individual CNTs is too high, the existing CNT paths will not endow better conductivity. Several main factors may influence the contact resistance between CNTs, such as the intrinsic transport properties of CNTs, the way of one CNT contacting with the others (overlap, end to end, one to one or one to more), the insulating layer coating the CNTs as well as its thickness. Based on these analyses, it is necessary to decrease the contact resistivity and improve transport properties between individual CNTs. For example, to improve their intrinsic transport properties, CNTs are treated under high temperature for improving their structural integrity and reducing the functional groups on the surface. The contact means between CNTs can be designed by adjusting the content and orientation of CNTs within a matrix. Huang *et al.* [101] proposed an ideal CNT structure, in which all the CNTs embedded in the matrix are aligned form one surface to the opposite side with all the CNT tips revealed on both surfaces. In addition, for the structural CNT/polymer composites, it is important to solve the slippage within the nanotubes.

1.3. Processing of CNT/Polymer nanocomposites

Because the structure of composites is formed during the synthesis and processing steps, knowledge of the processing-structure-property relations will enable the tailoring of material properties through the control of processing conditions. The effective utilization of CNTs in the composite is greatly dependent on their intrinsic morphology and dispersion state within the matrix. Besides, better CNT/polymer interfacial interaction will result in an efficient load

transfer from CNTs to the polymer matrix. These important issues that affect the composite properties have been focused on by attempting different processing routes. The common fabrication methods which are available for the issues mentioned above will be summarized in this part.

1.3.1. Calendering (Three roll mill)

Calendering, which is commonly known as three roll mill, as shown in Fig. 1-15, is a dispersion method that employs shear force created by the rolls with different rotating speed to mix, disperse or homogenize viscous materials. The general configuration of the machine consists of three adjacent cylindrical rollers. The first and third rollers, called the feeding and apron rollers (n1 and n3 in Fig. 1-15), rotate in the same direction while the center roller rotates in the opposite direction. The narrow gaps (controllable from 500 to 5 μm) between the rollers, combined with the mismatch in angular velocity of the adjacent rollers, result in locally high shear forces in a short residence time. In order to create high shear rates, angular velocity of the center roll should be higher than that of feed roll ($\omega_2 > \omega_1$). One of the unique advantages of this technique is that the gap width between the rollers can be adjusted, thus it is easy to get a controllable and narrow size distribution of particles in viscous materials [102, 103]. In some operations, the width of gaps can be decreased gradually to achieve the desired level of particle dispersion. This method has become a very promising approach to achieve relatively good CNT dispersion [104]. Thostenson *et al.* [105] utilized a scalable calendering approach for achieving dispersion of CNTs through intense shear mixing. The degree of mixing of the resin and fillers is controlled by the spacing of the gap between neighboring cylinders, through which the mixture must pass. Fig. 1-16 shows the progressive development of nanocomposite structure during the calendering process.

However, there are several concerns should be focused on in using this technique for CNT dispersion: the feeding materials should be in viscous state when mixing with CNTs. In addition, the minimum gap between the rollers is about 1-5 μm, which is comparable to the length of CNTs, but is much larger than the diameter of individual CNTs.

Fig. 1-15 *(a) Calendering (Three roll mill) machine used for particle dispersion; (b) Schematic of the general configuration and its working mechanism.*

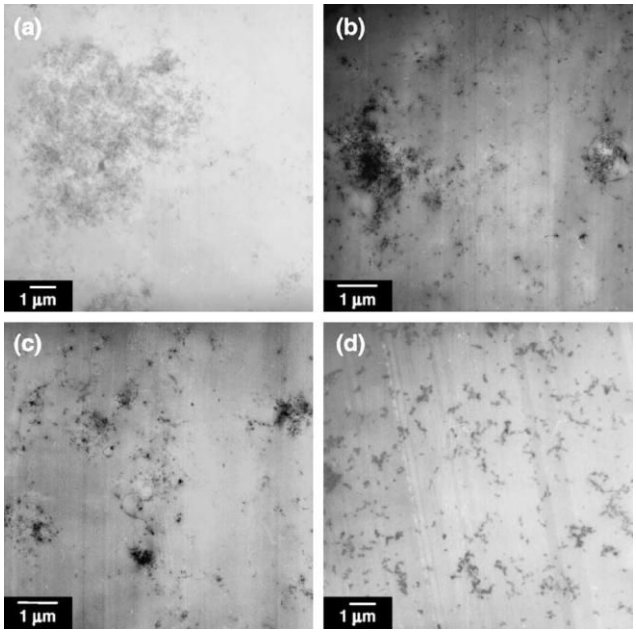

Fig. 1-16 *Nanocomposite structure development after processing at different gap settings (a) 50 µm, (b) 20 µm, (c) 10 µm and (d) 5 µm [39].*

1.3.2. Solution processing

Carbon nanotubes are generally dispersed in a certain solvent then mixed with polymer (solution) by vigorous stirring and/or sonication, i.e., mechanical mixing (high shear stirring), magnetic agitation or high energy sonication. Then, the CNT/polymer composites could be

obtained by controlled evaporation of the solvent with or without vacuum conditions at a certain temperature. In this method, though prolonged high-energy sonication has the potential to introduce defects, ultrasonication process is considered to effectively aid nanotube dispersion in liquid media [106]. In Addition, polymer-functionalized nanotubes [107], surfactants [108] and other chemical treatments [109] are often employed.

With regard to the thermosetting matrices, the CNT/epoxy composites were fabricated by Windle *et al.* [110] using the solution mixing and excellent electrical properties was achieved, resulting in a matrix conductivity around $\sigma=10^{-2}$ S/m with filler volume fractions as low as 0.1 vol.%. Ajayan *et al.* [111] reported the MWNT/epoxy composites prepared by this method and the load transfer from nanotubes to the matrix was studied in both tension and compression testing. In our research, the MWNT were first dispersed in methanol solution under magnetic agitation then mixed with the epoxy matrix [112]. The Young's modulus and the yield strength of the resulted MWNT/epoxy composites was doubled and quadrupled with respectively 1 and 4 wt.% nanotubes, compared to the pure resin matrix samples. Dang *et al.* [113-115] mainly focused on the CNT/PVDF composites with high permittivity and low percolation threshold prepared using this method, i.e., PVDF was firstly dissolved in DMF and then MWNT mixed in the PVDF solution.

For the thermoplastic matrices, the CNT based composites could also be prepared by the solution mixing. Since common solvents such as toluene, chloroform, tetrahydrofurane (THF), or dimethylformamide (DMF) are of high toxicity, a number of aqueous systems have been explored. Jin *et al.* have reported a similar method consisting of solution mixing, casting and drying [89]. Polyhydroxyaminoether (PHAE) was dissolved in the arc discharge grown CNTs in chloroform under sonication. In this work, the CNT orientation and degree of alignment was determined. Solution casting as an alternative processing method has been used to prepare the MWNT-based PS [116, 117], PVA [118, 110], ultrahigh molecular weight polyethylene (UHMWPE) [92], and acrylonitrile butadiene styrene (ABS) [119] composite films with homogeneous nanotube dispersions. Similarly, SWNT-based PP [120], PVA [107], composite films have also been prepared. Since the casting/evaporation process results in the CNT reagglomeration within the composite film, Winey *et al.* proposed coagulation as an alternative approach for fabricating composites with individually dispersed

CNTs [121]. After solution mixing, the CNT/PMMA suspension was dripped into a large excess of bad solvent (water) so as to induce instant precipitation of the polymer chains. The precipitating chains entrapped the carbon nanostructures and prevented them from bundling again. Oliva-Avilés *et al.* introduced the aligned MWNT/polysulfone (PSF) composite films which were prepared by solution casting under alternating electric field [122]. The electrical conductivity and piezoresistive response of electric-field-aligned and randomly oriented MWNT/PSF films are evaluated.

1.3.3. Melting blending

Melting blending has been a very practical method for the fabrication of CNT-based composites on the basis of the fact that thermoplastic polymers will soften when it is close to or above their melting point. Once the polymer was molten, the appropriate percentage of filler was added. Besides, this technique is suitable for polymers that could not easily be prepared using the solution processing due to their insolubility in common solvents. In general, the melt processing involves mixing nanoutbes with the polymer viscous fluid by using high shear forces to break down the CNT aggregates and to improve CNT dispersion. Then the final composite samples with specific geometric shapes could be processed by several techniques, such as extrusion.

Due to their good dispersive and distributive mixing capability, twin screw extruders have been the most popular equipment for dispersing and processing CNT-based composites [83]. In our previous studies, the conductive fillers [carbon black (CB), CNTs or the CB and CNT mixture] were mixed with the PVDF and UHMWPE melts using the melting method by a lab-scale Haake rheometer equipped with a pair of high shear roller-type rotors [123-125]. The preferential distribution of conductive fillers in the polymer matrix was observed and desirable positive temperature co-efficient (PTC) effect was achieved. In our group, the MWNT/PVDF nanocomposites were also fabricated by melt-blending the pristine MWNTs in PVDF matrix [126]. A giant dielectric permittivity (~ 3800) was observed when MWNT content is above the percolation threshold (f_c) of the system. However, a high value of f_c (~10.4 vol.%) was found in the composites possibly due to a significant polymer layer wrapping on the nanotubes. Kenny *et al.* [127] incorporated SWNTs into isotactic PP matrix

by melt mixing using Haake Rheomix internal mixer. The low concentration of SWNTs (0.75 wt.%) resulted in considerable improvement in Young's modulus and tensile strength. Besides, a noticeable increase in the storage modulus was also found. Park *et al.* reported the MWNT/PMMA strain sensors prepared with via either melt processing or solution casting [128]. The developed sensors exhibited a broad range of sensitivity. Nanni *et al.* fabricated the aligned MWNT loaded PET composites with different MWNT content, were prepared via twin-screw extrusion from a PET/MWNT masterbatch [91]. Both their self-sensing and mechanical properties are directly related to MWNT content and to the direction of applied stress with respect to CNT orientation.

1.3.4. In situ polymerization process

In situ polymerization processes for fabricating functional composites have been focused on in some investigations. It could produce polymer grafted nanotubes, mixed with free polymer chains. Importantly, this method allows the preparation of composites with high CNT weight fraction. Park et al. [129] prepared the SWNT/PI composites by an in situ polymerization process. This process enabled uniform dispersion of SWNTs in the PI matrix. The electrical conductivity of the resultant SWNT/PI nanocomposite films were significantly improved by 10 orders of magnitude at a low SWNT loading (0.1 vol.%). Mechanical properties as well as thermal stability were also improved with the incorporation of the SWNTs. Feng et al. [130] reported that MWNTs encapsulated by polyaniline (PANI) of nanometer size have been synthesized by in-situ polymerization. Hu et al. [131] prepared the CNT/polymer strain sensor using in-situ polymerization. The numerical calculation and experimental measurement are used to understand the piezoresistivity of the composites. Kang et al. [132] investigated the high piezoresistive characteristics of SWNT/PI composites from below to above the percolation threshold (~ 0.05 wt.%). The maximum piezoresistive stress coefficient of 1.52×10^{-3} MPa^{-1} was found when f_{SWNT} is just above f_c. This coefficient value exceeds those of the metallic piezoresistive materials by two orders of magnitude (4.25×10^{-5} MPa^{-1} for aluminum).

In situ polymerization processes allow for homogenous dispersion of functional fillers and therefore ensure strong interfacial interaction between the fillers and the polymer. As a

result, the resulted composites display excellent properties. However, the narrow monomer alternative window impedes its wide application in various composites.

1.3.5. Electrospinning

Electrospinning technique as an electrostatic induced self-assembly process has been developed for decades. It was used to align CNTs in a variety of polymeric matrixes and produce CNT/polymer composite nanofiber in a continuous manner. The alignment of CNTs enhances the axial mechanical and physical properties of the filaments. As shown in Fig. 1-17, a high voltage is applied between an oppositely charged polymer fluid and a metallic collection screen. The fluid is contained in a glass syringe which has a capillary tip (spinneret). When the voltage reaches a critical value, the electric field overcomes the surface tension of the suspended polymer and a jet of ultra-fine fibers is produced. As the solvent evaporates, a mesh of nano to micro size fibers is accumulated on the collection screen. The fiber diameter and mesh thickness can be controlled through the variation of the electric field strength, polymer solution concentration and the duration of electrospinning. Due to the sink flow and the high extension of the electrospun jet, it is expected to align CNTs during the electrospinning process. However, the distribution and alignment of the nanotubes in the nanofibers are strongly associated with the quality of the nanotube dispersion prepared before addition of the spinnable polymer solution. Generally, the well-dispersed CNTs were incorporated as individual elements mostly aligned along the nanofiber axis. Conversely, the irregular nanotubes were poorly aligned and appeared curled, twisted, and entangled. It is also indicated that the nanofiber diameter, the interaction between the spun polymer and nanotubes as well as the wetting ability are important factors affecting the alignment and distribution of the nanotubes. This was demonstrated by the difference in the alignment of SWNTs in polyacrylonitrile (PAN) and polylactic acid (PLA) nanofibers [78]. The investigations about the SWNTs/poly(ethylene oxide) (PEO) nanofibers by the electrospinning process exhibited that SWNTs were embedded in the PEO matrix in a more regular form because SWNTs are much smaller and uniform in shape and size, as compared to MWNTs. Besides, their stronger tendency to bundle up into coiled aggregates introduces a pronounced difficulty. As a result, more attention was given to the dispersion

process, which is essential for successful alignment of the nanotubes by the electrospinning process.

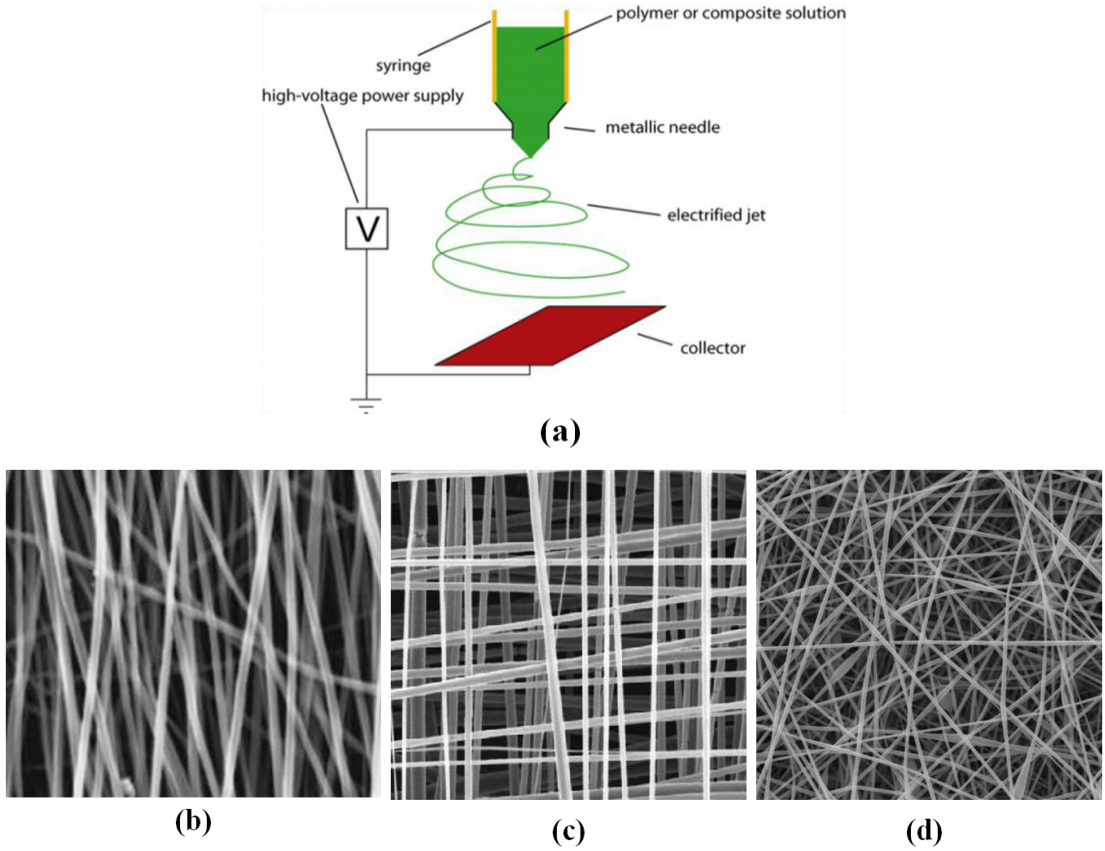

Fig. 1-17 *(a) Schematic of the electrospinning setup; (b) the obtained composite nanofiber.*

In summary, it should be noted that the techniques for CNT dispersion and alignment are not limited to the described above. Many of the recent studies are often based on the use of a combination of these techniques, such as ultrasonication plus ball milling [133], and ultrasonication plus extrusion [134, 135]. In addition, Many factors, such as physical (solid or liquid) and chemical (thermoplastic or thermoset) states of polymer matrix, dimensions and content of CNTs to be added, alternative of the fabrication processes, should be taken into account when selecting a proper technique for CNT dispersion. There is no almighty tool to achieve perfect dispersion of different CNTs in various types of polymer matrices. In addition, to obtain CNT/polymer nanocomposites with a very high CNT content or for some specific applications, new methods have been developed including densification, spinning of coagulant, layer-by-layer deposition and pulverization. It should be noted that as composite

materials are an emerging field, many studies are being made to devise new processing methods that can produce nanocomposites with unique structures and properties for specialty end applications.

1.4. Multifunctional applications of CNT/Polymer composites

It is known that nanostructure composites could produce and enhance multifunctionality in ways that the conventional composites could not. Multifunctional materials are necessarily composite materials. The extraordinary electric and thermal properties combined with their specific modulus and strength as well as their high aspect ratio has made nanotubes outstanding candidates for multifunctional nanofillers in composites, which have stimulated the development of CNT/polymer composites with the capability to serve as structural reinforcements, and a material platform for sensing, actuation, energy storage, electrostatic discharging, electromagnetic interference shielding, etc. The research paid attention on the CNT/polymer multifunctional materials has increased markedly in recent years. Baur *et al.* [136] reviewed the challenges and opportunities in the multifunctional nanocomposite aerospace structures. Thostenson *et al.* [58] and Chou *et al.* [105] reviewed recent advances related to the science and technology of carbon nanotubes and their composites. Li *et al.* [137] surveyed the recent advances related to the use of carbon nanotubes and their composites as sensors and actuators.

1.4.1. CNT-polymer nanocomposite for structural materials

Among the most important structural functions that a system can provide are stiffness, strength, fracture toughness, ductility, fatigue strength, energy absorption, etc. In recent years, the composite materials with lightweight and simultaneous improvement in multiple structural functions are extremely needed. As discussed above, carbon nanotubes exhibit exceptional mechanical properties with Young's modulus as high as ~ 1 TPa and tensile strength of 50-200 GPa. The combination of the superior mechanical properties as well as the low density, high aspect ratio and high surface area make them ideal candidates for reinforcement in the composites. Both SWNTs and MWNTs have been utilized for reinforcing thermosetting and thermoplastic polymers. The CNT reinforced nanocomposites

can be considered as a kind of particulate composites with the filler dimensions on nanometer scale and high aspect ratio. The addition of a small amount of CNTs in polymer composites has produced significant improvements in mechanical properties relative to the un-reinforced resin material.

Tai *et al.* [138] examined the mechanical properties of SWNT/phenolic composites. The change of Young's modulus and strength of the composites with nanotube percentage were investigated by perimental and Halpin-Tsai criterion, as shown in Fig. 1-18. With the addition of SWNT, Young's modulus and strength was increased. However, high loading of

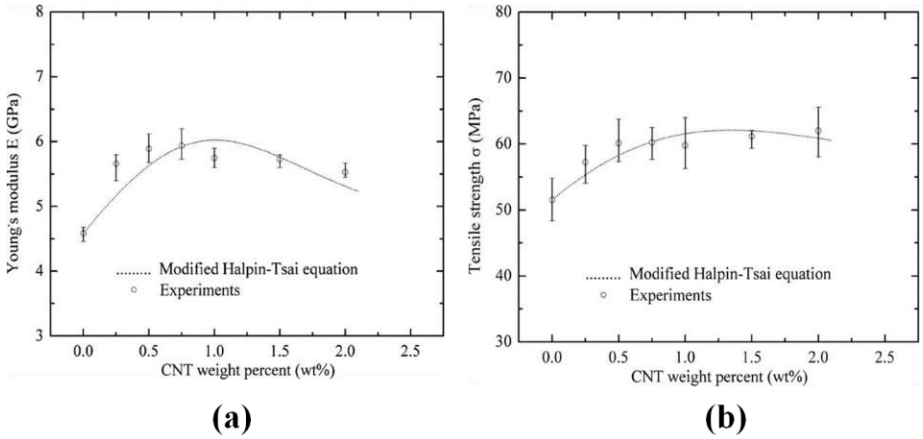

Fig. 1-18 *The experimental data of (a) Young's modulus and (b) tensile strength fitted by the modified Halpin-Tsai equation.[138]*

nanotubes causes insufficient impregnation of the resin within the SWNT networks, thus reducing the mechanical properties. Thostenson *et al.* [104] reported that the low CNT concentrations resulted in significant enhancements in fracture toughness and the overall fracture toughness were dependent on the dispersed and agglomerated structure of the composites, i.e., larger agglomerate was able to more effectively interact with crack front. Grimmer and Dharan [139] demonstrated that incorporating of 1 wt.% CNTs improved the fatigue life of woven glass fiber/epoxy composites by 60%. The added CNTs inhibit the formation of large cracks and the crack bridging by the CNTs as well as nanotube pull-out from the matrix enhance energy absorption and inhibit damage propagation. Koratkar *et al.* [140] reported that the loss modulus of polycarbonate composites was improved more than 1000% by addition of 2 wt.% SWNTs. It was hypothesized that frictional sliding at the

SWNT/PC interfaces was the reason for the enhanced energy dissipation.

In summary, the CNT/polymer composites could be used as structural materials for improved elastic modulus, strength, and fracture toughness and enhanced fatigue life in the glass/epoxy composites at low CNT loadings. However, if nanotube agglomerations are not well dispersed, the enhancement in mechanical properties of nanocomposites may not be significant and there may be even degradation. Surface functionalization of the nanotubes is a way to improve dispersion and strengthen nanotube-polymer interaction, but it may be detrimental to electrical properties of the nanocomposite. Besides, there is optimal nanotube concentration for improving the nanocomposite mechanical properties. In the case of higher nanotube content, the agglomerations and ends of nanotubes will act as stress concentrations and degrade mechanical properties of the nanocomposites. It is worth noting that, due to their distinctive architecture and well dispersed CNTs in the matrix, the CNT-mircoparticle nano/micro hybrids have been excellent reinforcements in the composites. In our research, compared to the SiC microparticles, the use of CNT-SiC hybrids in the epoxy matrix could provide more evident improvement in mechanical properties of the composites [52]. Besides, as shown in Fig. 1-19, the CNT-clay hybrids were demonstrated to be ideal and excellent nanofillers for mechanical reinforcement for fabricating nylon-6 nanocomposites, due to their homogeneous dispersion and strong interfacial interaction with the matrix [56].

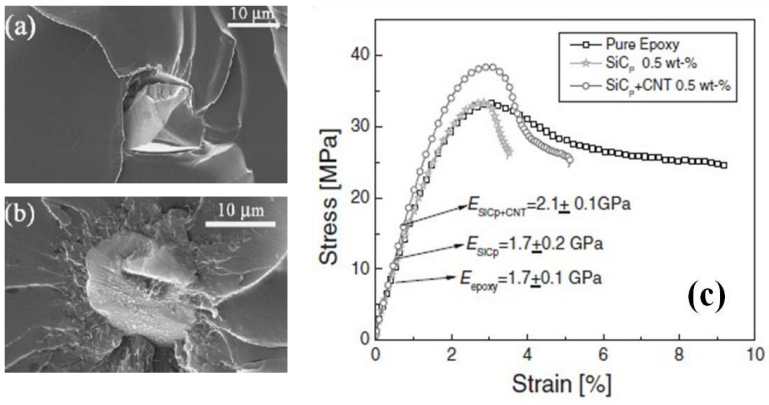

Fig. 1-19 *SEM images of the fracture surface of the composites with (a) SiC microparticle; (b) CNT-SiC hybrids; (c) The typical stress-strain curves of the SiC and CNT-SiC hybrids reinforced composites.[52]*

1.4.2. Electrical behavior of CNT-Polymer nanocomposites

In addition to serving as structural materials, the CNT/polymer composites have been considered to be electrically conducting materials used in various engineering applications including conductive adhesives, antistatic coatings and films, electromagnetic interference shielding, etc. Importantly, for aircraft structures, the conductive CNT/polymer composites are being substitute for the metallic conductors, which are too heavy and difficult to repair.

As show in Fig.1-20, with the gradual increase of CNT content, the composites undergo an insulator-to-conductor transition. The critical CNT content is referred to the percolation threshold, where the electrical conductivity of the composites sharply jumps up several orders of magnitude due to the formation of conductive networks. Percolation theory is usually applied to explain the electrical behavior of the CNT/polymer composites. Below the percolation transition range, the conductive paths do not exist and their electrical properties are mainly dominated by the matrix. Above the percolation transition range, the continuous networks are formed and the conductivity of the composites shows a saturation plateau.

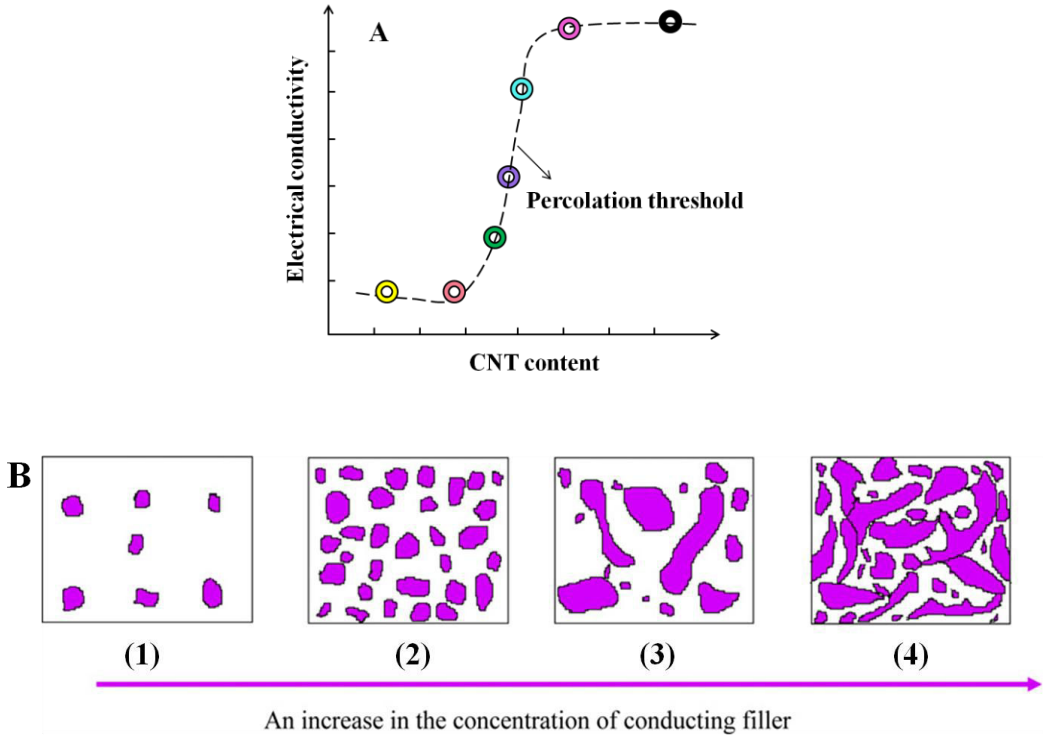

Fig. 1-20 *Schematics of (A) percolation phenomenon and (B) the evolution of conducting networks in composites with increasing conductive fillers.[113]*

The investigation about electrical percolation threshold of the CNT/polymer composites has been a challenging and major concern. It turns out that small concentration of CNTs can lead to very large improvements in the electrical conductivity of the composites. Moisala *et al.* [141] identified the percolation threshold of 0.005 wt.% for MWNT/epoxy composites, and 0.05-0.23 wt.% for SWNT/epoxy composites. However, there is no apparent consensus on percolation threshold values of CNTs: their values reported for CNT/epoxy composites varied from 0.002 to more than 7 wt.% [66, 141, 65]. This large variation indicates that the type of nanotubes (SWNT or MWNT), their surface functionalization, content, dispersion state, aspect ratio as well as the processing techniques used to produce the composites are important factors in determining the electrical properties of CNT/polymer composites. Gojny *et al.* [98] performed an extensive experimental research on the electrical conductivity of CNT/epoxy composites with relation to the contributing factors above. Li *et al.* [66] produced CNT/epoxy nanocomposites with percolation thresholds varying in the range from 0.1 to above 1 wt.% by controlling the dispersion state and aspect ratio of CNTs. They noted that the critical factors determining the percolation threshold were: (i) aspect ratio of CNTs; (ii) disentanglement of CNT agglomerates on the nanoscopic scale; and (iii) uniform distribution of individual CNTs or CNT agglomerates on microscopic scale. There is a critical value of CNT aspect ratio, above which the percolation threshold was sensitive to dispersion state, while below which the percolation threshold increased rapidly with decreasing aspect ratio. The importance of waviness was confirmed by Li *et al.* [142], who used Monte Carlo simulations to show that the electrical conductivity of composites with wavy nanotubes is less than that of composites with straight nanotubes. Thostenson and Chou [104] concluded that the electrical resistivity are higher for the highly dispersed than for the partially agglomerated structure, particularly at lower fractions of CNTs.

Apart from the dc electrical properties, the nanotubes offer the potential to tailor the frequency-dependent electrical and dielectric properties of the composites. Dang *et al.* [113] comprehensively investigated the varying ac electrical and dielectric properties of the CNTs filled PI and PVDF composites. For the CNT contents below the percolation threshold, the nanocomposites usually exhibit a typical dielectric behavior: the ac conductivity increases almost linearly as the increase of frequency. For CNT concentration above the percolation

threshold, the ac conductivity is almost independent of frequency, suggesting an effective connection of the conducting networks in the composites. Arjmand at al. [143] studied the electromagnetic interference (EMI) shielding effectiveness of MWNT/PC nanocomposites. It was found that the EMI shielding effectiveness increases linearly with MWNT content because the number of conductive networks and the number of free electrons increases with increasing MWNT content.

In summary, nanotubes are excellent reinforcements to prepare electrically conducting polymer composites with exceptionally low percolation thresholds. The electrical behaviors of the composites are greatly related to the CNT aspect ratio, dispersion state. As a result, the comprehensive research about the processing-structure-property relationship of composites is extremely needed. As our recently reported, the CNT-SiC multiscale hybrids significantly improve the dielectric permittivity of the CNT-SiC/PVDF composites with an extremely low CNT loading [144], as shown in Fig. 1-21. Thus, the CNT-microsubstrate hybrids are likely to have potential applications for improving the electrical properties of the composites.

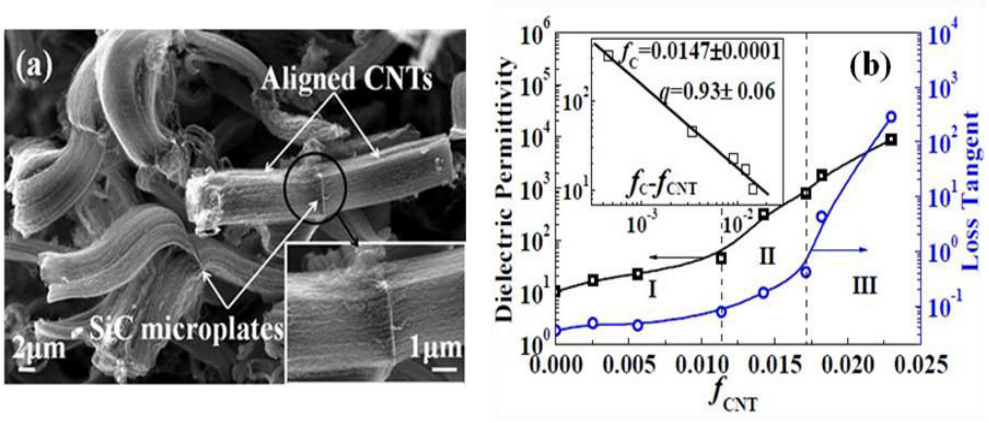

Fig. 1-21 *(a) SEM micrograph of the multi-directions SiC-CNT hybrids; (b) Dielectric permittivity and loss tangent of the SiC-CNT/PVDF composites as a function of f_{CNT}, measured at 100 Hz and at room temperature.[144]*

1.4.3. Piezoresistivity of CNT-Polymer nanocomposites

As discussed in the previous part, once percolation threshold is reached, the connected CNT networks result in continuous electron transport paths across the composites. When the

composites are subjected to an external load, the percolated CNT networks will be disrupted, resulting in an increase in electrical resistivity. The variation in resistivity is attributed to the following reasons: (1) the variation of contact configurations (percolation theory); (2) the increase of tunnelling distances among the CNTs with increase of strain (tunneling theory); (3) piezoresistive behavior of individual CNT themselves.

Early research about the piezoresistivity involved free-standing CNT films or sheets, i.e., 'buckypaper' bonded to the surface of various substrates (brass, aluminium, etc). When the load is applied on the substrates, the resistance between two electrodes attached to the CNT sheet was measured *in situ* [145]. Most of the related studies employed isotropic, randomly oriented CNT networks, and showed that the resistance increase linearly under tension and decreased linearly under compression. As recently reported, the piezoresistivity of the composites with CNTs added to the polymers including the general thermoplastics and thermosets, shape memory polymers, elastomers, and concrete have been investigated.

Kang *et al.* [146] reported the strain sensing behavior of the SWNT-PMMA composites, showing linear symmetric strain response trends in both compression and tension. Pham *et al.* [128] reported the development of the MWNT-filled polymer composite films that can be used as strain sensors with tailored sensitivity. The electrical resistance of MWNT-PMMA films subjected to tensile strains was measured, and the potential applications of the films as strain sensors with a broad range of tunable sensitivity were studied. The largest sensitivity achieved was almost an order of magnitude greater than conventional resistance strain gages. A semi-empirical model, based on the percolation theory, was developed to identify the relationship between the applied strain and sensitivity factor. Not only can the sensitivity be tailored over a broad, but also it can be increased significantly when CNT content is close to the percolation threshold. Zhang *et al.* [147] demonstrated the MWNT-PC composites as multifunctional strain sensors. The composites with 5 wt.% MWNT showed instantaneous electrical resistance response to linear and sinusoidal dynamic strain inputs and a sensitivity of ~3.5 times that of a typical strain gage. Billoti *et al.* [148] investigated the good strain sensing abilities of the MWNT filled polyurethane (TPU) nanocomposite fibers fabricated via an extrusion process and the piezoresistivity can be tunable by controlling the extrusion temperature. Bautista-Quijanoa *et al.* [149] reported the piezoresistive responses of the

MWNT filled polysulfone (PSF) thin films. The films were bonded to aluminum specimens and evaluated as strain sensing elements during quasi-static and cycling tensile loading. Excellent piezoresistive capabilities were found for the films with MWNT loadings as low as 0.5 *wt.%*. De la Vega, *et al.* [150] characterized the local and global stress response of SWNT-epoxy composites by simultaneous Raman spectroscopic and electrical measurement on the specimens subjected to various levels of strain. Both the Raman G-band resonance frequency and the electrical resistance of the composite are found to change monotonically with strain until an inflection point is reached at 1.5% strain. Anand at al. also [151] studied the quasi-static and dynamic piezoresistivity of the CNT-epoxy composites. Wichmann *et al.* [152] found that distinct piezoresistive behavior in the regime of elastic deformation of the MWNT/epoxy composites, which is in good agreement with prevalent theories about charge carrier transport mechanisms in isolator/conductor composites. Dang *et al.* [153] reported the high sensitivity and linear piezoresistive behavior of the MWNT filled methylvinyl silicone rubber (VMQ) nanocomposites. Zha *et al.* [154] investigated the effect of aspect ratio of MWNT on the piezoresistive behavior of thermoplastic elastomer (TPE) based composites in details. By introducing the effective MWNT aspect ratios which are length-dependent and diameter-dependent, it has been demonstrated that the piezoresistivity will decrease with the increase of effective aspect ratios. The piezoresistivity of the CNT-based nanocomposites exhibits a much higher sensitivity as compared to traditional strain gages. Future research in improving the repeatability of nanotube based strain sensors and the effect of CNT aspect ratio and orientation on the piezoresistive behavior is needed.

1.5. CNT-based multiscale hybrid composites

Conventional fiber-reinforced polymer composites (FRPs) have considered to be high strength structural materials and have been widely used in many fields including aerospace, automobile, marine and military due mainly to their high specific strength and stiffness, lower density and flexible tailoring, easy processability, etc [155]. Extensive research in the fiber-reinforced composites has achieved excellent in-plane properties (fiber-dominated), such as, high tensile modulus and strength. However, the relatively weak out of-plane properties (matrix-dominated) which control compression and delamination performance

still remain major obstacles [156]. It has been found that the factors most contributing to the weak out-of-plane properties are the brittle nature of matrix resins and weak interfacial adhesion of matrix and fiber, which relates to the wettability of fibers. Considerable effort towards solving the problems has been made, by introducing the through-the-thickness reinforcement (3D textiles) to change the architecture of the reinforcement [157]. However, these modifications of the micro-structure of the reinforcement do not change the intrinsic interface and matrix properties. This can be done through surface modification of the fibers (for interface) and toughening of the matrix (for the both).

As discussed in the previous part, it was demonstrated that the addition of CNTs in the matrix can increase the toughness of the matrix and improve the interface properties of CNT-composites. Therefore, the poor properties of the traditional FRPs may be improved at nanoscale by introduction of multiscale reinforcements. That is, the nanotubes are dispersed uniformly throughout the polymer matrix, as shown in Fig. 1-18, or integrated by selectively depositing directly on the fiber surfaces (Fig. 1-22) [158]. The multiscale hybrid composites consist of nanoscale CNTs as well as continuous microscale (unidirectional or woven) fiber and the polymer matrix (macro) have drawn significant interest in the field of advanced, high-performance materials.

The small size of CNTs enables them to penetrate into the narrow matrix-rich regions between individual fibers in a bundle as well as between layers of laminated composites. It is important to understand the synergistic interactions of the multiscale nanotube/fiber hybrid system. At the single fiber level, the interaction of the nanoscale reinforcement is on the level of the fiber/matrix interface where selective local stiffening or strengthening of the polymer matrix surrounding the fiber could occur. At the bundle level, nanotubes could interact to share load in the transverse direction and also create electrically or thermally conductive pathways between or around the fiber reinforcements. At the microstructural level of the composite laminate, the nanotubes could provide reinforcement to improve interlaminar or through-thickness reinforcement and alter other matrix-dominated structural or functional properties.

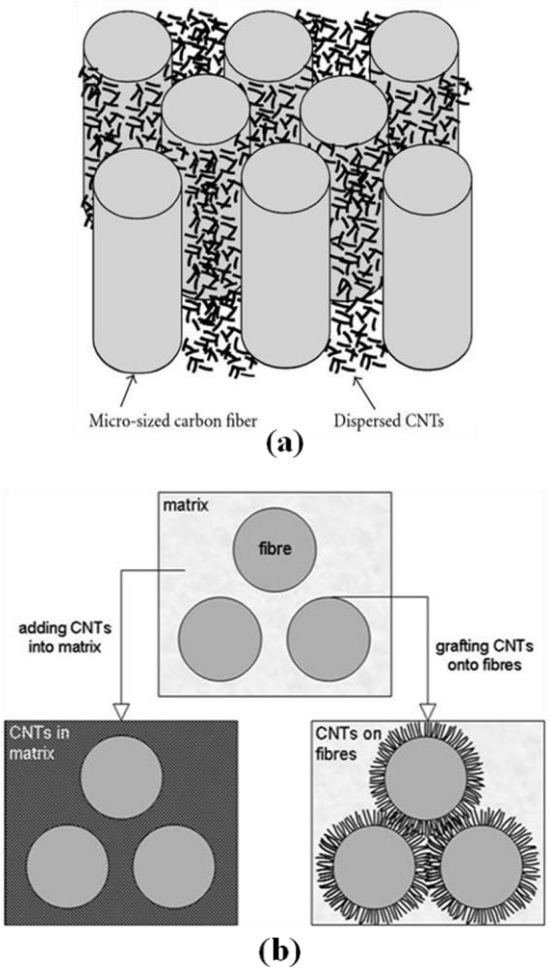

Fig. 1-22 *Fiber reinforced multiscale hybrid polymer composites with CNTs (a) dispersed in the matrix; (b) grown on the surface of fibers.[159]*

The nanoscale CNT holds the potential to tailor structural and functional properties and change the micro-scale damage mechanisms of through the fiber reinforced composites. The challenges associated with understanding the structure/property relations still remain in the CNT-based multiscale hybrid composites. In this part, we briefly review the critical issues and results associated with the development of these systems and highlight a multifunctional application of utilizing CNTs to *in situ* detect damage in composite materials.

1.5.1. Dispersed CNTs in the matrix

Dispersing CNTs into the polymer matrix for producing multiscale hybrid composites can be realized using conventional composite manufacturing process, such as prepregging,

filament winding, pultrusion, or resin transfer molding (RTM). But the dispersion of CNTs in the polymer matrix has some processing challenges. Inadequate dispersion of CNTs in the matrix can result in agglomerations. Due to the very small inter-fiber spacing in the fiber reinforced composites, the CNT agglomerates are usually filtered-out by the fiber bundles, leading to the non-uniform infiltration of the fiber bundles. In addition, the dispersion of nanotubes also results in increased viscosity of the polymer suspension, creating difficulties for the infusion and wetting of the fibers. Thus, the addition of CNTs into the matrix is typically limited to relatively low concentrations and the improvement of CNT dispersion is extremely needed for the FRPs with CNT modified matrix.

Some promising enhancements of the matrix-dominated mechanical properties in the fiber composites have been observed by modifying the matrix with CNTs. Bekyarova *et al.* [160] reported that the carboxylic acid functionalized SWNTs were dispersed in epoxy matrix and then infused into unidirectional carbon fibers using RTM, resulting in a 40% enhancement of the interlaminar shear strength at just 0.5 *wt.%* of CNTs. Yokozeki *et al.* [161, 162] reported that the interlaminar fracture toughness of carbon fiber reinforced composite laminates with cup stacked carbon nanotubes (CSCNTs) in epoxy matrix was improved up to 100%. Wichmann *et al.* [163] found a 16.8% increase in the inter-laminar shear strength (ILSS) of the glass fiber/epoxy composites with the addition of 0.3 *wt.%* DWNTs in the epoxy matrix. However, there was no significant improvement in interlaminar fracture toughness of the multiscale hybrid composites.

Besides their structural properties, if the nanotubes are uniformly dispersed in the matrix and infused through the fiber bundles, the electrically percolating networks can be formed throughout the composites [163, 164]. In this case, it can result in the improvement of electrical conductivity especially in the FRPs with insulating fibers, such as glass or advanced polymer fibers. Thostenson *et al.* [164] fabricated the CNT/glass fiber/vinyl ester composites and measured the influence of both processing conditions and fiber orientation on the electrical properties of the composites at different CNT contents. Obvious anisotropy of the electrical properties in the longitudinal and transverse directions was observed, as shown in Fig. 1-23. There is approximately a one order of magnitude difference between the longitudinal and transverse directions. The theoretical modeling showed that the percolating

pathways are closely related to the microstructure of the fiber composites which influences spanning cluster formation. It is probable that the spanning clusters will form in the regions between the fibers along longitudinal direction instead of around the fibers in the transverse direction. In addition, the clusters follow a longer mean path to go around the fibers in the transverse direction, resulting in higher overall resistances of the spanning clusters.

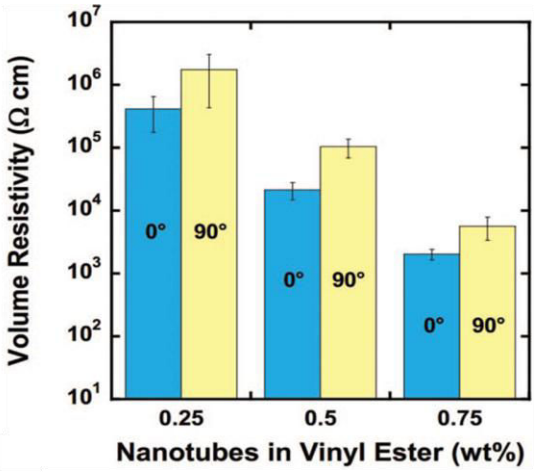

Fig. 1-23 *Electrical anisotropy in carbon nanotube/fiber hybrid composites. [164]*

1.5.2. CNTs grown on surface of fibers

Unlike dispersing CNTs into the matrix, depositing nanotubes on the fiber surface could offer the possibility to achieve higher CNT concentrations but requires the development of new processing methods. The ways of fabricating the CNT-grafted fiber multiscale hybrids mainly include chemical reactions between modified fibers and CNTs [165, 166], integration CNTs into fiber sizing [167-169], electrophoretic deposition [170, 171] and direct growth of CNTs onto fibers via catalytic chemical vapor deposition [172, 38], as discussed above. Each of these techniques has its own potential benefits and drawbacks [173]. Amongst them, CCVD appears to be a most frequently used way for its controllable diameter size [4] and orientation [174, 175].

Gao *et al.* [167] have utilized a fiber sizing approach for depositing uniformly dispersed CNTs onto glass fiber surfaces and investigated the electrical properties of the composites compared to composites with CNTs well dispersed throughout the matrix. The schematics in

Fig. 1-24 show the CNT distribution in the two kinds of as-processed multiscale composites. Using, CNTs are locally segregated near the fiber surface. Unlike the traditional calendering approach, with the fiber sizing method, the distribution of CNTs in the composite can be controlled and substantial amount of CNTs agglomerates on the glass fiber surface, which results in a 2-3 orders improvement in the composite electrical conductivity in the axial, transverse and through-thickness directions (Fig. 1-24).

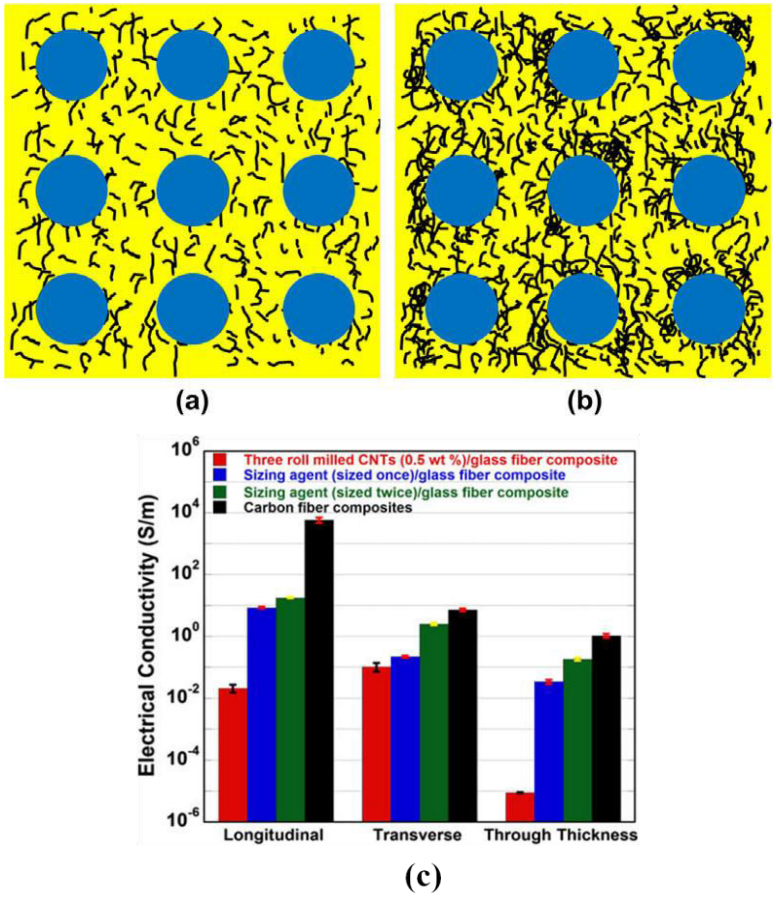

Fig. 1-24 *Schematics of (a) CNTs evenly distributed in the matrix using the three-roll mill process; (b) CNT agglomeration on the surface of sized fibers; (c) Comparative study of electrical conductivity of three roll milled CNT/fiber/epoxy, fiber/sizing agent (sized once)/epoxy, fiber/sizing agent (sized twice)/epoxy, and fiber/epoxy composites.[167]*

An *et al.* [40] synthesized vertically aligned CNT arrays onto the carbon fiber fabric using CCVD method. After CNTs growth, single fiber tensile tests indicated slight tensile strength degradation within 10% for all different lengths of fibers, while the fiber modulus has not been significantly damaged. Compared with the as-received carbon fibers, a nearly

110% increase of interfacial shear strength (IFSS) from 65 to 135 MPa has been identified by single fiber pull-out tests for the micro-droplet composite with CNT-grafted carbon fiber.

Wardle *et al.* [176] utilized vertically aligned CNT arrays transfer-printed the surfaces of prepreg plies to modify the interlaminar properties of carbon fiber reinforced composites. The improvement of both Mode I and Mode II fracture toughness was observed, which was attributed to the CNT bridging of interlaminar cracks (Fig. 1-25).

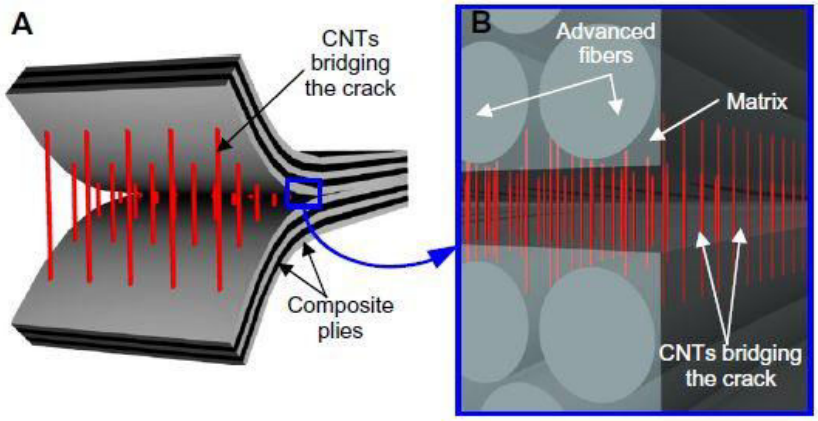

Fig. 1-25 *Illustration of the ideal hybrid interlaminar architecture: (A) VACNTs placed in between two plies of a laminated composite; and (B) close-up of the crack, showing VACNTs bridging the crack between the two plies. Illustrations are not to scale.[176]*

Veedu *et al.* [177] demonstrated the growth of aligned CNT forests perpendicular to the surface of 2D woven SiC fabric cloth consisting of micron size SiC fibers using a CVD process shown in Fig. 1-26. The fabrics were then infiltrated with epoxy resin and stacked to form 3D composites. Significant improvements in interlaminar fracture toughness were achieved due to the presence of the CNT forests.

Garcia *et al.* [39] reported that direct growth of aligned CNTs on the surface of advanced fibers in a woven fabric resulted in enhancement of multifunctional performance, 69% increase in the interlaminar shear strength and 10^6 (in-plane) and 10^8 (through-thickness) increment in laminate-level electrical conductivity. A capillarity-driven mechanism is used to explain the observed effective and uniform wetting of the aligned CNTs in the interior of the laminate by unmodified thermoset polymer resins, as shown in Fig. 1-27.

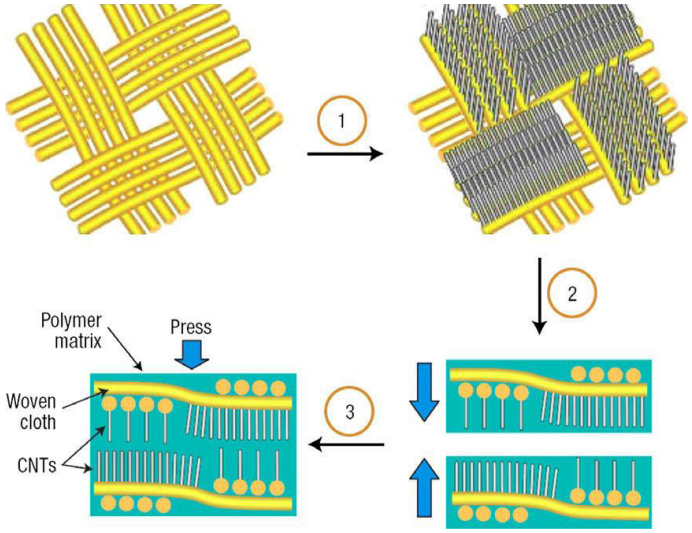

Fig. 1-26 *Schematic diagram of the steps involved in the hierarchical nanomanufacturing of a laminated composite. (1) Aligned nanotubes grown on the fiber cloth; (2) Stacking of matrix-infiltrated CNT-grown fiber cloth; (3) Nanocomposite laminates fabrication by hand lay-up. [177]*

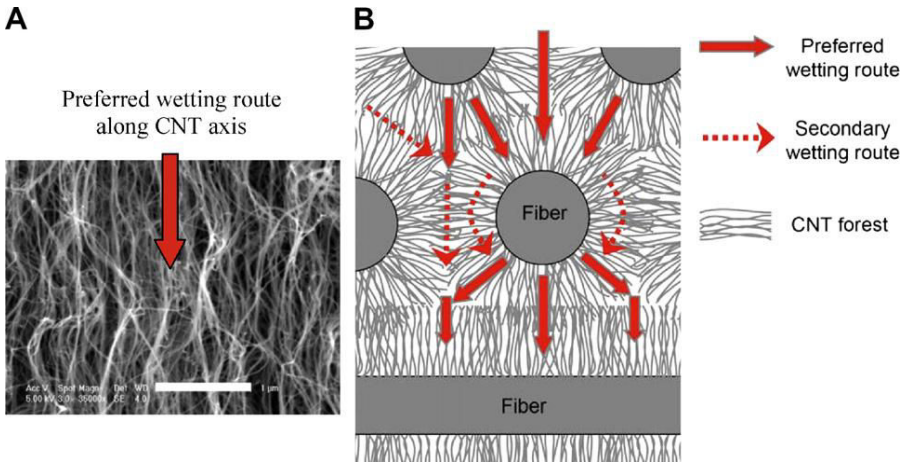

Fig. 1-27 *Routes for polymer wetting of the CNTs in the hybrid composites: (A) high magnification SEM of aligned CNT forest indicating preferred wetting route via capillary action; (B) illustration of CNT wetting in the interior of the composites. [39]*

In summary, with regard to using CNT-grafted fiber as multiscale reinforcement for preparing the FRPs, there still exists some disagreement. Though these positive results have been reported, some researchers deduce that a poor interfacial adhesion probably appears due to the hydrophobicity of CNT grafting. Therefore, more deeply research in this field is needed in future.

1.5.3. CNT-based damage sensing

As discussed in the last part, the advanced fiber-reinforced polymer composites are now widely used in aircraft and other industries due to their high specific strength and modulus. However, they are especially sensitive to the intrinsic damages with various scales including fiber/matrix interfacial debonding, transverse microcracking in the matrix, delamination at ply interfaces, and fiber fracture. Thus, during their service life, many structural components require inspection and evaluation to detect these damages that may lead to failure, and the development of techniques for damage detection is crucial to expanding their applications.

In the composite materials, the damage usually initiates in the polymer matrix in the form of microcracks or delaminations. Though the in-plane properties of composites are dominated principally by breakage of load-carrying fibers, the initiation of damage in the matrix leads to premature fracture and reduced durability. These matrix dominated damage mechanisms often occur at low strain or because of out-of-plane loading. Because of the micro-scale nature of damage in the composites, many non-destructive techniques are used to detect the initiation and accumulation of microcracks. Improved understanding of the damage mechanisms in composite materials is essential for enhanced methodologies for life prediction and also the development of in-service damage monitoring techniques.

For the carbon fiber reinforced composites, utilizing electrical resistance measurements have been established as one of the noninvasive ways for damage monitoring under static and dynamic loading conditions [178-181]. Due to their inherent electrical conductivity, the breakage of load-carrying carbon fibers will result in the changes of the composite electrical resistance. But the electrical response of carbon fiber reinforced composites is dominated by fiber breakage and is less sensitive to the onset of matrix-dominated damage, where damage is first initiated. Besides, it is not applicable to the composites reinforced with fibers are non-conducting, such as glass or aramid fibers. Some researchers have attempted to locally modify the electrical properties of glass fiber yarn bundles via coating with carbon powder and utilizing them for damage sensing [182]. Fiedler *et al.* [183] first introduced the concept of conductive modification with nanotubes as having potential for damage sensing.

As compared to traditional microscale fibrous reinforcements, carbon nanotubes have

dimensions that are three orders of magnitude smaller. Due to their extremely small size, it is possible for nanotubes to penetrate the matrix-rich regions around the fibers and between the plies of the composite. Due to their exceptionally high current carrying capacity, CNTs are able to form electrically conductive networks in polymer matrix at very low volume contents. The formed conductive networks in the matrix surrounding the fibers enables CNTs to be a distributed sensing network that can be utilized for sensing of deformation and damage in situ, as shown in Fig. 1-28 [184, 137, 185]. When the cracks propagate in the composite, the conducting pathways are broken in the percolating network. The capability to sense damage is unique to nanostructured materials since a nano-scale conductor is necessary to sense the formation of a micro-sized crack.

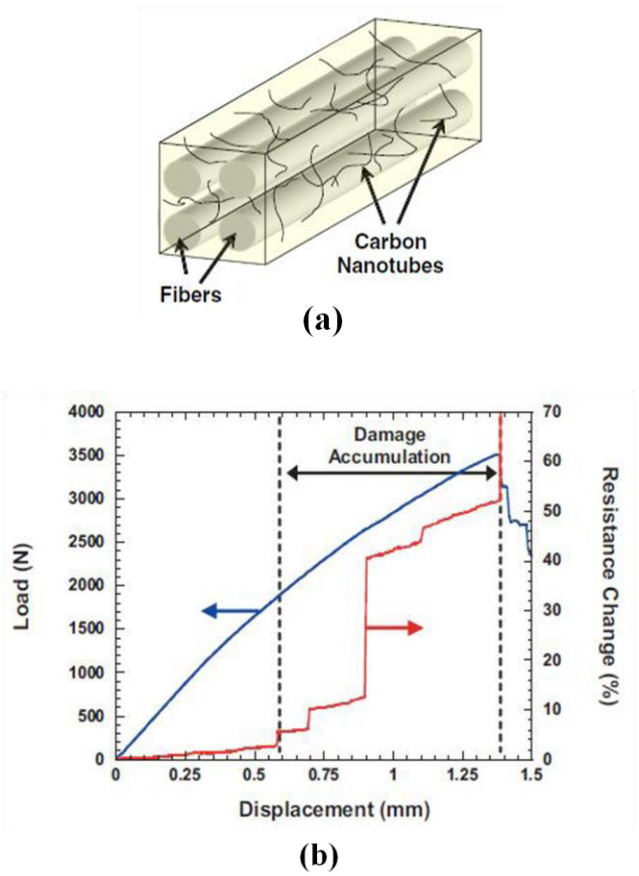

Fig. 1-28 *(a) Three-dimensional model showing the penetration of nanotubes throughout a fiber array due to their relative scale;[137] (b) Load-displacement and resistance curves for the 0/90 specimen.[184]*

Thostenson *et al.* [184] utilized MWNTs dispersed in the epoxy matrix as distributed sensors to evaluate the onset and evolution of damage in the glass fiber reinforced cross-ply

laminate composites, as shown in Fig. 1-28b. The initial slight increase of resistance change is due to the elastic deformation of the material and the subsequent rapid resistance increase is the result of damage accumulation. Fig. 1-29 shows the images of a transverse crack where nanotubes are observed in the narrow regions between fibers. Nofar *et al.* [186] used MWNT networks as sensors to predict the failure region and monitor the degradation of mechanical properties in the glass fiber reinforced composites subjected to tensile and cyclic fatigue loadings.

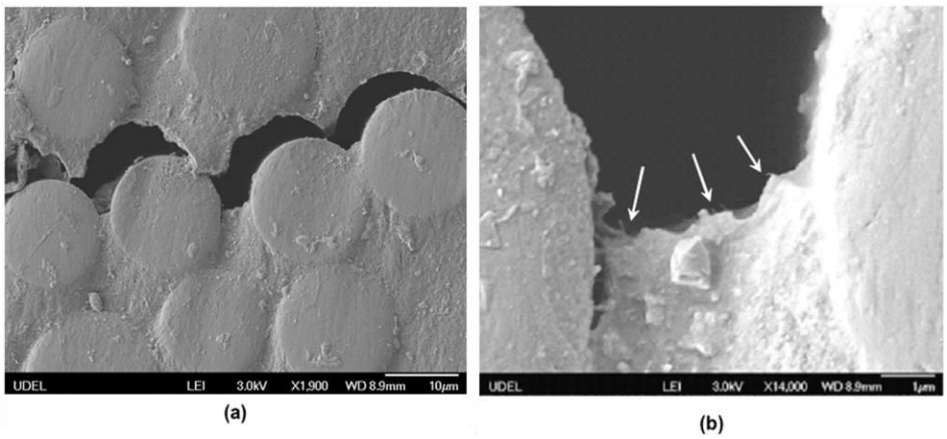

Fig.1-29 *SEM images of (a) formation of microscale transverse cracks and (b) MWNTs protruding from the matrix in the region between two glass fibers.[185]*

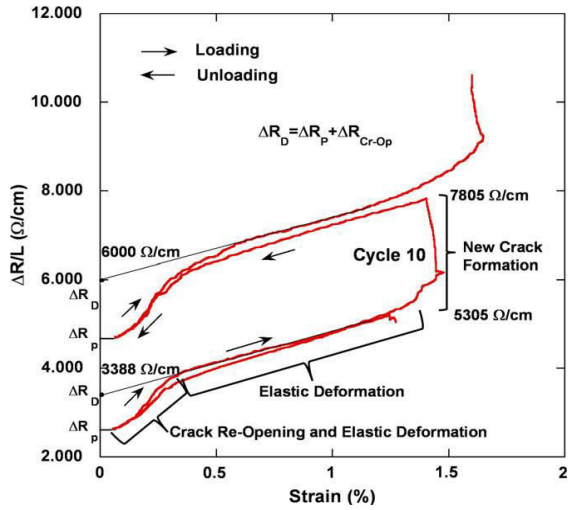

Fig. 1-30 *(a) Resistance change behaivor with tensile strain and damaged resistance change (DRD) defined as a measure of damage. [187]*

With increasing tensile load and number of cycles, different resistance changes are detected and the failure occurs as higher resistance change was detected. During the cyclic loading, the resistance change show more sensitivity to identify the crack location. Gao *et al.* [187] investigated the damage mechanism under cyclic loading in cross-ply fiber reinforced composite laminates via the CNT sensors in the matrix. Fig. 1-30 shows a typical cycle of an incremental tensile test. At the beginning of a loading cycle, the re-opening of previously closed cracks accounts for the initial increase in resistance. The following linear portion of the curve is due to elastic deformation of the material. Then there are large resistance increases due to the formation of new cracks. Kim *et al.* [188] analyzed the damage mechanisms of 3D braided composites were using a low fraction of CNTs dispersed in the resin matrix. Piezoresistive behavior was observed during the tensile testing and the electrical resistance varied with a discontinuous slope when the CNT conductive networks were broken-up due to the damage formation. Four characteristic strains were identified from the resistance change. Using X-ray CT, these characteristic stains were confirmed as critical strain levels, between which different damage mechanisms were involved.

Besides, the CNTs incorporated into the FRPs through surface treat or coat of the fibers, instead of dispersing them in the matrix, also could be used *in situ* sensors. Gao *et al.* [189] reported semiconductive MWNT-glass fibers with MWNTs deposited on the fiber surface. The unidirectional composites containing MWNT-glass fibers exhibit ultrahigh anisotropic electrical properties and an ultralow electrical percolation threshold. And the fiber/polymer interphases was used as *in-situ* multifunctional sensors. Sureeyatanapas *et al.* [190] prepared the glass fiber reinforced composites with SWNTs incorporated as a strain sensor on the fiber surface. Alexopoulos *et al.* [191] embedded CNT fibers to the glass fiber reinforced composites for structural monitoring of the materials. The CNT fibers were used as damage sensor in both tensile and compression loadings. Under high stress (or strain) level loadings, residual resistance measurements were observed after unloading. Accumulating damage in the composites was calculated and was correlated to the resistance change.

In summary, a number of studies have focused on tailoring mechanical and electrical properties of the CNT-based nanocomposites by controlling CNT dispersion, orientation, and CNT-matrix interface at the nanoscale. The insights gained from multifunctional properties

of the CNT nanocomposites have opened up the potential to tailor structural and functional properties of the advanced fiber reinforced polymer composites using the nanoscale CNTs. Introduction of small amount of CNTs can achieve electrically conductive networks in composites, which could serve as *in situ* damage sensor for structural monitoring. The CNTs can be well dispersed in the polymer matrix or grown directly on the fiber surfaces. However, with regard to the former, the uniform dispersion of CNTs in the matrix is extremely needed. And for the later, the processing laminations and difficulties for the applications in industry scale as well as some controversy are the main issues.

1.6. Concluding remarks

The nanoscale structures with high aspect ratio as well as exceptional mechanical and multifunctional properties of CNTs have attracted extensive attention since their discovery. CNTs have tremendous potential for applications in many scientific and technological fields. This chapter provides a detailed overview on the structure and properties of CNTs and their utilization as multifunctional fillers in the polymer matrix to achieve improved mechanical, electrical and desirable piezoresistive properties of the resulting composites.

CNT aspect ratio is an important factor that influences the composite properties. An optimal aspect ratio is needed to provide an efficient load transfer from the nanotubes to matrix, and it is also helpful for the formation of conductive networks for improved mechanical and electrical properties. CNT orientation is another key issue for design the CNT/polymer composites. The desirable CNT orientation gives rise to CNT/polymer composites with higher electrical conductivity and mechanical reinforcement. The control of CNT alignment towards the pre-determined direction is important to take advantage of their anisotropic properties. Besides, there are two major interrelated issues that should be addressed, namely, dispersion of CNTs in the matrix and CNT/polymer interfacial adhesion. Both the mechanical technique and surface treatment of CNTs are employed for improve their dispersion. The chemical and physical functionalizations of CNTs not only facilitate dispersion of CNTs, but also improve the interfacial interactions between the CNTs and polymer matrix. Various processing methods can be adopted to prepare the CNT/polymer nanocomposites. Based on the processing-structure-property relations of the composites, the

issues can be realized by selection of the CNT synthesis and CNT/polymer preparation methods or controlling the conditions during process. Selection of a proper method or a combination of several methods has to be based on the desired properties of the composites. The multifunctional CNT/polymer composites with the outstanding mechanical, electrical and piezoresistive properties have capability to serve as structural materials, and a platform for sensing, actuation, energy storage and so on. Besides, the fiber-reinforced composites modified with CNTs, known as multiscale composites as they are reinforced with microscale fibers and nanoscale nanotubes have drawn significant attention in the field of advanced high-performance materials. The multiscale reinforcements, containing fibers together with CNTs in the matrix or on the surface of the fibers can increase holds the potential to tailor structural and functional properties of the fiber reinforced composites. The electrically conductive networks of CNTs could serve as *in situ* sensor to detect the damage evolution in the composites.

More recently, it is worth noting that large scale controlled growth of aligned CNTs on microsubstrates could solve the problems above. The CCVD process has been successfully used to synthesize various nano/micrometer hybrid structures with CNTs selectively grown on fibers or micrometer particles including metal or oxide nanoparticles, microsized ceramic particles, fullerenes and two dimensional graphene. This hybrid structures show superior multifunctional properties in the composites, mainly due to the uniformly dispersed CNTs in the matrix as well as reinforced interfacial connection and charge transfer between CNTs and the matrix in composites. As a result, the nano/micro multiscale hybrids probably endow CNTs as multifunctional reinforcements for many potential applications in a wide range of fields including conductive and high-strength composites, strain sensors and actuators, etc. In this thesis, the CNT-microparticle multiscale hybrids with various architectures will be used as novel multifunctional fillers in the composites, taking place of the conventional randomly orientated CNTs. Their mechanical, electrical, piezoresistive and damage sensing behavior in the nanocomposites or fiber-reinforced composites will be focused on.

Chapter II
CNT-Microparticle Hybrids Reinforced Epoxy Nanocomposites

2.1. Introduction

Carbon nanotubes with exceptional mechanical and electrical properties [10, 11] have emerged as superior multifunctional nanofillers for the polymer composites. A significant improvement of composite properties would be achieved by incorporating a small amount of CNTs [58, 59]. Such CNT-based polymer composites are ideal candidates for numerous engineering applications including automotive, aerospace and electronics. It is well known that the efficient stress transfer from CNTs to the matrix is prerequisite to attain required mechanical properties of the composites, which is greatly dependent on the CNT dispersion [74], orientation [90] and aspect ratio [61], and the CNT/matrix interfacial properties [192]. It has been generally accepted that the uniform dispersion and larger aspect ratios of CNTs enabled enhanced mechanical properties in the composites. Graphene platelets (GNPs) with two-dimensional structure and high aspect ratio which are composed of several layers of graphite nanocrystals stacked together become ideal reinforcing and conducting fillers [193]. According to the up-to-date research, GNPs could offer more advantages towards highly improving mechanical properties of the composites [194] because their planar structure and ultrahigh aspect ratio are expected to endow better stress transfer from GNPs to the matrix during loading. However, in many cases, the potential applications of GNPs are limited because and they tend to restack due to their large Van der Waals and strong π-π interactions [195].

Besides, with regard to the structural composites based on CNTs, their reliability and long-term safety is a critical issue. For electrically conductive CNT/polymer composites, it is worth noting that their electrical resistance change makes them capable to *in-situ* monitor deformation or damage evolution under loading [137]. For the composites with self-sensing capabilities, the formation of continuous conductive networks is needed. In this case, the

percolation threshold is also related to the CNT dispersion, aspect ratio and orientation [98]. However, most of the available research on the self-sensing composites are mainly limited to randomly distributed CNTs as *in-situ* sensors [196, 197]. In general, their *in-situ* electrical resistance monotonically increases under tensile loading till the catastrophic failure. More recently, the effect of CNT alignment on the self-sensing properties of the composites has also been addressed [91]. The anisotropy of the aligned networks results in improved sensing capabilities. It could be concluded that the *in-situ* sensing behaviors are structure-dependent, which can be controlled by tailoring morphology of CNT conductive networks. As a result, the mechanical and self-sensing performances of the polymer composites depend on the intrinsic characteristics of carbon fillers including their morphology (dimension, aspect ratio, alignment, etc) as well as their dispersion state within the polymeric matrix.

Nowadays, the development of multifunctional CNT/polymer composites with excellent structural and self-sensing properties has been focused on. And the challenging tasks consist in attaining uniform CNT dispersion, optimal CNT aspect ratio and arrangement as well as a strong interface interaction between the CNTs and polymer matrix. Regarding the key issues mentioned above, the design of novel architecture based on the traditional fillers, their modification and the exploitation of other multifunctional fillers may be necessary to achieve outstanding mechanical and desirable self-sensing performance in the polymer composites. The CNT-microparticle multiscale hybrids have been reported to possess certain advantages in achieving more controllable CNT dispersion and improved interfacial properties in the polymer matrix, compared to randomly distributed CNTs [56]. These hybrid architectures were obtained by self-organizing CNTs grown on micosubstrate surface, rather than simply mechanically mixed them. And the CNT aspect ratio can be controlled by varying the growth parameters [53]. These multi-scale hybrids with CNTs grown on SiC microplates or graphene platelets showed enhanced mechanical [52], electrical properties [144] and novel self-sensing behaviors at low CNT concentrations. However, the related research on these multifunctional hybrids is still at an early stage and their underlying reinforcement mechanisms in the composites are not clear to date. Understanding the effect of the hybrid structure on the mechanical and self-sensing properties of the composites is extremely desired in order to fully take advantage of these nano/micro hybrids.

In this chapter, three kinds of hybrids with CNTs grown on SiC microplates (CNT-SiC), Al_2O_3 microparticles (CNT-Al_2O_3) and graphene nanoplatelets (CNT-GNP) were synthesized by chemical vapor deposition (CVD) process. The CNT aspect ratios and organizations of the hybrids can be adjusted by optimizing the CVD conditions. Then epoxy nanocomposites with the various hybrids were prepared by calendaring method. Mechanical, electrical and self-sensing properties of the nanocomposites were investigated in details. The underlying mechanisms associated to the composite properties with relation to the hybrid structure (CNT aspect ratio, orientation and substrate morphology) were analyzed.

2.2. Experimental

2.2.1. Raw materials for the hybrid and composite preparation

Micro-spherical alumina particles (μAl_2O_3, with 3~10 μm in size, 99.8% purity) (Fig. 2-1a) were purchased from the Performance Ceramic Company (Peninsula, OH, USA). SiC microplates with the size of ~2 μm (Fig. 2-1b) were provided by Marion Technologies, France. Graphene nanoplatelets with high aspect ratio, i.e., 3~4 μm in length and ~30 nm in thickness (Fig. 2-1c) were obtained from Xiamen Knano Graphene Technology Co., Ltd. GNPs are platelets like graphite nanocrystals with stacks of multi-layered graphene sheets and there are some wrinkles on their surfaces. This microstructure reveals that GNPs may be difficult to be uniformly dispersed in the matrix. The Al_2O_3, SiC and GNP were respectively employed as the substrates for the CNT growth. Commercial CNTs (randomly distributed), with the diameter of 30~50 nm and length about 20 μm as shown in Fig. 2-1d, supplied by Chengdu Organic Chemicals Co., Ltd., Chinese Academy of Sciences were used as-received. The long and tortuous CNTs entangle with each other, which reveals that this kind of CNTs are difficult to be uniformly dispersed in the polymer matrix. Epoxy resin (1080S, Resoltech Ltd, France) and the curing agent (1084, Resoltech Ltd) was used as the matrix materials.

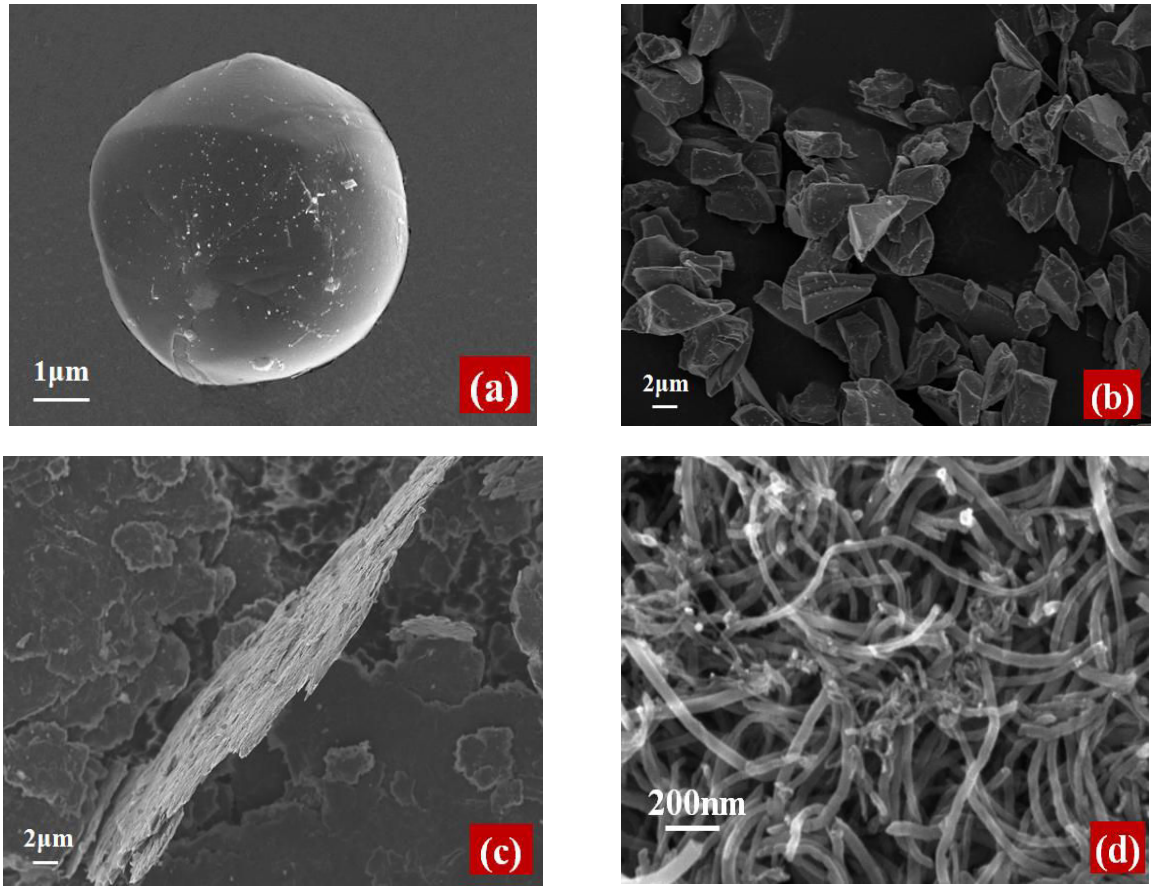

Fig. 2-1 *SEM micrographs of (a) Al_2O_3 microparticle, (b) SiC microplates, (c) GNP and (d) randomly distributed CNTs.*

2.2.2. Preparation of the hybrids and composites

2.2.2.1. Hybrid preparation

Multi-walled nanotubes were *in situ* synthesized on three different substrates (Al_2O_3 microspheres, SiC microplates and GNPs), respectively, by using CVD procedure without any pre-treatment. The acetylene (C_2H_2) was selected as the carbon source and ferrocene Fe $(C_5H_5)_2$ as catalyst precursor [52, 53, 198]. In brief, ferrocene (concentrated at 0.05 g ml^{-1}) was dissolved in xylene solution to serve as catalyst precursor. Then, the mixture was fed by a syringe system and carried into the preheated stable reaction zone in the form of spray by carrier gas argon mixed with 10 ~ 40 % hydrogen. The total gas flow rate was fixed at 1 L min^{-1}. Acetylene (10 ml min^{-1}) was injected as another carbon source. The CNT synthesis

temperatures used were between 550-600 °C. The CNT growth time varied from 2 to 30 min in order to obtain CNTs of different lengths. After, the reactor was cooled down to room temperature under argon atmosphere (1 L min^{-1}). The CNT morphology of the hybrids is strongly dependent upon the nature of substrates. That is, the well-aligned CNTs generally form into symmetric six-orthogonal branches on the spherical Al_2O_3 particles, whereas, the CNTs perpendicularly aligned on the flat surfaces of SiC microplates as well as on the GNPs. The CNT length and density of the hybrids can be tuned by the CVD conditions, for instance, the growth time and temperature.

2.2.2.2. Composite fabrication

The randomly distributed CNTs (commercial) or as-synthesized hybrids (CNT-Al_2O_3, CNT-SiC, CNT-GNP) were firstly mixed manually with the epoxy resin as per calculated weight ratio. Then to further improve the dispersion of the reinforcement, the mixture was passed through a three-roll mill (EXAKT, Germany), following a well-established protocol. In this mixing process, the 1st and 3rd rollers rotate in the same direction whereas the 2nd roller placed in between rotates in the opposite direction thereby inducing high shearing in the mixture. In order to induce high shear force in the mixture, a varying gap setting between the rolls was used according to the size of every kind of fillers. The induction of high shear forces allowed the separation of the entangled CNTs and their uniform dispersion in the epoxy matrix. The parameters of the three-roll mill used for preparing the composites are listed in Table 2-1. After the calendering procedure, the suspension was collected and then the curing agent was added to the obtained suspension by stirring at mass ratio of 1/3 to the epoxy resin, according to the manufacturer's recommendations. The resulting mixture was degassed for 30 min to eliminate the entrapped air and then injected into the mold. The composites were cured at 60 ^{o}C under 10 MPa for 2 h, and then at 60 ^{o}C for 15h under atmospheric pressure. Dumbbell-shape samples with ~ 1 mm in thickness, ~50 mm in length and ~4 mm in gage width were obtained and edge-polished for the mechanical testing. The schematic in Fig. 2-2 depicts the detailed procedure used for the composite preparation.

Table 2-1

The parameters of three-roll mill for preparing the composites

Epoxy composites	Rotation speed of rollers (r/min)	Rotation time (min)	Roll gap (μm)
CNT+SiC (AR1200)	120	30	25
CNT+GNP (AR1200)	120	30	25
CNT+Al_2O_3 (AR1200)	120	30	25
CNT-SiC (AR1200)	80	10	35
CNT-GNP (AR1200)	80	10	35
CNT-Al_2O_3 (AR500)	80	10	15
CNT-Al_2O_3 (AR1200)	80	10	35
CNT-Al_2O_3 (AR2000)	80	10	50
CNT-Al_2O_3 (AR3200)	80	10	70

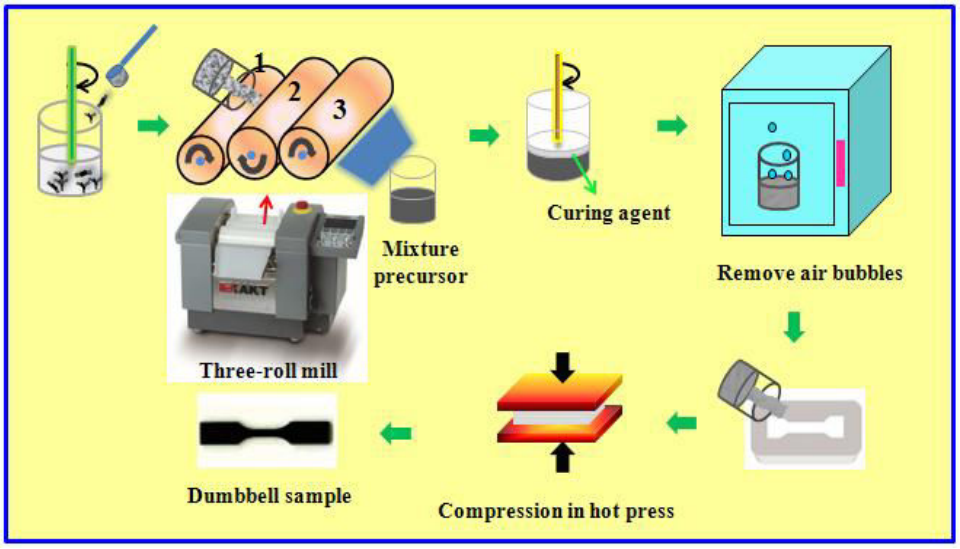

Fig.2-2 *Schematic of the preparation process of the epoxy nanocomposites*

2.2.3. Characterization and instruments

2.2.3.1. Thermogravimetric analysis

The thermogravimetric analysis (TGA) of the as-prepared hybrid fillers were conducted on a thermal analyzer (NETZSCH STA 449F3) in air atmosphere from 30 °C to 800 °C.

2.2.3.2. Calculation of the filler and matrix volume fraction

The corresponding filler and matrix volume fraction can be calculated using the density of the constituents as follows:

$$W_{Particle} = W_M \times \phi_{Hybrid} \times (1 - \varphi_{CNT}) \quad 2\text{-}1$$

$$W_{CNT} = W_M \times \phi_{Hybrid} \times \varphi_{CNT} \quad 2\text{-}2$$

$$V_{Particle} = \frac{W_{Particle} / \rho_{Particle}}{W_{CNT} / \rho_{CNT} + W_{Particle} / \rho_{Particle} + W_M / \rho_M} \quad 2\text{-}3$$

$$V_{CNT} = \frac{W_{CNT} / \rho_{CNT}}{W_{CNT} / \rho_{CNT} + W_{Particle} / \rho_{Particle} + W_M / \rho_M} \quad 2\text{-}4$$

where W_M, W_{Hybrid}, $W_{Particle}$ and W_{CNT} are the mass of the matrix, hybrid, particle substrate and CNT of the hybrids; V_M, V_{Hybrid}, $V_{Particle}$ and V_{CNT} are the volume fraction of the matrix, hybrid, particle substrate and CNTs; ρ_M, $\rho_{particle}$ and ρ_{CNT} is the density of the matrix, particle substrate and CNT, respectively. Φ_{Hybrid} is the weight fraction of the hybrid in the matrix. φ_{CNT} is the weight fraction of the CNT in the hybrids.

2.2.3.3. Micrographic analysis

SEM observations of the reinforcements and fracture surfaces of the nanocomposites were performed on ZEISS, LEO 1530 Gemini. For morphological observation, the obtained composite samples were frozen in liquid nitrogen then quickly fractured.

2.2.3.4. Mechanical characterization

Quasi-static and incremental cyclic tensile tests for the dumbbell-shape samples of the randomly distributed CNTs and hybrids reinforced epoxy composites were carried out on a micro-tensile machine (Instron 5544 with a 2 kN load cell) at a fixed displacement rate of 0.2mm/min. Toward determining the statistics of the modulus, strength and fracture strain of the composites, between three to five samples for each kind of composites are tested under the same condition. For the cyclic tensile testing, the specimens were loaded and un-loaded at the same rate with progressively increasing peak values of cyclic load.

2.2.3.5. Thermo-mechanical characterization

Thermo-mechanical properties of the samples were determined by dynamic mechanical analysis (DMA). Dynamic mechanical analyzer (Netch 242C, Germany) was employed for the tests. The samples with dimensions ~ 60 mm in length and ~ 10 mm in width were tested under a three point bending mode from 30 ^{o}C to 180 ^{o}C at a heating rate of 3 ^{o}C /min and a frequency of 1.0 Hz in nitrogen atmosphere. The storage modulus (E'), loss modulus (E'') and loss tangent (tan δ) were determined as a function of the temperature. Between three to five samples for each kind of the composites were tested. Their storage modulus and glass transition temperature achieved from the DMA curves are used to evaluate the viscoelastic and damping properties of the composites.

2.2.3.6. Electrical measurement

The alternating current (AC) conductivity of the composites was measured using a precision impedance analyzer (Agilent 4294A) over the frequency range from 10^2 to 10^7 Hz at room temperature. Prior to measurements, the silver paste electrodes were applied to both sides of the samples in order to reduce the contact resistance.

2.2.3.7. In situ sensing behavior

To determine the self-sensing behaviors of the composites, *in situ* electrical resistance measurements were performed for monitoring the deformation evolution of the composites. A Keithley 2400 voltage-current meter was used to measure the in-plane volume electrical resistance of the specimens by sourcing a constant voltage and measuring the current using a two point technique. Prior to the electrical measurements, the silver paste electrodes were also applied on both sides of the samples. The schematic in Fig. 2-3 illustrates the testing system for the *in situ* sensing. Due to the nature of the electrically percolative specimens the electrical contact resistance is very small relative to the overall specimen resistance. The electrical resistance data were *in situ* recorded using data acquisition software LabView.

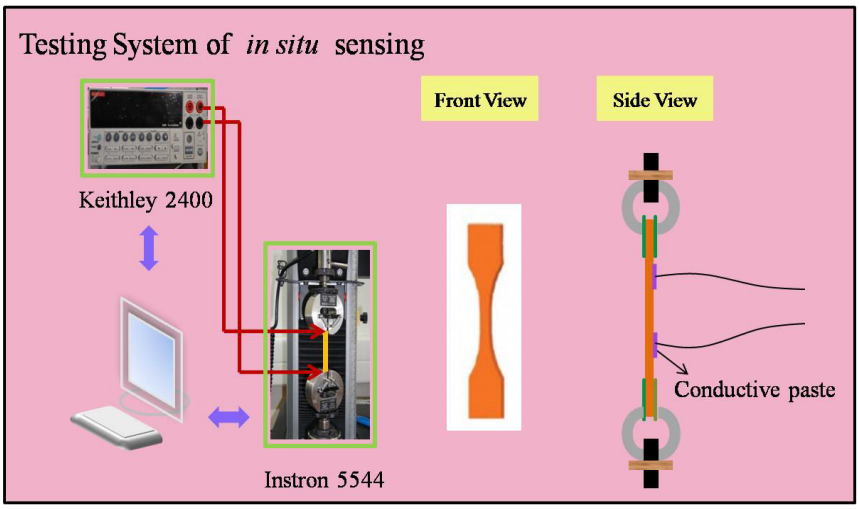

Fig.2-3 *Schematic of the testing system for in situ sensing of the materials.*

2.2. Morphologies of the nano/micro CNT-microparticle hybrids

SEM images in Fig. 2-4 show the morphologies of the nano/micro CNT-microparticle hybrids. These hybrids were prepared using CVD synthesis. It can be seen that the CNTs on each substrate have high number density, but organize into varied architectures. As shown in Fig. 2-4a and b, the CNTs were vertically aligned on the flat surfaces of SiC microplates and the GNPs with a thickness less than 100 nm (see the high magnification image in Fig. 2-4h). The CNT lengths on the two substrates were about 10~15 μm. However, the well-aligned nanotubes generally form into symmetric six-orthogonal branches on the spherical Al_2O_3 microparticles (Fig. 2-4c ~ g), due to their specific crystallographic structures. It is worth underlining that the flake structure of SiC and GNP makes the CNTs mainly aligned on their two opposite sides, differing from the six-branch organization on the spherical Al_2O_3. The hybrids with varied CNT lengths were obtained by adjusting the CVD conditions, such as the growth temperature, time and hydrogen ratio, etc. Therefore, the CNT distribution and arrangement patterns in the hybrids are dependent on the geometry and microstructure of the substrates. The basic information of the various hybrids used is listed in Table 2-2. The aspect ratios (AR) of the CNTs are defined as the ratio of their average length (l) to the diameter (d), i.e., $AR=l/d$.

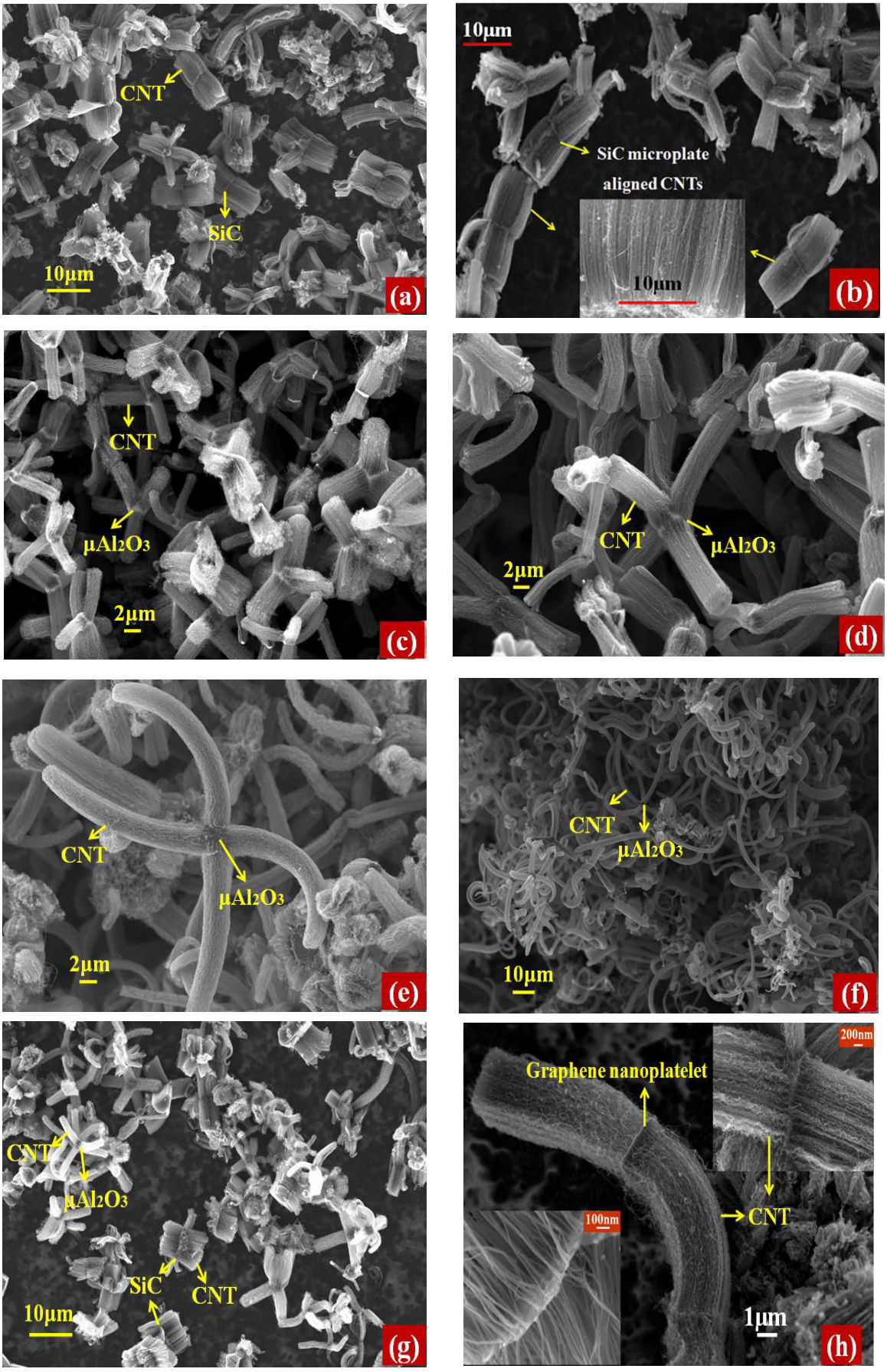
CNT
SiC
10μm
(a)
10μm
SiC microplate
aligned CNTs
10μm
(b)
CNT
μAl2O3
2μm
(c)
CNT
μAl2O3
2μm
(d)
CNT
μAl2O3
2μm
(e)
CNT
μAl2O3
10μm
(f)
CNT
μAl2O3
SiC
CNT
10μm
(g)
Graphene nanoplatelet
200nm
CNT
100nm
1μm
(h)

Fig.2-4 *SEM micrographs of the various CNT-microparticle hybrids (a) and (b) CNT-SiC hybrids with CNT aspect ratio (AR1200); (c) ~ (f) CNT-Al_2O_3 hybrids with different CNT aspect ratios; (c) AR500, (d) AR1200, (e) AR2000, (f) AR3200; (g) the mixture of CNT-SiC and CNT-Al_2O_3 with CNT AR1200 (h) CNT-GNP hybrids with CNT AR1200.*

Table 2-2

Basic information of the randomly distributed CNTs (rand-CNTs), the CNTs grown on the particles and the particle substrates

Materials	CNT length (μm)/ diameter (nm)	Average CNT aspect ratio	CNT density (g/cm^3)	Substrate density (g/cm^3)
rand-CNTs	(10~15[a])/(~10[a])	1200		
[1]CNT-Al_2O_3	(4~6)/(~10)	500		
[2]CNT-Al_2O_3	(10~15)/(~10)	1200	1.78	3.1
[3]CNT-Al_2O_3	(18~22)/(~10)	2000		
[4]CNT-Al_2O_3	(30~35)/(~10)	3200		
CNT-SiC	(10~15)/(~10)	1200	1.78	3.9
CNT-GNP	(10~15)/(~10)	1200	1.78	2.25[a]

[a] According to the values provided by the companies.

2.3. Microstructure of the epoxy nanocomposites

SEM images of the fracture surfaces of epoxy nanocomposites are presented in Fig. 2-5. As shown in Fig. 2-5a, most of the tortuous CNTs are individually separated and randomly distributed within the epoxy matrix. Fig. 2-5b ~ h demonstrates the SEM micrographs of the fractured surfaces of the epoxy composites with different hybrids. It can be seen that the hybrids are well dispersed in the epoxy matrix and their original architectures are almost retained, which endows controlled CNT layout. By comparing Fig. 2-5d ~ g, one can see that the dispersion state of CNT-Al_2O_3 hybrids in the composites depends on the CNT aspect ratio. In the case of relatively short CNTs, Al_2O_3 microparticles are surrounded in the center by the CNTs and the hybrid structure is symmetric and isotropic (Fig. 2-5d ~ f). However, for too long CNTs, Al_2O_3 particles are wrapped at the end by CNTs and the hybrids exist like bundles in the composites (Fig. 2-5g).

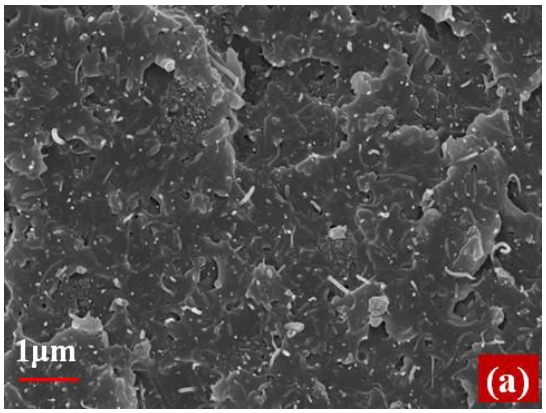
1μm
(a)

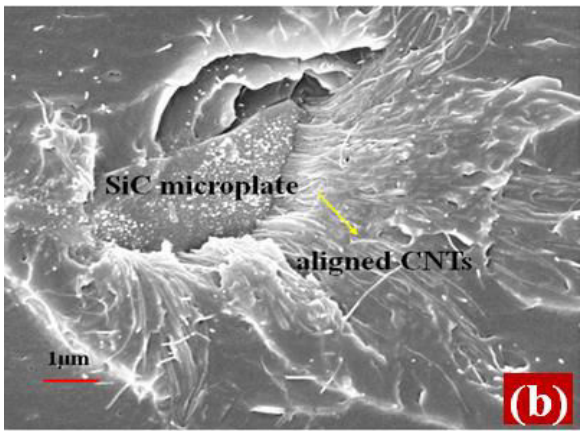
SiC microplate
aligned CNTs
1μm
(b)

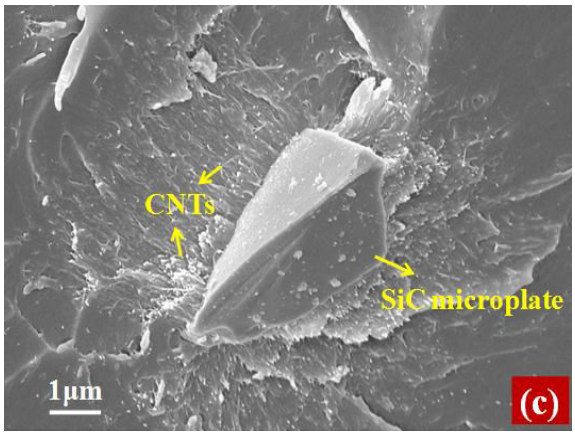
CNTs
SiC microplate
1μm
(c)

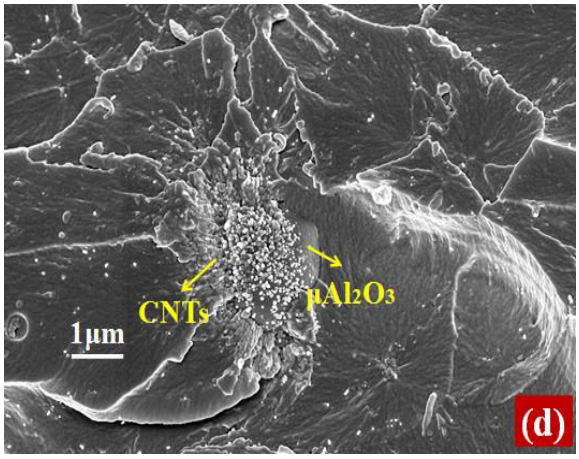
CNTs
μAl2O3
1μm
(d)

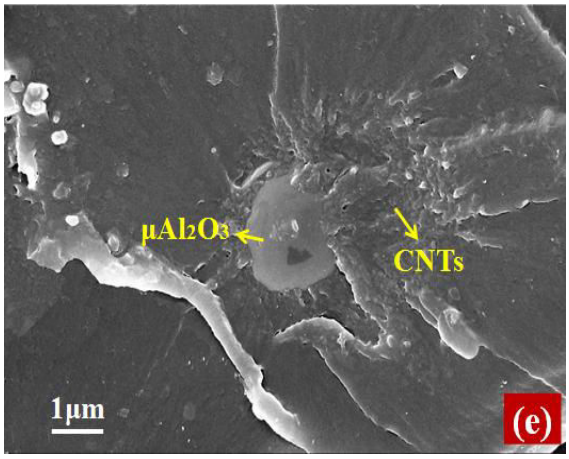
μAl2O3
CNTs
1μm
(e)

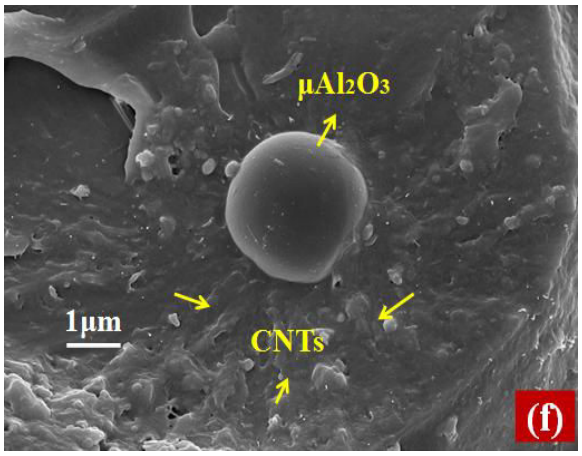
μAl2O3
1μm
CNTs
(f)

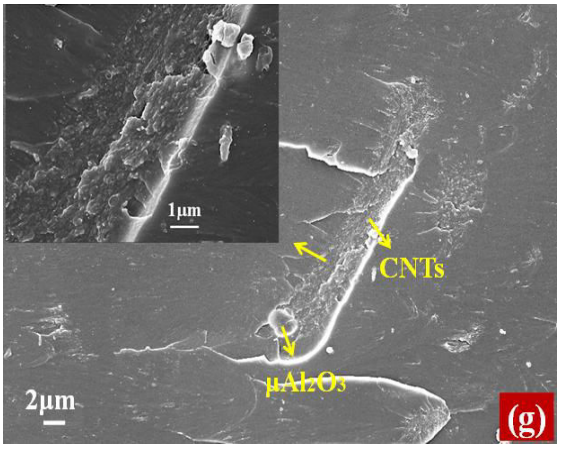
1μm
CNTs
μAl2O3
2μm
(g)

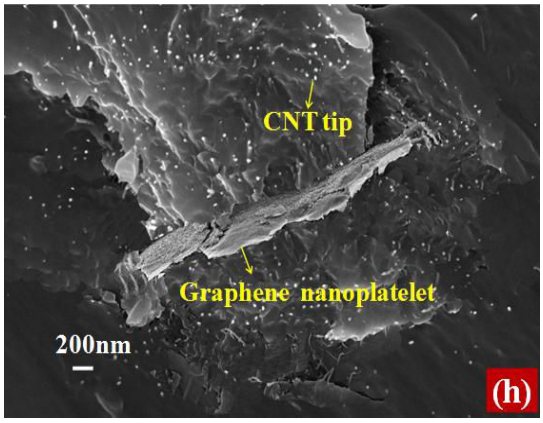

Fig.2-5 *SEM micrographs of the fracture surfaces of epoxy composites based on different fillers (a) CNT/epoxy composites (b) and (c) CNT-SiC/epoxy composites with aspect ratio (1200); (d) ~ (g) CNT-Al_2O_3/epoxy composites with different aspect ratios, (d) AR500; (e) AR1200; (f) AR2000; (g) AR3200; (h) CNT-GNP/epoxy composites (AR1200).*

As shown in Fig. 2-5b, c and h, most of the CNTs are distributed on the opposite surfaces of the SiC and GNP substrates. Besides, it can be viewed that most of the CNTs retain aligned in the matrix at their actual lengths instead of curved states. The dispersion states of the hybrids can ensure large contact area and good interfacial interaction between the CNTs and polymer matrix. All the CNTs of the hybrids are strongly fixed on the microsubstrates. Their orientation during tensile loading is possibly different from that of the randomly distributed CNTs. Thus, the introduction of these hybrids is expected to achieve the desired self-sensing and mechanical properties of the composites.

2.4. Electrical properties of the epoxy nanocomposites

Fig. 2-6 shows the frequency dependence of the ac conductivities measured at room temperature of the epoxy composites containing different volume fractions of the conductive fillers, which indicates the overall connectivity of conducting networks in all the composites. With regard to the randomly distributed CNTs or the hybrids filled epoxy nanocomposites, it is obvious that almost three different behaviors could be identified with increasing the filler content. When only a small amount of the conductive fillers is incorporated into the epoxy matrix, they are considered to be isolated to each other and the ac conductivities of the composites increased almost linearly as the frequency increases from 10^2 Hz to 10^7 Hz. That

is, the conductivity is strongly dependent upon the frequency. In this case, the exhibited typical dielectric behavior indicates the absence of conductive path in the composites, which are largely due to the formation of CNT clusters. The conductivity is mainly determined by the polarization effects and electron motion in the matrix. While with the concentration of the fillers approaching a critical value f_c, the conductivity values are significantly improved and almost independent of the change of frequency in the low frequency range (10^2-10^4 Hz). In this case, the conductive fillers are very close to each other. When f is above f_c, the greatly improved conductivities are observed and their values are almost independent of frequency within the low frequency range. In this case, the corresponding composites exhibit a DC conductivity behavior, since their conductivity does not change with the frequency. Such DC characteristic in the low frequency range is induced by few percolating paths formed through the polymer matrix. With regard to these systems, a moderate increase in conductivity is observed when the volume fraction of conductive filler is below the percolation threshold, while it becomes significant after the volume fraction is above the percolation threshold. The variation of conductivity shows a good agreement with the typical power law:

$$\sigma \propto (f - f_c)^t \qquad as \qquad f > f_c \tag{2-5}$$

Where σ is the conductivity of the composites, f is the volume fraction of conductive fillers, f_c is defined as percolation threshold and t is the critical exponent in the conducting region which is dependent on the dimensionality of the conductive networks. In our research concerning the nano/micro hybrids filled epoxy systems, f represents the volume fraction of the CNTs instead of the hybrids. The best fits of the experimental conductivity data to the log-log plots of the power law could give the value of the percolation threshold and critical exponent in every system. In order to achieve the value of f_c in the composites based on the hybrids, the fraction of CNTs in the hybrids is needed.

According to the Eqs. 2-1 ~ 4, the concentrations for each component in the as-prepared epoxy composites reinforced with the nano/micro hybrids can be calculated and the results are shown in Table 2-3. We can see that the percolation thresholds in the CNT-microparticle hybrids filled composites are much lower than the composites with the randomly distributed CNTs, which are primarily contributed to the unique architecture of the hybrids with various

morphologies of the CNTs grown on the microparticle substrates. These nano/micro hybrids could endow high degree of CNTs, which efficiently increases its utilization ratio in forming conducting network at lower loading.

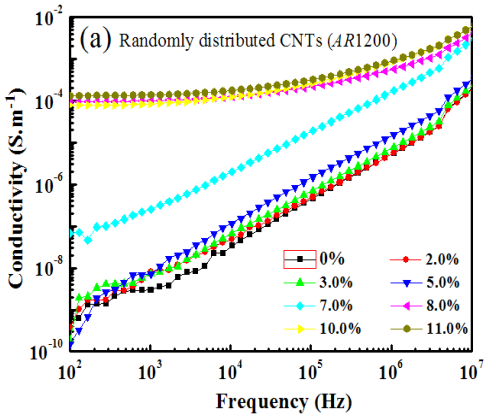

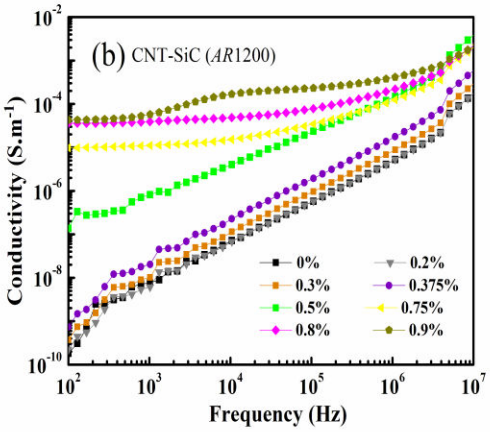

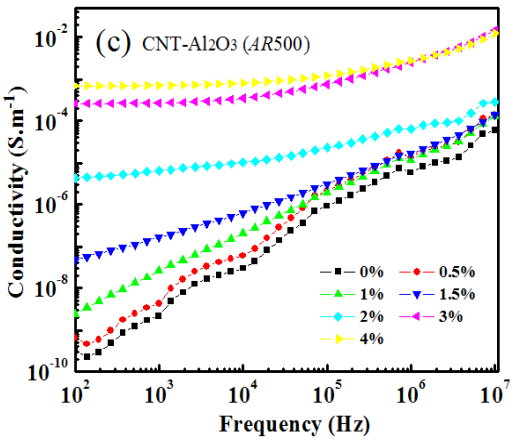

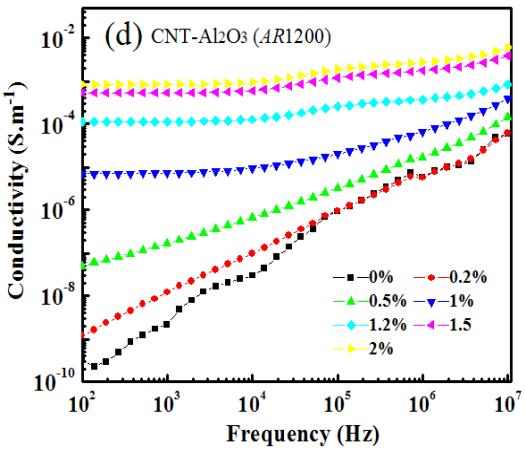

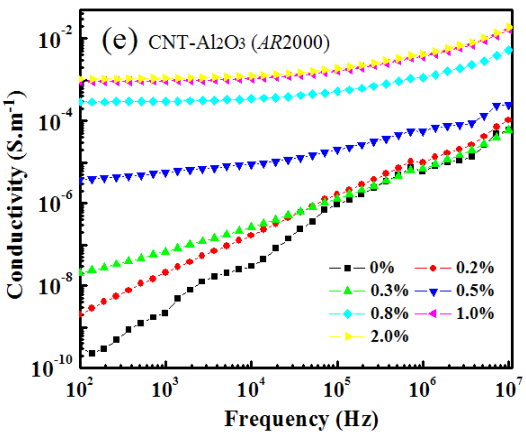

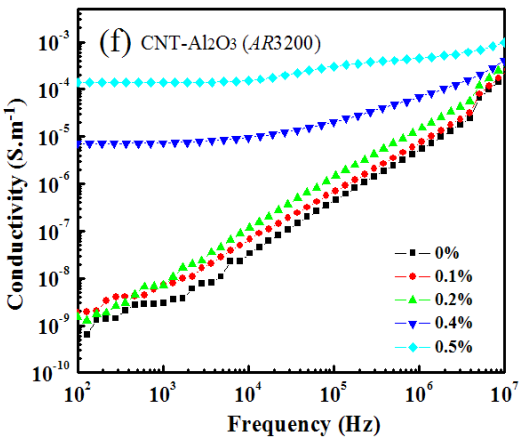

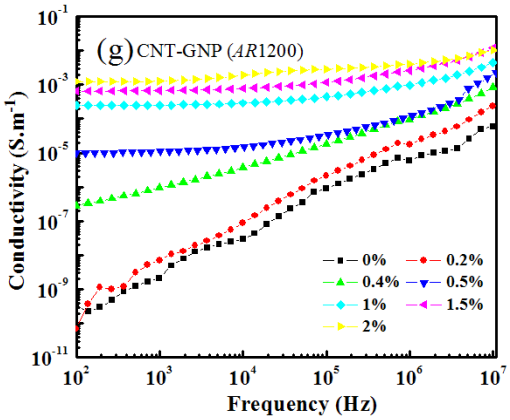

Fig.2-6 *Electrical properties of the epoxy composites based on different fillers: (a) randomly orientated CNTs; (b) CNT-SiC hybrids with CNT AR1200; (c) ~ (f) CNT-Al_2O_3 hybrids with different CNT aspect ratios, (c) AR500; (d) AR1200; (e) AR2000; (f) AR3200; (g) CNT-GNP hybrids with CNT AR1200.*

Table 2-3

Percolation thresholds of the CNTs in the epoxy composites based on different hybrid fillers

Materials	f_{hybrid} (wt.%)	f_{CNT} (wt.%)	f_{CNT} (vol.%)
Randomly distributed CNTs		7.92	5.05
CNT-SiC (*AR*1200)	0.7	0.21	0.16
CNT-Al_2O_3 (*AR*500)	1.95	0.27	0.16
CNT-Al_2O_3 (*AR*1200)	0.96	0.24	0.15
CNT-Al_2O_3 (*AR*2000)	0.52	0.12	0.08
CNT-Al_2O_3 (*AR*3200)	0.40	0.25	0.16
CNT-GNP (*AR*1200)	0.50	0.24	0.15

With regard to the hybrids with the different substrate microparticles (SiC, GNP and Al_2O_3) and the same CNT aspect ratios, it is observed that there is not much difference the of percolation thresholds between the hybrids with different substrates. However, in the case of the CNT-Al_2O_3 hybrids with the different CNT aspect ratios, it is found that the percolation threshold is dependent on the aspect ratios. With the increase of the CNT aspect ratio from 500 to 2000, its value consistently decreases, however, it begins to increase when the aspect

ratio is up to 3200. The effect of aspect ratio on the percolation behavior and conductivity of the composites is illustrated in Fig. 2-7.

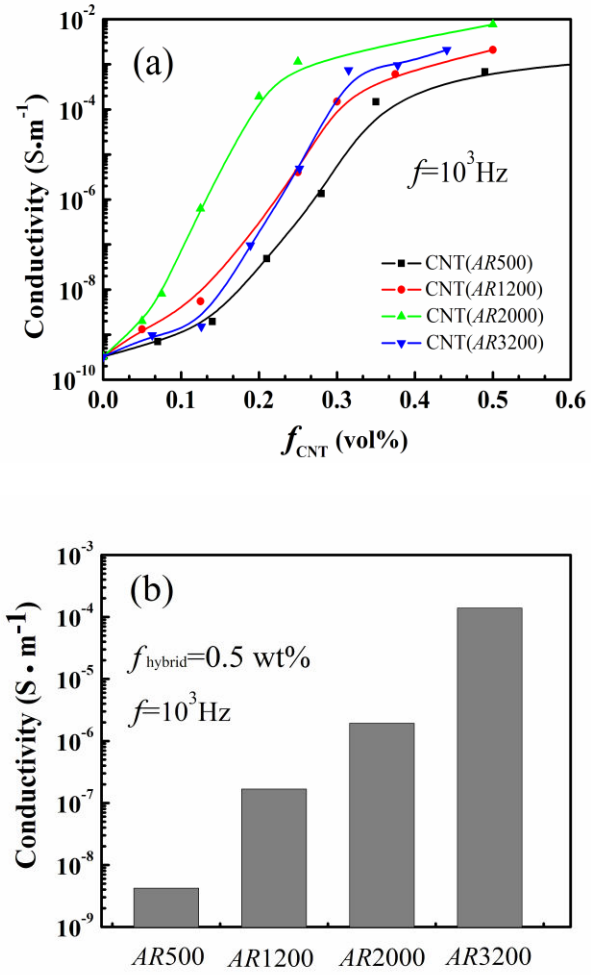

Fig.2-7 *(a) The influence of CNT aspect ratio on the conductivity of the composites with different hybrid concentrations at f=10^3 Hz; (b) The influence of CNT aspect ratio on the conductivity of the composites with the same hybrid concentration (0.5 wt.%) at f=10^3 Hz.*

As shown in Fig. 2-8, the mass change of CNTs in each kind of hybrids was recorded and presented from the TGA curves. The oxidation of CNTs always begins at about 450 °C and ends at about 550 °C. The abrupt mass drop in this range could give the mass fraction of CNTs in the various hybrids. We can see from Fig. 2-8b that the relationship between the aspect ratio and CNT concentration in the hybrids is obviously monotonous. With increasing the CNT aspect ratio, the concentration of CNTs in the hybrids also increases.

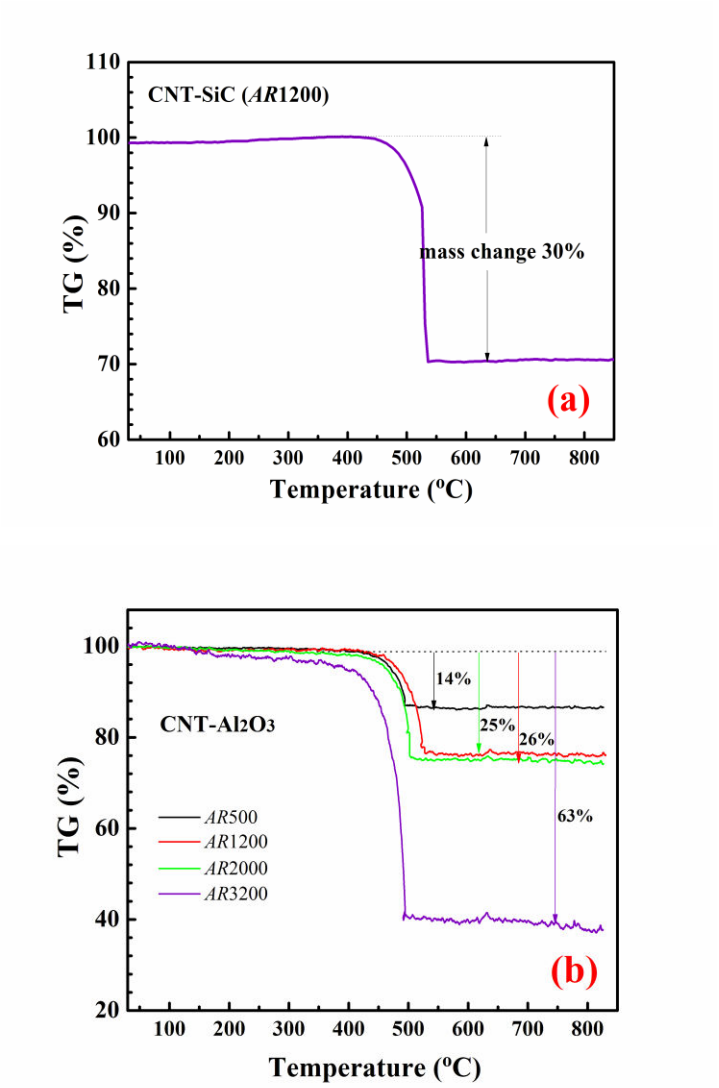

Fig.2-8 *Thermogravimetric analysis (TGA) of the various CNT-microparticle nano/micro hybrids.*

2.5. Tensile properties of the epoxy nanocomposites

2.5.1. Tensile properties of the hybrids reinforced epoxy nanocomposites

In order to demonstrate the superiority of the nano/micro hybrids fillers on improving the mechanical performance of the composites, the multi-scale hybrids and traditional fillers reinforced epoxy nanocomposites were respectively investigated. As previously reported, the mechanical properties of epoxy composites with 0.5 *wt.%* filler (SiC microparticles with or without CNTs grown) were investigated [52]. Compared to neat epoxy, there was no obvious improvement in mechanical properties of the SiC/epoxy composites and their fracture strain

was greatly reduced. However, the CNT-SiC hybrids provide an evident improvement on the mechanical properties. The elastic modulus and tensile strength of their composites were significantly enhanced and the fracture strain was also higher than the SiC/epoxy composites. The CNT-SiC hybrids could improve the interfacial properties between the SiC particles and epoxy matrix and the stress is efficiently transferred from the reinforcements to the matrix through the excellent interface during tensile loading. Therefore, the CNT-SiC hybrids have been considered to be one of the ideal candidates on improving the mechanical properties of the composites.

Graphene nanoplatelets composed of multi-graphene layers have emerged as promising fillers in the polymer composites due to their extremely high aspect ratio, unique graphitized plane structure and low manufacturing cost. The larger surface area can increase the contact area with the polymer matrix, maximizing the stress transfer from the polymer matrix to the fillers. Therefore, they are expected to exhibit better reinforcement than CNTs. However, the larger surface area between the planar nanosheets results in large Vander Waals forces and strong π-π interactions. The aggregation and inter-planer stacking of the nanosheets will limit the composite performance. Thus, their dispersion in the polymer is still a challenging task. The idea of using hybrid filler comprised of GNPs and CNTs has already been explored. It was demonstrated that the improved composite performance can be achieved by combining the advantages of the GNPs and CNTs [195]. Unlike the simple mixture of the GNPs and CNTs, it is required to achieve the essential connection between them, and especially the optimal CNT distribution and orientation in the matrix. Hence, the CNT-GNP hybrids with CNTs vertically grown on the opposite surfaces of the GNPs are expected to be utilized as reinforcements for the composites.

Fig. 2-9 illustrates the typical stress-strain response of the baseline epoxy and their composites with the same concentration (0.5 *wt.%*) of CNTs, GNPs, CNT+GNP mixture and CNT-GNP hybrids under quasi-static tensile loading. Introducing such small amount of these reinforcements, the mechanical behavior of the composites apparently shows different levels of enhancing trend compared to that of baseline epoxy. It is obvious that the elastic modulus and ultimate tensile strength (UTS) of the CNT-GNP/epoxy nanocomposites are dramatically increased compared to the composites with other kinds of fillers.

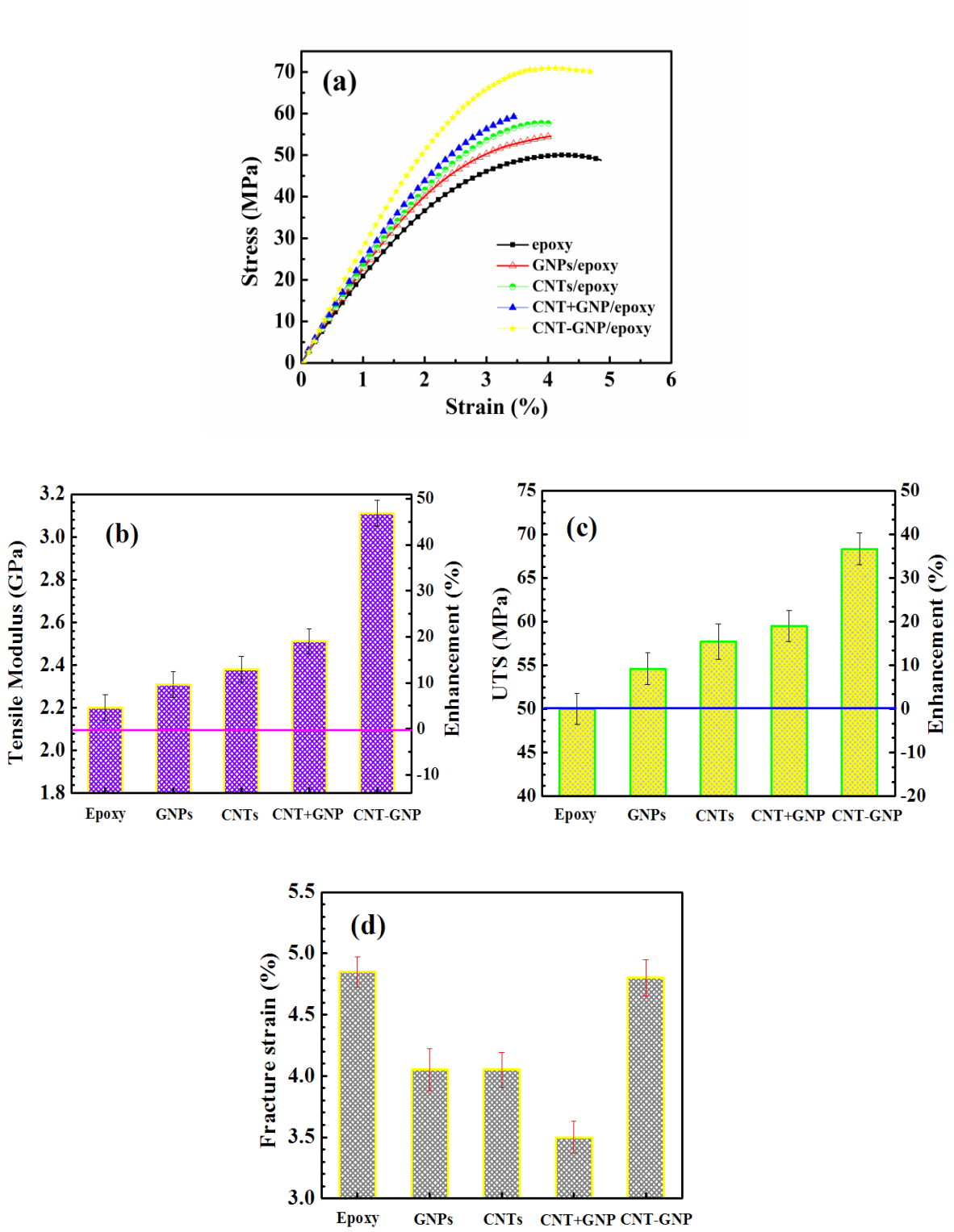

Fig.2-9 *Tensile properties of baseline epoxy and the epoxy composites with 0.5 wt.% reinforcements (a) Typical strain-stress curves; (b) Tensile modulus; (c) Ultimate tensile strength; (d) Fracture strain.*

Toward determining the statistics of the tensile modulus, UTS and fracture strain of the composites, between three to five samples for each kind of composite are tested under the same condition. The results of the tensile properties of baseline epoxy and their composites are summarized in Fig. 2-9b ~ d. The tensile modulus of the CNT-GNP/epoxy composite is up to about 3GPa and shows ~40% increase compared to that of pristine epoxy. However, there are only moderate enhancements of the tensile modulus for the CNTs/epoxy (~8%), GNPs/epoxy (~5%) and CNT+GNP/epoxy (~14%) nanocomposites. The variation tendency of the tensile strength in these composites is similar to that of tensile modulus. The tensile strength of the CNT-GNP/epoxy nanocomposites also acquires significant enhancement (+36%) compared to other kinds of composites. The lower improvement of the tensile modulus and tensile strength in the epoxy composites reinforced with CNTs, GNPs or CNT+GNP may be attributed to the waviness of pristine CNTs and the stacking behavior of GNPs arising from their large aspect ratio and van der Waals force. It is generally accepted that CNT orientation is a key parameter for the mechanical properties of the composites. The rotation of graphene substrate and the orientation of aligned CNT bundles gradually appear with the increase of strain, which potentially leads to the rearrangement of CNT networks. This rearrangement behavior possibly inhibits the rapid growth of the emerging microcracks and some mechanical energy could be dissipated during this rearrangement process. Besides, it could weaken the stress concentrations to a certain extent. All of these factors may account for the increase of toughness and fracture strain in the CNT-GNP/epoxy composites.

SEM images of the fracture surfaces of epoxy composites are presented in Fig. 2-10. Fig. 2-11 schematically depicts the distribution of the reinforcements in the epoxy matrix. Most of the tortuous CNTs are individually separated and randomly distributed within the epoxy matrix (see Fig. 2-10a). As shown in Fig. 2-10b, some GNPs are non-uniformly dispersed and aggregated in the matrix. It indicates that CNTs are much easier to be dispersed than GNPs. That is because the van der Waals forces resulted from the plane-to-plane contact of the adjacent GNPs may be stronger than that of CNTs. Besides, the GNP agglomerates lead to the formation of defects or flaws in the matrix, possibly limiting their reinforcement effect on the composite mechanical properties. Compared to the GNPs/epoxy composite, it seems that better dispersion of GNPs is obtained in the CNT+GNP mixture reinforced composite

(Fig. 2-10c). Therefore, the incorporation of CNTs has great influence on the dispersion of GNPs in the matrix, which has been explained by the synergetic effect of the CNTs and GNPs. In the case of the CNT-GNP hybrids reinforced composite, the original architecture of the hybrids is retained (Fig. 2-10d). With the help of GNPs, the highly dispersed CNTs as well as uniform CNT networks are achieved in the matrix. These factors could lead to larger contact area and better interaction between CNTs and the matrix. Besides, the CNT bundles grown on the GNP surface could inhibit the plane-to-plane aggregations of GNPs and the GNP/matrix interfacial properties are also improved. As a result, it is expected that the mechanical properties of the composites could be significantly enhanced by addition of the CNT-GNP hybrids. Moreover, the slippage of the overlapped GNPs is also considered to appear during tensile loading. It is well known that a high degree of load transfer from the reinforcement to matrix is an important issue for the improvement of elastic modulus and strength.

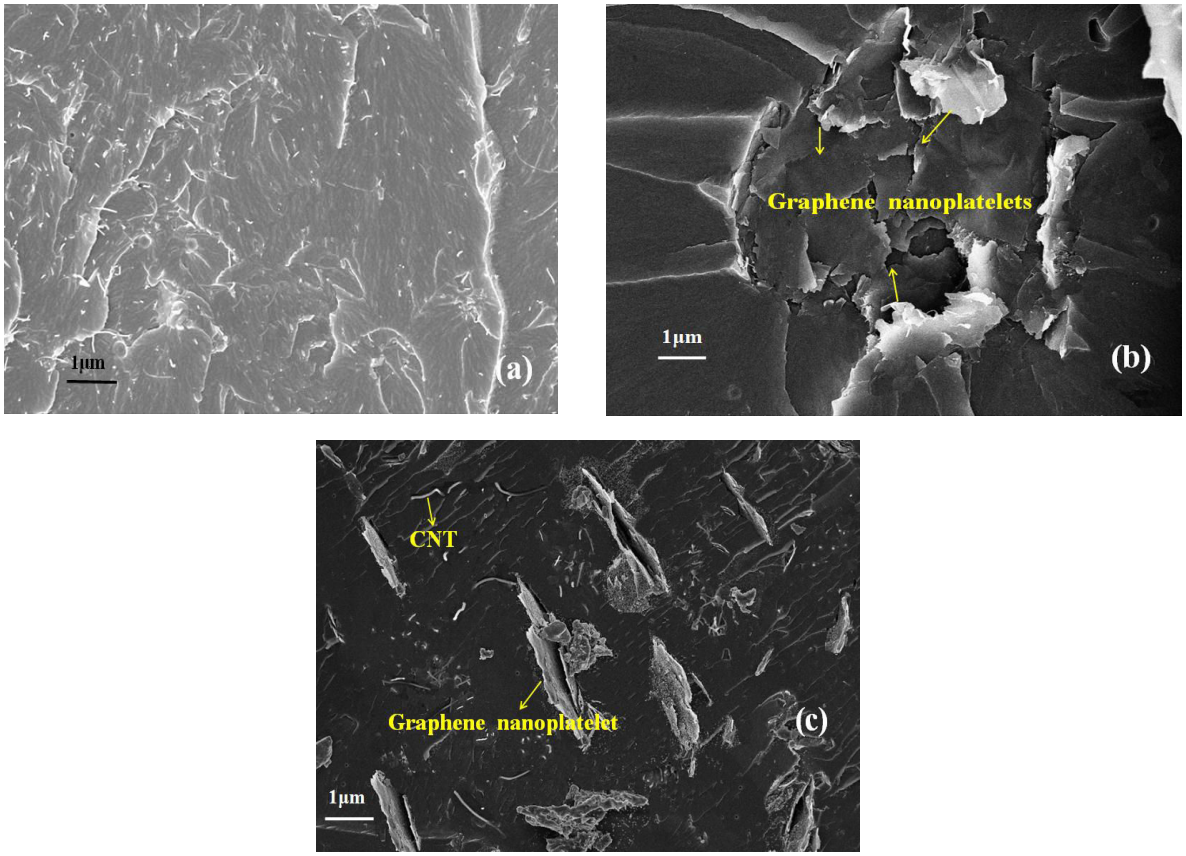

Fig.2-10 *SEM micrographs of the fractured surface of the epoxy composites with 0.5 wt.% reinforcements (a) CNTs; (b) GNPs; (c) CNT+GNP mixture.*

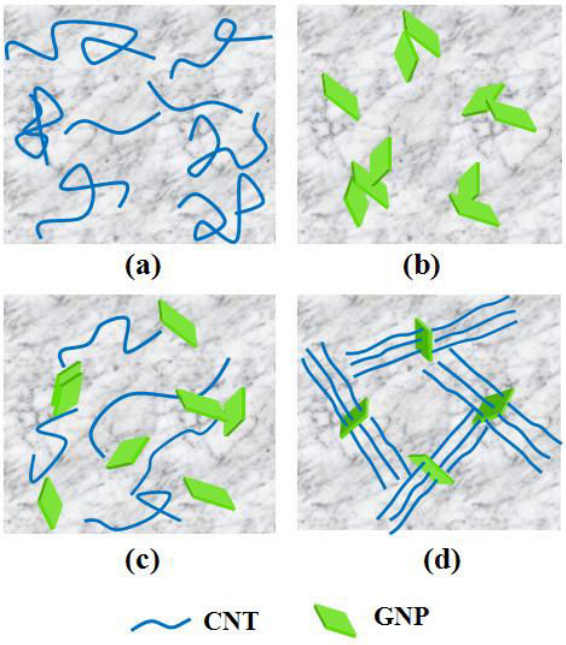

Fig.2-11 *Schematic images of the reinforcement dispersion in the epoxy composites (a) CNTs; (b) GNPs; (c) CNT+GNP mixture; (d) CNT-GNP hybrids.*

However, the adverse factors of CNTs and GNPs may restrain the stress transfer, limiting the reinforcement efficiency. Aside from the tensile modulus and strength, the fracture strain of the baseline epoxy and their composites is shown in Fig. 2-9d. The fracture strain of the CNT-GNP/epoxy composite is almost the same as that of neat epoxy, which is different from the CNTs, GNPs or CNT+GNP mixture reinforced composites with much lower fracture strain. In the case of poor dispersion of the reinforcements, the formation of nano or micro flaws results in local stress concentration in the matrix. The brittleness and ultimate failure of the composites isprobably caused by these voids and defects resulted from the GNP and CNT agglomerations. On the basis of the experimental results and analysis mentioned above, it could be inferred that the CNT-GNP/epoxy composite demonstrates better stiffness as well as toughness than other kinds of composites. The reinforcement effect is generally a complex issue involving the load transfer, stress concentration and defect distribution. Some explanations are proposed to reveal the underlying reinforcing mechanism of the CNT-GNP hybrids with distinctive architecture. First, the perfectly dispersed CNTs grown on GNPs could not only form uniform CNT networks but also inhibit the stacking and aggregation of GNPs. This three-dimensional hybrid structure leads to the larger surface contact and strong

molecular coupling between CNTs and the matrix. It is possible that the excellent interfacial interaction between the CNT networks and surrounding polymer matrix plays an important role on the effective stress transfer. Second, the aligned CNTs can be viewed to retain in the epoxy matrix at their actual lengths instead of curly state for optimizing their reinforcement efficiency. Third, the uniform dispersion of the CNTs and GNPs is not conducive to the formation of flaws, which is very important for stress transfer from the reinforcements to the matrix. Fourth, the orientation of the CNT grown on GNPs are much more difficult than the randomly orientated CNTs under low strain because of their stable junctions with graphene substrate and excellent molecular couplings with the polymer chains, which could give a good explanation to the higher elastic modulus in the CNT-GNP/epoxy composites.

Our experimental results of the tensile modulus are compared with the calculated values based on empirical formulas. The well-established Halpin-Tsai equation can be utilized to predict the tensile modulus of the unidirectional or randomly distributed fibers reinforced composites [194]. In our calculation, CNT was considered as discontinuous fiber and GNP was assumed as effective rectangular solid fiber. Considering both random orientation and unidirectional dispersion of the CNTs and GNPs in the composites, the Halpin-Tsai equation could be rewritten as follows:

$$E_{rand} = \left[\frac{3}{8} \frac{1 + 2(l_{NT} / d_{NT}) \eta_L V_{NT} + (2l_{GN} / 3w) \varsigma_L V_{GN}}{1 - \eta_L V_{NT} - \varsigma_L V_{GN}} + \frac{5}{8} \frac{1 + 2\eta_T V_{NT} + 2\varsigma_T V_{GN}}{1 - \eta_T V_{NT} - \varsigma_T V_{GN}} \right] \times E_M \quad 2\text{-}6$$

$$E_{paral} = \left[\frac{1 + 2(l_{NT} / d_{NT}) \eta_L V_{NT} + (2l_{GN} / 3w) \varsigma_L V_{GN}}{1 - \eta_L V_{NT} - \varsigma_L V_{GN}} \right] \times E_M \quad 2\text{-}7$$

$$\eta_L = \frac{(E_{NT} / E_M) - 1}{E_{NT} / E_M + 2(l_{NT} / d_{NT})} \quad 2\text{-}8$$

$$\eta_T = \frac{(E_{NT} / E_M) - 1}{(E_{NT} / E_M) + 2} \quad 2\text{-}9$$

$$\varsigma_L = \frac{(E_{GN} / E_M) - 1}{E_{GN} / E_M + (2l_{GN} / 3w)} \quad 2\text{-}10$$

$$\varsigma_T = \frac{(E_{GN} / E_M) - 1}{(E_{GN} / E_M) + 2} \quad 2\text{-}11$$

In this modified Halpin-Tsai model, E_{rand} and E_{paral} represents the tensile modulus of the composites with randomly oriented and unidirectionally distributed fillers, respectively. E_{NT}, E_{GN} and E_M are the tensile modulus of CNT, GNP and epoxy matrix. l_{NT}, d_{NT}, l_{GN} and w

is the average CNT length and diameter, GNP length and thickness, respectively. The values of these related parameters are listed in Table 2-4. The tensile modulus of the composites based on the two presumed dispersion of CNTs and GNPs are calculated and compared with our experimental data in Table 2-5.

Table 2-4

The values of related parameters of CNT, GNP and epoxy matrix

Materials	Tensile modulus	Length(μm)	Diameter/Thickness	Density (g/cm^3)
CNT	450GPa[a]	~13μm	~13nm	1.78
GNP	1.0TPa[b]	~30nm[c]	~3[c]μm	2.25[c]
Epoxy	2.2GPa[d]			1.1[c]

[a] According to Rafiee et al. [199] [b] According to Zhao et al. [194] [c] According to the values provided by the companies.
[d] According to our experimental results.

Table 2-5

Tensile modulus (E) as calculated using Halpin-Tsai equation and measured from tensile tests

Systems	E_{rand} (GPa) by Halpin-Tsai	E_{paral} (GPa) by Halpin-Tsai	E (GPa) experimental data	Comparison
CNTs/epoxy	2.71	3.51	2.36	$E_1 < E_{rand1} < E_{paral1}$
GNPs/epoxy	2.32	2.52	2.26	$E_2 < E_{rand2} < E_{paral2}$
CNT+GNP/epoxy	2.51	2.99	2.45	$E_3 < E_{rand3} < E_{paral3}$
CNT-GNP/epoxy			3.11	$E_4 > E_{paral3} > E_{rand3}$

The experimental values of the tensile modulus of the CNTs/epoxy, GNPs/epoxy and CNT+GNP/epoxy composites are generally lower than their values calculated using the Halpin-Tsai equation. However, the experimental tensile modulus of the CNT-GNP/epoxy composite is found to outperform that of the CNT+GNP/epoxy composite predicted using the Halpin-Tsai modeling. Hence, high reinforcing effectiveness is achieved by introduction of CNT-GNP hybrid as reinforcement. In this case, the uniform dispersion of CNTs and

GNPs mainly contributes to the higher tensile modulus. In addition, it can be considered that better synergetic effect between CNTs and GNPs is established on improving the mechanical properties of the composites.

However, it is difficult to calculate the tensile modulus of the CNT-GNP hybrids based composites using this equation because the modulus of the hybrids is unknown. Based on the dispersed morphologies of the hybrids in the matrix, the CNT-SiC, CNT-GNP hybrids and the CNT-Al_2O_3 (AR3200) can be considered as bundle like structures. The CNT-Al_2O_3 hybrids with AR 500, 1200, 2000 can be regarded as the spherical particles. To predict the reinforcing effect of these hybrids, the following Guth -Gold-Smallwood (GGS) equation was put forward which deals mainly for the static and dynamic moduli: [200-202]

$$E = E_m\left[1+0.67\alpha f+1.62(\alpha f)^2\right] \qquad 2\text{-}12$$

where, E is tensile modulus of the composites, E_m is the matrix's tensile modulus, f is the volume fraction of filler and α is a shape factor that allows the application of the equation to non-spherical fillers, particularly when the fillers are either platelet like structure or rod like structure. This equation is more commonly applied to understand the degree of dispersion of various nano-structured anisotropic fillers. The tensile modulus of the hybrids reinforced composites are calculated and compared with our experimental data in Table 2-6. It can be seen that the experimental values of the tensile modulus are generally higher than the values calculated using the GGS equation.

Table 2-6

Tensile modulus of the hybrids reinforced composites as calculated using the GGS equation and measured from tensile tests

Composites with hybrids	α	f_{hybrid} (*vol.%*)	Calculated E (GPa)	Experimental E (GPa)
CNT-GNP (1200)	4	0.15	2.21	3.1
CNT-SiC (1200)	3	0.13	2.21	2.3
CNT-Al_2O_3 (500)	1	0.667	2.21	2.4
CNT-Al_2O_3 (1200)	1	0.368	2.20	2.6
CNT-Al_2O_3 (2000)	1	0.185	2.20	2.8
CNT-Al_2O_3 (3200)	8	0.179	2.22	2.5

2.5.2. Effect of the hybrid content on tensile properties of the nanocomposites

Based on the discussions above, it has been well established the CNT-microparticle nano/micro hybrids could enable their utilization as high-performance structural additives for improving the mechanical performance of the composites. In this part, the influence of the hybrid content on the mechanical properties of epoxy composites will be investigated. In order to determine the statistics of the tensile modulus, tensile strength and fracture strain of the composites, five specimens of every kind of samples are tested under the same condition.

2.5.2.1. Tensile properties of the CNT-GNP/epoxy nanocomposites

Fig. 2-12 displays the influence of CNT-GNP hybrid concentration on the mechanical performances of epoxy nanocomposites. Fig. 2-12a depicts the typical stress-strain curves of the baseline epoxy and their composites with varying weight fractions of CNT-GNP hybrids under quasi-static tensile loading. The curves show evident non-linear relationship between the stress and strain before reaching the maximum stress, but no obvious yield point could be found in the curves. In order to have a better view of the reinforcement effect of the hybrids, the experimental results of the tensile properties of baseline epoxy and their composites as function of the CNT-GNP contents are summarized in Fig. 2-12b ~ d. When $f_{CNT\text{-}GNP}$ reaches 0.5 *wt.%*, the strengthening effect has been notable. The tensile modulus of the composites is nearly up to 3GPa, which reveals the greatest improvement (~ 40%) compared to that of pure epoxy. With further increasing the CNT-GNP content, the tensile modulus unfortunately begins to degrade. The tensile strength of the composites shows the similar trend, acquiring the highest enhancement of ~36% at $f_{CNT\text{-}GNP}$=0.5 *wt.%* (Fig. 2-12c).

In addition to the tensile strength and modulus, we also compared the ductility (fracture strain) and toughness (energy absorbed at failure) of the baseline epoxy and their composites. As demonstrated in Fig. 2-12d, at low hybrid concentration, there is no obvious decrease of the fracture strain in the composites. In general, for the epoxy matrix, the 10 ~ 15% loss in ductility could be tolerated provided that other mechanical properties such as modulus and strength are enhanced. When the hybrid content is up to 1 *wt.%* or more, the fracture strain is found to be distinctly decreases. In this case, the CNT-GNP/epoxy composites demonstrate

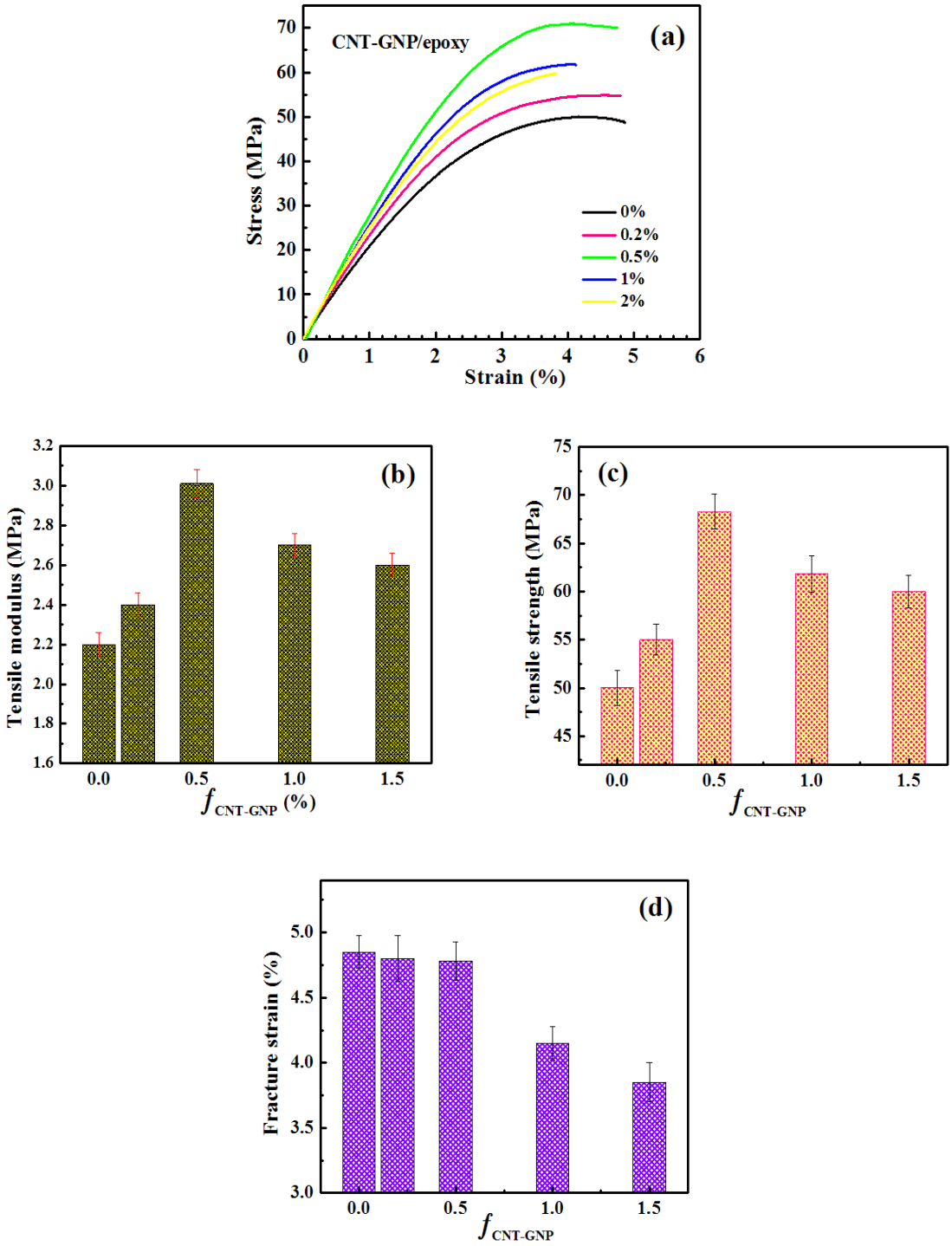

Fig.2-12 *Tensile properties of baseline epoxy and the epoxy composites with varying weight fractions of CNT-GNP hybrids (AR1200), (a) Typical strain-stress curves; (b) Tensile modulus; (c) Tensile strength; (d) Fracture strain.*

lower ductility than the baseline epoxy. Because of the non-linear stress-strain behavior, it is difficult to calculate the absorption energy from the typical tensile curves (Fig. 2-12a) during the fracture process. The total area under the stress-strain curves can be used to characterize the absorption energy before the emergence of facture, and then we can judge the composite toughness. From Fig. 2-12a, it can be seen that, as the CNT-GNP content increases from 0.2 *wt.%* to 0.5 *wt.%*, the areas under the stress-strain curves clearly increase, implying that the composite toughness is moderately improved owing to the introduction of CNT-GNP hybrids. However, when $f_{CNT\text{-}GNP}$ is up to 1 *wt.%*, their toughness is obviously reduced. The reduced ductility may be caused by the stress concentration resulted from the hybrid fillers. This phenomenon typically occurs when hard fillers are incorporated into a brittle matrix. Besides, the higher hybrid content possibly leads to defects in the matrix, which serves as seed points for crack initiation and premature fracture.

2.5.2.2. Tensile properties of the CNT-SiC/epoxy nanocomposites

Fig. 2-13 shows the influence of CNT-SiC concentration on the tensile properties of the CNT-SiC/epoxy nanocomposites. The typical stress-strain response of the pristine epoxy and their composites containing 0.2, 0.6, 0.7, 0.9, 1.0 *wt.%* CNT-SiC reinforcements are depicted in Fig. 2-13a. The relationship between the tensile modulus, tensile strength, fracture strain of the composites and the hybrid concentration are plotted in Fig. 2-13b ~ d. When $f_{CNT\text{-}SiC} <$ 0.7 *wt.%*, the strengthening effect is not remarkable at low CNT-SiC concentration. With increasing the CNT-SiC content, the tensile modulus and strength consistently increase. When $f_{CNT\text{-}SiC}$ is close to 0.7 *wt.%*, the reinforcement effect of the CNT-SiC hybrids reaches the maximum value. The average tensile modulus rises from ~ 2.16 GPa of neat epoxy to ~ 2.64 GPa of the 0.7 *wt.%* CNT-SiC reinforced epoxy composite, namely, ~ 22% increment. Similarly, the average tensile strength increases from ~ 45 MPa of the pure epoxy matrix to ~57 MPa, a rise scope of ~ 27%. Then further increase of the hybrid concentrations would cause the decrease in the tensile strength and modulus of the composites. At much higher hybrid content, the tensile properties of the CNT-SiC/epoxy composites are even lower than that of pure epoxy. This variation trend is almost the same as that of the CNT-GNP/epoxy system. Moreover, it is found that the fracture strain in this system is much lower than the

pure epoxy with the addition of the CNT-SiC hybrids (Fig. 2-13d). And evident loss of the ductility and toughness is observed with the introduction of CNT-SiC hybrids.

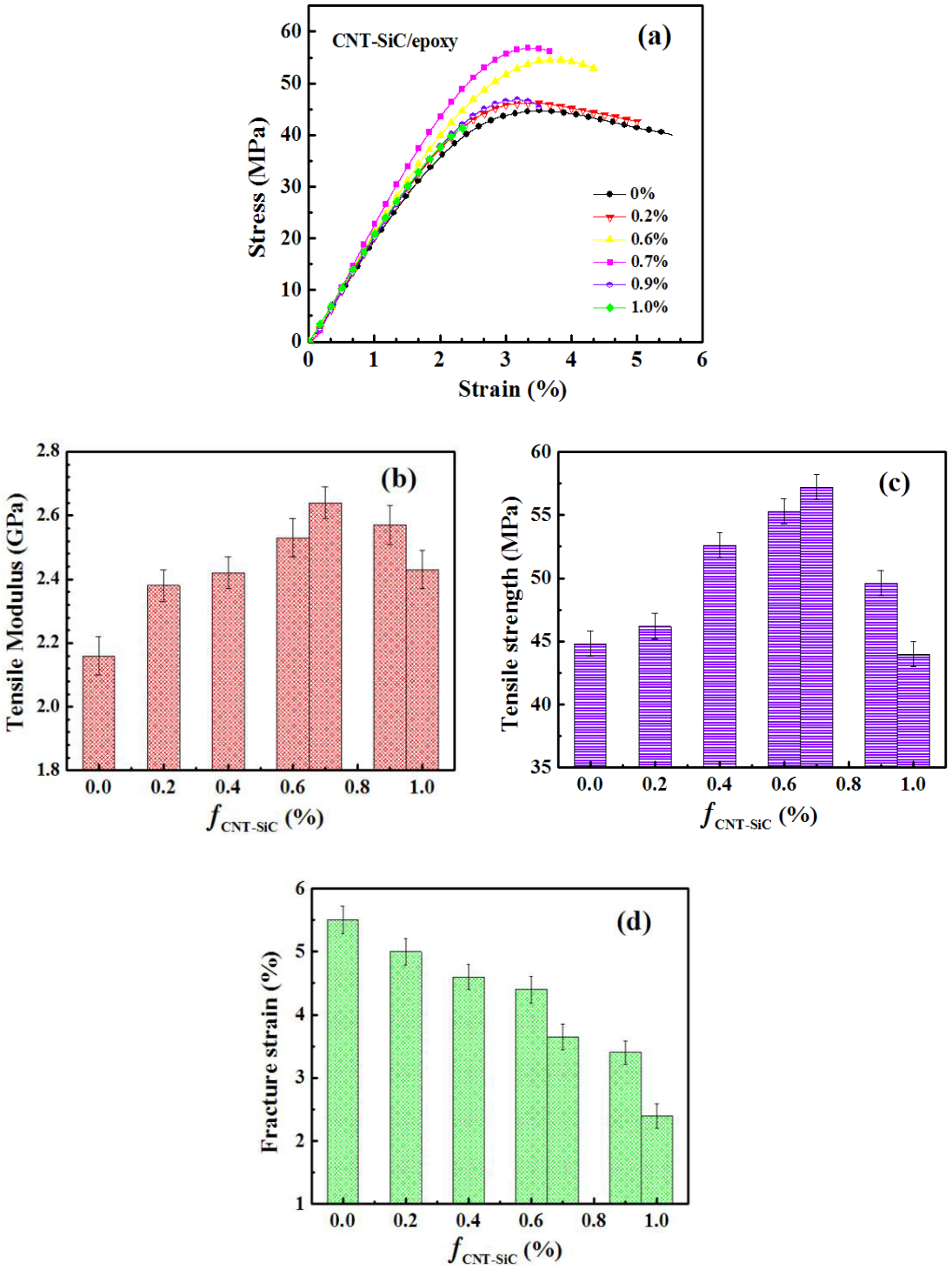

Fig.2-13 *Tensile properties of baseline epoxy and the epoxy composites with varying fractions of CNT-SiC hybrids (AR1200), (a) Typical strain-stress curves; (b) Tensile modulus; (c) Tensile strength; (d) Fracture strain.*

2.5.2.3. Tensile properties of the CNT-Al_2O_3/epoxy nanocomposites

Fig. 2-14 shows the influence of the concentration of CNT-Al_2O_3 hybrids with different aspect ratios (500, 1200, 2000 and 3200) on mechanical properties of the epoxy composites. From the typical stress-strain curves, we can see that the whole variation trend of the tensile modulus and strength as function of the CNT-Al_2O_3 content in the four systems is nearly the same as that of the CNT-GNP/epoxy and CNT-SiC/epoxy systems discussed above. The optimal loading of CNT-Al_2O_3 hybrids is found to exist in every system. And it is very close to the percolation threshold f_c mentioned above. Before f_c, the tensile modulus and strength continuously increase with the embedding of the hybrids. As f_{hybrid} approaches f_c, the results indicate that they approximately reach the maximum values. However, when $f_{hybrid} > f_c$, they begin to degrade with the hybrid loading. Moreover, as shown in Fig. 2-14, the composites based on the CNT-Al_2O_3 hybrids (*AR*500) exhibit more favorable ductility and toughness, compared to the other three systems with larger CNT aspect ratios (*AR*1200, 2000, 3200). A slight increase in the strain to failure was also observed in the CNT-Al_2O_3 (*AR*500) filled epoxy composites at 1 wt. % loading, compared to the neat epoxy. This phenomenon may be mainly contributed to their different dispersion states in the matrix, as illustrated in Fig. 2-5d ~ g.

With regard to the short CNTs, the well-aligned CNTs grown on the Al_2O_3 microparticle are more inclined to retain at their actual lengths in the matrix instead of curly state. This dispersion state is not conducive to the formation of flaws in the matrix. Besides, the unique three-dimensional architecture of the CNT-Al_2O_3 hybrids leads to large surface contact and strong molecular coupling between the CNTs and epoxy matrix. The CNTs are well wrapped by the host polymer, suggesting the existence of a very thin polymer layer embedded into the interspaces between any two aligned CNTs. This is helpful for achieving better wetting and adhesion strong interfacial interaction between CNTs and the matrix. It has been reported that the addition of CNTs with better CNT/polymer interfacial adhesion could increase the fracture energy because the crack propagation could be restrained by bringing up the crack faces of CNTs. Zhou *et al.* [194] reported that the crack propagation changes direction as it crosses CNTs during failure process due to bridge effect which prevents crack opening. As a

result, the crack initiation and propagation becomes more difficult in the system reinforced by CNTs than that without CNTs. It may be one of the reasons due to which the flexural strain to failure in the composites was increased. CNTs have a high aspect ratio and shows highly flexible elastic behavior during loading. Due to the strong interfacial bonding between this reinforcement and epoxy matrix, the composites exhibit higher absorption of energy. The increase in strain energy thus can be attributed to increase in strain to failure. Besides, it is worth noting that the CNT aspect ratio of the hybrids takes an important role on the mechanical properties of the composites. With increasing the aspect ratio, the required hybrid content is lowered to achieve better reinforcement effect.

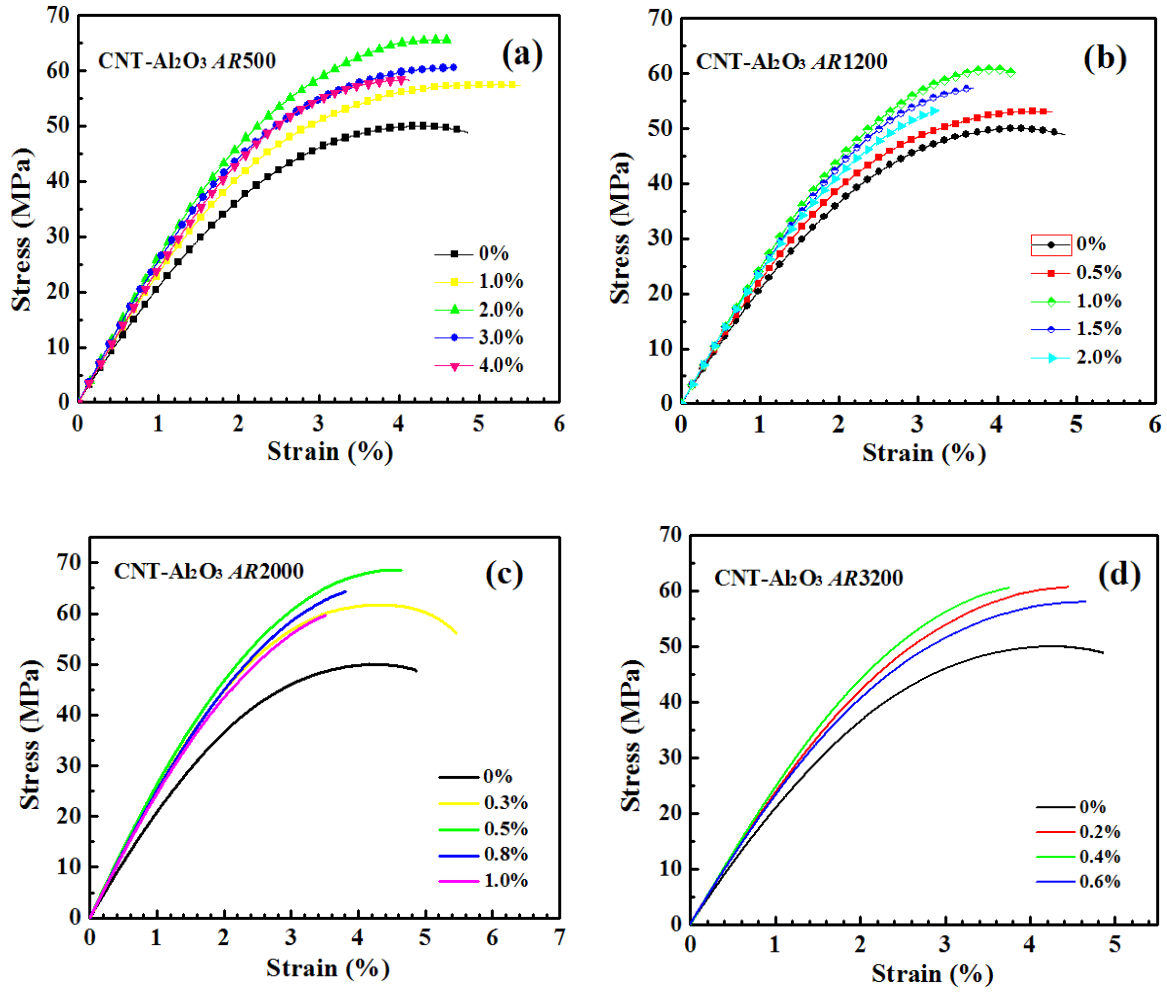

Fig.2-14 *Typical strain-stress curves of baseline epoxy and the epoxy composites reinforced with varying weight fractions of CNT-Al_2O_3 hybrids with different CNT aspect ratios, (a) AR500; (b) AR1200; (c) AR2000; (d) AR3200.*

The general variation trend of mechanical properties of the composites with the hybrids (CNT-GNP, CNT-SiC and CNT-Al_2O_3) can be explained as follows. The dispersion of CNTs and hybrids is more homogeneous at small concentrations. The uniformly dispersed fillers could restrict the mobility of polymer chains under tensile loading, resulting in improved tensile modulus and strength. However, concerning the decrease of mechanical properties at higher hybrid content, it is possibly contributed to the voids or other defects in the matrix. Besides, in this case, the modification of the crystalline section of the matrix considerably decreases the plastic range, which causes a decrease in ductility and an increase in brittleness. Moreover incorporation of higher loading of hybrids increased the viscosity of matrix which may have impeded the dispersion. Song *et al.* [203] stated that poorly dispersed CNTs within epoxy have a higher viscosity than that of uniformly dispersed suspensions. In addition, high viscosity of the resin resulting from poor CNT dispersion may cause poor wetting and adhesion between CNTs and the matrix. Thus, it could be concluded that the tensile properties of the CNT-Al_2O_3/epoxy nanocomposites show the sensitivity on the dispersion state of the hybrids.

In summary, the CNT-microparticle multi-scale hybrids could be used reinforcements in the composites. It is most often the case that mechanical properties of the hybrids reinforced composites degrade or become saturated after a peak when the hybrid content exceeds a certain value. As a result, the optimal concentration of the hybrid is necessary to achieve the desirable reinforcement effect. The varying threshold hybrid contents also depend on their type. Besides, for the same hybrid or CNT concentration, the mechanical properties of the composites are greatly dependent on the microsubstrates and CNT aspect ratio of the hybrids. This observation has a practical implication in that one can tailor the composite properties with an optimal hybrid content and desirable CNT aspect ratio and substrates depending on their applications with different property requirements.

2.5.3. Influence of the substrate and CNT aspect ratio of the hybrids on tensile properties of the composites

Concerning the CNT-GNP and CNT-SiC hybrids with the same CNT aspect ratio (1200), it is clearly seen that the substrates of the hybrids have some influence on the mechanical properties of the composites, as shown in Figs. 2-12 and 2-13. From the results indicated in Fig. 2-14, whatever the CNT aspect ratio, the most satisfactory reinforcement effect of the CNT-Al_2O_3 hybrids can be achieved at their optimal loading in every system. However, the hybrid content in each system has obvious difference. In this section, the influence of the substrate and CNT aspect ratio of the hybrids on mechanical performance of the composites will be discussed. Here the optimal concentration of hybrids where the preferable composite properties are acquired is listed in Table 2-7.

Table 2-7

The concentrations of CNT-Al_2O_3 hybrids in the epoxy composites with different CNT aspect ratios

[a] Materials	Φ_{hybrid} (*wt.%*)	Φ_{CNT} (*wt.%*)	Φ_{matrix} (*vol.%*)	Φ_{hybrid} (*vol.%*)
*AR*500-Al_2O_3	2.0	0.28	99.3	0.667
*AR*1200-Al_2O_3	1.0	0.25	99.6	0.368
*AR*2000-Al_2O_3	0.5	0.13	99.8	0.185
*AR*3200-Al_2O_3	0.4	0.25	99.8	0.197
*AR*1200-SiC	0.67	0.26	99.7	0.13
*AR*1200-GNP	0.5	0.28	99.7	0.15

[a] The epoxy composites based on the different hybrids will be identified as *CNT AR*-substrate.

The mechanical properties of the CNT-Al_2O_3/epoxy nanocomposites with different CNT aspect ratios are compared in Fig. 2-15. Table 2-8 summarizes the experimental results of the mechanical properties of the composites containing the hybrids with the same CNT aspect ratio (1200). Table 2-9 displays the experimental results of the CNT-Al_2O_3/epoxy composites with different CNT aspect ratios (500, 1200, 2000 and 3200). The neat epoxy matrix tensile modulus and strength are E_m = 2.2±0.1 GPa and σ_m=50.0±1.6 MPa. By introducing such

small amount of the hybrids, the composites show obvious enhancements of mechanical properties compared to the baseline epoxy.

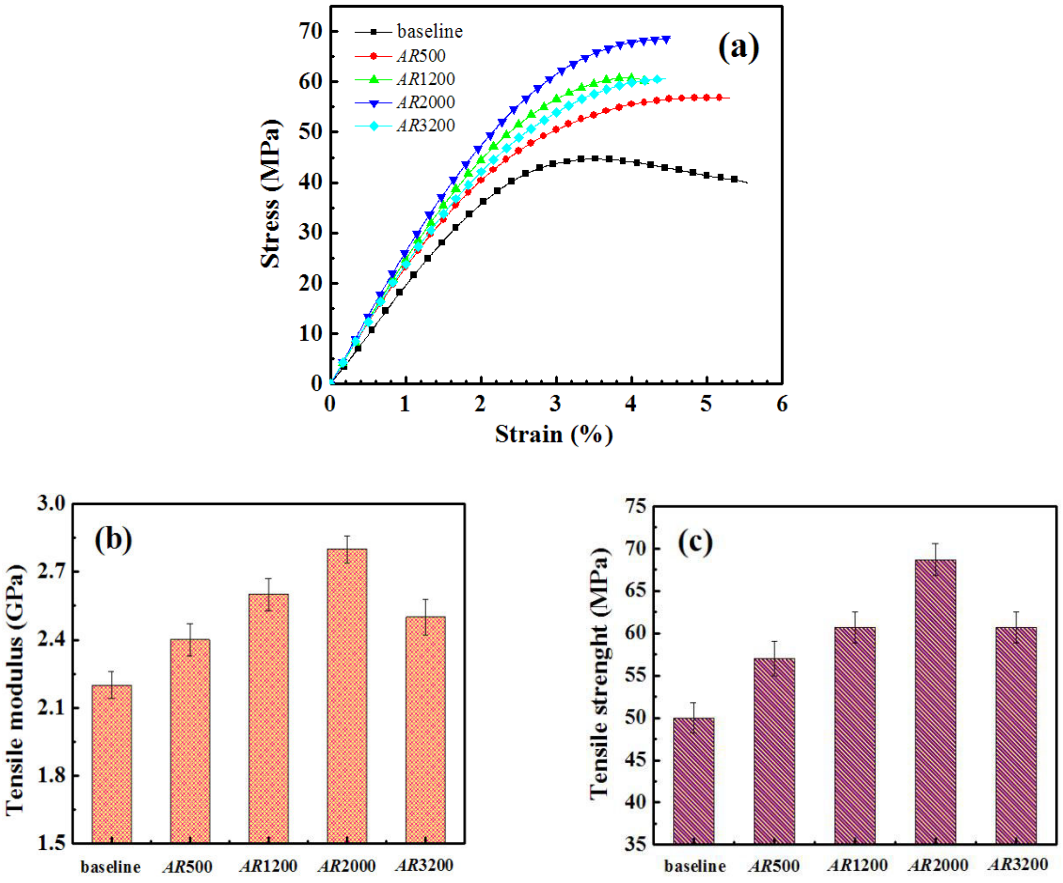

Fig.2-15 *Comparison of the mechanical properties of the CNT-Al_2O_3/epoxy composites with different CNT aspect ratios when $f_{hybrid} = f_c$ (a) Typical strain-stress curves; (b) Tensile modulus; (c) Tensile strength.*

The reinforcing mechanism of these hybrids could be explained as follows. First, the distribution states of the hybrid fillers in the matrix could restraint the CNT agglomeration. Second, their three-dimensional architectures give rise to larger contact surface and stronger molecular interaction between the CNTs and the matrix, resulting in an improved load transfer. Third, the alignment of CNTs in the hybrids retains their actual lengths in the matrix, enhancing their reinforcement efficiency. Fourth, the strong junction between the CNTs and the substrates makes CNT reorientation much more difficult under low strain, compared with the randomly distributed CNTs. This can explain the higher elastic modulus of the composites based on the hybrids.

Table 2-8

Comparison of the mechanical properties of the CNT-Al_2O_3/epoxy composites with different CNT aspect ratios

Materials	Tensile modulus (GPa)	Effective reinforcing modulus (GPa)	Tensile strength (MPa)	Effective reinforcing strength (MPa)
epoxy	2.2±0.1		50±2	
*AR*500-Al_2O_3	2.4±0.1	32±9	57±2	1099±240
*AR*1200-Al_2O_3	2.6±0.1	111±19	61±2	2955±462
*AR*2000-Al_2O_3	2.8±0.1	326±32	69±2	10143±918
*AR*3200-Al_2O_3	2.5±0.1	154±25	61±2	5476±1014

Table 2-9

Comparison of the mechanical properties of the epoxy composites based on different hybrids with the same CNT aspect ratio

Materials	Tensile modulus (GPa)	Effective reinforcing modulus (GPa)	Tensile strength (MPa)	Effective reinforcing strength (MPa)
*AR*1200-SiC	2.3±0.1	35±19	56±2	1995±518
*AR*1200- Al_2O_3	2.6±0.1	111±19	61±2	2955±462
*AR*1200-GNP	3.1±0.1	328±29	68±2	6679±652

As shown in Table 2-8, the mechanical properties of the composites are dependent on substrates of the hybrids. The tensile modulus and tensile strength in the CNT-GNP/epoxy composites are dramatically increased compared to the other hybrids reinforced composites. Their tensile modulus is up to 3GPa, corresponding to about 40 % increase compared to that of the pristine epoxy. However, only moderate enhancements of the tensile modulus are achieved in the other composites, ~4 % for CNT-SiC/epoxy, ~18 % for CNT-Al_2O_3/epoxy and ~9 % for CNT-SiC+CNT-Al_2O_3/epoxy. As presented in Table 2-9, the tensile modulus and tensile strength of the CNT-Al_2O_3/epoxy composites strongly depend on the CNT aspect ratios. With the increase of aspect ratio from 500 to 2000, the experimental tensile modulus

and strength show monotonically increasing trend. However, for the aspect ratio up to 3200, it is found that the mechanical properties of the composites unexpectedly decrease.

According to the simple Rule of Mixtures (ROM) for predicting the composite modulus and strength, the effective reinforcement modulus (E_{hy}) and strength (σ_{hy}) of the hybrids in the composites could be given as:

$$E_{hy} = \frac{E_c - E_m}{v_f} + E_m \qquad 2\text{-}12$$

$$\sigma_{hy} = \frac{\sigma_c - \sigma_m v_m}{v_f} \qquad 2\text{-}13$$

where, E_c, E_m, σ_c, σ_m, v_m and v_f are the composite tensile modulus, the matrix tensile modulus, the composite tensile strength, the matrix tensile strength, the matrix and the hybrid volume fraction, respectively. The results of E_{hy} and σ_{hy} for each system calculated from Eqs. 2-12 and 2-13 are also presented in Table 2-8 and 2-9.

It can be seen from Table 2-8 that the variation trend of E_{hy} and σ_{hy} with the hybrid substrate is similar to that of E_c and σ_c, respectively. For nearly the same weight ratio of CNTs with *AR*1200, the CNT-GNP hybrids offer the highest reinforcement effectiveness among the three hybrids. Their E_{hy} is as high as ~330 GPa, which is about three and nine times of that of CNT-Al_2O_3 and CNT-SiC, respectively. Their σ_{hy} is up to ~ 6600 MPa, corresponding to almost two and three times of that of CNT-Al_2O_3 and CNT-SiC, respectively. The more prominent enhancement of CNT-GNP hybrids lies in their superior mechanical properties, larger contact area with the matrix as well as the better synergistic effect of the perfectly dispersed GNPs and CNTs on the structural reinforcements. As shown in Table 2-9, the E_{hy} and σ_{hy} of the CNT-Al_2O_3 hybrids increase and then decrease with the CNT aspect ratio, as do the E_c and σ_c . The highest E_{hy} (320 GPa) and σ_{hy} (10^4 MPa) are obtained at *AR*2000. When the CNT aspect ratio is relative small, the aligned CNTs can retain their actual lengths in the matrix instead of curved state. In this case, the reorientation of short CNTs grown on Al_2O_3 is not easy to happen. However, with regard to *AR*2000, the reorientation of the aligned CNTs gradually appears with increasing the applied strain, which leads to the rearrangement of conductive networks. It has been demonstrated that the CNT reorientation is a key parameter for the mechanical properties of the composites, which

weakens the stress concentration. And this behavior can inhibit the rapid growth of emerging microcracks and dissipate certain mechanical energy during tensile loading. However, in the case of *AR*3200, this nominal aspect ratio of CNTs is not the same as their actual one in the composites because of the waviness of some CNTs. Besides, many adjacent CNTs form the CNT bundles which may introduce some flaws in the matrix. These are the reasons why the incorporation of the CNT-Al_2O_3 with too high CNT aspect ratios results in the decrease of the mechanical properties. Therefore, the hybrids with optimal aspect ratio and substrates are essential to achieve high performance composites.

2.6. Thermo-mechanical properties of the epoxy nanocomposites

Dynamic-mechanical properties of the composites were performed using a dynamic mechanical thermo-analyzer to study their mechanical properties as function of temperature. This analysis could determine a variety of fundamental material parameters like the storage modulus, loss modulus, glass transition temperature (T_g) and damping behavior (ratio of loss/storage modulus). Three point bending mode was used on the specimens. The storage modulus (E') and loss modulus (E'') of the samples were measured at the oscillation frequency of 1 Hz and collected automatically at the temperature ranging from 20 ^oC to 160 ^oC at a constant heating rate of 3 ^oC/min. E' represents the elastic behavior of materials and its value decreases with increasing temperature. In general, the E' curve can be divided into three phases. The glassy phase usually occurs at low temperature. Then a transition from the glassy to rubbery phase is characterized by a narrow temperature region in which a sharp increase in macromolecular fragment mobility occurs. After that, it is the rubbery phase at the high temperature.

2.6.1. DMA analysis of the hybrids reinforced epoxy composites

As shown in Fig. 2-16a and b, E' and loss factor (tan δ) were plotted as a function of temperature for baseline epoxy and their composites with the same weight fraction (0.5%) of CNTs, GNPs, CNT+GNP mixture and CNT-GNP hybrids. At low temperature all the samples show very high value of the elastic modulus, followed by one significant drop in the range of 60 ^oC to 100 ^oC due to the glass transition. In this temperature range the

corresponding tan δ curves also display a peak, indicating the glass transition temperature of the materials. It is clearly seen that the value of E' shows varying degrees of growth with the addition of these reinforcements. It is worth noting that, compared to other kinds of reinforcements, the introduction of CNT-GNP hybrids results in a more evident increment of E' both in the glassy and rubbery region as well as significant shift of glass transition of the CNT-GNP/epoxy composites. As shown in Fig. 2-16c, the value of E' for pure epoxy at 40 ^{o}C is about 3.7 GPa which increases up to ~5.0 GPa for the CNT-GNP/epoxy composites, i.e., the corresponding enhancement is around 37%. This may be attributed to the stronger interfacial interaction between the CNTs of the hybrids and the polymer matrix. As shown in Fig. 2-16b, with the addition of reinforcements, we can clearly see that T_g of the composites shifts to higher temperature, implying improved thermo-stabilities. The average T_g obtained from the typical tan δ ~ temperature curves has been plotted in Fig. 2-16d. Particularly, T_g was shifted from 82 ^{o}C for neat epoxy sample to 97 ^{o}C for 0.5 *wt.%* CNT-GNP concentration obtained from the peak of the glass transition temperature of the CNT-GNP/epoxy composites, and a maximum change of T_g is achieved. The origin of such T_g shifts has been attributed to the presence of so-called 'interphase' polymer, which arises due to the interaction of the chains with the filler surface. In our system, as discussed above about the dispersion state of the hybrids, most of the aligned CNTs are wrapped by the host polymer, suggesting the existence of a very thin polymer layer embedded into the interspaces between any two well-aligned CNTs. This is equivalent to a wetting polymer-particle interface, which is proposed to possibly influence T_g of the composites. The attractive interactions will restrict the mobility of the polymer chains. Percolation of this network of interphase polymer could then manifest the large T_g shift of the bulk composite. This T_g change also represents that the hybrids make strong interfacial bonding with the matrix, resulting in large free movement of the polymer chains to a large extent. It is well known that a relatively free movement of the polymer chains often affects the induce effect on T_g of the composites. This improvement of T_g is obviously due to the reduction of polymer chain mobility resulted from the increase of intermolecular interaction between CNTs and polymer chain molecules.

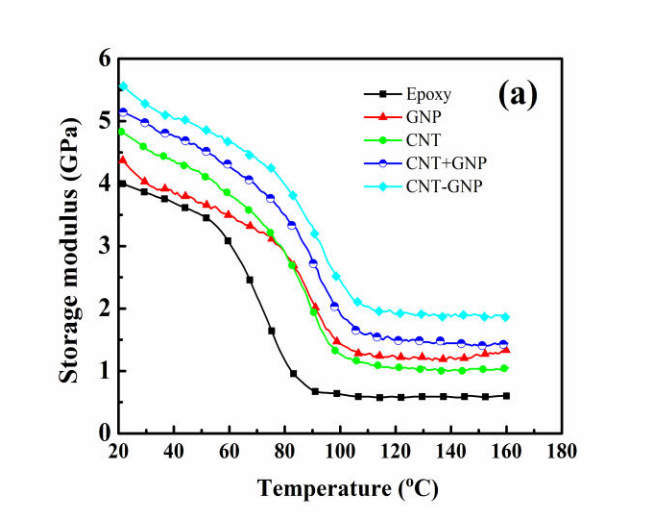

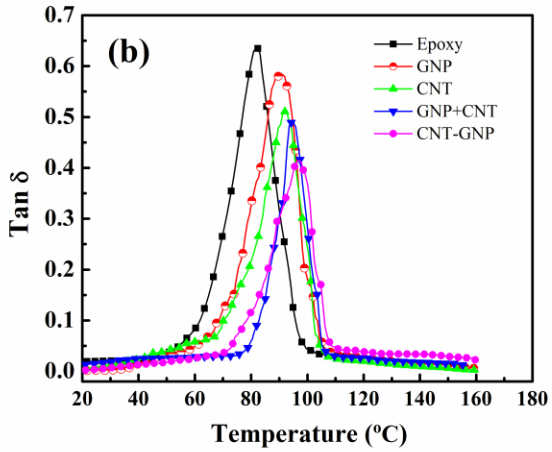

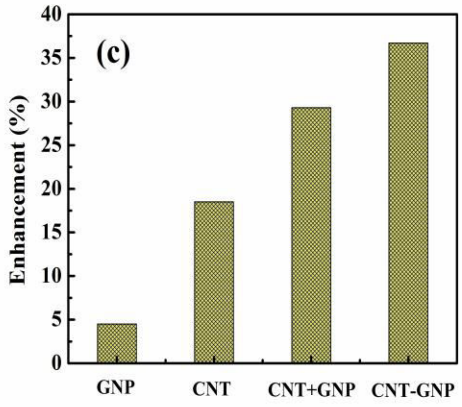

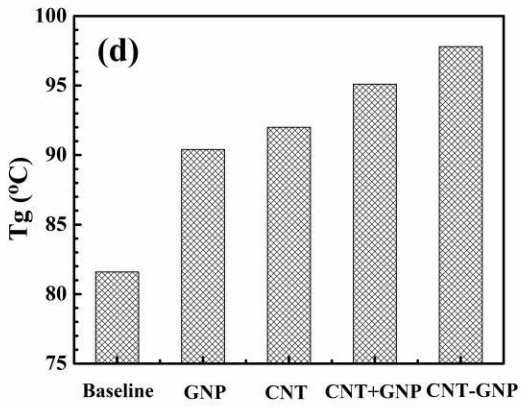

Fig. 2-16 *Thermomechanical analysis of the pure epoxy and epoxy composites from DMA results (a) Storage modulus vs. temperature; (b) Loss factor (tan δ) vs. temperature; (c) Enhancement of the storage modulus compared to pure epoxy at 40°C;(d) Glass transition temperature (T_g).*

2.6.2. The influence of CNT aspect ratio on DMA behavior of the composites

In order to investigate the effect of CNT aspect ratio on thermomechanical properties of the CNT-Al_2O_3 hybrids reinforced epoxy composites. The variation of E' and tan δ as a function of temperature in dynamic measurements is presented in Fig. 2-17a and b. Fig. 2-17c and d shows the mean E' enhancement and glass transition temperature obtained from the DMA experiments. These results indicate that E' of the CNT-Al_2O_3/epoxy composites are increased substantially relative to neat epoxy, and T_g are shifted to higher temperature.

Besides, the E' and T_g are dependent on the CNT aspect ratio of the hybrids. As shown in Fig. 2-17a and c, the storage modulus of the composites in the glassy and rubbery regions was increased upon incorporation of CNT-Al_2O_3 hybrids with AR from 500 to 2000, and then begins to decrease with further increasing AR up to 3200. Likewise, the largest shift of glass transition temperature could be observed at AR=2000. And then the incremental changes in T_g is reduced with further increase of AR. This variation trend is consistent with the results from tensile testing discussed above. And the similar mechanisms related to the hybrids can account for this phenomenon. For the CNTs with relatively smaller aspect ratio, the aligned CNTs hen the CNT aspect ratio is relative small, the aligned CNTs are more inclined to retain at their actual lengths in the matrix. And Al_2O_3 microparticles are surrounded in the center by the CNTs. With increasing the CNT aspect ratio up to 3200 or more, some of the CNTs may exist as the curved state and Al_2O_3 particles are wrapped at the end by CNTs and the hybrids exist like bundles in the composites. In this case, the nominal CNT aspect ratio is not the same as their actual one in the composites due to their waviness. Besides, this dispersion state more easily introduces the defects between the adjacent CNTs in the matrix. The improvement in thermo-stability of the composites is closely related to the reduction in mobility of the matrix around the CNTs by interfacial interactions. Because this interaction induces different cross-linking regions in epoxy matrix which will eventually reduce the polymer chain motion, a strong shift of glass transition temperature in nanocomposites was observed. However, additionally, increases in the viscosity of the matrix by the addition of CNTs with too high aspect ratio could alter its flow behaviour both during impregnation as well as during the curing process, resulting in nanometer/micron scale porosities. This could

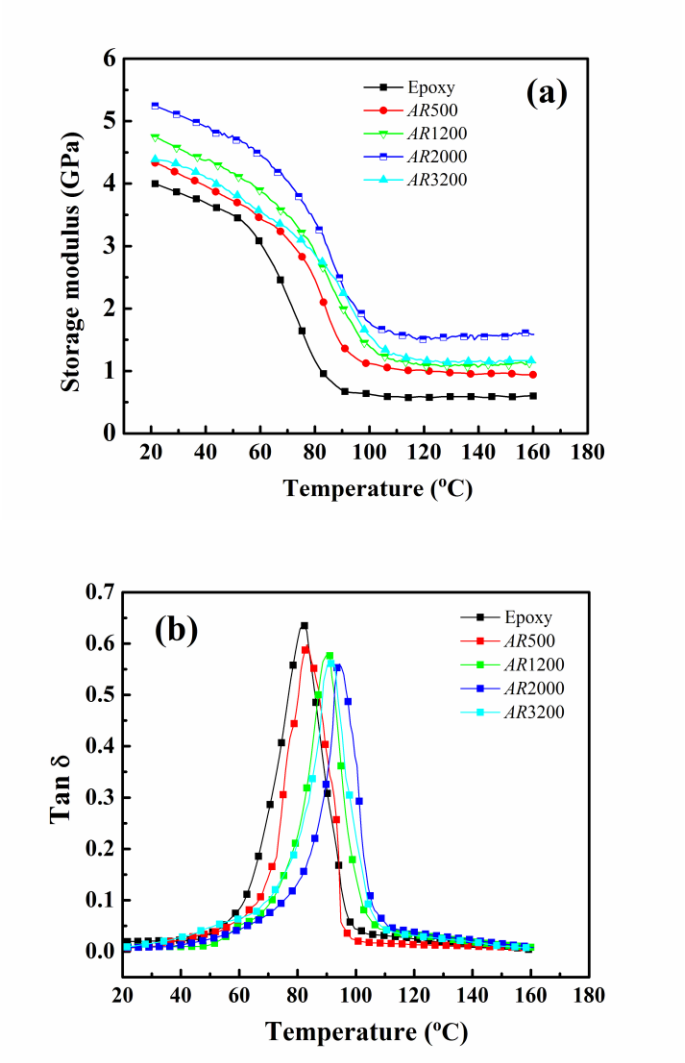

Fig. 2-17 *Influence of CNT aspect ratio on the thermomechanical properties of the CNT-Al_2O_3/epoxy composites (a) Storage modulus vs. temperature; (b) Loss factor (tan δ) vs. temperature; (c) Enhancement of the storage modulus compared to pure epoxy at 35°C;(d) Glass transition temperature (T_g).*

lead to an increase in free volume of the polymer molecules in the matrix allowing additional mobility of molecules possibly contributing to the unexpected onset of decrease in T_g of the CNT-Al_2O_3/epoxy composites at AR=3200.

2.7. Self-sensing behaviors of the epoxy nanocomposites

The CNT/polymer composites are increasingly being reviewed as a realistic alternative to conventional smart materials. Significant advances have been made in using CNT based polymer films as strain sensors. As compared to conventional sensors, higher sensitivity has been observed in these novel sensors. In general, the piezoresistivity observed in these strain sensors made from CNT/polymer composites can be mainly attributed to the variation of conductive networks with strain, such as loss of contact between the fillers, tunneling effect in neighbouring fillers and the conductivity change resulted from deformed CNTs. Recently, great interest has been generated in building highly sensitive strain sensors with randomly oriented CNTs. Besides, some studies have been focused on the aligned CNTs in the matrix. It was found that aligned CNT network resulted in improved electrical and piezoresistive sensing capabilities of the composites [91]. In this part, the varying self-sensing behaviors of the composites filled with *ran*-CNTs and the hybrids (CNT-GNP, CNT-SiC and CNT-Al_2O_3) will be comparatively investigated. The underlying mechanisms with relation to the substrates and CNT aspect ratios of the hybrids will be mainly discussed. The distinctive *in situ* sensing behaviors of the hybrids could offer great advantages for their potential applications.

2.7.1. Self-sensing behavior of the composites during quasi-static tensile tests

Fig. 2-18 ~ 2-20 demonstrates the typical stress-strain curves (solid lines) and the *in-situ* electrical resistance responses (dotted lines) of the epoxy composites with different fillers during quasi-static tensile loading until final fracture. Here, the filler concentration in each system is close to its percolation threshold, as listed in Table 2-3.

2.7.1.1. Self-sensing behavior of the epoxy nanocomposites with randomly distributed CNTs (ran-CNTs)

Fig. 2-18a and b demonstrate the self-sensing behavior of the composites containing the *ran*-CNTs and mechanical mixture of *ran*-CNTs and microparticles (Al_2O_3, SiC and GNP), respectively.

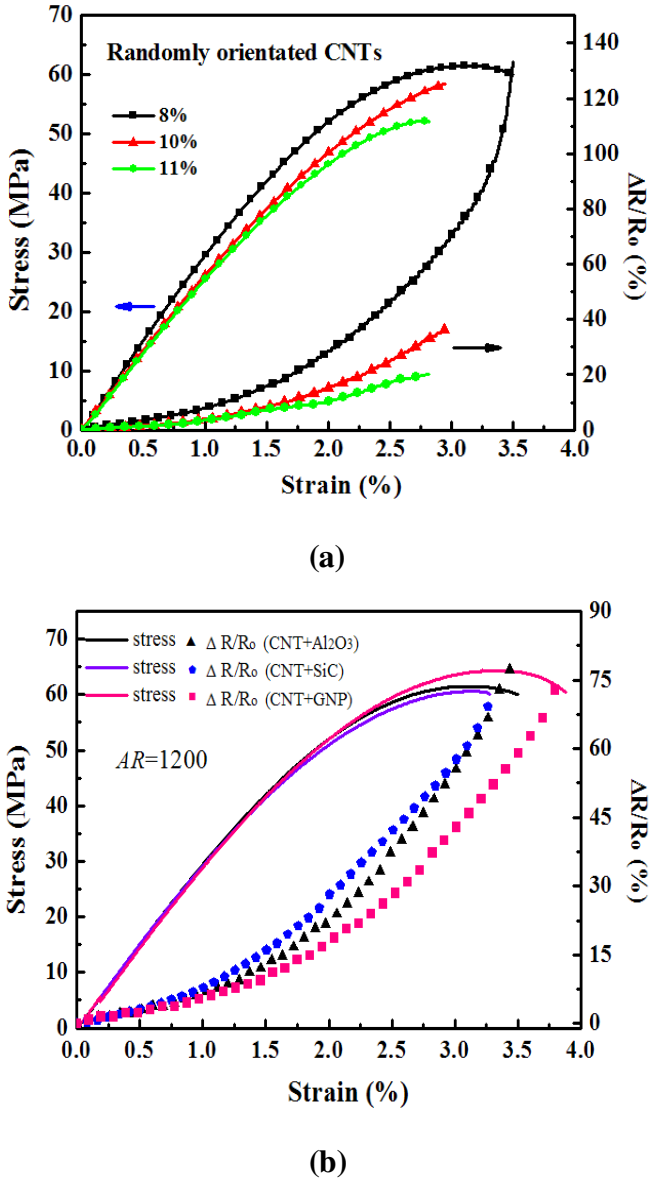

Fig. 2-18 *In situ sensing behavior of the composites with different concentrations of fillers under quasi-static tensile loading: (a) randomly distributed CNTs filled epoxy composites, (b) randomly distributed CNTs and microparticles co-filled composites.*

As shown by the dotted lines in Fig. 2-18a, the *in-situ* electrical resistance increases monotonically with the applied strain until catastrophic fracture of the composites. We can see from Fig. 2-18b that the self-sensing properties of the mixture of *ran*-CNTs and microparticles filled composites is almost the same as that shown in Fig. 2-18a. And this behavior is almost independent of the microparticle types. Besides, it should be noted that the *in situ* electrical resistance in the two systems increases in a fairly linear way at small strain and then exhibits a similar exponential behavior, increasing more significant per strain unit with the increase of strain. When the strain is near the fracture, a sudden increase of ΔR is observed. This phenomenon of the resistance-change is also independence of the *ran*-CNT content.

2.7.1.2. Self-sensing behavior of the CNT-GNP/epoxy and CNT-SiC/epoxy nanocomposites

An example of the typical stress-strain curve and *in-situ* electrical resistance response of the CNT-GNP/epoxy and CNT-SiC/epoxy nanocomposites during quasi-static tensile loading are plotted in Fig. 2-19a and b, respectively. It can be clearly seen that the *in situ* resistance increases to its maximum value and then begins to decrease at a critical strain, which is absolutely different from that of the *ran*-CNTs filled composites.

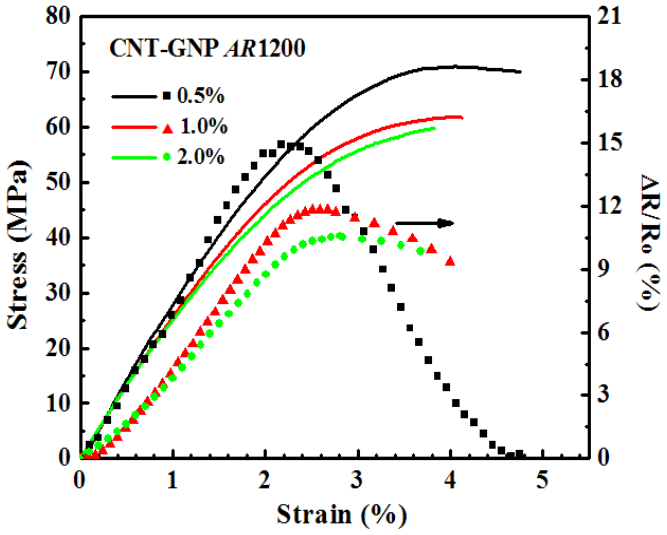

(a)

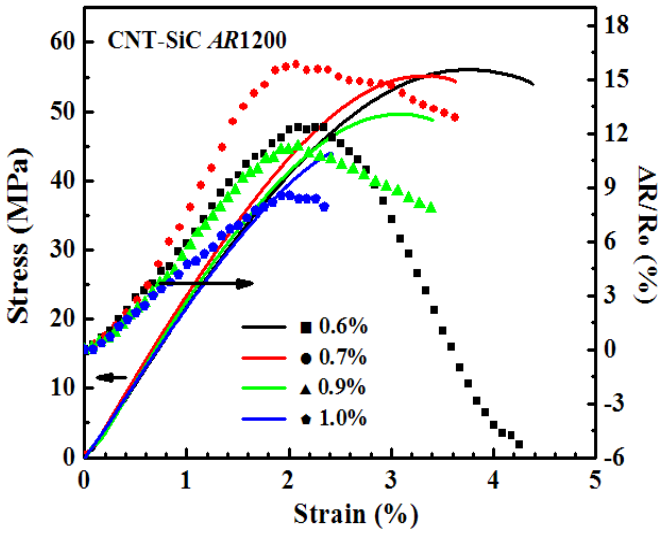

(b)

Fig. 2-19 *Self-sensing behavior of the composites containing different contents of the hybrid under quasi-static tensile loading, (a) CNT-GNP/epoxy; (b) CNT-SiC/epoxy composites.*

2.7.1.3. Self-sensing behavior of the CNT-Al_2O_3/epoxy nanocomposites

Fig. 2-20 exhibits the self-sensing behavior of the CNT-Al_2O_3/epoxy composites with different CNT aspect ratios. It is found that the response of the *in-situ* electrical resistance is strongly dependent on the CNT aspect ratio. In the case of *AR*500 and *AR*1200, the *in-situ* resistance exhibits a similar behavior to that shown in Fig. 2-18 with a consistent increase of electrical resistance until the ultimate failure of the composites. However, with increasing CNT aspect ratio up to 2000 or more, the self-sensing properties of the composites become similar to that shown in Fig. 2-19.

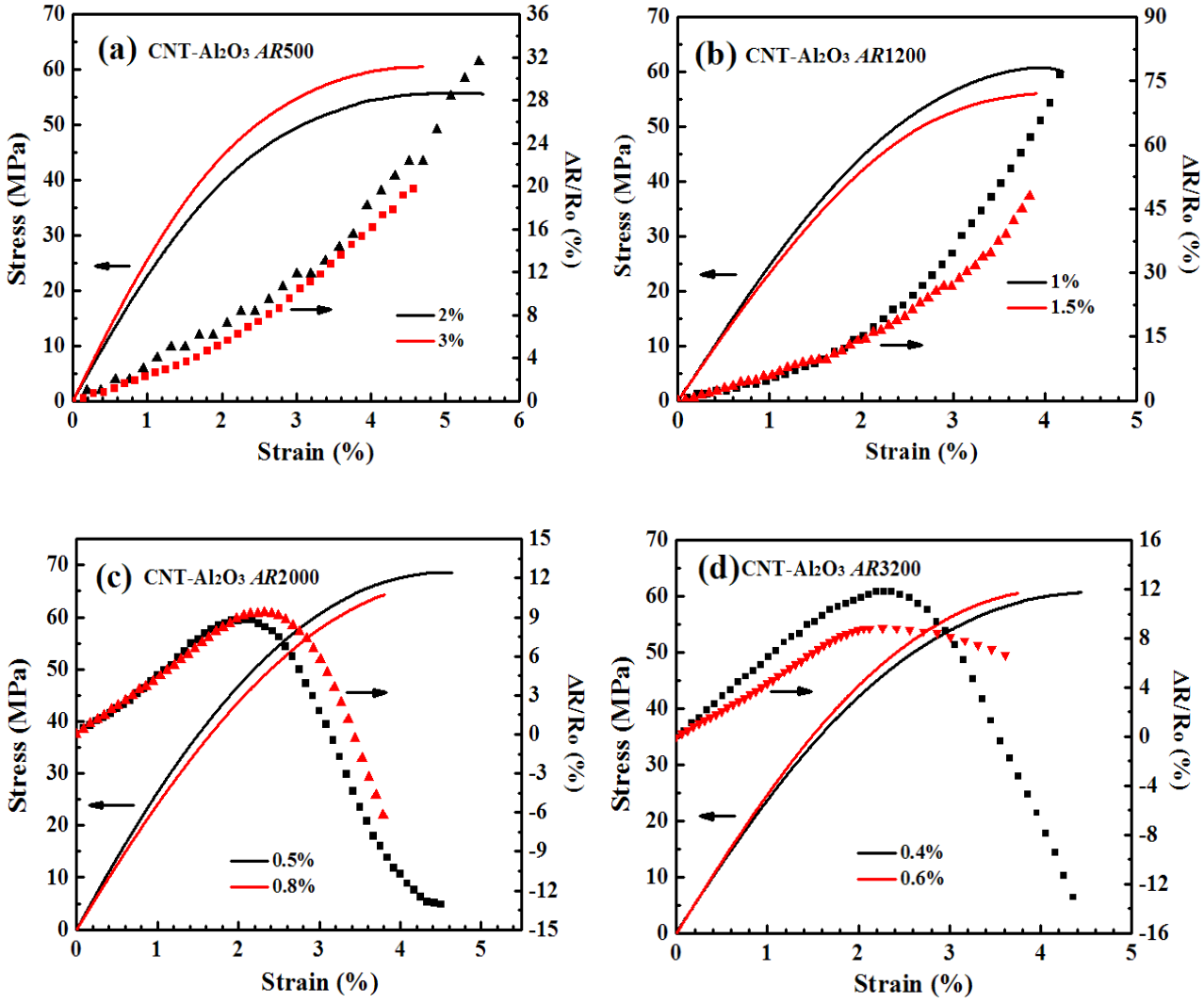

Fig. 2-20 *Self-sensing behavior of the composites containing different concentrations of the CNT-Al_2O_3 hybrids with different CNT aspect ratios under quasi-static tensile loading; (a) AR500, (b) AR1200, (c) AR2000, (d) AR3200.*

2.7.2. Self-sensing behavior of the epoxy composites during cyclic loading

In order to explore the underlying mechanisms behind these different self-monitoring behaviors aforementioned, the evolution of deformation occurred in the composites during tensile loading are investigated. Accordingly, the incremental cyclic loading tests of the composites are carried out.

2.7.2.1. Self-sensing behavior of randomly distributed CNTs/epoxy composites

Fig. 2-21 shows the detailed research about characteristic stress ~ strain curve and the *in situ* sensing behavior of the composite containing 8 *wt.%* randomly distributed CNTs. A fairly linear behavior is detected for small deformations ($\varepsilon < \varepsilon_c$), but the complete curve is clearly nonlinear. As it exceeds the critical strain (ε_c), the resistance increases nonlinearly, gradually increasing the curve slope until the ultimate fracture. When the strain is close to the fracture, a sudden increase in ΔR occurs since the continuity of the CNT networks inside the matrix is disrupted. This nonlinear piezoresistive behavior in the *ran*-CNT/polymer composites under high deformation has been observed. Park *et al.* [204] suggested that for deformations in the elastic range of the polymer matrix, CNTs are still in contact inside the Matrix, and thus the piezoresistive effects can be explained by common percolative theories. However, for higher deformations (close to the elasto-plastic mechanical transition), CNT contacts decrease and the tunneling resistance may play a dominant role in the nonlinear behavior. According to Hu *et al.* [131, 196], increasing the tunneling resistance can improve piezoresistivity of the composites, which may be the reason for increased sensitivity (slope) observed in the large deformation zone. In our case, it is also possible that the large applied strain yields certain CNT reorientation inside the polymer.

Besides, an incremental cyclic loading has also been conducted as shown in Fig. 2-21b and c. After the fourth loading cycle ($\sigma \approx 49$ MPa), some residual strain occurs when the specimen is unloaded to $\sigma = 0$, which can be attributed to the plastic deformation. The *in situ* electrical resistance increases and decreases monotonically with the cyclic stress and strain, however, an irreversible resistance change occurs after the fourth loading cycle which directly correlates with the emerging residual strain. That is, once the yield point where $\sigma_y \approx$ 49 MPa is passed, the plastic deformation happened. However, from the *in situ* resistance change, there is not obvious inflexion region or other information to identify the elastic and plastic region.

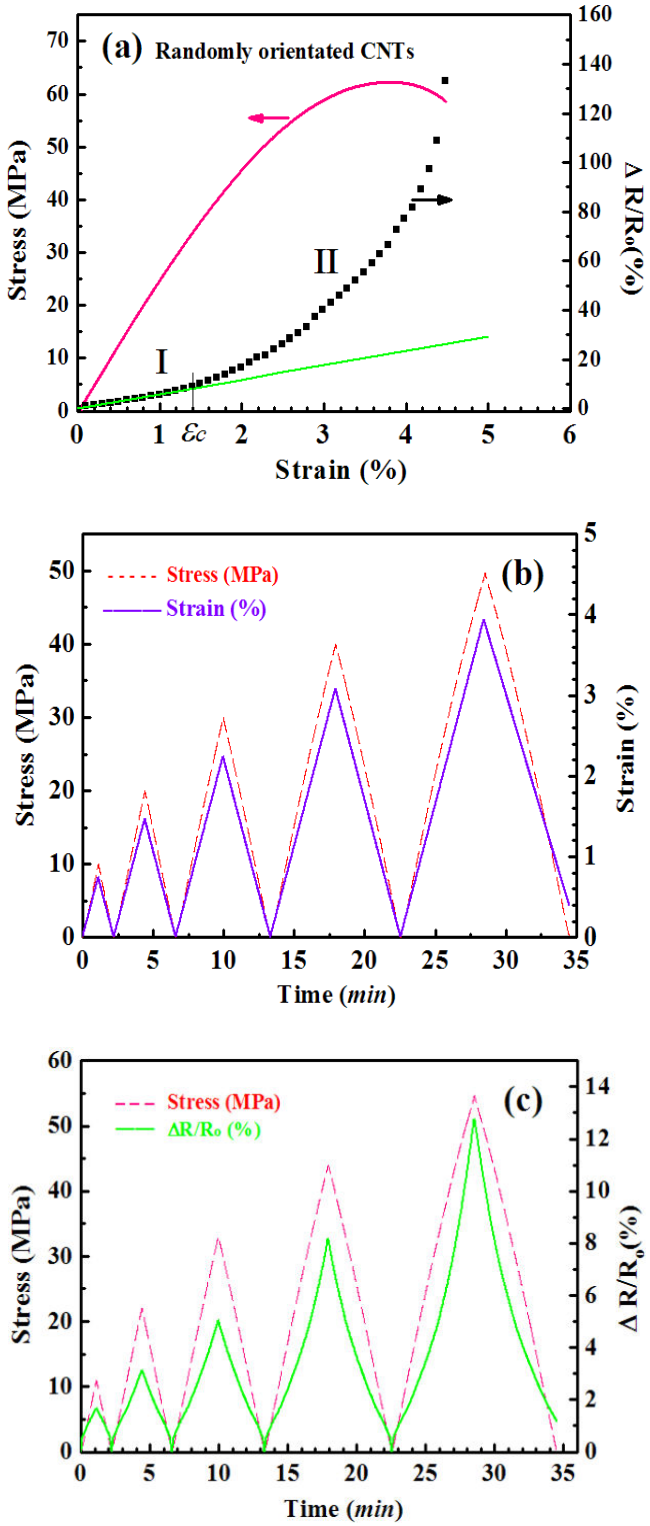

Fig. 2-21 *In situ sensing behavior of the epoxy composite incorporated with 8 wt.% of randomly distributed CNTs; (a) The stress-strain and electrical resistance-change response curves of the composite under quasi-static, (b) and (c) Incremental cyclic loading with transient stress, strain, and resistance response versus time.*

2.7.2.2. Self-sensing behavior of the CNT-GNP/epoxy nanocomposites

In attempt to further exploit CNT-GNP hybrid as novel *in situ* sensor, the electrical resistance response of the CNT-GNP/epoxy composite with 0.5 *wt.%* CNT-GNP hybrids is tracked in real-time when the specimens are subjected to quasi-static and incremental cyclic tensile loading. Between three to five samples are tested under the same condition. An example of the typical stress-strain curve and the *in-situ* electrical resistance response during quasi-static tensile loading is plotted in Fig. 2-22a. It is clearly seen that the *in situ* resistance increases to its maximum value and then begins to decrease at a critical strain (ε_c). This self-sensing behavior is similar to that of the composites based on CNT-SiC hybrids [205]. When $\varepsilon < \varepsilon_c$, the CNTs grown on the substrates are very difficult to orientate due to their strong junctions with the substrate and excellent molecular coupling with the polymer chains. Then the matrix deformation makes the number of contact points between CNTs decrease. Therefore, the formed conductive networks are broken up and the *in situ* electrical resistance increases. With the increase of applied strain ($\varepsilon > \varepsilon_c$), it is helpful for the CNT orientation in the composites due to the formation of certain microvoids, shear bands and crazing. In this case, the rotation of the GNP substrates could also facilitate the rotation of the CNTs and hybrids. These rearrangement behaviors could make the separated conductive networks closer again, giving rise to the decrease of electrical resistance. In addition, the electrical tunneling resulted from the closing of some micro-cracks because of Poisson's contraction also contributes to the reformation of the conductive networks.

In order to further shed light on the deformation evolution in the composites, the incremental cyclic loading tests are also performed. Fig. 2-22b and c shows an example of the transient stress, strain and electrical resistance response as function of time under cyclic tensile loading. During the first three loading and unloading cycles, the transient resistance change closely follows the response of applied stress and strain. The *in situ* resistance increases and decreases monotonically with the cyclic stress and strain. That is because the reversible deformation induces the break-up and intact reformation of the conductive networks with the open and closing of microcracks during tensile loading.

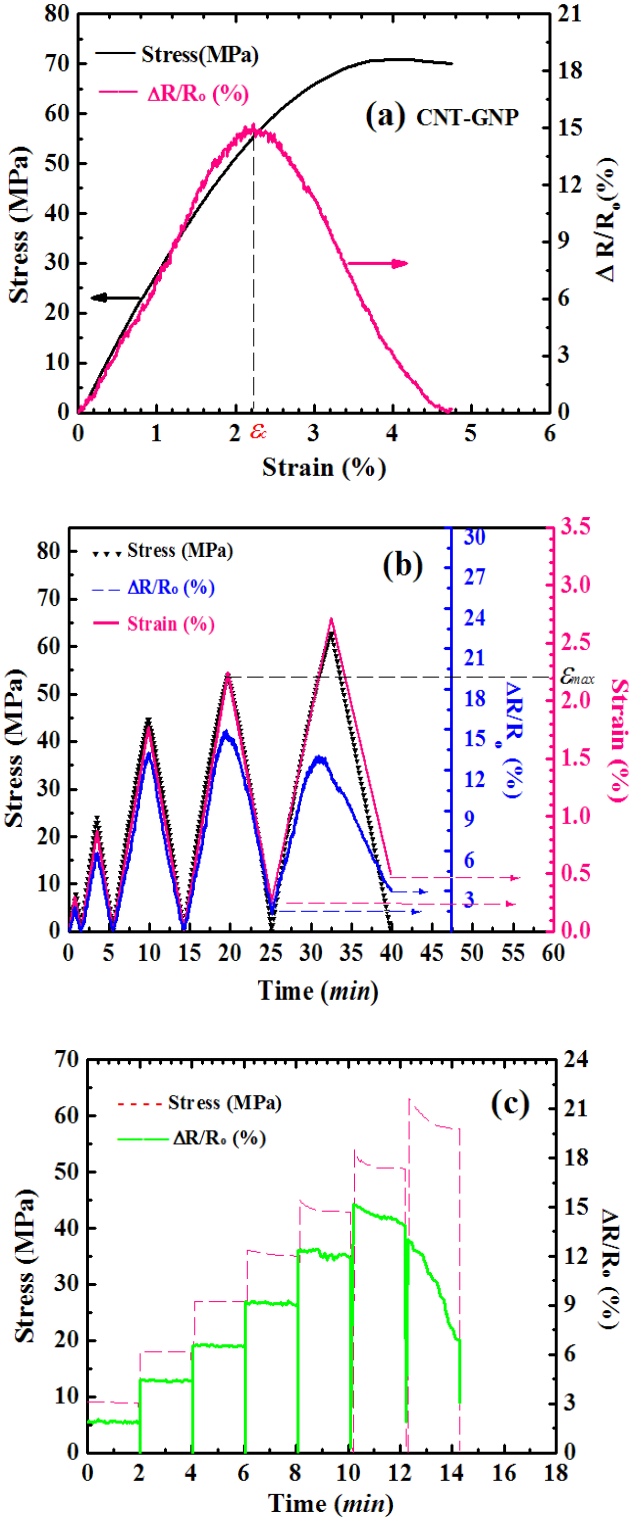

Fig. 2-22 *In situ sensing behavior of the epoxy composites with 0.5 wt.% CNT-GNP hybrids: (a) Resistance change and the corresponding stress as function of strain under quasi-static loading, (a) Cyclic loading with transient stress, strain, and resistance response versus time; (b) Incremental cyclic loading and the corresponding resistance change.*

Besides, during the first three cycles, the strain and *in situ* $\Delta R/R_o$ always return to zero after each cycle. However, the slight deviation of the electrical resistance response to strain response could be observed during the fourth cycle. Upon unloading after the fourth cycle, the strain and $\Delta R/R_o$ could not return to their original values, indicating that the residual strain, irreversible deformation and permanent resistance change has occurred during this cycle. It is noteworthy that the amplitude of strain in the fourth cycle (ε_{max}) is very close to the critical strain (ε_c) in Fig. 2-22a where $\Delta R/R_o$ begins to decrease. The subsequent cycles show more evident deviation of the resistance curve to the strain response with the appearance of larger permanent resistance change and residual strain. Additionally, the amplitude of $\Delta R/Ro$ begins to decrease in the fifth cycle. In order to gain an insight into the general tendency of resistance change with different applied stress, Fig. 2-22c illustrates the stress and *in situ* resistance response of one sample undergoing cyclic loading with a progressively increasing step load. In the first fifth cycles, there is larger resistance change in the latter cycle as compared to the previous cycle upon re-loading and the resistance change is relatively stable in each cycle. In this case, the resistance increase in the following cycles may be attributed to the formation of new micocracks which break apart the electrically percolating networks in the matrix. However, the resistance change begins to decrease and becomes unstable from the sixth re-loading cycle. Besides, the permanent resistance change appears in the unloaded state after the sixth cycle. The stress in the sixth cycle (σ_{max}) is very close to the stress corresponded to ε_c in Fig. 2-22a. Consequently, from these results one can see that the specimen experiences reversible elastic deformation during the first fifth cycle and the irreversible plastic deformation is initiated from the sixth cycle. The decrease of resistance change may be attributed to the reformation of new conductive networks induced by the orientation of CNT bundles and GNP substrate in the permanent deformation region. Based on the results above, we conclude that the onset of *in situ* resistance decrease can be used to identify the irreversible deformation onset in the CNT-GNP/epoxy composite, where the permanent resistance change and residual strain also begin to appear. The distinctive architecture of CNT-GNP hybrids endows possibility of the reformation of conductive networks with the emergence of irreversible deformation. As a result, the CNT-GNP hybrids as potential self-sensing materials could open up new opportunities in the field of smart

sensing and structural health monitoring.

2.7.2.3. Self-sensing behavior of the CNT-SiC/epoxy nanocomposites

Fig. 2-23a presents the stress-strain curve (solid line) as well as *in situ* electrical resistance change (dotted line) in the CNT-SiC/epoxy composites during tensile loading. The resistance monotonically increases then begins to decrease when the strain passes a critical value ε_r, which obviously divides the dotted line into Region I and II. The stress-strain curve (0~ε_r) displays a typical linear-elastic behavior (see the inset), which is reconciled with the Hooke's Law. Traditionally, the elastic and plastic region could be identified via the offset yield point [206, 207]. A 0.2% residual strain has been taken to define the offset yield point (Y) and the corresponding ε_y is very close to ε_r. In order to further verify the yield point and the appearance of the permanently plastic deformation near yield point, the specimen is also subjected to tensile loading cycles with increasing maximum per cycle and unloaded to zero stress at the end of each cycle. After the fifth loading cycle (σ_{max}=46 MPa), some residual strain occurs when the specimen is unloaded to σ=0 (Fig. 2-23b), which can be attributed to the permanently plastic deformation. As shown in Fig. 2-23c, the *in situ* electrical resistance increases and decreases monotonically with the cyclic stress and strain, however, an irreversible resistance change occurs after the fifth loading cycle when the specimen is unloaded, which directly correlates with the emerging residual strain. That is,once the yield point σ_y≈46 MPa is passed, the plastic deformation happened. Besides, as shown in the SEM image of Fig.4a, some permanent micro-cracks in the matrix are initiated and observed at 4% strain. As a result, this *in situ* sensing behavior of our CNT-SiC hybrids in the composites could offer valuable information for identifying the elastic and plastic region.

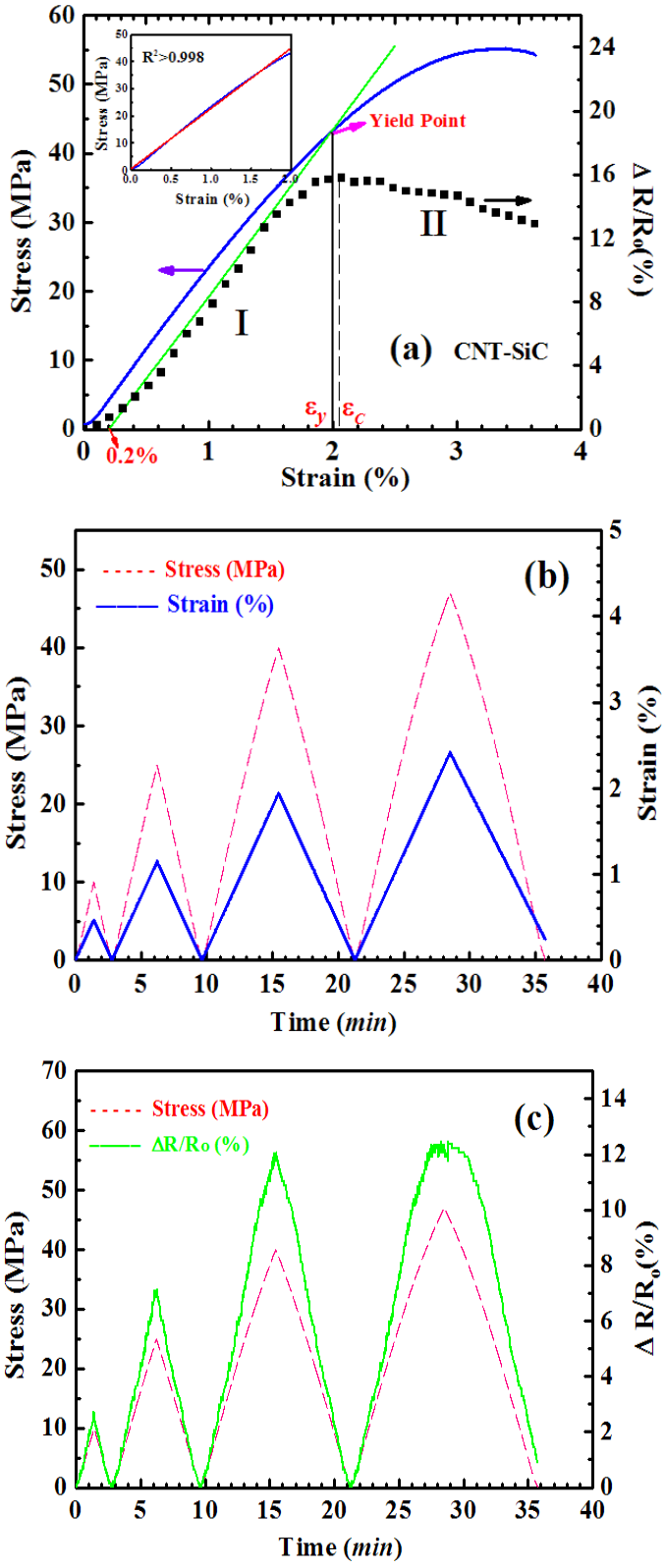

Fig. 2-23 *In situ sensing behavior of the epoxy composite with 0.7 wt.% CNT-SiC hybrids; (a) The stress-strain and electrical resistance-change response curves of the composite under quasi-static, (b) and (c) Cyclic loading with transient stress, strain, and resistance response versus time.*

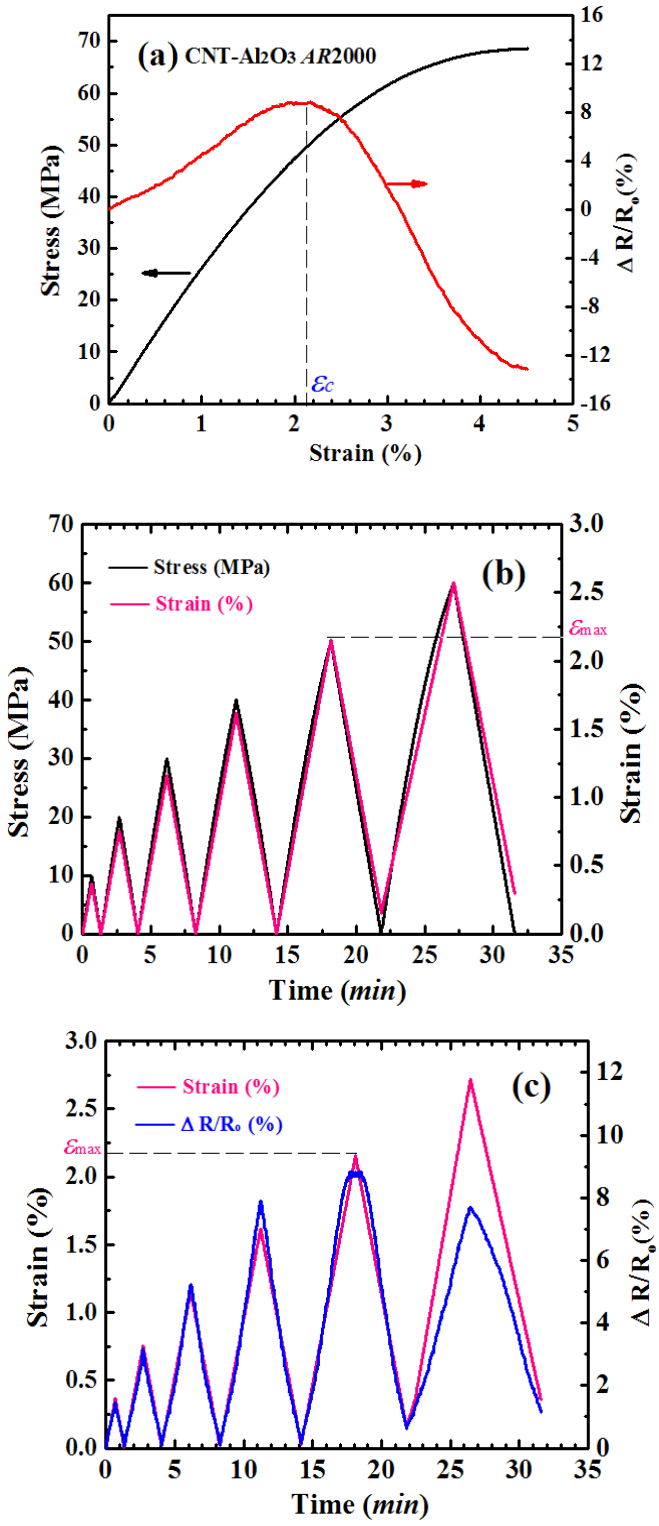

Fig. 2-24 *In situ sensing behavior of the epoxy composite with 0.5 wt.% CNT-Al_2O_3 hybrids (AR2000); (a) The stress-strain and electrical resistance-change response curves of the composite under quasi-static, (b) and (c) Cyclic loading with transient stress, strain, and resistance response versus time.*

2.7.2.4. Self-sensing behavior of the CNT-Al_2O_3/epoxy nanocomposites

The tensile loading-unloading cycles of the CNT-Al_2O_3/epoxy composites (*AR*2000) is shown in Fig. 2-24b and c. The stress, strain and *in-situ* electrical resistance are plotted as function of time. During the first four cycles, the strain and *in-situ* $\Delta R/R_o$ always return to zero after each cycle, indicating that no irreversible deformation occurs in the composites. However, in the fifth cycle, the strain and $\Delta R/R_o$ could not return to their original values after unloading. This indicates that the appearance of the residual strain and irreversible deformation as well as the permanent electrical resistance change at this strain level. Besides, the amplitude of $\Delta R/R_o$ gradually increases with the loading-reloading number during the first five cycles, whereas, it begins to decrease in the sixth cycle. It is noteworthy that the amplitude of strain in the fifth cycle (ε_{max}) is very close to the critical strain (ε_c) shown in Fig. 2-24a where the $\Delta R/R_o$ begins to decrease. In addition, the critical strain values in each system are almost close to each other, as shown in Fig. 2-22a and Fig. 2-23a. Hence, one can say that the reversible elastic deformation mainly occurs in the composites when $\varepsilon<\varepsilon_c$, and then the irreversible deformation or permanent damage is initiated when $\varepsilon>\varepsilon_c$. The onset of irreversible deformation in the composite could be identified by the onset of the decrease of *in-situ* electrical resistance where the permanent resistance change begins to appear.

2.7.3. Influence of the substrate and CNT aspect ratio of the hybrids on the self-sensing behavior of the composites

As shown in Fig. 2-25a, the composites based on the hybrids (CNT-SiC, CNT-GNP and CNT-SiC+CNT-Al_2O_3) with the same CNT aspect ratio (*AR*1200) behave remarkably differently. These composites display a similar self-monitoring ability during tensile loading, that is, the *in-situ* electrical resistance monotonically increases to its maximum value and then begins to decrease. For the composites with the CNT-SiC+CNT-Al_2O_3 mixture, the mass ratio of the two hybrids is set as 1:1. Fig. 2-25b displays the self-sensing behavior of the CNT-Al_2O_3/epoxy composites with different CNT aspect ratios. It is found that the response of *in-situ* electrical resistance also depends on the CNT aspect ratio. In the case of

*AR*500 and *AR*1200, the *in-situ* resistance exhibits a similar behavior to that of the *ran*-CNTs filled composites. However, with increasing aspect ratio up to 2000 or more, the self-sensing properties of the composites become similar to that shown in Fig. 2-25a.

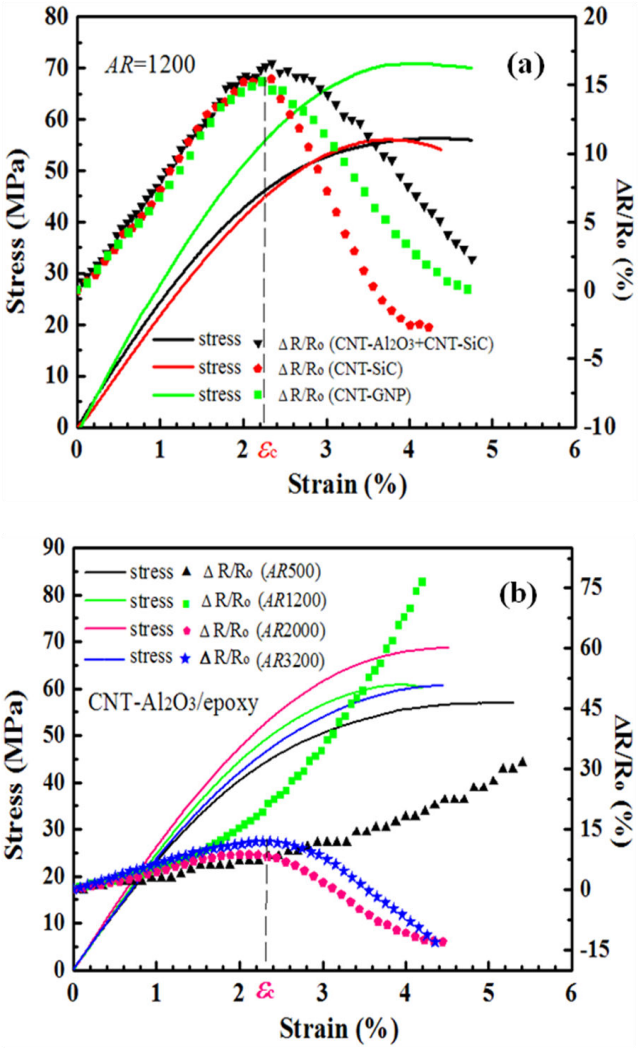

Fig. 2-25 *Self-sensing behaviors of the epoxy composites with (a) hybrid fillers with the same aspect ratio (AR1200), (b) CNT-Al_2O_3 hybrids with different aspect ratios.*

Before tensile loading, the vertically aligned CNTs well dispersed in the matrix and the conductive networks are formed (Fig. 2-26). In the elastic region, the elastic deformation makes the number of contact points between CNTs on different SiC microplates decrease (Fig. 2-26). As a result, the *in situ* electrical resistance increases in this region. When the plastic deformation occurs, there is reformation of the conductive networks after their break-ups, which can be explained by the electrical tunneling resulted from the closing of the

micro-cracks because of Poisson's contraction. There is a good dispersion of the vertically aligned CNTs and two neighboring CNTs grown on SiC are not overlapping yet still situated closely enough to allow electrical tunneling, which is different from the case of randomly orientated CNTs. Besides, Poisson's ratio effect and the intense movement of the polymer chain may result in the rotation of some CNT bundles grown on SiC along the stress direction (Fig. 2-26 and Fig. 2-27). This rotation of CNT bundle is different from that of randomly orientated CNTs because only free ends of them could be rotated and the other ends are attached to SiC microplate. Besides, the possible reorientation of the SiC microplate could not be seen from the optical image because the SiC microplate is much smaller compared to the CNTs. Therefore, it is possible for this kind of nano/micro hybrid to reform the conductive networks in the plastic region. This may explain the decrease of electrical resistance when it entered into the plastic region.

The self-sensing behavior of the composites is strongly dependent on the formed CNT conductive networks. Therefore, we try to explain the *in-situ* sensing behaviors mentioned by exploring the different evolutions of the conductive networks provided by the randomly distributed CNTs and the CNTs grown on the microsubstrates. The randomly distributed CNTs are generally supposed to more easily orientate in the polymer matrix compared to the CNTs grown on the microsubstrates. They are inclined to align along the stress direction during tensile loading, as shown in Fig. 2-26a. However, this rearrangement is not conducive to the reformation of conductive networks. Thus, the composites with randomly distributed CNTs show a monotonic increase of the *in-situ* electrical resistance until their ultimate fracture. However, the composites based on the CNT-SiC or CNT-GNP hybrids (*AR*1200) display a noticeable recovery of resistance when $\varepsilon>\varepsilon_c$. Moreover, the electrical resistance at high strain becomes even lower than that at $\varepsilon=0$, as shown in Fig. 5b. When $\varepsilon<\varepsilon_c$, the CNTs grown on the substrates are very difficult to orientate under low strain due to the strong junctions with the substrate and excellent molecular coupling with polymer chains. In this case, the broken of the formed conductive networks mainly happens. With the increase of applied stress, it may be helpful for the orientation of the CNTs and hybrids in the composites. As indicated previously, the SiC and GNP substrates are anisotropic. When $\varepsilon>\varepsilon_c$, their rotation could facilitate the rotation of the CNTs and hybrids, due to the formation of

certain microvoids, shear bands and crazing. Besides, the CNT-SiC and CNT-GNP hybrids show the asymmetric morphology in the composites, as shown in Fig. 2-26b. Then the rearrangement of the CNTs and hybrids can make the separated conductive networks closer again, giving rise to the decrease of electrical resistance. However, this does not happen in the case of the CNT-Al_2O_3/epoxy composites (*AR*1200). The *in-situ* electrical resistance continues to increase even at high strain ratio ($\varepsilon > \varepsilon_c$).

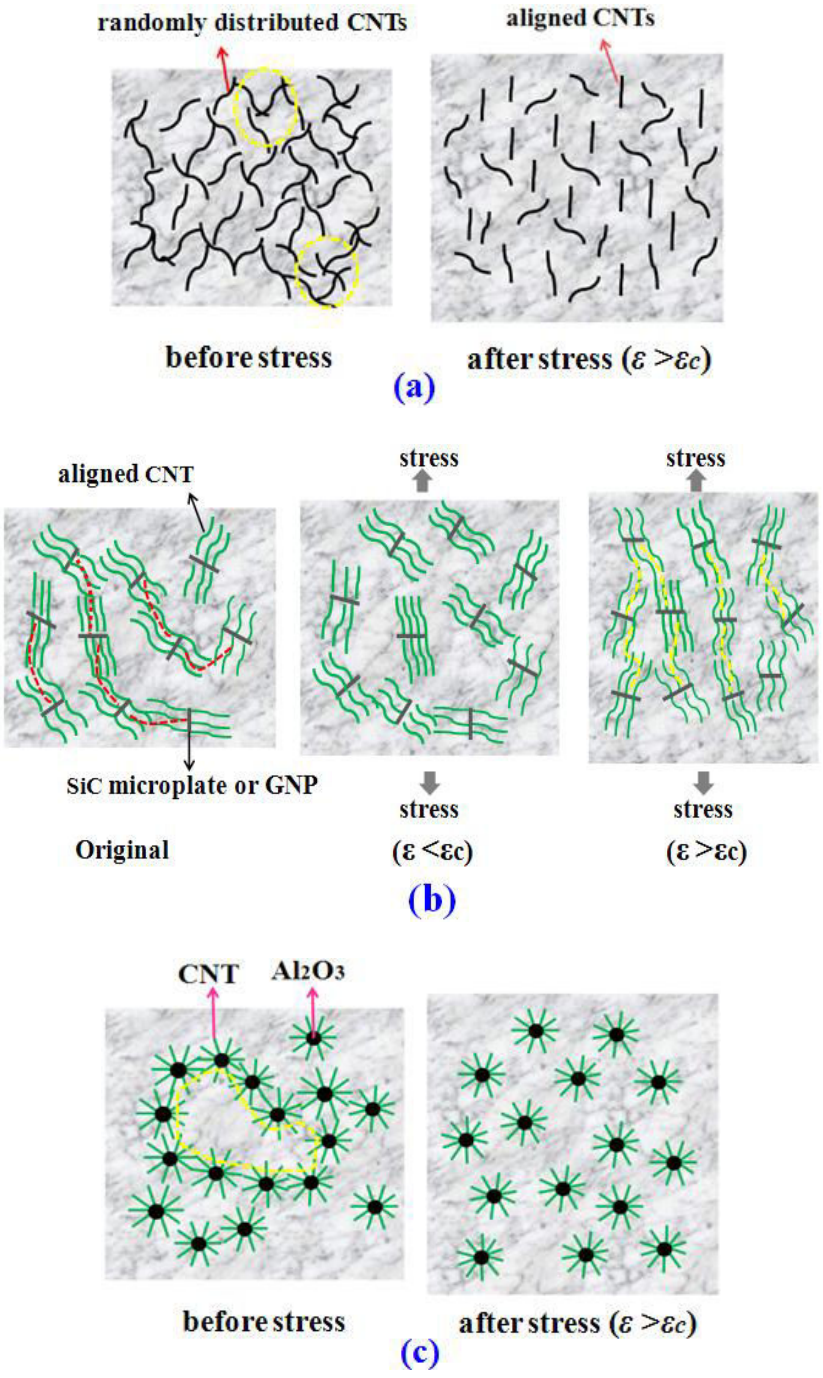

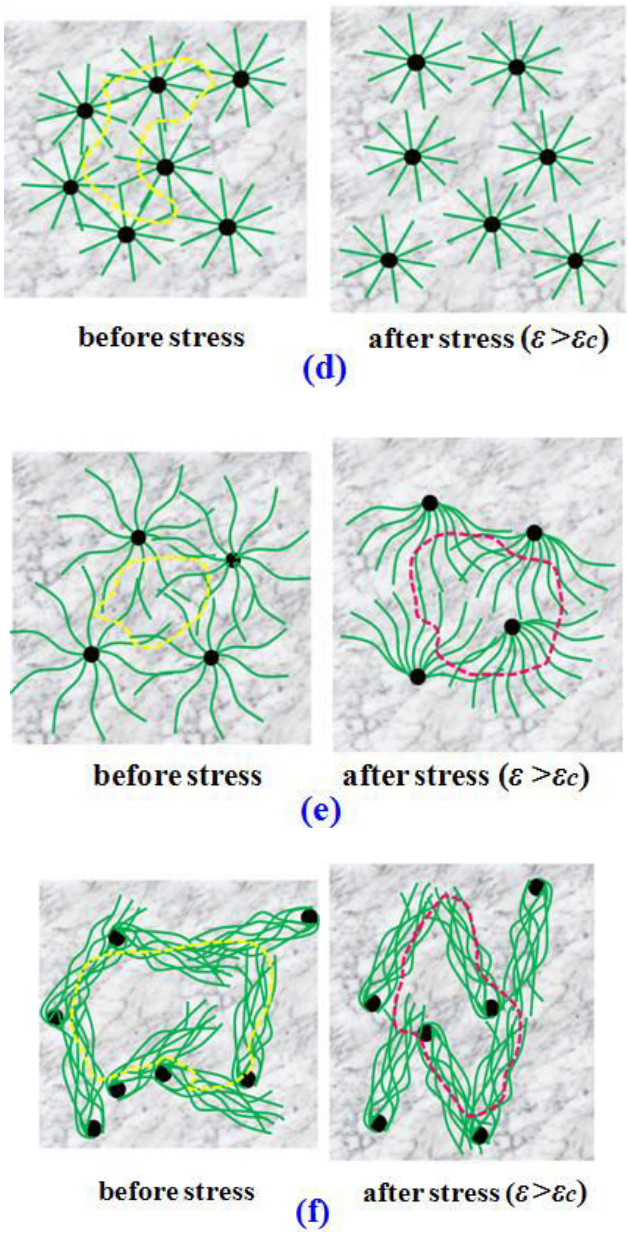

Fig.2-26 *Schematic of the evolution of conductive networks provided by the fillers during tensile loading (a) randomly distributed CNTs; (b) CNT-SiC or CNT-GNP hybrids; (c) ~ (f) CNT-Al_2O_3 hybrids with different aspect ratios: (c) AR500; (d) AR1200; (e) AR2000; and (f) AR3200. The dotted line represents the conductive networks.*

It is known that the morphology of Al_2O_3 is spherical, and the CNT-Al_2O_3 hybrids with relative small length exist in a symmetric form in the composites (Fig. 2-26c and d). Therefore, the rotation of the CNTs and hybrids could not change their existing morphology in the composites. Besides the substrate morphologies, the CNT aspect ratio also has an important effect on the self-sensing behavior of the composites. As discussed in Fig. 2-25

concerning the self-sensing behaviors of the CNT-Al_2O_3/epoxy composites with different aspect ratios, when *AR* is equal to 500 and 1200, the *in situ* electrical resistance of the composites monotonically increases with the applied strain, whereas when *AR* is up to 2000 or more, it begins to decrease when $\varepsilon>\varepsilon_c$. Asides from the rotation of the CNTs and hybrids resulted from that of the substrates, the reorientation of CNTs with high aspect ratio along the stress is much more evident than that of small ones under tensile loading, as shown in Fig. 2-26e. With the help of this orientation behavior, the conductive networks could easily reform during tensile loading. Moreover, for *AR* 3200, the Al_2O_3 substrate seems to be wrapped by the CNTs in one end instead of in the center (Fig. 2-5g and Fig. 2-26f). These distribution states provide more chance for the reorientation of CNTs, which will contribute to the reformation of conductive networks when $\varepsilon>\varepsilon_c$. Besides, most of the curved CNTs with higher aspect ratios may be stretched along the tensile loading, which also helps to reform the conductive networks. In addition, the variation tendency of percolation thresholds in CNT-Al_2O_3/epoxy composites could also be explained by the aspect ratio dependent CNT dispersion. With the increase of aspect ratio from 500 to 2000, the percolation threshold of the composites shows obvious downward trends, however, it begins to increase with further increasing aspect ratio to 3200. To some extent, the waviness of some CNTs in this system (*AR*3200) also decreases their actual length in the composites.

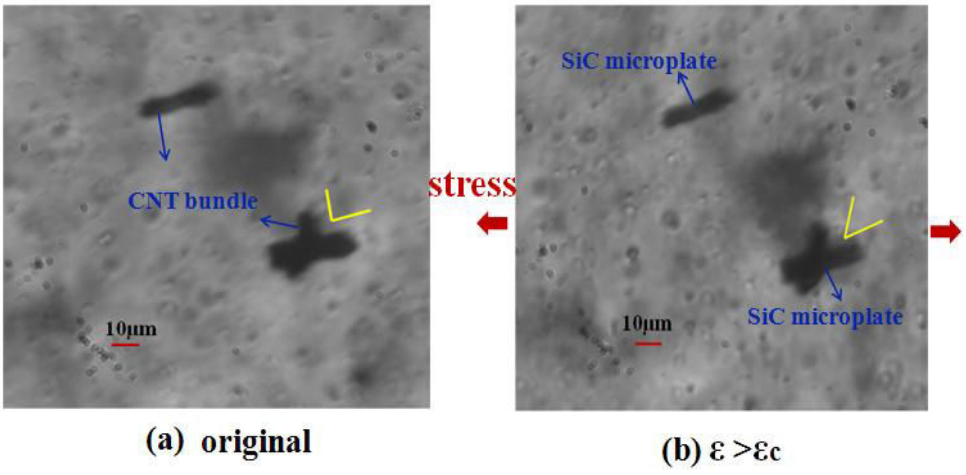

Fig. 2-27 *Optical images of CNT-SiC hybrids during tensile loading.*

Based on the above discussion, it can be concluded that the self-sensing behavior of the composites greatly depends on the evolution of conductive networks during tensile loading. And this evolution is closely related to the CNT aspect ratio and reorientation as well as the microsubstrate geometry.

2.8. Concluding remarks

In order to develop the high performance CNT/polymer composites, the critical issues, such as, preparing the structure controllable CNTs (aspect ratio and orientation), creating uniform dispersion and desirable alignment of CNTs within the polymer matrix, improving load transfer from CNT to the matrix, etc, still exist and extremely need to be solved. Their hybridizations with other materials, like nanosized metal or oxide particles, microsized ceramic particles, fullerenes and two dimensional graphene could control CNT distribution and arrangements in polymer matrix and exhibit superior multifunctional properties of the composites than the pristine CNTs. In this chapter, three kinds of well-organized hybrid structures are respectively achieved by in situ grafting multi-walled carbon nanotubes on SiC microplates, graphene nanoplatelets, micro-spherical Al_2O_3 during CVD synthesis process, without any pre-patterned catalyst treatment. The CNT organization and distribution patterns on the substrates is strongly dependent on their diameter, length and area number density by controlling CNT growth temperature, time and hydrogen ratio, etc. The CNT-SiC, CNT-GNP and CNT-Al_2O_3 nano/micro hybrids reinforced epoxy composites were fabricated using calendaring method. Compared to the randomly orientated CNTs filled composites, the more improved mechanical, electrical and obviously different self-sensing properties of the multiscale hybrids filled composites were comprehensively investigated. The relationship between the composite properties and hybrid structure (CNT aspect ratio, orientation and substrate morphology) has been well established. The major conclusions are summarized as follows:

(I) The CNT-microparticle multiscale hybrids could be used as high-performance structural additives for improving the composite mechanical properties. Such as, with respect to neat epoxy, significantly enhanced mechanical properties in the CNT-GNP filled composites were achieved at ultralow hybrid loading (0.5 *wt.*%). The tensile modulus showed ~40% increase and the tensile strength was improved by ~36%. But, it was found that the optimal concentration of the hybrids (f_c) is necessary to achieve the desirable reinforcement effect. It is most often the case that mechanical properties of the hybrids reinforced composites become saturated when the hybrid content exceeds a certain value. When $f_{\text{hybrid}} < f_c$, the

tensile modulus and strength continuously increase with the embedding of the hybrids. As f_{hybrid} approaches f_c, the results indicate that they approximately reach the maximum values. However, when $f_{hybrid} > f_c$, they begin to degrade with the hybrid loading. Besides, the value of percolation threshold of the hybrids filled systems is much lower, ~ 0.2 *vol.%* in the CNT-SiC composites.

(II) The epoxy composites with CNT-GNP, SiC-CNT or CNT-Al_2O_3 hybrids could exhibit distinctive self-sensing behavior for *in situ* monitoring the onset of irreversibly permanent deformation. The *in situ* electrical resistance initially increases to its maximum value and then begins to decrease with the appearance of residual strain and irreversible deformation, which is remarkably different from the randomly oriented CNTs filled composites only with monotonic increase of the resistance until their catastrophic fracture.

(III) The mechanical and self-sensing properties of the composites are closely related to the substrate morphology of the hybrids. For the same aspect ratio (1200), the *in-situ* electrical resistances of CNT-SiC/epoxy and CNT-GNP/epoxy composites increase when $\varepsilon<\varepsilon_c$ and then decreases when $\varepsilon>\varepsilon_c$, which is different from that of the CNT-Al_2O_3/epoxy composites with monotonic increase until their ultimate failure. Moreover, the CNT-GNP/epoxy composite shows the most significant improvement of the tensile modulus and tensile strength compared to the baseline epoxy. Besides, the self-sensing and mechanical properties of the composites also strongly depend on the CNT aspect ratio and organization. With increasing *AR* up to 2000 or more, the change of *in-situ* electrical resistance of CNT-Al_2O_3 filled composites becomes similar to that of the CNT-SiC/epoxy and CNT-GNP/epoxy composites. The tensile modulus and strength of CNT-Al_2O_3/epoxy composites increase with increasing *AR* from 500 to 2000, but then decrease at *AR*=3200.

(IV) For the reinforcing mechanism of these hybrids, the uniform distribution states of the hybrids in the matrix can restraint CNT agglomeration. Their three dimensional architectures give rise to larger contact surface and stronger molecular interaction between the CNTs and the matrix, resulting in an improved load transfer. The alignment of CNTs in the hybrids retains their actual lengths in the matrix, enhancing their reinforcement efficiency. Besides, the strong junction between the CNTs and the substrates makes CNT reorientation much

more difficult under low strain, compared to the randomly distributed CNTs. This could explain the higher elastic modulus of the composites based on the hybrids.

With regard to the underlying mechanisms of self-sensing properties of the composites, it is found that the evolution of conductive networks resulted from the rotation of the substrates and hybrids as well as the reorientation of CNTs during tensile loading plays an important role on the self-sensing behavior of the composites. And the CNT reorientation, dispersion state and substrate also have significant influence on the composite mechanical properties. Proper selection of hybrid structure (CNT aspect ratio, organization and substrate) is critical for achieving desired mechanical and self-sensing performances in the nano/micrometer hybrids reinforced composites.

Chapter III
The mutiscale glass fabric/epoxy composites

3.1. Introduction

Glass fiber-reinforced plastic laminated composites are widely used in many structural applications, such as wind energy, transportation, aerospace, etc, due to their high specific modulus and strength as well as significant weight reduction relative to metallic materials [156]. The fiber plays an important role in the load carrying capacity of the composites along the fiber direction, endowing them with superior in-plane performance. The epoxy adhesives are usually incorporated to hold together the load-bearing fibers. These glassy networks offer high creep and corrosion resistance and good adhesion to the fibers, yet they are also highly brittle and insulating. Hence, the composites suffer from poor matrix-dominated mechanical properties, such as interlaminar toughness and transverse electrical and thermal conductivity, particularly in matrix-rich interlaminar regions between the fibers.

Many studies have focused on toughening the matrix of the composites to improve their mechanical robustness. Rubber-toughening through the addition of discrete rubber particles enhances toughness but degrades the thermomechanical properties of crosslinked polymer networks [208]. The addition of rigid thermoplastics is another method of toughening the matrix low degradation in its thermomechanical properties [209]. Even so, the new methods to improve toughness while maintaining or improving thermal properties and simultaneously addressing additional needs such as transverse electrical conductivity are also needed. In this point, nanofillers have the potential to toughen the matrix phase and offer multifunctionality for the enhancements of other properties. Besides, the out-of-plane or through thickness properties of the composites also depend on the fiber/matrix interface [155]. Generally, the decreased in-plane and out-of-plane performance of the composites are attributed to the breakage of load-carrying fibers and the matrix dominated cracks occurring at low strain. In order to improve the overall mechanical properties and long-term durability, modifying the

fiber/matrix interface by nanofiller is a more achievable method. Even so, with the increase of their service time, many structural components require damage detection. As a result, it is imperative for the development of *in situ* damage sensor for their life prediction. Currently, electrical resistance measurement has been established as a nondestructive way for damage sensing [180, 181], but it is not applicable for the glass fiber (non-conducting) reinforced composites. In this case, more interest has emerged in developing the electrically conductive matrix by introducing conductive fillers into the matrix. Then the conductive networks offer potential for *in situ* monitoring the damage evolution of the composites. It is expected that matrix modification via incorporation of multifunctional filler could provide feasibilities for attaining desirable mechanical and self-sensing properties in the fiber reinforced composites.

Carbon nanotubes with extraordinary strength and stiffness and high aspect ratio have emerged as potential candidates for the matrix modification. As inherently multifunctional nanofiller, CNTs could serve as a structural reinforcement, conductive additives and strain sensor at a nanoscale [187, 177]. It was demonstrated that the addition of CNTs in the matrix improved the toughness of the matrix and the intrinsic interface properties of the composites. Besides, due to the small scale of CNTs relative to that of the fiber reinforcement, CNTs can penetrate into matrix-rich regions among fibers to form electrically conductive networks. The formed networks were utilized as sensitive sensors for monitoring the matrix-dominated damage. In recent years, significant attention has been paid to the multiscale, multifunctional structural composites containing conventional continuous fiber reinforcement together with the CNTs modified matrix [184]. Bekyarova et al. grew CNTs on carbon fiber surfaces for enhanced interactions, yielding tensile modulus and strength improvements of ~ 30% and 15% over the base composites, respectively [171]. Unfortunately, CNT growth from carbon fibers often results in non-uniform coverage or damage to the fibers, making this method difficult to optimize the composites.

However, the incorporation of CNTs in fibrous polymer composites still remains a challenging task. In view of the processability affected by the viscosity of the CNT-polymer mixtures, lower CNT content is required to simultaneously improve both mechanical and electrical properties of the composites. In this case, a prerequisite is the preferential CNT distribution in the matrix because more agglomerations of CNTs will severely reduce the

matrix-dominated mechanical properties and increase the percolation threshold to some extent. In this respect, different approaches are selected, covering a wide range from stirring, high shear mixing to chemical functionalization. Additionally, interfacial adhesion between the matrix and CNTs is another critical issue. Strong polymer/CNT interaction results in efficient load transfer from the matrix to CNTs which may increase the mechanical performance. As previously reported [98], it was found that functionalization of CNTs could improve their degree dispersion and interfacial properties, whereas, unexpectedly increasing the percolation threshold and decreasing the electrical conductivity of the system. Besides, the CNT alignment is also one of the most parameters in influencing the mechanical and self-sensing properties of the composites.

With regard to the critical issues discussed above, the multiscale hybrids with CNTs grown on the surface of other microparticle has been introduced into the matrix, resulting in uniform CNT dispersion and improved interfacial properties [56]. The CNT organization can be tailored by varying the growth parameters. Moreover, the hybrids were proposed to be utilized as multifunctional fillers in the composites. As our recently reported, the CNT-SiC and CNT-graphene nanoplatelet hybrids with CNTs grown on the surfaces of SiC or GNP microparticles have respectively served as high-performance reinforcement [210] and *in situ* strain sensor to detect the onset of irreversibly permanent deformation in the matrix [205]. To the best of our knowledge, the research on the glass fabric reinforced polymer composites incorporated with the CNT-microparticle multiscale hybrids has not yet been reported up to now. We hope that the hybrids become desirable alternative for matrix modification and *in situ* damage sensor in the fiber reinforced composites.

Epoxy is widely used as the polymer matrix for high performance laminated composites due to their good mechanical performance, processability, compatibility with most fibers, chemical resistance, wear resistance and low cost. In our work, the CNT-Al_2O_3 hybrids with well-aligned CNTs forming six-orthogonal branches on the spherical Al_2O_3 microparticles were prepared by chemical vapor deposition (CVD) process. The multiscale glass fabric (GF) reinforced epoxy (EP) composites (GF/EP) using the particles [randomly distributed CNTs (*ran*-CNT), *ran*-CNT+Al_2O_3 mixture and CNT-Al_2O_3 hybrids] were fabricated, respectively. Dynamic mechanical analysis and three point bending were performed for a comparative

research regarding the influence of reinforcements on the flexural and thermo-mechanical properties of the glass fiber/epoxy composites. *In situ* electrical resistance measurements were conducted to monitor the damage states and evolution of the continuous glass fiber reinforced composites. The potential of the CNT-Al_2O_3 hybrids as structural reinforcement and *in situ* damage sensor in the composites were analyzed.

3.2. Experimental

3.2.1. Materials

Randomly distributed CNTs (commercial) with a diameter of 30~50 nm and length ~20 μm supplied by Chengdu Organic Chemicals Co., Ltd., Chinese Academy of Sciences were used as-received (Fig. 2-1d). Micro-spherical alumina particles with 3~10 μm in size (99.8% in purity) were purchased from Performance Ceramic Company (Peninsula, OH, USA) (Fig. 2-1a). Graphene nanoplatelets (GNPs) with high aspect ratio, i.e., 3~4 μm in length and ~30 nm in thickness were obtained from Xiamen Knano Graphene Technology Co., Ltd. The plain woven glass fiber fabric used as-received with a density of 206g/m^2 and warp 51%, weft 49% was manufactured by Hexcel Corporation. The CNT-microparticle nano/micro hybrids used were synthesized using CVD procedure in our lab. The detailed preparation process has been illustrated in the last part. Epoxy resin (1080S, Resoltech Ltd, France) and the curing agent (1084, Resoltech Ltd) was used as the polymer matrix.

3.2.2. Preparation of the composites

The multiscale composites were manufactured using the glass fabric and epoxy matrix doped with three kinds of particle reinforcements, such as, the *ran*-CNTs, *ran*-CNT+Al_2O_3 mixture and CNT-Al_2O_3 hybrids. The composite laminates without particle reinforcements were also fabricated for comparative purposes. The fabrication procedure of the composite laminates consists of two steps: (I) Preparation of the particle/epoxy suspensions and (II) Impregnation of the suspension into a mold containing the glass fiber performs.

3.2.2.1. Preparation of particle/epoxy suspensions

The present research concentrates on manufacturing of the initial epoxy suspension by dispersing 0.5 *wt.%* of particles in the epoxy matrix. The fraction of the *ran*-CNTs and Al_2O_3 in the *ran*-CNT+Al_2O_3 mixture is respectively the same as that of the CNT-Al_2O_3 hybrids. In order to well disperse these particles, we manually added them into the neat resin and then added the resulting suspension to a lab scale three-roll mill for final high shear mixing. The gap distance between the three rollers and the roller spend was set according to the particle size. The detailed processing methods have been stated in the last part. The prepared epoxy suspensions were collected and then mixed with the added the harder with a mechanical stirrer for 10 min.

3.2.2.2. Fabrication of composite laminate

The glass fabric/epoxy composite laminates were fabricated by using an autoclave after typical manual hand layup and vacuum bagging of plies, then hot compression techniques. In our research, the volume percentage of the glass fiber fabric in the composite laminate is set about 50%. The glass fiber layers were properly stacked into four plies and the orientation of fiber within the glass fabric was kept constant without alternating warp direction. The epoxy suspensions prepared above was spread uniformly on each fabric layer. After the infusion, the preformed composites were put into a vacuum bag in the autoclave. After completing the degassing process, the laminates were cured under 3 bar at 60^{o}C for 2h in the autoclave. Elevated temperature was selected 5^{o}C/min to reduce the curing period and production time. After curing, the temperature of the hot press was gradually reduced at a rate of 2^{o}C/min to avoid the unwanted shrinkage in the laminates. Finally, the cured panel was taken out and post cured in an oven for 15 h at 60 ^{o}C under atmospheric pressure. The final thickness of the panel was measured to be about 1.1 mm. The schematic in Fig. 3-1 shows the fabrication of the glass fabric reinforced epoxy composite laminates.

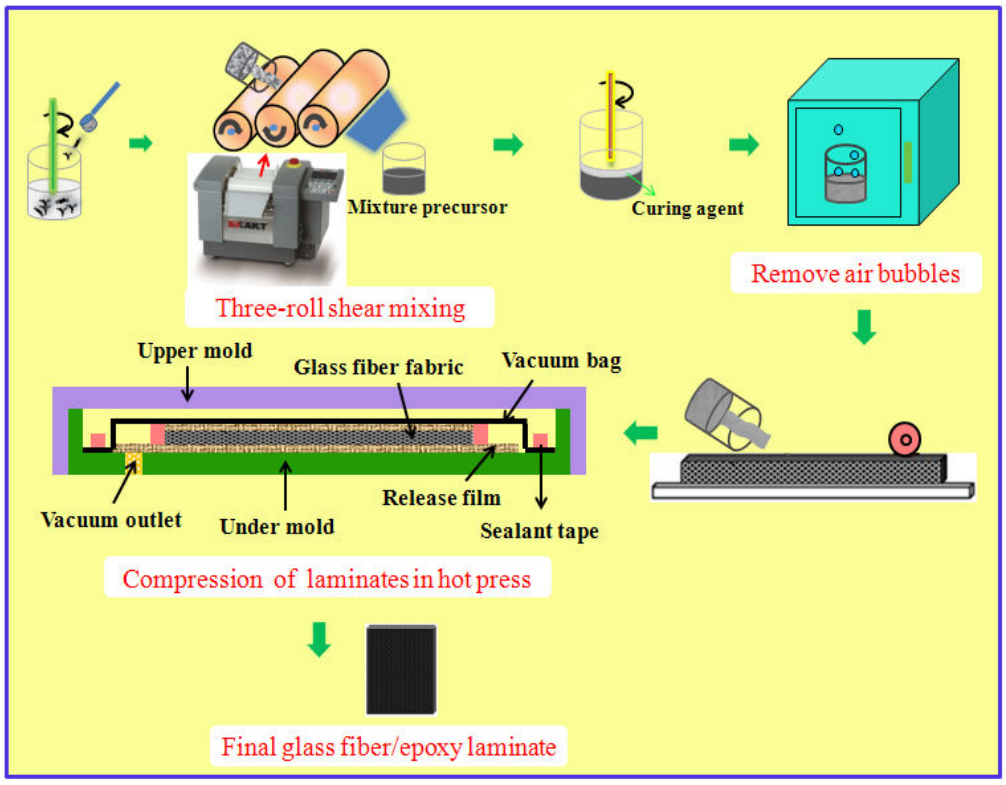

Fig.3-1 *Schematic of the preparation process of the glass fiber/epoxy laminates.*

3.2.3. Characterization and instruments

3.2.3.1. Micrographic analysis

Optical microscopy (OM) and Scanning Electron Microscope (SEM) observations were conducted to investigate the reinforcement dispersion and the local failure mechanisms in the fractured composites. The samples used for microscopic analysis were cut from the failure region of the fractured specimens and then polished using the grit abrasive wheel.

3.2.3.2. Mechanical characterization

Mechanical tests of the glass fabric/epoxy composites were performed on a universal testing machine (Instron 5000) equipped with a 25 KN load cell for the quasi-static tensile tests, and with a 5 kN one for the flexural testing. From each composite panel, the tensile and flexural specimens were cut using garnet-abrasive-assisted water-jet. The tensile tests were performed according to ASTM D3039 standard and the specimen dimensions were 160 mm

in overall length and 12.7 mm in gage width. Dimensions of the specimens for tensile testing are shown in Fig. 3-2. Toward determining the statistics of the modulus, strength and fracture strain of the composites, between three to five samples for each kind of composites are tested under the same condition.

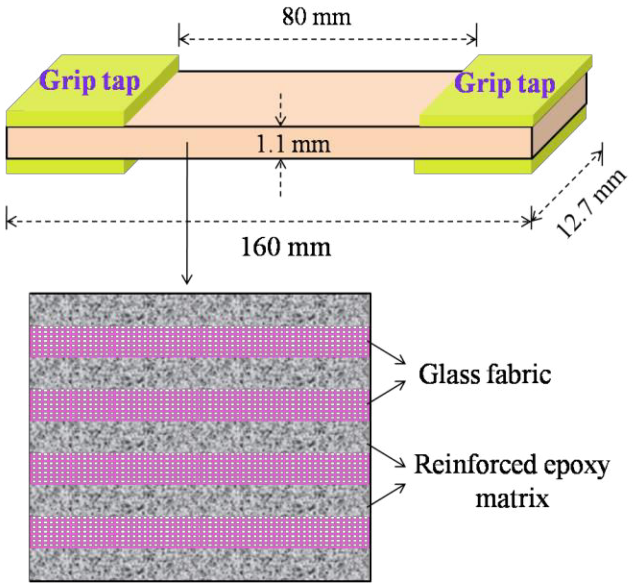

Fig.3-2 *Schematic of the glass fabric/epoxy specimens for tensile testing.*

Flexural modulus was calculated from the slope of the tangent to initial straight line portion of stress-strain plot. It was determined by the following equation Eq. 3-1:

$$\text{Flexural modulus}=\frac{\text{slope of tangent}\times(\text{span length})^2}{4\times width\times(thickness)^2} \qquad 3\text{-}1$$

The maximum stress at failure on the tension side of a flexural specimen was considered as the flexural strength of the material. The flexural strength in a 3-point flexural test was determined using Eq. 3-2:

$$\text{Flexural strength}=\frac{3\times\text{peak load}\times\text{span length}}{2\times width\times(thickness)^2} \qquad 3\text{-}2$$

3.2.3.3. Thermo-mechanical characterization

Thermo-mechanical properties of the glass fabric/epoxy composite were determined

using dynamic mechanical analysis (DMA). It was conducted using a dynamic mechanical analyzer (DMA 242c, Germany) under three-point bending mode from 30 ^{o}C to 180 ^{o}C at a heating rate of 3 ^{o}C /min and a frequency of 1.0 Hz in nitrogen atmosphere. The samples with dimensions ~ 60 mm in length and ~ 10 mm in width were tested. The storage modulus (E'), loss modulus (E'') and the loss tangent (tan δ) were determined as a function of the temperature. Between three to five samples for each kind of composites were tested. The maximum point on the tan δ curve was chosen as the glass transition temperature (T_g) of the composites. The storage modulus and glass transition temperature achieved from the DMA curves were used to evaluate the viscoelastic and damping properties of the composites.

3.2.3.4. Electrical conductivity measurement

The alternating current (ac) conductivity of the composites was measured using a precision impedance analyzer (Agilent 4294A) over the frequency range 10^2~10^6 Hz at room temperature. The measurements were performed by using the rectangle specimens with dimensions of 1.1×10×10 mm. Prior to the measurements, the silver paste electrodes were applied to both sides of the samples in order to reduce the contact resistance.

3.2.3.5. In situ sensing behavior

To determine the self-sensing behaviors of the composites, *in situ* electrical resistance measurements were performed for monitoring the deformation evolution of the composites. A Keithley 2400 voltage-current meter was used to measure the in-plane volume electrical resistance of the specimens by sourcing a constant voltage and measuring the current using a four point technique. Prior to the electrical measurements, the silver paste electrodes were also applied on both sides of the samples. Due to the nature of the electrically percolative samples, the contact resistance is very small relative to their overall resistance. The electrical resistance data were *in situ* recorded using software LabView.

3.3. Morphologies of the reinforcements

The SEM morphology of the CNT-Al_2O_3 hybrids is demonstrated in Fig. 3-3a. It can be seen that the well-aligned CNTs generally form into symmetric six-orthogonal branches on

the surface of the spherical Al_2O_3 particles, due to their specific crystallographic structures. The CNT grown on the substrates were with a length ranging from 20 to 25μm. The CNT length and density can be adjusted by the CVD conditions, such as growth temperature, time and hydrogen ratio. The morphology of the glass fabric as-received is shown in Fig. 3-3b.

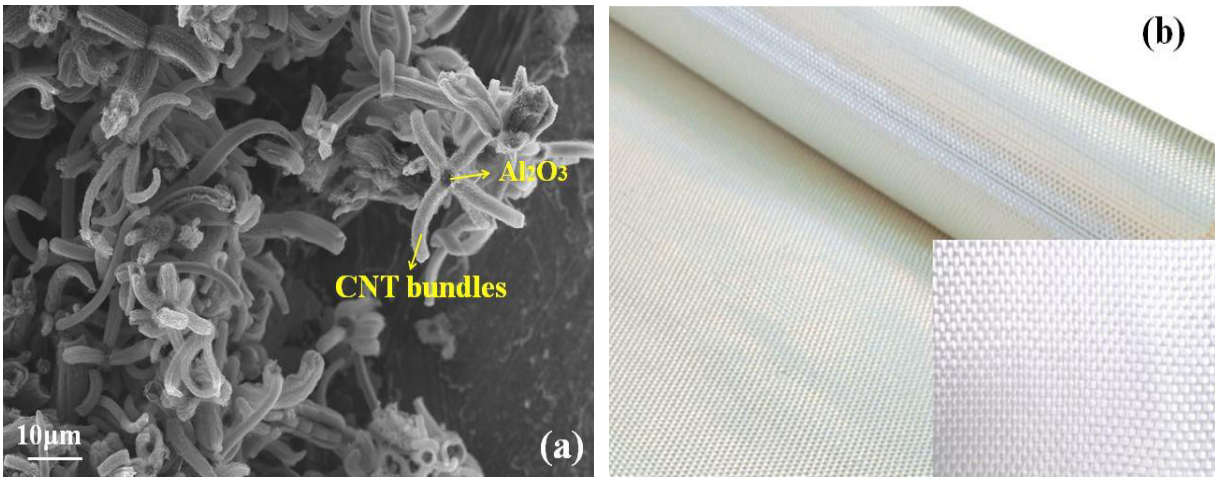

Fig.3-3 *Morphologies of the reinforcements in the composite laminates (a) SEM image of the CNT-Al_2O_3 hybrids; (b) Optical images of the glass fabric.*

Fig. 3-4 shows the distribution state of the CNT-Al_2O_3 hybrids in the epoxy matrix. The SEM observation reveals that the hybrids are well dispersed in the epoxy matrix and their original architectures are almost retained, endowing controlled CNT layout. And the Al_2O_3 microparticles are surrounded in the center by the CNTs, demonstrating symmetric hybrid structure. Besides, most of the CNTs retain aligned in the epoxy matrix at their actual lengths instead of curved states, confirmed by the SEM micrograph at high magnification (Fig. 3-4c). In this case, the nanotubes may break with low extraction lengths because most of them are coated by a matrix layer. It can be viewed that the dispersion states of the hybrids can ensure large contact area and good interfacial interaction between the matrix and CNTs. A good dispersion not only makes more filler surface area available, but also prevents aggregation of the filler acting as stress concentrators and the slippage of nanotubes during applied loading. Therefore, it is expected that the mechanical properties of the composites could be improved by addition of the hybrids. In addition, the introduction of the special uniform CNT networks are expected to be utilized as *in situ* damage sensors in the multiscale glass fabric/epoxy

composite laminates.

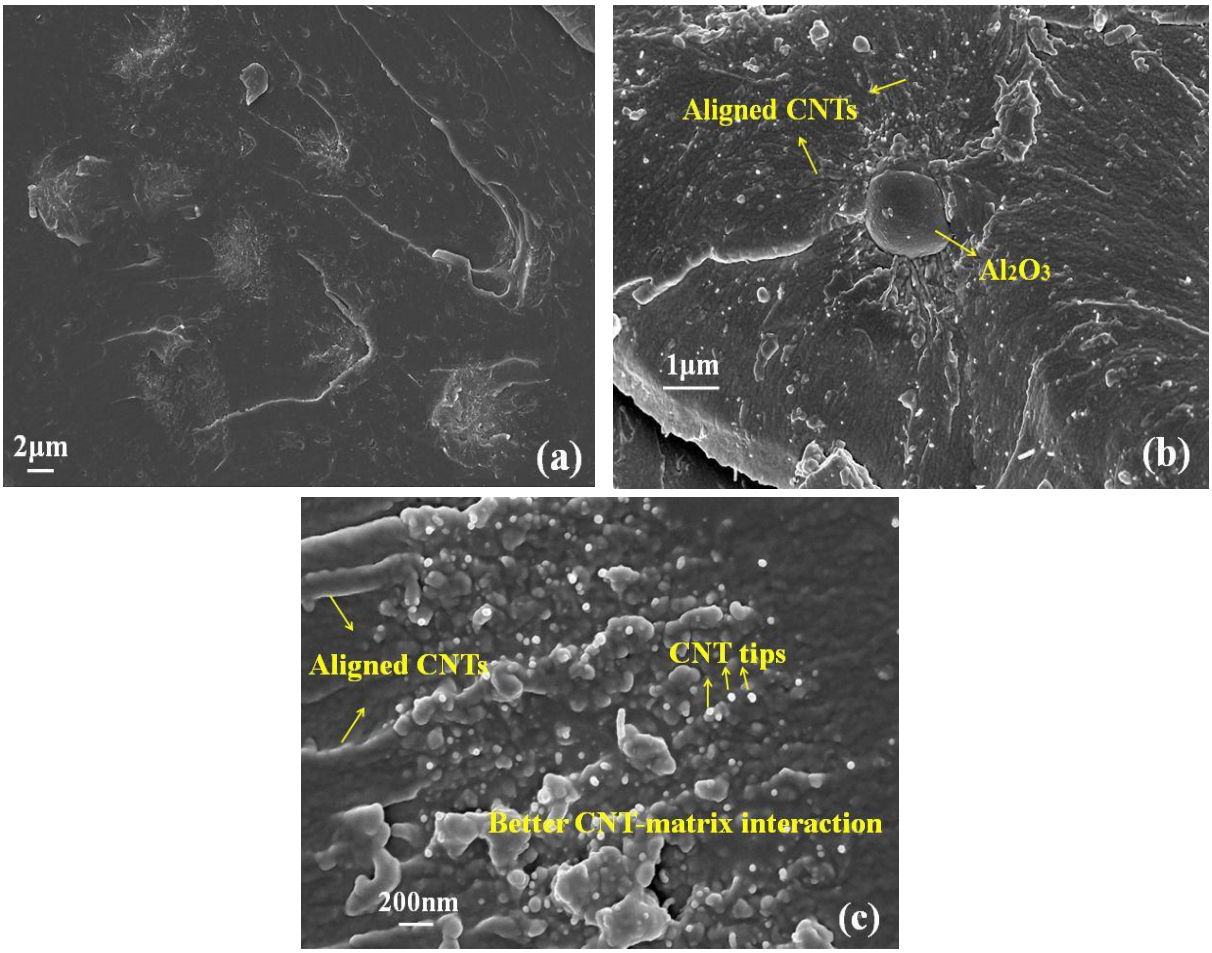

Fig.3-4 *SEM images of the dispersion of CNT-Al_2O_3 hybrids in the epoxy matrix at lower magnification (a) and (b); aligned CNTs grown on Al_2O_3 at high magnification level (c).*

3.4. Electrical properties of the glass fabric/epoxy composites

The ac conductivity measurements of the composites were performed in the frequency range between 10^2 and 10^7 Hz. The ac conductivities of the glass fabric/epoxy composite laminates with and without the nanofillers as function of frequency in the through thickness and in-plane directions are shown in Fig. 3-5a and b, respectively. It can be clearly seen that the conductivities are enhanced in both in-plane and through-thickness directions, indicating the effect of matrix modification by incorporation of nanofillers on the electrical properties of the laminates.

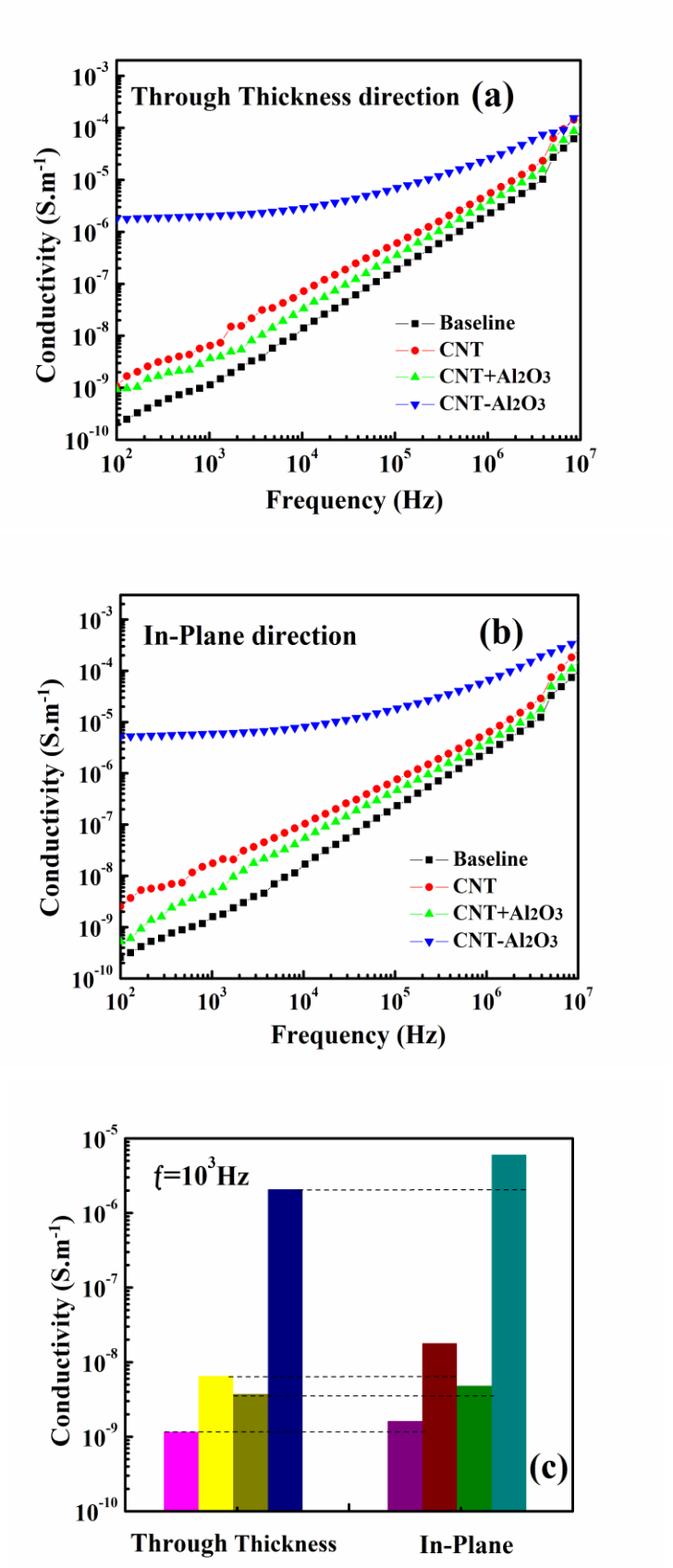

Fig.3-5 *AC electrical conductivities of the glass fabric/epoxy composite laminates with and without*

nanofillers as function of frequency in the range of 10^2 to 10^7 Hz through the thickness direction (a) and in-plane direction (b); comparative study of the ac conductivities of these composites in the two directions at $f=10^3$ Hz.

The resulting conductivities of the baseline laminates and the laminates reinforced with three kinds of nanofillers at $f=10^3$ Hz in the two directions are summarized in Fig. 3-5c. It is worth noting that the conductivities of the laminates containing 0.5 *wt.*% CNT-Al_2O_3 hybrids are 3 ~ 4 orders of magnitude higher than that of the reference samples for both in-plane and through-thickness directions, up to values on the order of 10^{-5} ~ 10^{-6} S/m. This is attributed to the formation of a percolating conductive nanotube networks in the material. Moreover, the addition of CNT-Al_2O_3 hybrids can easily bridge the insulating epoxy interlaminar region between plies. In this case, the well dispersed CNTs and the distinctive architecture formed by the multiscale hybrids play an important role in determining the significantly improved conductivity. However, as shown in Fig. 3-5c, for all the composites with or without nanofillers, the through-thickness conductivity is turned out to be lower than the in-plane value. The anisotropy observed is due to the differences between the resistivity of the epoxy and glass fibers and the geometry of the glass fibers which form a continuous path in the laminate plane whereas discontinuous path across ply interfaces. The conductive epoxy/CNT regions will be continuous in the in-plane direction at the layers of the fabric, not influencing by the insulating glass fiber. However, the conductive epoxy/CNT regions are interrupted by the glass fibers in the through thickness direction, resulting in a serial configuration which is influenced more strongly by the low conductivity phase. The presence of insulating glass fiber reinforcements in plane precludes the formation of the conductive paths, which could explain the lower conductivities in the through-thickness direction.

The Rule of Mixture (ROM) is generally used to predict the properties of the composites made up of continuous and unidirectional fibers. According to ROM, the conductivity of the glass fiber/CNT-Al_2O_3/epoxy composites in the parallel directions to the fibers calculated using the equations given by:

$$\sigma_{para} = \sigma_f V_f + \sigma_m \left(1 - V_f\right) \qquad 3\text{-}1$$

Here σ_{para} is the conductivity of the composites in the parallel direction; V_f is the volume

fraction of the fiber; σ_f is the conductivity of the glass fiber; σ_m is the conductivity of the CNT-Al_2O_3/epoxy composite matrix. The experimental results obtained from Fig. 3-5c and the predicted values are compared in Table 3-1. As demonstrated in Table 3-1, there is not obvious difference between the experimental values of $\sigma_{in\text{-}plane}$ and calculated results of σ_{para}. The conductivity of the glass fiber/CNT-Al_2O_3/epoxy multiscale composites is dependent on that of the CNT-Al_2O_3/epoxy matrix.

Table 3-1

σ_m	5.7×10^{-6} S/m
σ_f	1.0×10^{-13} S/m
$\sigma_{in\text{-}plane}$ (Experimental)	5.97×10^{-6} S/m
σ_{para} (Calculation)	2.85×10^{-6} S/m

3.5. *In situ* sensing behavior of the multiscale glass fabric/epoxy composites with CNT-Al_2O_3 hybrids

Fig. 3-6a demonstrates the typical electrical resistance change as function of the applied strain for the composite laminates during a quasi-static tensile test until ultimate failure. Fig. 3-6b shows the crack density as a function of the applied strain. When the strain reaches a certain value, the samples were unloaded. After polish, the crack number was counted under SEM. For the non-transparent composites, the *in situ* observation of the crack propagation is a challenging. As shown in Fig. 3-6a, it is clearly seen that the resistance increases all the time and it can be classified into three stages according to the different slopes of the resistance curves, which implies the varying damage mechanisms existed in the three stages. The macroscopic damage mechanisms of the laminates generally include the matrix micro-cracking, localized warp fiber fracture, weft fiber pull-out, and delamination along the middle plies. SEM and optical micrographs of the damaged specimens are shown in Fig. 3-7. Fig. 3-8 schematically illustrates the damage propagation in different stages of the laminates.

In the initial stage (I), the resistance response with the strain is almost linear. At the

onset of the loading, the incipient matrix-dominated damages such as the microcracks or flaws are initiated in the regions between the glass fiber and matrix. As demonstrated in Fig. 3-7a and Fig. 3-8a, the microcracks were found propagating along the fiber-matrix interface or through the glass fiber plies. Fig. 3-7b shows a microcrack passing through a hybrid. The formation of these microcracks causes the damage of the CNT conductive networks. In this stage, the crack density increases slightly due to the initiation of some microcracks (Fig. 3-6b). With the gradual increase of the strain in the following stage, when $\varepsilon_1 < \varepsilon < \varepsilon_2$, one can see that the electrical resistance begins to deviate from the initial linear resistance-strain curve and increases more evidently than in the previous stage. In this case, some of the matrix microcracks propagate which results in the interfacial debonding. The increased steep growth in this stage is attributed to the accumulation of the matrix-dominated damage (Fig. 3-6c), the debonding of fiber-epoxy interface (Fig. 3-6d) and the transverse crackings (Fig. 3-6e and g). These factors possibly result in more broken-up of the conducting paths in the composites. However, when it enters into the III stage ($\varepsilon>\varepsilon_2$), the slope of the resistance change curve is decreased compared to the II stage, suggesting the slight increase of the resistance. Besides the debonding of fiber-epoxy interface and transverse crackings, the fiber breakage along the direction of applied load and interply delamination will also take place, as shown in Fig. 3-6f and Fig. 3-8c. These factors further accelerate the broken of conductive networks. However, with regard to the decreased slope, it is worth noting that the Poisson contraction of the matrix possibly plays an important role on the evolution of the conductive networks, which possibly lead to the closing of the microcracks in the matrix. Then the two neighboring CNTs may be situated close enough to endow the tunneling effect, enabling the reformation of conductive networks. Moreover, the orientation of the CNTs grown on the Al_2O_3 microparticles resulted from the increasing strain is also responsible for the formation of the conductive networks. As a result, during the III stage, there exist two kinds of factors which mainly influence the conductive networks in the matrix. One can give rise to the increasing resistance and the other often causes the decreasing resistance. But the former has much greater effect on the resistance change than the latter, which could be used to explain the consistently slight increase of the resistance.

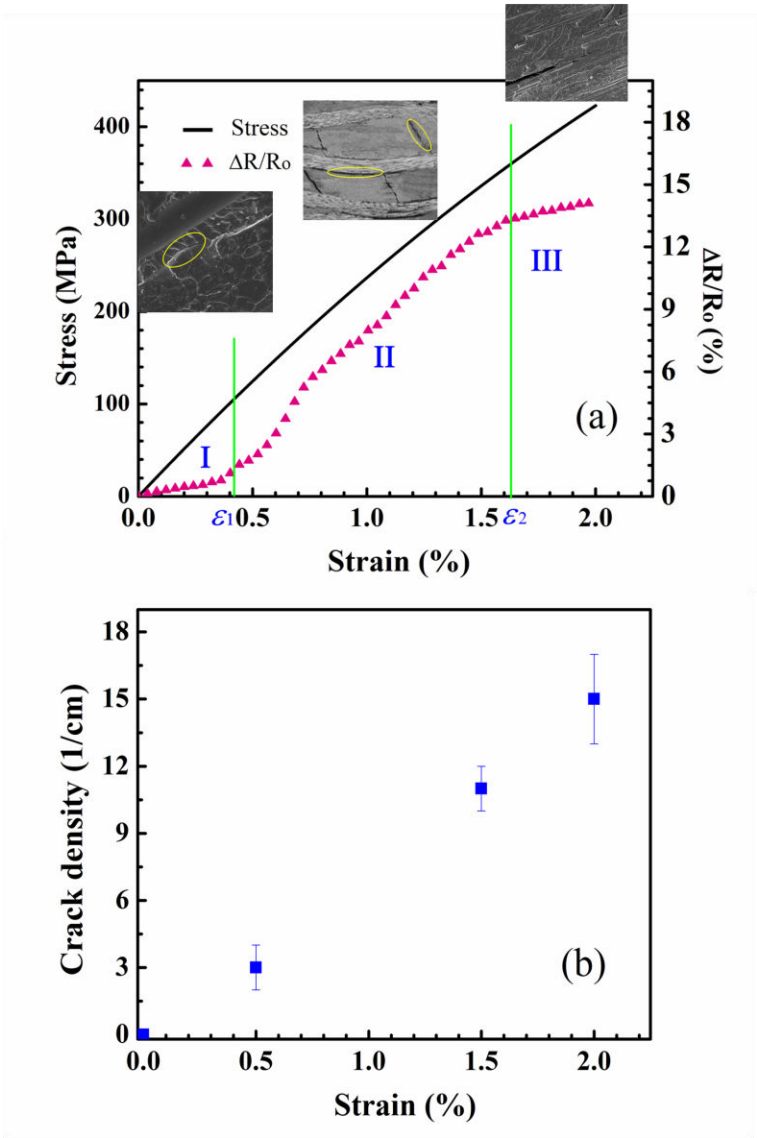

Fig. 3-6 *Piezoresistive behavior of the multiscale glass fabric reinforced epoxy composites with CNT-Al_2O_3 hybrids.*

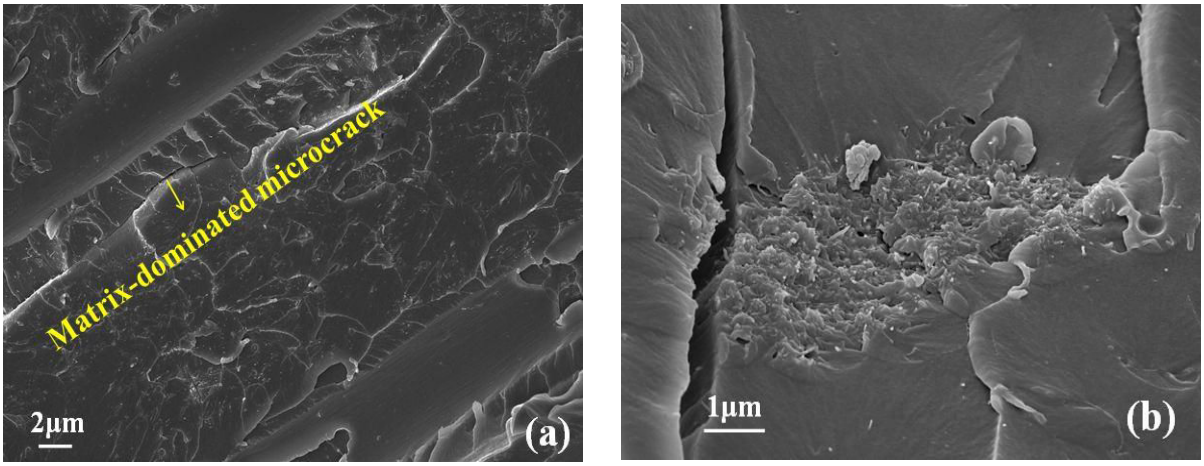

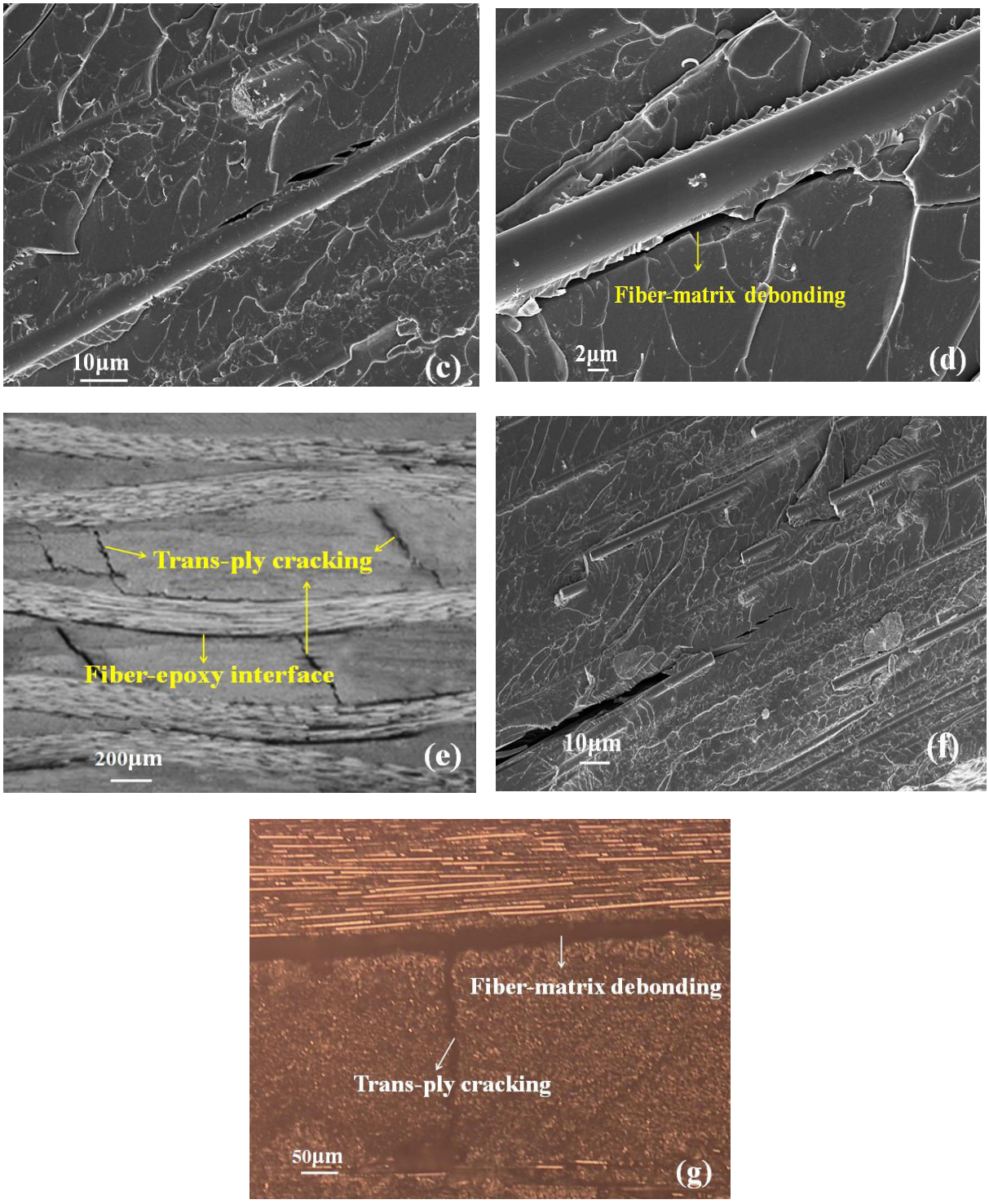

Fig. 3-7 *Damage evolution in the multiscale glass fabric/epoxy/CNT-Al_2O_3 composites during tensile loading (a) ~ (f) SEM images; (g) Optical microscopy.*

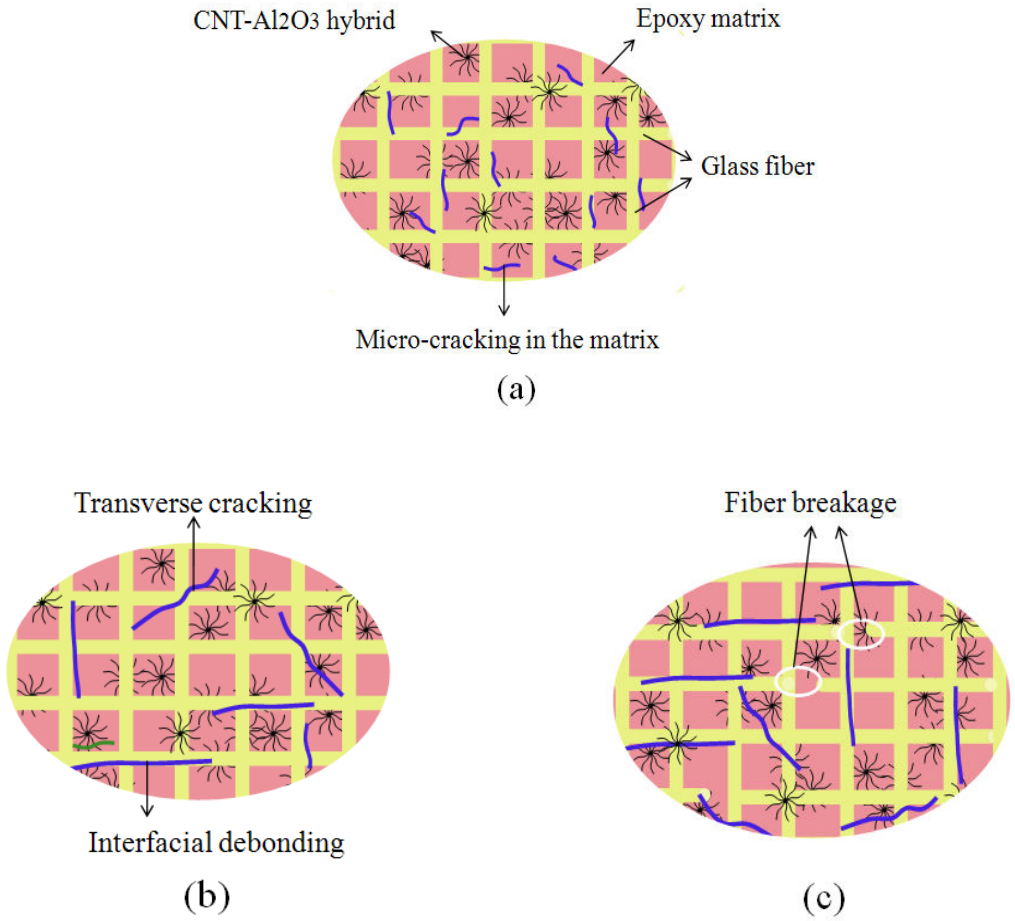

Fig. 3-8 *Schematics of the damage evolution in the multiscale glass fabric/epoxy/CNT-Al_2O_3 composites during tensile loading.*

The different *in situ* sensing behaviors of the CNT-Al_2O_3/epoxy composite matrix and the glass fabric/CNT-Al_2O_3/epoxy multiscale composites are compared in Fig. 3-9 (with 0.5 *wt.%* CNT-Al_2O_3 of the matrix for both two systems). It can be clearly seen that the introduction of glass fibers plays an important role on the mechanical properties of the composites and the *in situ* electrical resistance change during tensile loading. The tensile modulus of the multiscale composites is greatly improved, but the fracture strain is reduced compared to the CNT-Al_2O_3/epoxy matrix. Besides, for the glass fabric/CNT-Al_2O_3/epoxy composites, the *in situ* resistance shows no obvious decrease, but the sensitivity of the *in situ* sensing behavior is larger. In this case, due to the addition of glass fiber, the volume fraction of CNT-Al_2O_3 hybrids of the total volume of the matrix and reinforcements (glass fiber) is lower. Under the same strain, the conductive networks are easy to be broken up. And the

damage of glass fiber also influences the change of conductive networks. It can be considered that the deformation (strain) of the composites is mainly contributed to the reorientation of CNTs, resulting in the reformation of conductive networks and the decrease of the *in situ* resistance.

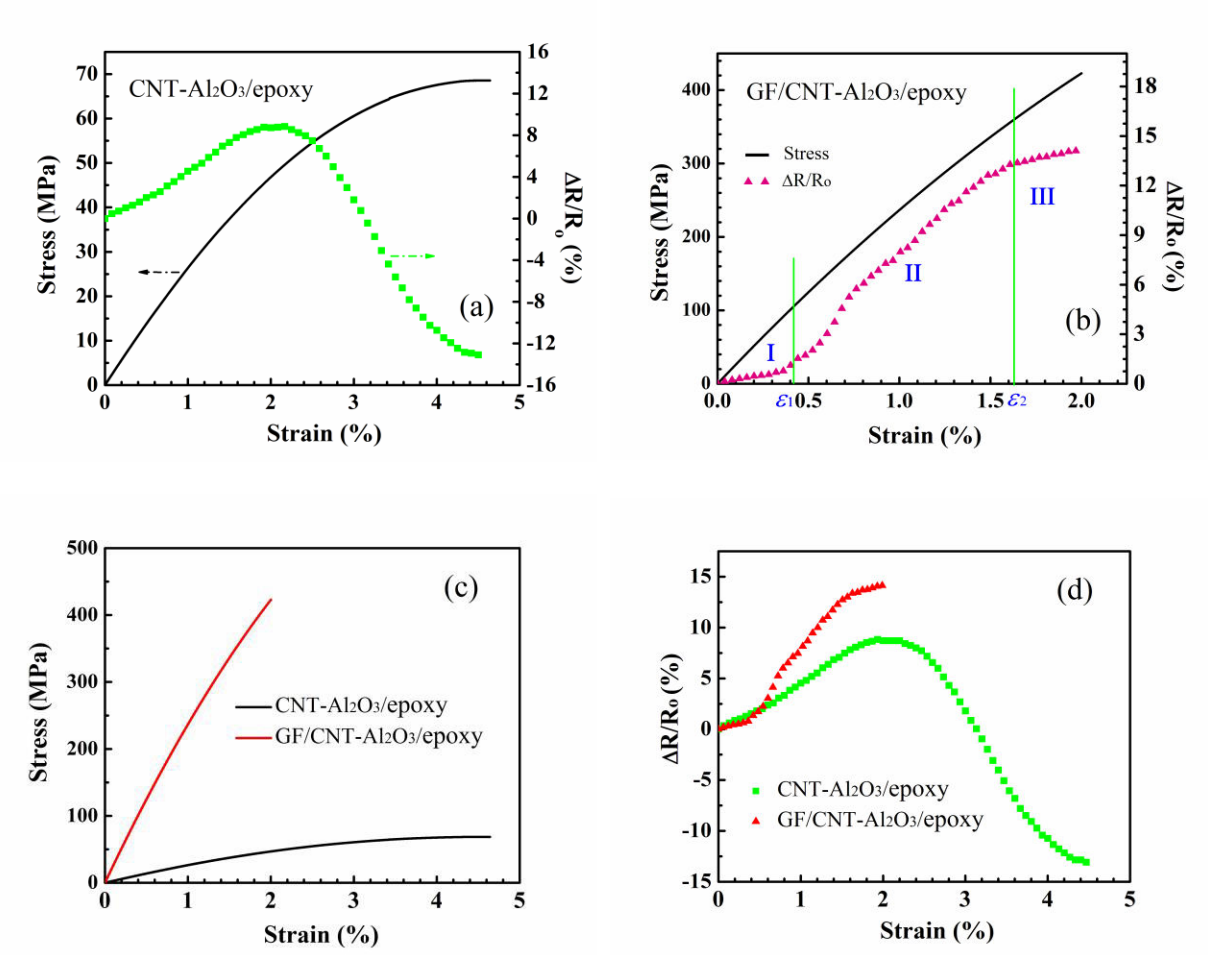

Fig. 3-9 *Comparison of the in situ sensing behaviors of the CNT-Al_2O_3/epoxy composite matrix and the glass fabric/CNT-Al_2O_3/epoxy composite laminate.*

3.6. Mechanical properties of the glass fabric/epoxy composites

3.6.1. Flexural properties of the glass fabric/epoxy composites

Fig. 3-10 demonstrates the typical stress-strain curves of the glass fabric reinforced neat epoxy and the modified epoxy matrix with the same concentration (0.5 *wt.*%) of *ran*-CNTs, *ran*-CNT+Al_2O_3 and CNT-Al_2O_3 hybrids under three-point bending test. In comparison to

the reference sample, different levels of improvement of the flexural properties are observed in the composites with these fillers incorporated as reinforcements. The experimental results obtained from the stress-strain curves are summarized in Figs. 3-10b and c. The flexural modulus and strength of the glass fabric/epoxy composite laminates reinforced with the CNT-Al_2O_3 hybrids are more evidently increased. Their average flexural modulus is up to about 26 GPa and demonstrates ~ 19% increase over that of the reference sample, whereas there are only moderate enhancements of the flexural modulus in the other two kinds of composites. Likewise, their average flexural strength also shows a maximum increment (~13%) compared to that of the reference sample. It indicates that reinforcement provides a mechanism of matrix strengthening, such as crack bridging phenomenon, which is more effective in the case of adding CNT-Al_2O_3 hybrids to the matrix.

From the SEM images in Fig. 3-4c, it is clearly seen that the bright dots, i.e., the CNTs, are well dispersed in the matrix. The well-aligned CNTs grown on the Al_2O_3 microparticles retain in the matrix at their actual lengths instead of curly state. This dispersion state is not conducive to the formation of flaws in the matrix. Besides, the unique three-dimensional architecture of the CNT-Al_2O_3 hybrids leads to large surface contact and strong molecular coupling between CNTs and the matrix. The CNTs are well wrapped by the host polymer, suggesting the existence of a very thin polymer layer embedded into the interspaces between any two aligned CNTs. The hybrids play an important role in the toughening of matrix. In addition, compared to neat epoxy, the introduction of CNT-Al_2O_3 hybrids cannot easily result in more increased viscosity, which is different from other fillers. This is helpful for the adhesion between the modified matrix and the glass fiber. Hussain et al. [211] proposed that the addition of nano-sized fillers to an epoxy matrix caused higher thermal residual stresses on the surface of the fibers, which could increase the fiber-matrix interfacial bonding. These factors play an important role in achieving efficient stress transfer from the matrix to reinforcement, leading to the improved mechanical properties. SEM images of the delaminated surface of the glass fabric reinforced epoxy composites were illustrated in Fig. 3-11. As shown in Fig. 3-11a, the composites made from neat epoxy exhibited remarkable river stripes of brittle fracture in the matrix, including some islands of matrix and the matrix among the fibers. The cracks propagated along the fiber-matrix interface, also reflecting the

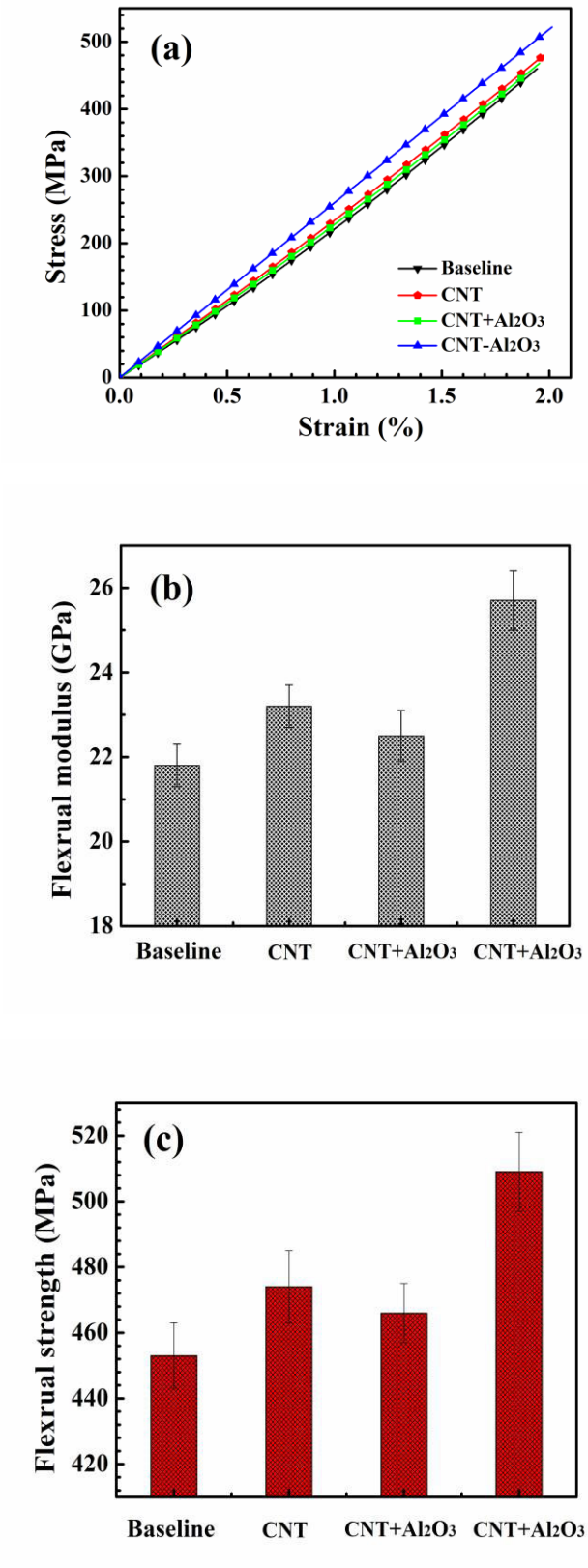

Fig. 3-10 *Flexural properties of the glass fabric/epoxy composites with and without nanofillers (a) typical stress-strain curves; (b) and (c) the obtained experimental results of flexural modulus and strength.*

weak fiber-matrix interfacial adhesion. Debonding between the fibers and the epoxy matrix due to weak interfacial bonding is also obviously observable. As shown in Fig. 3-11b~c, Fig. 3-7a and c, the composites with the CNT-Al_2O_3 hybrids demonstrated a rougher matrix surface than those with the neat epoxy. Interconnecting CNT-Al_2O_3 hybrids was observed between the neighboring glass fibers, greatly improving the matrix toughness. That is, the composite surfaces showed a higher interaction between the matrix and the fibers. These results indicate that the incorporation of nanofillers into the conventional fiber composites could create the anchor effect against the matrix cracking, which enhances their mechanical properties.

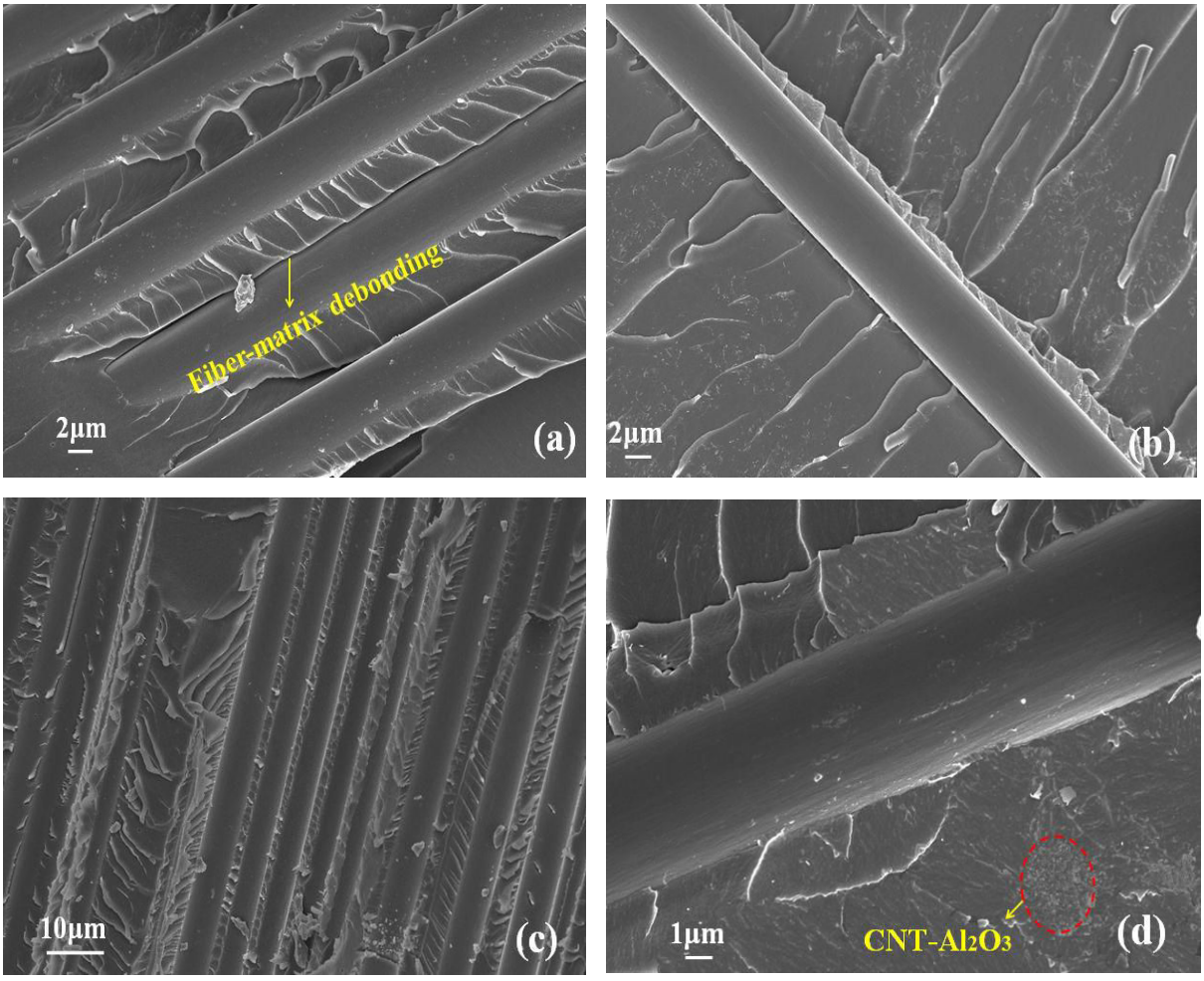

Fig.3-11 *SEM images of the surfaces of the glass fabric/epoxy composites (a) without nanofillers; (b) with ran-CNTs; (c) with CNT-Al_2O_3 hybrids; (d) the enlarged image of Fig. 3-9c showing the toughened epoxy matrix by the CNT-Al_2O_3 hybrids.*

A further examination of the fracture surface of the glass fabric/epoxy composites with the CNT-Al_2O_3 hybrids is demonstrated in Fig. 3-12. For the composites made from the neat epoxy, it is clearly seen that there is fiber-matrix debonding on their fracture surface and their failure surface is brittle-like (Fig. 3-12a). The matrix detached from the fiber surface due to the weak adhesion with smooth fiber surface. The interfacial debonding of the matrix from the fiber can be regarded as the dominant mechanism for flexural failure of composites without CNT-Al_2O_3 hybrids. For the composites containing the CNT-Al_2O_3 hybrids, one can see from Fig. 3-12b that better fiber-matrix bonding was observed from many locations of the fracture surfaces of the specimens and the cracks propagated through the breaking of the fibers but not along the fiber-matrix interface, suggesting the better adhesion between the fibers and the matrix. Besides, the glass fibers as continuous reinforcement tend to be broken rather than being pulled out, implying desirable ductile-like features in the modified matrix and ensuring the effective load transfer from the modified matrix to glass fibers.

A detailed investigation of the damages in the hybrids filled regions from the higher resolution SEM micrograph (Fig. 3-12c) revealed that the micro-cracks were stabilized by the bridging of the aligned CNT bundles, which can absorb a substantial amount of energy and stop or slow down the crack propagation, making the system tougher and stronger. We can see that several nanotubes bridged a micro-crack of several hundred nanometers. Due to the nanotube bridging, the micro-cracks were arrested and prevented from developing into larger and more harmful cracks. Though numerous micro-cracks were created in the epoxy matrix, the growth of the micro-cracks was arrested by the bridging or prevented by the hybrids. Thus, the CNT networks which serve as microcrack arrester enhance the composites toughness through the bridging mechanism in resin-rich region. The above mechanisms contributed to the enhancement of flexural modulus and strength. The SEM observations are in agreement with the experimental results of the mechanical properties. The introduction of the CNT-Al_2O_3 hybrids seems to be responsible for the increase in the flexural performance of the multiscale glass fiber reinforced composites.

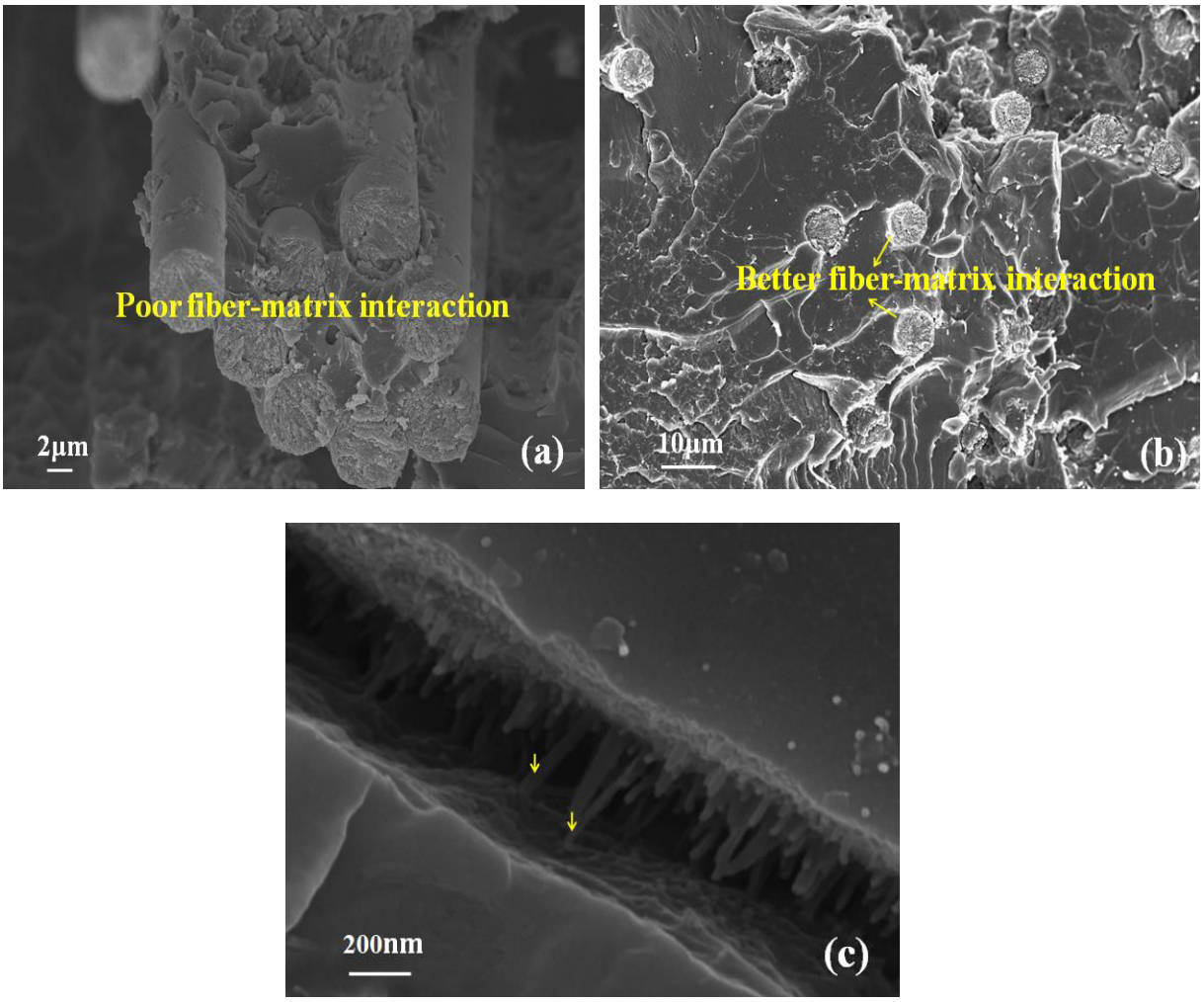

Fig.3-12 *SEM images of the fracture surface under tensile failure of the glass fabric reinforced pure epoxy matrix (a); and CNT-Al_2O_3 modified epoxy matrix (b).*

3.6.2. Tensile properties of the glass fabric/epoxy composites

Tensile testing was performed to evaluate the effect of addition of nanoreinforcement on the mechanical properties of glass fabric reinforced laminates. The representative tensile stress-strain curves of the reference composite and the laminates containing 0.5 *wt.%* *ran*-CNTs, *ran*-CNTs+Al_2O_3 mixture and *ran*-CNTs-Al_2O_3 hybrids are plotted in Fig. 3-13a for comparison. The tensile modulus and strength obtained from these curves are collected in Fig. 3-13b and c. In general, the tensile modulus and strength of the studied composites was not greatly affected by the addition of nanoreiforcements at the experimental contents. Only

slight increase of the tensile properties in all tested multiscale composites over the neat material could be observed, though there are higher values of the tensile modulus and strength in the case of the composites reinforced with CNT-Al_2O_3 hybrids. These results show that the method used to incorporate the nanoreinforcements into the composite matrix has not diminished the structural integrity of the glass fiber composite for the tested CNT contents. Tensile properties are dominated by the continuous fiber when they are measured in the longitudinal direction. Therefore, the addition of the nanoreinforcement had produced defects during manufacturing, but its incorporation cannot change appreciably the properties with regard to those obtained for the neat resin composite material. Some authors have observed that it is difficult to achieve higher values of elastic modulus and even small drops have been measured with regard to the carbon fiber/epoxy composites reinforced with CNTs.

For the plain-weave composites, the longitudinal and transverse yarns (warp and weft) pass over and under each other alternately. The longitudinal yarns are subject to uniform strains whereas the strains of transverse yarns are insignificant. The longitudinal yarns are under combined effect of bending and stretching due to the crimp. Based on the Rule of Mixture (ROM), the longitudinal modulus and transverse modulus of the yarns could be respectively calculated as follows [212, 213]:

$$E_{II} = V_f E_f + E_m \left(1 - V_f\right) \qquad 3\text{-}2$$

$$E_{\perp} = \frac{E_f E_m}{V_f E_m + \left(1 - V_f\right) E_f} \qquad 3\text{-}3$$

Here E_1^y is the longitudinal modulus of the composites; E_2^y is the transverse modulus of the composites; V_f is the volume fraction of the fiber; E_m is the Young's modulus of the matrix; E_{11} is the longitudinal modulus of the fiber. The underlying assumptions of these rules are: the reinforcements are uniformly distributed in the matrix; perfect bonding between the reinforcements and matrix; the matrix and reinforcements behave as perfectly linear elastic materials. The transverse modulus of the composites can be described more accurately using the Halpin-Tsai equation:

$$E_{\perp} = \frac{\left(1 + \xi \eta V_f\right) E_m}{1 - \eta V_f} \qquad 3\text{-}4$$

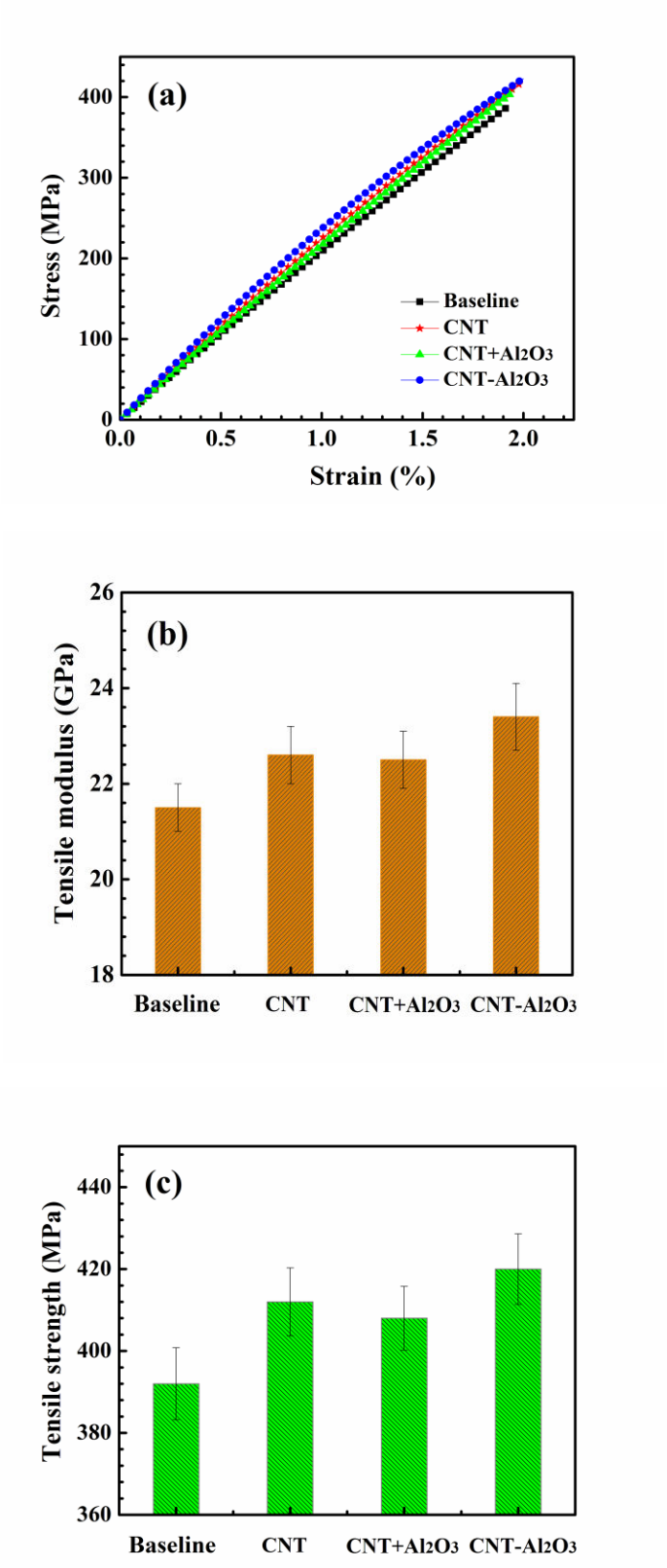

Fig.3-13 *Tensile properties of the glass fabric/epoxy composite laminates with and without nanofillers (a) typical stress-strain curves; (b), (c) the obtained experimental results of flexural modulus and strength;*

(d) Improvement of the tensile modulus and strength in the composites reinforced with different fillers.

In our research, E_m is the Young's modulus of the epoxy matrix reinforced with CNT-Al_2O_3 hybrids; V_f is the volume fraction of glass fiber (V_f =0.5); E_f=70GPa. If the effect of weave on the modulus was neglected, the modulus of the composites can be calculated as follows:

$$E_C = (E_{11} + E_{\perp})/2 \qquad 3\text{-}5$$

The experimental and predicted Young's modulus of the GF/epoxy composites with CNT-Al_2O_3 hybrids (0.5 *wt.*%) are listed in Table 3-2.

Table 3-2

$E_{CNT\text{-}Al2O3/epoxy}$	2.6 (±0.1) Gpa
E_c (Experimental)	23.4 (±0.7) Gpa
E_{11}	36.3 GPa
$E_{\perp}$ (ROM)	5.0 GPa
$E_{\perp}$ (Halpin-Tsai)	8.9 GPa
E_c (Predicated)	20.6 GPa

As shown in Table 3-2, the Young's modulus of the GF/CNT-Al_2O_3/epoxy multiscale composites is obviously larger than that of the CNT-Al_2O_3/epoxy composite matrix, showing the reinforcing effect of the glass fibers. Noticeably, the predicted Young's modulus of the composites is a little higher than the experimental values. Thus, the crimp of the yarns has less influence on the longitudinal modulus. However, it is lower than the predicted value of the longitudinal modulus.

3.7. Thermomechanical properties of the glass fabric reinforced epoxy composites

The influence of matrix modification by the reinforcements on the thermo-mechanical performance of the glass fiber/epoxy composites laminates was investigated via dynamic mechanical analysis (DMA). The variation of the storage modulus and loss tangent of the composites with and without fillers as a function of temperature was plotted in Fig. 3-14a and b, respectively. The temperature corresponding to the peak value of tan δ is generally considered as glass transition temperature (T_g) of the composites, which is the characteristic temperature signifying the motion of polymer chains. As shown in Fig. 3-14a, by modifying the epoxy matrix, the storage modulus of the laminates was increased both in the glassy and rubbery regions in comparison to the control samples, but it demonstrates much stronger improvement in the glassy than in the rubbery region. The addition of low concentrations of CNT-Al_2O_3 hybrids has improved the elastic properties of the composites at elevated temperatures. This behavior can be contributed to the enhanced CNTs dispersion in epoxy and improved interfacial interactions between CNTs and the epoxy matrix. This interfacial interaction reduces the mobility of the epoxy matrix around the CNTs and results in the observed increase in thermal stability. Besides, the T_g was also found to shift toward higher temperature, suggesting improved thermo-stabilities. This behavior can be ascribed to the effects of interfacial interactions and entanglements between the fillers and epoxy matrix. In the glassy region, the presence of fillers will influence the alignment of the chain segment and molecular chains and thus restrict their movement, resulting in stronger amplitude variation of the elastic properties of the composites. However, above the glass transition temperature, the molecular chain shows intense movement and viscous state. In this case, some polymer molecular could not come into contact with the fillers, decreasing shear force between them. Thus, a relatively slight enhancement of storage modulus was observed in the rubbery region.

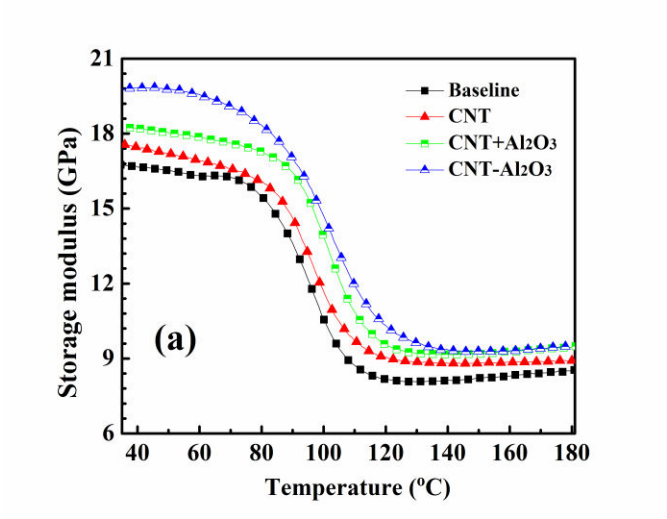

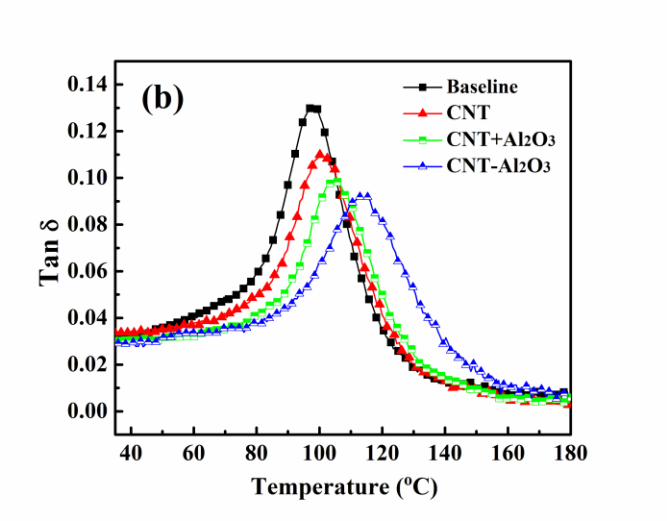

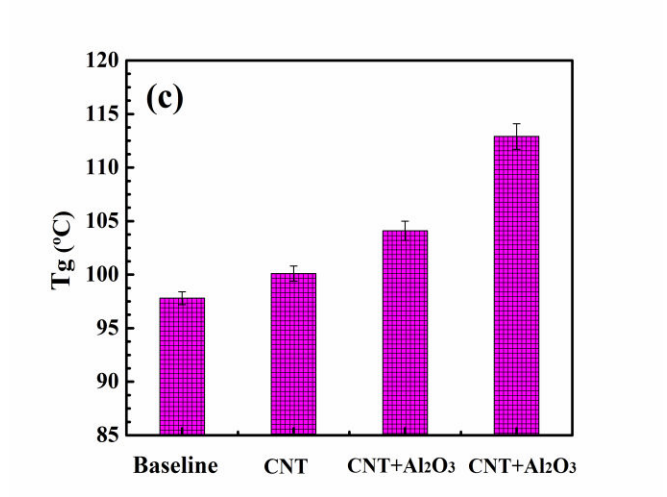

Fig.3-14 *Thermomechanical analysis of the glass fabric/epoxy/CNT-Al_2O_3 composite laminates from DMA results (a) Storage modulus vs. temperature; (b) Loss factor (tan δ) vs. temperature; (c) Glass transition temperature (T_g).*

The gain in thermo-stability could be explained by the fact that the augmentation of cross-linking density resulted from the addition of particles requires a higher temperature to provide the necessary thermal energy to induce the glass transition in the composites. Moreover, the T_g is considered to be sensitive to interfacial interactions between the matrix and fillers. It is worth noting that the introduction of CNT-Al_2O_3 hybrids gave rise to a more remarkable increment of storage modulus. The mean storage modulus values at 50 ^oC and 150 ^oC from the DMA results of the glass fiber/epoxy composite laminates are summarized in Table 3-3. The storage modulus of the glass fabric/epoxy multiscale composites with 0.5 *wt.%* CNT-Al_2O_3 hybrids increases dramatically to 19.8 GPa (at 50 ^oC) in the glassy region, which is 20% larger than that (16.5 GPa) of the reference samples. In addition, one can see that there is more noticeable shift of T_g by addition of CNT-Al_2O_3 hybrids, compared to other fillers. The T_g was shifted from ~ 98 ^oC for control samples to about 113 ^oC for thesamples containing 0.5 *wt.%* CNT-Al_2O_3 hybrids. The addition of 0.5 *wt.%* CNT-Al_2O_3 significantly improved the T_g of the multiscale composites up to 25 ^oC. These results also indicate that the hybrid fillers are uniformly dispersed throughout the polymer matrix and have strong interfacial adhesion with the surrounding matrix. As discussed above in Fig. 3-4c, we can see that the CNTs are wrapped by the host polymer, suggesting the existence of a very thin polymer layer embedded into the interspaces between any two well-aligned CNTs. This is equivalent to a wetting polymer-particle interface, which is proposed to possibly influence the T_g of the composites. Thus, the significant reinforcement of the mechanical properties is primarily contributed to the homogenous dispersion of the hybrids and the strong interfacial interaction between the fillers and matrix.

Table 3-3

Temperature	Storage Modulus (GPa)			
	Baseline	CNT	CNT+Al_2O_3	CNT-Al_2O_3
50^{o}C	16.5	17.2	18.0	19.8
150^{o}C	8.2	8.8	9.2	9.3

3.8. Concluding remarks

In this part, the hybrid multiscale composite laminates based on the plain woven glass fabric and particle reinforcements modified epoxy matrix were fabricated. The influence of particle reinforcements on improving the flexural and thermomechanical properties of the glass fabric/epoxy laminates was investigated with respect to the unmodified composites.

It is worth noting that the multiscale composite incorporated with 0.5 *wt.*% CNT-Al_2O_3 hybrids showed maximum increment in the flexural modulus ~ 19% and flexural strength ~ 13% over that of the reference sample. Similar, from the DMA results, the samples exhibited considerable improvement of ~ 20% in storage modulus at 50 ^oC and an increase of 15 ^oC in glass transition temperature compared to the control samples. In this case, the efficient stress transfer from the CNT-Al_2O_3 hybrids modified epoxy matrix to the glass fiber resulted from the strong fiber/matrix interfacial interaction.

With the addition of 0.5 *wt.*% CNT-Al_2O_3 hybrids, ac conductivities of the composites at f=10^3 Hz are up to values on the order of 10^{-5} ~ 10^{-6} S/m and 3 ~ 4 orders of magnitude higher than that of the reference samples for both in-plane and through-thickness directions, indicating the effect of matrix modification by the nanofillers on the electrical properties of the laminates. It is worth noting that, for all the composites with or without nanofillers, the through-thickness conductivity is turned out to be lower than that in the in-plane direction. This anisotropy observed in the composites is due to the differences between the resistivity of the epoxy and glass fibers and the geometry of the glass fibers which form a continuous path in the laminate plane whereas discontinuous path across ply interfaces.

As multifunctional reinforcements, the CNT-Al_2O_3 hybrids could be utilized as *in situ* damage sensor to monitor the damage evolution of the glass fabric/epoxy composites when they are subjected to uniaxial tensile loading. With the increase of strain, the *in situ* electrical resistance increases all the time until ultimate failure and it can be classified into three stages according to the different slopes of the resistance curve, which implies the different damage mechanisms in the three stages. When $\varepsilon < \varepsilon_1$, the matrix-dominated damages such as the microcracks or flaws are initiated in the region between the glass fiber and matrix. When $\varepsilon_1<\varepsilon<\varepsilon_2$, the accumulation of matrix-dominated damages and the emergence of the transverse

cracking and interfacial debonding contribute to the increased steep growth of the resistance curve. In the III stage, the interfacial debonding, interply delamination and fiber breakage along the strain direction will take place. However, Poisson contraction of the matrix and orientation of the CNT-Al_2O_3 hybrids facilitate the reformation of the conductive networks, leading to the slight increase of the resistance in this stage.

General conclusions and perspectives

General conclusions

This thesis is focused on developing the CNT-microparticle multiscale hybrids with controllable CNT architecture to replace the pristine CNTs as superior multifunctional fillers in the composites. The mechanical, electrical and piezoresistive properties of these hybrids based epoxy nanocomposites and fiber-reinforced composite laminates were investigated in detail. The main results can be concluded as follows:

I. The CNT-microparticle hybrids reinforced epoxy nanocomposites

Three kinds of nano/micro multiscale hybrids with CNTs *in situ* grown on the SiC microplates, graphene nanoplatelets and Al_2O_3 microparticles, i.e., CNT-SiC, CNT-GNP and CNT-Al_2O_3 were used for preparing the epoxy nanocomposites using calendaring method.

The CNT-microparticle hybrids can serve as high-performance structural reinforcements. With respect to the neat epoxy, significantly improved mechanical properties in the CNT-GNP filled nanocomposites were obtained at ultralow hybrid loading (0.5 *wt.%*). The tensile modulus exhibited up to 40% increase and the tensile strength was enhanced by ~36%. It was found that the optimal concentration of the hybrids (f_c) is necessary to achieve the desirable reinforcement effect.

Besides, the CNT-microparticle hybrids can be used as *in situ* sensors. The hybrids filled epoxy nanocomposites also exhibit distinctive self-sensing behaviors for *in situ* monitoring the onset of irreversibly permanent deformation. The *in situ* resistance initially increases to its maximum value and then begins to decrease with the appearance of residual strain and irreversible deformation, which is different from the randomly distributed CNTs filled composites only with monotonic increase of the resistance until their ultimate fracture.

The relationship between hybrid structure (CNT aspect ratio, orientation and substrate morphology) and the mechanical and self-sensing properties was investigated. For the same aspect ratio (1200), the *in-situ* electrical resistance of CNT-SiC/epoxy and CNT-GNP/epoxy

composites increases when $\varepsilon<\varepsilon_c$ and then decreases when $\varepsilon>\varepsilon_c$, which is different from that of the CNT-Al_2O_3/epoxy composites only with monotonic increase. Besides, the self-sensing and mechanical properties of the composites are also strongly dependent on the CNT aspect ratio and organization. With increasing *AR* to 2000 or more, the change of *in-situ* electrical resistance of CNT-Al_2O_3 filled composites becomes similar to that of the CNT-SiC/epoxy and CNT-GNP/epoxy composites. The tensile modulus and strength of CNT-Al_2O_3/epoxy composites increase with increasing *AR* from 500 to 2000, but then decrease at *AR*=3200.

With regard to the reinforcing mechanism of these hybrids, the well dispersed CNT is one important reason. The three dimensional architectures of the hybrids give rise to larger contact surface and stronger CNT/matrix interaction, resulting in improved load transfer. The alignment of CNTs in the hybrids retains their actual lengths in the matrix, enhancing their reinforcement efficiency. The underlying mechanisms of the self-sensing properties can be contributed to the evolution of conductive networks resulted from the rotation of substrates and the reorientation of CNTs during tensile loading. Proper selection of hybrid structure (CNT aspect ratio, organization and substrate) is critical for achieving desired mechanical and self-sensing performances in the nano/micrometer hybrids reinforced composites.

II. The multiscale glass fabric/epoxy laminates with CNT-microparticle hybrids

The effect of CNT-microparticle reinforcements on the flexural and thermomechanical properties of the glass fabric/epoxy composite laminates was investigated. It was found that the composites incorporated with 0.5 *wt.*% CNT-Al_2O_3 hybrids exhibit ~ 19% increment in the flexural modulus and about 13% enhancement in the flexural strength over the reference sample. The composites also show considerable improvement of ~ 20% in storage modulus at 50 ^oC and an increase of 15 ^oC in glass transition temperature compared to the control samples. In this case, the efficient stress transfer from the CNT-Al_2O_3 hybrids modified matrix to the glass fiber resulted from the strong fiber/matrix interfacial interaction.

By introduction of 0.5 *wt.*% CNT-Al_2O_3 hybrids, ac conductivities of the composites at $f=10^3$ Hz are up to values on the order of 10^{-5} ~ 10^{-6} S/m and 3 ~ 4 orders of magnitude higher than that of the reference composites in the in-plane and through-thickness directions. It was found that the through-thickness conductivity is lower than the in-plane value.

The CNT-Al_2O_3 multifunctional reinforcements can be utilized as *in situ* damage sensor to monitor damage evolution in the glass fabric reinforced laminates during tensile loading. With the increase of strain, the *in situ* electrical resistance always increases until the ultimate failure. According to its different slopes, the electrical resistance curve can be classified into three stages, which implies the different damage mechanisms in the three stages. When $\varepsilon < \varepsilon_1$ (I), the matrix-dominated damages such as the microcracks or flaws are initiated in the region between the glass fiber and matrix. In the II stage ($\varepsilon_1<\varepsilon<\varepsilon_2$), the increased steep growth of the curve are mainly contributed to the accumulation of the matrix-dominated damage, the fiber/matrix debonding and the transverse cracking. When enter into III stage ($\varepsilon>\varepsilon_2$), besides the interfacial debonding and tans-ply cracking, the fiber breakage along the strain direction also take place. However, Poisson contraction of the epoxy matrix and the reorientation of the CNT-Al_2O_3 hybrids possibly facilitate the reformation of the conductive networks, resulting in the slight increase of the resistance in this stage.

Perspectives

1. For the CNT-microparticle hybrids filled epoxy nanocomposites, the hybrid morphology (CNT aspect ratio, orientation and the substrate structure) has great effect on their *in-situ* sensing behaviors. However, establishing the correlation between the hybrid morphology and the sensitivity of the self-sensing composites are still interesting issues.
2. According to some existing models and empirical equations, the tensile modulus of the epoxy nanocomposites filled with the hybrids was calculated, which are generally lower than the experimental results. The modified equations used for calculation of the tensile modulus of the hybrids as reinforcements are needed.
3. The CNT-microparticle hybrids can be used as *in situ* damage sensor in the composites. Besides, the measurements of the *in situ* resistance during loading, it is also necessary for the *in situ* observation of the crack propagation and the hybrid movement or orientation by microscopes. This is a challenging for the non-transparent composites with CNTs.
4. The introduction of the CNT-microparticle hybrid plays an important role on toughening the epoxy matrix. The improved mechanical properties were achieved in the multiscale glass fabric/epoxy composites with the hybrids. Further research on the influence of the hybrids on the fiber/epoxy interface and how to improve the interfacial properties is also needed.

References

[1] Iijima S. Helical microtubules of graphitic carbon. nature 1991, **354**(6348): 56-8.

[2] Dresselhaus M S, Dresselhaus G, Eklund P C, *Science of fullerenes and carbon nanotubes: their properties and applications*. 1996: Academic Press.

[3] Krishnan A, Dujardin E, Ebbesen T, Yianilos P, Treacy M. Young's modulus of single-walled nanotubes. Physical Review B 1998, **58**(20): 14013.

[4] Siegal M, Overmyer D, Provencio P. Precise control of multiwall carbon nanotube diameters using thermal chemical vapor deposition. Applied physics letters 2002, **80**(12): 2171-3.

[5] Wilder J W, Venema L C, Rinzler A G, Smalley R E, Dekker C. Electronic structure of atomically resolved carbon nanotubes. nature 1998, **391**(6662): 59-62.

[6] Yakobson B, Samsonidze G, Samsonidze G. Atomistic theory of mechanical relaxation in fullerene nanotubes. Carbon 2000, **38**(11): 1675-80.

[7] Yakobson B I, Brabec C, Bernholc J. Nanomechanics of carbon tubes: instabilities beyond linear response. Physical review letters 1996, **76**(14): 2511-4.

[8] Nardelli M B, Yakobson B, Bernholc J. Brittle and ductile behavior in carbon nanotubes. Physical review letters 1998, **81**(21): 4656-9.

[9] Salvetat J-P, Briggs G A D, Bonard J-M, Bacsa R R, Kulik A J, Stöckli T, et al. Elastic and shear moduli of single-walled carbon nanotube ropes. Physical review letters 1999, **82**(5): 944-7.

[10] Salvetat J-P, Bonard J-M, Thomson N, Kulik A, Forro L, Benoit W, et al. Mechanical properties of carbon nanotubes. Applied Physics A 1999, **69**(3): 255-60.

[11] Ebbesen T, Lezec H, Hiura H, Bennett J, Ghaemi H, Thio T. Electrical conductivity of individual carbon nanotubes. 1996.

[12] De Pablo P, Graugnard E, Walsh B, Andres R, Datta S, Reifenberger R. A simple, reliable technique for making electrical contact to multiwalled carbon nanotubes. Applied physics letters 1999, **74**(2): 323-5.

[13] Kaneto K, Tsuruta M, Sakai G, Cho W, Ando Y. Electrical conductivities of multi-wall carbon nano tubes. Synthetic Metals 1999, **103**(1): 2543-6.

[14] Bandaru P R. Electrical properties and applications of carbon nanotube structures. Journal of nanoscience and nanotechnology 2007, **7**(4-5): 4-5.

[15] Tombler T W, Zhou C, Alexseyev L, Kong J, Dai H, Liu L, et al. Reversible electromechanical characteristics of carbon nanotubes under local-probe manipulation.

nature 2000, **405**(6788): 769-72.

[16] Minot E, Yaish Y, Sazonova V, Park J-Y, Brink M, McEuen P L. Tuning carbon nanotube band gaps with strain. Physical review letters 2003, **90**(15): 156401.

[17] Cao J, Wang Q, Dai H. Electromechanical properties of metallic, quasimetallic, and semiconducting carbon nanotubes under stretching. Physical review letters 2003, **90**(15): 157601.

[18] Rochefort A, Avouris P, Lesage F, Salahub D R. Electrical and mechanical properties of distorted carbon nanotubes. Physical Review B 1999, **60**(19): 13824.

[19] Ong K G, Zeng K, Grimes C A. A wireless, passive carbon nanotube-based gas sensor. Sensors Journal, IEEE 2002, **2**(2): 82-8.

[20] Cho W-S, Moon S-I, Lee Y-D, Lee Y-H, Park J-H, Ju B K. Multiwall carbon nanotube gas sensor fabricated using thermomechanical structure. Electron Device Letters, IEEE 2005, **26**(7): 498-500.

[21] Kim P, Shi L, Majumdar A, McEuen P. Thermal transport measurements of individual multiwalled nanotubes. Physical review letters 2001, **87**(21): 215502.

[22] Kawano T, Chiamori H C, Suter M, Zhou Q, Sosnowchik B D, Lin L. An electrothermal carbon nanotube gas sensor. Nano letters 2007, **7**(12): 3686-90.

[23] Njuguna M, Yan C, Hu N, Bell J, Yarlagadda P. Sandwiched carbon nanotube film as strain sensor. Composites Part B: Engineering 2012.

[24] Martel R a, Schmidt T, Shea H, Hertel T, Avouris P. Single-and multi-wall carbon nanotube field-effect transistors. Applied physics letters 1998, **73**: 2447.

[25] Iijima S, Ichihashi T. Single-shell carbon nanotubes of 1-nm diameter. 1993.

[26] Bethune D, Klang C, De Vries M, Gorman G, Savoy R, Vazquez J, et al. Cobalt-catalysed growth of carbon nanotubes with single-atomic-layer walls. 1993.

[27] Philippe R, Caussat B, Falqui A, Kihn Y, Kalck P, Bordère S, et al. An original growth mode of MWCNTs on alumina supported iron catalysts. Journal of Catalysis 2009, **263**(2): 345-58.

[28] Jose-Yacaman M, Miki-Yoshida M, Rendon L, Santiesteban J. Catalytic growth of carbon microtubules with fullerene structure. Applied physics letters 1993, **62**(2): 202-4.

[29] Choy K. Chemical vapour deposition of coatings. Progress in Materials Science 2003, **48**(2): 57-170.

[30] Hao Y, Qunfeng Z, Fei W, Weizhong Q, Guohua L. Agglomerated CNTs synthesized in a fluidized bed reactor: agglomerate structure and formation mechanism. Carbon 2003, **41**(14): 2855-63.

[31] Mora E, Tokune T, Harutyunyan A R. Continuous production of single-walled carbon

nanotubes using a supported floating catalyst. Carbon 2007, **45**(5): 971-7.

[32] Li W, Xie S, Qian L X, Chang B, Zou B, Zhou W, et al. Large-scale synthesis of aligned carbon nanotubes. Science 1996, **274**(5293): 1701-3.

[33] Huang S. Growing carbon nanotubes on patterned submicron-size SiO_2 spheres. Carbon 2003, **41**(12): 2347-52.

[34] Zhang Q, Huang J-Q, Zhao M-Q, Qian W-Z, Wang Y, Wei F. Radial growth of vertically aligned carbon nanotube arrays from ethylene on ceramic spheres. Carbon 2008, **46**(8): 1152-8.

[35] Qian H, Bismarck A, Greenhalgh E S, Kalinka G, Shaffer M S. Hierarchical composites reinforced with carbon nanotube grafted fibers: the potential assessed at the single fiber level. Chemistry of Materials 2008, **20**(5): 1862-9.

[36] Thostenson E, Li W, Wang D, Ren Z, Chou T. Carbon nanotube/carbon fiber hybrid multiscale composites. Journal of Applied physics 2002, **91**(9): 6034-7.

[37] Yamamoto N, John Hart A, Garcia E J, Wicks S S, Duong H M, Slocum A H, et al. High-yield growth and morphology control of aligned carbon nanotubes on ceramic fibers for multifunctional enhancement of structural composites. Carbon 2009, **47**(3): 551-60.

[38] Zhang Q, Liu J, Sager R, Dai L, Baur J. Hierarchical composites of carbon nanotubes on carbon fiber: Influence of growth condition on fiber tensile properties. Composites Science and Technology 2009, **69**(5): 594-601.

[39] Garcia E J, Wardle B L, John Hart A, Yamamoto N. Fabrication and multifunctional properties of a hybrid laminate with aligned carbon nanotubes grown *In Situ*. Composites Science and Technology 2008, **68**(9): 2034-41.

[40] An F, Lu C, Guo J, He S, Lu H, Yang Y. Preparation of vertically aligned carbon nanotube arrays grown onto carbon fiber fabric and evaluating its wettability on effect of composite. Applied Surface Science 2011, **258**(3): 1069-76.

[41] Dupuis A-C. The catalyst in the CCVD of carbon nanotubes-a review. Progress in Materials Science 2005, **50**(8): 929-61.

[42] Bae E J, Choi W B, Jeong K S, Chu J U, Park G-S, Song S, et al. Selective growth of carbon nanotubes on pre-patterned porous anodic aluminum oxide. Advanced Materials 2002, **14**(4): 277.

[43] Han Z, Yang B, Kim S, Zachariah M. Application of hybrid sphere/carbon nanotube particles in nanofluids. Nanotechnology 2007, **18**(10): 105701.

[44] Hart A J, Slocum A H. Rapid growth and flow-mediated nucleation of millimeter-scale aligned carbon nanotube structures from a thin-film catalyst. The Journal of Physical Chemistry B 2006, **110**(16): 8250-7.

[45] Sohn J I, Lee S, Song Y-H, Choi S-Y, Cho K-I, Nam K-S. Patterned selective growth of carbon nanotubes and large field emission from vertically well-aligned carbon nanotube field emitter arrays. Applied physics letters 2001, **78**(7): 901-3.

[46] Wei B, Vajtai R, Jung Y, Ward J, Zhang R, Ramanath G, et al. Assembly of highly organized carbon nanotube architectures by chemical vapor deposition. Chemistry of Materials 2003, **15**(8): 1598-606.

[47] Zhu S, Su C-H, Lehoczky S, Muntele I, Ila D. Carbon nanotube growth on carbon fibers. Diamond and Related Materials 2003, **12**(10): 1825-8.

[48] Liu H, Zhang Y, Arato D, Li R, Mérel P, Sun X. Aligned multi-walled carbon nanotubes on different substrates by floating catalyst chemical vapor deposition: critical effects of buffer layer. Surface and Coatings Technology 2008, **202**(17): 4114-20.

[49] De Resende V G, Antunes E F, de Oliveira Lobo A, Oliveira D A L, Trava-Airoldi V J, Corat E J. Growth of carbon nanotube forests on carbon fibers with an amorphous silicon interface. Carbon 2010, **48**(12): 3655-8.

[50] Lv P, Feng Y-y, Zhang P, Chen H-m, Zhao N, Feng W. Increasing the interfacial strength in carbon fiber/epoxy composites by controlling the orientation and length of carbon nanotubes grown on the fibers. Carbon 2011, **49**(14): 4665-73.

[51] Bozlar M, He D, Bai J, Chalopin Y, Mingo N, Volz S. Carbon nanotube microarchitectures for enhanced thermal conduction at ultralow mass fraction in polymer composites. Advanced Materials 2010, **22**(14): 1654-8.

[52] Ci L, Bai J. Novel micro/nanoscale hybrid reinforcement: multiwalled carbon nanotubes on SiC particles. Advanced Materials 2004, **16**(22): 2021-4.

[53] He D, Bozlar M, Genestoux M, Bai J. Diameter-and length-dependent self-organizations of multi-walled carbon nanotubes on spherical alumina microparticles. Carbon 2010, **48**(4): 1159-70.

[54] He D, Li H, Bai J. Experimental and numerical investigation of the position-dependent growth of carbon nanotube–alumina microparticle hybrid structures in a horizontal CVD reactor. Carbon 2011, **49**(15): 5359-72.

[55] He D, Li H, Li W, Haghi-Ashtiani P, Lejay P, Bai J. Growth of carbon nanotubes in six orthogonal directions on spherical alumina microparticles. Carbon 2011, **49**(7): 2273-86.

[56] Zhang C, Tjiu W W, Liu T, Lui W Y, Phang I Y, Zhang W-D. Dramatically Enhanced Mechanical Performance of Nylon-6 Magnetic Composites with Nanostructured Hybrid One-Dimensional Carbon Nanotube-Two-Dimensional Clay Nanoplatelet Heterostructures. The Journal of Physical Chemistry B 2011, **115**(13): 3392-9.

[57] Pandey G, Thostenson E T. Carbon nanotube-based multifunctional polymer

nanocomposites. Polymer Reviews 2012, **52**(3-4): 355-416.
[58] Thostenson E T, Ren Z, Chou T-W. Advances in the science and technology of carbon nanotubes and their composites: a review. Composites Science and Technology 2001, **61**(13): 1899-912.
[59] Thostenson E T, Li C, Chou T-W. Nanocomposites in context. Composites Science and Technology 2005, **65**(3): 491-516.
[60] Gibson R F. A review of recent research on mechanics of multifunctional composite materials and structures. Composite structures 2010, **92**(12): 2793-810.
[61] Wu D, Wu L, Zhou W, Sun Y, Zhang M. Relations between the aspect ratio of carbon nanotubes and the formation of percolation networks in biodegradable polylactide/carbon nanotube composites. Journal of Polymer Science Part B: Polymer Physics 2010, **48**(4): 479-89.
[62] Qian D, Dickey E C, Andrews R, Rantell T. Load transfer and deformation mechanisms in carbon nanotube-polystyrene composites. Applied physics letters 2000, **76**: 2868.
[63] Zhang W, Picu R, Koratkar N. The effect of carbon nanotube dimensions and dispersion on the fatigue behavior of epoxy nanocomposites. Nanotechnology 2008, **19**(28): 285709.
[64] Zhang H, Zhang Z. Impact behaviour of polypropylene filled with multi-walled carbon nanotubes. European polymer journal 2007, **43**(8): 3197-207.
[65] Sandler J, Kirk J, Kinloch I, Shaffer M, Windle A. Ultra-low electrical percolation threshold in carbon-nanotube-epoxy composites. Polymer 2003, **44**(19): 5893-9.
[66] Li J, Ma P C, Chow W S, To C K, Tang B Z, Kim J K. Correlations between percolation threshold, dispersion state, and aspect ratio of carbon nanotubes. Advanced Functional Materials 2007, **17**(16): 3207-15.
[67] Tucker III C L, Liang E. Stiffness predictions for unidirectional short-fiber composites: Review and evaluation. Composites Science and Technology 1999, **59**(5): 655-71.
[68] Ma P C, Tang B Z, Kim J-K. Effect of CNT decoration with silver nanoparticles on electrical conductivity of CNT-polymer composites. Carbon 2008, **46**(11): 1497-505.
[69] Kosmidou T V, Vatalis A, Delides C, Logakis E, Pissis P, Papanicolaou G. Structural, mechanical and electrical characterization of epoxy-amine/carbon black nanocomposites. Express Polymer Letters 2008, **2**: 364-72.
[70] Gojny F H, Nastalczyk J, Roslaniec Z, Schulte K. Surface modified multi-walled carbon nanotubes in CNT/epoxy-composites. Chemical physics letters 2003, **370**(5): 820-4.
[71] Cooper C A, Ravich D, Lips D, Mayer J, Wagner H D. Distribution and alignment of carbon nanotubes and nanofibrils in a polymer matrix. Composites Science and Technology 2002, **62**(7): 1105-12.

[72] Dai J, Wang Q, Li W, Wei Z, Xu G. Properties of well aligned SWNT modified poly (methyl methacrylate) nanocomposites. Materials Letters 2007, **61**(1): 27-9.

[73] Xie X-L, Mai Y-W, Zhou X-P. Dispersion and alignment of carbon nanotubes in polymer matrix: a review. Materials Science and Engineering: R: Reports 2005, **49**(4): 89-112.

[74] Ma P-C, Siddiqui N A, Marom G, Kim J-K. Dispersion and functionalization of carbon nanotubes for polymer-based nanocomposites: A review. Composites Part A: Applied Science and Manufacturing 2010, **41**(10): 1345-67.

[75] Kim J-K, Mai Y-W. Engineered interfaces in fiber reinforced composites. 1998.

[76] Thostenson E T, Chou T-W. Aligned multi-walled carbon nanotube-reinforced composites: processing and mechanical characterization. Journal of physics D: Applied physics 2002, **35**(16): L77.

[77] Sen R, Zhao B, Perea D, Itkis M E, Hu H, Love J, et al. Preparation of single-walled carbon nanotube reinforced polystyrene and polyurethane nanofibers and membranes by electrospinning. Nano letters 2004, **4**(3): 459-64.

[78] Ko F, Gogotsi Y, Ali A, Naguib N, Ye H, Yang G, et al. Electrospinning of continuous carbon nanotube-filled nanofiber yarns. Advanced Materials 2003, **15**(14): 1161-5.

[79] Hou H, Ge J J, Zeng J, Li Q, Reneker D H, Greiner A, et al. Electrospun polyacrylonitrile nanofibers containing a high concentration of well-aligned multiwall carbon nanotubes. Chemistry of Materials 2005, **17**(5): 967-73.

[80] Choi E, Brooks J, Eaton D, Al-Haik M, Hussaini M, Garmestani H, et al. Enhancement of thermal and electrical properties of carbon nanotube polymer composites by magnetic field processing. Journal of Applied physics 2003, **94**(9): 6034-9.

[81] Kimura T, Ago H, Tobita M, Ohshima S, Kyotani M, Yumura M. Polymer composites of carbon nanotubes aligned by a magnetic field. Advanced Materials 2002, **14**(19): 1380-3.

[82] Russell J M, Oh S, LaRue I, Zhou O, Samulski E T. Alignment of nematic liquid crystals using carbon nanotube films. Thin Solid Films 2006, **509**(1): 53-7.

[83] Lynch M D, Patrick D L. Organizing carbon nanotubes with liquid crystals. Nano letters 2002, **2**(11): 1197-201.

[84] Fan Z, Advani S G. Characterization of orientation state of carbon nanotubes in shear flow. Polymer 2005, **46**(14): 5232-40.

[85] Xu A-Z, Yang M-S, Wu Q, XM HU J L. Flow field induced steady alignment of oxidized multi-walled carbon nanotubes. Chin Chem Lett 2005, **7**: 849.

[86] Fornes T, Baur J, Sabba Y, Thomas E. Morphology and properties of melt-spun polycarbonate fibers containing single-and multi-wall carbon nanotubes. Polymer 2006,

47(5): 1704-14.

[87] Haggenmueller R, Gommans H, Rinzler A, Fischer J E, Winey K. Aligned single-wall carbon nanotubes in composites by melt processing methods. Chemical physics letters 2000, **330**(3): 219-25.

[88] Park S J, Cho M S, Lim S T, Choi H J, Jhon M S. Synthesis and Dispersion Characteristics of Multi-Walled Carbon Nanotube Composites with Poly (methyl methacrylate) Prepared by In-Situ Bulk Polymerization. Macromolecular Rapid Communications 2003, **24**(18): 1070-3.

[89] Jin L, Bower C, Zhou O. Alignment of carbon nanotubes in a polymer matrix by mechanical stretching. Applied physics letters 1998, **73**: 1197.

[90] Wang Q, Dai J, Li W, Wei Z, Jiang J. The effects of CNT alignment on electrical conductivity and mechanical properties of SWNT/epoxy nanocomposites. Composites Science and Technology 2008, **68**(7): 1644-8.

[91] Nanni F, Mayoral B, Madau F, Montesperelli G, McNally T. Effect of MWCNT alignment on mechanical and self-monitoring properties of extruded PET-MWCNT nanocomposites. Composites Science and Technology 2012.

[92] Hirsch A. Functionalization of single-walled carbon nanotubes. Angewandte Chemie International Edition 2002, **41**(11): 1853-9.

[93] Koval'chuk A A, Shevchenko V G, Shchegolikhin A N, Nedorezova P M, Klyamkina A N, Aladyshev A M. Effect of carbon nanotube functionalization on the structural and mechanical properties of polypropylene/MWCNT composites. Macromolecules 2008, **41**(20): 7536-42.

[94] Yuen S-M, Ma C-C M, Lin Y-Y, Kuan H-C. Preparation, morphology and properties of acid and amine modified multiwalled carbon nanotube/polyimide composite. Composites Science and Technology 2007, **67**(11): 2564-73.

[95] Kim K H, Jo W H. Improvement of tensile properties of poly (methyl methacrylate) by dispersing multi-walled carbon nanotubes functionalized with poly (3-hexylthiophene)-graft-poly (methyl methacrylate). Composites Science and Technology 2008, **68**(9): 2120-4.

[96] Sahoo N G, Jung Y C, Yoo H J, Cho J W. Effect of functionalized carbon nanotubes on molecular interaction and properties of polyurethane composites. Macromolecular chemistry and physics 2006, **207**(19): 1773-80.

[97] Ma P C, Kim J-K, Tang B Z. Effects of silane functionalization on the properties of carbon nanotube/epoxy nanocomposites. Composites Science and Technology 2007, **67**(14): 2965-72.

[98] Gojny F H, Wichmann M H, Fiedler B, Kinloch I A, Bauhofer W, Windle A H, et al.

Evaluation and identification of electrical and thermal conduction mechanisms in carbon nanotube/epoxy composites. Polymer 2006, **47**(6): 2036-45.

[99] Buldum A, Lu J P. Contact resistance between carbon nanotubes. Physical Review B 2001, **63**(16): 161403.

[100] Stadermann M, Papadakis S, Falvo M, Novak J, Snow E, Fu Q, et al. Nanoscale study of conduction through carbon nanotube networks, 2004, DTIC Document.

[101] Huang H, Liu C, Wu Y, Fan S. Aligned carbon nanotube composite films for thermal management. Advanced Materials 2005, **17**(13): 1652-6.

[102] Viswanathan V, Laha T, Balani K, Agarwal A, Seal S. Challenges and advances in nanocomposite processing techniques. Materials Science and Engineering: R: Reports 2006, **54**(5): 121-285.

[103] Meng H, Sui G, Fang P, Yang R. Effects of acid-and diamine-modified MWNTs on the mechanical properties and crystallization behavior of polyamide 6. Polymer 2008, **49**(2): 610-20.

[104] Thostenson E T, Chou T-W. Processing-structure-multi-functional property relationship in carbon nanotube/epoxy composites. Carbon 2006, **44**(14): 3022-9.

[105] Chou T-W, Gao L, Thostenson E T, Zhang Z, Byun J-H. An assessment of the science and technology of carbon nanotube-based fibers and composites. Composites Science and Technology 2010, **70**(1): 1-19.

[106] Koshio A, Yudasaka M, Zhang M, Iijima S. A simple way to chemically react single-wall carbon nanotubes with organic materials using ultrasonication. Nano letters 2001, **1**(7): 361-3.

[107] Paiva M, Zhou B, Fernando K, Lin Y, Kennedy J, Sun Y-P. Mechanical and morphological characterization of polymer-carbon nanocomposites from functionalized carbon nanotubes. Carbon 2004, **42**(14): 2849-54.

[108] Zhang X, Liu T, Sreekumar T, Kumar S, Moore V C, Hauge R H, et al. Poly (vinyl alcohol)/SWNT composite film. Nano letters 2003, **3**(9): 1285-8.

[109] Mitchell C A, Bahr J L, Arepalli S, Tour J M, Krishnamoorti R. Dispersion of functionalized carbon nanotubes in polystyrene. Macromolecules 2002, **35**(23): 8825-30.

[110] Shaffer M S, Windle A H. Fabrication and characterization of carbon nanotube/poly (vinyl alcohol) composites. Advanced Materials 1999, **11**(11): 937-41.

[111] Schadler L, Giannaris S, Ajayan P. Load transfer in carbon nanotube epoxy composites. Applied physics letters 1998, **73**: 3842.

[112] Coleman J N, Khan U, Gun'ko Y K. Mechanical reinforcement of polymers using carbon nanotubes. Advanced Materials 2006, **18**(6): 689-706.

[113] Dang Z-M, Yuan J-K, Zha J-W, Zhou T, Li S-T, Hu G-H. Fundamentals, processes and applications of high-permittivity polymer–matrix composites. Progress in Materials Science 2012, **57**(4): 660-723.

[114] Dang Z M, Wang L, Yin Y, Zhang Q. Giant Dielectric Permittivities in Functionalized Carbon-Nanotube/Electroactive-Polymer Nanocomposites. Advanced Materials 2007, **19**(6): 852-7.

[115] Wang L, Dang Z-M. Carbon nanotube composites with high dielectric constant at low percolation threshold. Applied physics letters 2005, **87**(4): 042903--3.

[116] Paul C, KuangáHsu W. A low resistance boron-doped carbon nanotube–polystyrene composite. Journal of Materials Chemistry 2001, **11**(10): 2482-8.

[117] Safadi B, Andrews R, Grulke E. Multiwalled carbon nanotube polymer composites: synthesis and characterization of thin films. Journal of applied polymer science 2002, **84**(14): 2660-9.

[118] Cadek M, Coleman J, Barron V, Hedicke K, Blau W. Morphological and mechanical properties of carbon-nanotube-reinforced semicrystalline and amorphous polymer composites. Applied physics letters 2002, **81**(27): 5123-5.

[119] Park K S, Youn J R. Dispersion and aspect ratio of carbon nanotubes in aqueous suspension and their relationship with electrical resistivity of carbon nanotube filled polymer composites. Carbon 2012, **50**(6): 2322-30.

[120] Grady B P, Pompeo F, Shambaugh R L, Resasco D E. Nucleation of polypropylene crystallization by single-walled carbon nanotubes. The Journal of Physical Chemistry B 2002, **106**(23): 5852-8.

[121] Du F, Fischer J E, Winey K I. Coagulation method for preparing single-walled carbon nanotube/poly (methyl methacrylate) composites and their modulus, electrical conductivity, and thermal stability. Journal of Polymer Science Part B: Polymer Physics 2003, **41**(24): 3333-8.

[122] Oliva-Avilés A, Avilés F, Sosa V. Electrical and piezoresistive properties of multi-walled carbon nanotube/polymer composite films aligned by an electric field. Carbon 2011, **49**(9): 2989-97.

[123] Dang Z-M, Li W-K, Xu H-P. Origin of remarkable positive temperature coefficient effect in the modified carbon black and carbon fiber cofillled polymer composites. Journal of Applied physics 2009, **106**(2): 024913-5.

[124] Zha J-W, Li W-K, Liao R-J, Bai J, Dang Z-M. High performance hybrid carbon fillers/binary–polymer nanocomposites with remarkably enhanced positive temperature coefficient effect of resistance. Journal of Materials Chemistry A 2013, **1**(3): 843-51.

[125] Xu H-P, Dang Z-M, Jiang M-J, Yao S-H, Bai J. Enhanced dielectric properties and positive temperature coefficient effect in the binary polymer composites with surface modified carbon black. Journal of Materials Chemistry 2008, **18**(2): 229-34.

[126] Yuan J-K, Yao S-H, Dang Z-M, Sylvestre A, Genestoux M, Bail J. Giant dielectric permittivity nanocomposites: realizing true potential of pristine carbon nanotubes in polyvinylidene fluoride matrix through an enhanced interfacial interaction. The Journal of Physical Chemistry C 2011, **115**(13): 5515-21.

[127] Manchado M, Valentini L, Biagiotti J, Kenny J. Thermal and mechanical properties of single-walled carbon nanotubes–polypropylene composites prepared by melt processing. Carbon 2005, **43**(7): 1499-505.

[128] Pham G T, Park Y-B, Liang Z, Zhang C, Wang B. Processing and modeling of conductive thermoplastic/carbon nanotube films for strain sensing. Composites Part B: Engineering 2008, **39**(1): 209-16.

[129] Park C, Ounaies Z, Watson K A, Crooks R E, Smith Jr J, Lowther S E, et al. Dispersion of single wall carbon nanotubes by in situ polymerization under sonication. Chemical physics letters 2002, **364**(3): 303-8.

[130] Feng W, Bai X, Lian Y, Liang J, Wang X, Yoshino K. Well-aligned polyaniline/carbon-nanotube composite films grown by in-situ aniline polymerization. Carbon 2003, **41**(8): 1551-7.

[131] Hu N, Karube Y, Yan C, Masuda Z, Fukunaga H. Tunneling effect in a polymer/carbon nanotube nanocomposite strain sensor. Acta Materialia 2008, **56**(13): 2929-36.

[132] Kang J H, Park C, Scholl J A, Brazin A H, Holloway N M, High J W, et al. Piezoresistive characteristics of single wall carbon nanotube/polyimide nanocomposites. Journal of Polymer Science Part B: Polymer Physics 2009, **47**(10): 994-1003.

[133] Ma P C, Wang S Q, Kim J-K, Tang B Z. In-situ amino functionalization of carbon nanotubes using ball milling. Journal of nanoscience and nanotechnology 2009, **9**(2): 749-53.

[134] Moniruzzaman M, Du F, Romero N, Winey K I. Increased flexural modulus and strength in SWNT/epoxy composites by a new fabrication method. Polymer 2006, **47**(1): 293-8.

[135] Isayev A, Kumar R, Lewis T M. Ultrasound assisted twin screw extrusion of polymer–nanocomposites containing carbon nanotubes. Polymer 2009, **50**(1): 250-60.

[136] Baur J, Silverman E. Challenges and opportunities in multifunctional nanocomposite structures for aerospace applications. MRS bulletin 2007, **32**(04): 328-34.

[137] Li C, Thostenson E T, Chou T-W. Sensors and actuators based on carbon nanotubes and their composites: a review. Composites Science and Technology 2008, **68**(6): 1227-49.

[138] Tai N-H, Yeh M-K, Peng T-H. Experimental study and theoretical analysis on the mechanical properties of SWNTs/phenolic composites. Composites Part B: Engineering 2008, **39**(6): 926-32.

[139] Grimmer C S, Dharan C. High-cycle fatigue of hybrid carbon nanotube/glass fiber/polymer composites. Journal of Materials Science 2008, **43**(13): 4487-92.

[140] Koratkar N A, Suhr J, Joshi A, Kane R S, Schadler L S, Ajayan P M, et al. Characterizing energy dissipation in single-walled carbon nanotube polycarbonate composites. Applied physics letters 2005, **87**(6): 063102--3.

[141] Moisala A, Li Q, Kinloch I, Windle A. Thermal and electrical conductivity of single-and multi-walled carbon nanotube–epoxy composites. Composites Science and Technology 2006, **66**(10): 1285-8.

[142] Li C, Thostenson E T, Chou T-W. Effect of nanotube waviness on the electrical conductivity of carbon nanotube-based composites. Composites Science and Technology 2008, **68**(6): 1445-52.

[143] Arjmand M, Mahmoodi M, Gelves G A, Park S, Sundararaj U. Electrical and electromagnetic interference shielding properties of flow-induced oriented carbon nanotubes in polycarbonate. Carbon 2011, **49**(11): 3430-40.

[144] Yuan J-K, Li W-L, Yao S-H, Lin Y-Q, Sylvestre A, Bai J. High dielectric permittivity and low percolation threshold in polymer composites based on SiC-carbon nanotubes micro/nano hybrid. Applied physics letters 2011, **98**(3): 032901--3.

[145] Vemuru S, Wahi R, Nagarajaiah S, Ajayan P. Strain sensing using a multiwalled carbon nanotube film. The Journal of Strain Analysis for Engineering Design 2009, **44**(7): 555-62.

[146] Kang I, Heung Y Y, Kim J H, Lee J W, Gollapudi R, Subramaniam S, et al. Introduction to carbon nanotube and nanofiber smart materials. Composites Part B: Engineering 2006, **37**(6): 382-94.

[147] Zhang W, Suhr J, Koratkar N. Carbon nanotube/polycarbonate composites as multifunctional strain sensors. Journal of nanoscience and nanotechnology 2006, **6**(4): 960-4.

[148] Bilotti E, Zhang R, Deng H, Baxendale M, Peijs T. Fabrication and property prediction of conductive and strain sensing TPU/CNT nanocomposite fibres. Journal of Materials Chemistry 2010, **20**(42): 9449-55.

[149] Bautista-Quijano J, Aviles F, Aguilar J, Tapia A. Strain sensing capabilities of a

piezoresistive MWCNT-polysulfone film. Sensors and Actuators A: Physical 2010, **159**(2): 135-40.

[150] De la Vega A, Kinloch I, Young R, Bauhofer W, Schulte K. Simultaneous global and local strain sensing in SWCNT–epoxy composites by Raman and impedance spectroscopy. Composites Science and Technology 2011, **71**(2): 160-6.

[151] Anand S V, Mahapatra D R. Quasi-static and dynamic strain sensing using carbon nanotube/epoxy nanocomposite thin films. Smart Materials and Structures 2009, **18**(4): 045013.

[152] Wichmann M H, Buschhorn S T, Böger L, Adelung R, Schulte K. Direction sensitive bending sensors based on multi-wall carbon nanotube/epoxy nanocomposites. Nanotechnology 2008, **19**(47): 475503.

[153] Dang Z-M, Jiang M-J, Xie D, Yao S-H, Zhang L-Q, Bai J. Supersensitive linear piezoresistive property in carbon nanotubes/silicone rubber nanocomposites. Journal of Applied physics 2008, **104**(2): 024114--6.

[154] Shehzad K, Ul-Haq A, Ahmad S, Mumtaz M, Hussain T, Mujahid A, et al. All-organic PANI–DBSA/PVDF dielectric composites with unique electrical properties. Journal of Materials Science 2013: 1-8.

[155] Tang L G, Kardos J L. A review of methods for improving the interfacial adhesion between carbon fiber and polymer matrix. Polymer composites 1997, **18**(1): 100-13.

[156] Hughes J. The carbon fibre/epoxy interface—a review. Composites Science and Technology 1991, **41**(1): 13-45.

[157] Mouritz A, Bannister M, Falzon P, Leong K. Review of applications for advanced three-dimensional fibre textile composites. Composites Part A: applied science and manufacturing 1999, **30**(12): 1445-61.

[158] Godara A, Gorbatikh L, Kalinka G, Warrier A, Rochez O, Mezzo L, et al. Interfacial shear strength of a glass fiber/epoxy bonding in composites modified with carbon nanotubes. Composites Science and Technology 2010, **70**(9): 1346-52.

[159] Vlasveld D, Daud W, Bersee H, Picken S. Continuous fibre composites with a nanocomposite matrix: Improvement of flexural and compressive strength at elevated temperatures. Composites Part A: Applied Science and Manufacturing 2007, **38**(3): 730-8.

[160] Bekyarova E, Thostenson E T, Yu A, Itkis M E, Fakhrutdinov D, Chou T-W, et al. Functionalized single-walled carbon nanotubes for carbon fiber-epoxy composites. The Journal of Physical Chemistry C 2007, **111**(48): 17865-71.

[161] Yokozeki T, Iwahori Y, Ishiwata S, Enomoto K. Mechanical properties of CFRP laminates manufactured from unidirectional prepregs using CSCNT-dispersed epoxy.

Composites Part A: Applied Science and Manufacturing 2007, **38**(10): 2121-30.
[162] Yokozeki T, Iwahori Y, Ishibashi M, Yanagisawa T, Imai K, Arai M, et al. Fracture toughness improvement of CFRP laminates by dispersion of cup-stacked carbon nanotubes. Composites Science and Technology 2009, **69**(14): 2268-73.
[163] Wichmann M H, Sumfleth J, Gojny F H, Quaresimin M, Fiedler B, Schulte K. Glass-fibre-reinforced composites with enhanced mechanical and electrical properties–benefits and limitations of a nanoparticle modified matrix. Engineering Fracture Mechanics 2006, **73**(16): 2346-59.
[164] Thostenson E T, Gangloff J J, Li C, Byun J-H. Electrical anisotropy in multiscale nanotube/fiber hybrid composites. Applied physics letters 2009, **95**(7): 073111--3.
[165] He X, Zhang F, Wang R, Liu W. Preparation of a carbon nanotube/carbon fiber multi-scale reinforcement by grafting multi-walled carbon nanotubes onto the fibers. Carbon 2007, **45**(13): 2559-63.
[166] Laachachi A, Vivet A, Nouet G, Ben Doudou B, Poilâne C, Chen J, et al. A chemical method to graft carbon nanotubes onto a carbon fiber. Materials Letters 2008, **62**(3): 394-7.
[167] Gao L, Chou T-W, Thostenson E T, Godara A, Zhang Z, Mezzo L. Highly conductive polymer composites based on controlled agglomeration of carbon nanotubes. Carbon 2010, **48**(9): 2649-51.
[168] Warrier A, Godara A, Rochez O, Mezzo L, Luizi F, Gorbatikh L, et al. The effect of adding carbon nanotubes to glass/epoxy composites in the fibre sizing and/or the matrix. Composites Part A: Applied Science and Manufacturing 2010, **41**(4): 532-8.
[169] Gao L, Chou T-W, Thostenson E T, Zhang Z. A comparative study of damage sensing in fiber composites using uniformly and non-uniformly dispersed carbon nanotubes. Carbon 2010, **48**(13): 3788-94.
[170] Schaefer J D, Rodriguez A J, Guzman M E, Lim C-S, Minaie B. Effects of electrophoretically deposited carbon nanofibers on the interface of single carbon fibers embedded in epoxy matrix. Carbon 2011, **49**(8): 2750-9.
[171] Bekyarova E, Thostenson E, Yu A, Kim H, Gao J, Tang J, et al. Multiscale carbon nanotube-carbon fiber reinforcement for advanced epoxy composites. Langmuir 2007, **23**(7): 3970-4.
[172] Qian H, Bismarck A, Greenhalgh E S, Shaffer M S. Carbon nanotube grafted carbon fibres: A study of wetting and fibre fragmentation. Composites Part A: Applied Science and Manufacturing 2010, **41**(9): 1107-14.
[173] Qian H, Greenhalgh E S, Shaffer M S, Bismarck A. Carbon nanotube-based hierarchical composites: a review. Journal of Materials Chemistry 2010, **20**(23): 4751-62.

[174] Sager R, Klein P, Lagoudas D, Zhang Q, Liu J, Dai L, et al. Effect of carbon nanotubes on the interfacial shear strength of T650 carbon fiber in an epoxy matrix. Composites Science and Technology 2009, **69**(7): 898-904.
[175] Lee K-H, Cho J-M, Sigmund W. Control of growth orientation for carbon nanotubes. Applied physics letters 2003, **82**(3): 448-50.
[176] Garcia E J, Wardle B L, John Hart A. Joining prepreg composite interfaces with aligned carbon nanotubes. Composites Part A: Applied Science and Manufacturing 2008, **39**(6): 1065-70.
[177] Veedu V P, Cao A, Li X, Ma K, Soldano C, Kar S, et al. Multifunctional composites using reinforced laminae with carbon-nanotube forests. Nature Materials 2006, **5**(6): 457-62.
[178] Schulte K, Baron C. Load and failure analyses of CFRP laminates by means of electrical resistivity measurements. Composites Science and Technology 1989, **36**(1): 63-76.
[179] Weber I, Schwartz P. Monitoring bending fatigue in carbon-fibre/epoxy composite strands: a comparison between mechanical and resistance techniques. Composites Science and Technology 2001, **61**(6): 849-53.
[180] Kupke M, Schulte K, Schüler R. Non-destructive testing of FRP by dc and ac electrical methods. Composites Science and Technology 2001, **61**(6): 837-47.
[181] Schueler R, Joshi S P, Schulte K. Damage detection in CFRP by electrical conductivity mapping. Composites Science and Technology 2001, **61**(6): 921-30.
[182] Muto N, Arai Y, Shin S, Matsubara H, Yanagida H, Sugita M, et al. Hybrid composites with self-diagnosing function for preventing fatal fracture. Composites Science and Technology 2001, **61**(6): 875-83.
[183] FIEDLER B, GOJNY F H, WICHMANN M H, BAUHOFER W, SCHULTE K. Can carbon nanotubes be used to sense damage in composites? in Annales de chimie. 2004. Lavoisier.
[184] Thostenson E T, Chou T W. Carbon nanotube networks: sensing of distributed strain and damage for life prediction and self healing. Advanced Materials 2006, **18**(21): 2837-41.
[185] Thostenson E T, Chou T-W. Real-time in situ sensing of damage evolution in advanced fiber composites using carbon nanotube networks. Nanotechnology 2008, **19**(21): 215713.
[186] Nofar M, Hoa S, Pugh M. Failure detection and monitoring in polymer matrix composites subjected to static and dynamic loads using carbon nanotube networks. Composites Science and Technology 2009, **69**(10): 1599-606.
[187] Gao L, Thostenson E T, Zhang Z, Chou T W. Sensing of Damage Mechanisms in Fiber-Reinforced Composites under Cyclic Loading using Carbon Nanotubes. Advanced

Functional Materials 2009, **19**(1): 123-30.
[188] Kim K J, Yu W-R, Lee J S, Gao L, Thostenson E T, Chou T-W, et al. Damage characterization of 3D braided composites using carbon nanotube-based *in situ* sensing. Composites Part A: Applied Science and Manufacturing 2010, **41**(10): 1531-7.
[189] Gao S l, Zhuang R C, Zhang J, Liu J W, Mäder E. Glass fibers with carbon nanotube networks as multifunctional sensors. Advanced Functional Materials 2010, **20**(12): 1885-93.
[190] Sureeyatanapas P, Young R J. SWNT composite coatings as a strain sensor on glass fibres in model epoxy composites. Composites Science and Technology 2009, **69**(10): 1547-52.
[191] Alexopoulos N, Bartholome C, Poulin P, Marioli-Riga Z. Structural health monitoring of glass fiber reinforced composites using embedded carbon nanotube (CNT) fibers. Composites Science and Technology 2010, **70**(2): 260-71.
[192] Coleman J N, Khan U, Blau W J, Gun'ko Y K. Small but strong: a review of the mechanical properties of carbon nanotube–polymer composites. Carbon 2006, **44**(9): 1624-52.
[193] Viculis L M, Mack J J, Mayer O M, Hahn H T, Kaner R B. Intercalation and exfoliation routes to graphite nanoplatelets. Journal of Materials Chemistry 2005, **15**(9): 974-8.
[194] Zhao X, Zhang Q, Chen D, Lu P. Enhanced mechanical properties of graphene-based poly (vinyl alcohol) composites. Macromolecules 2010, **43**(5): 2357-63.
[195] Yang S-Y, Lin W-N, Huang Y-L, Tien H-W, Wang J-Y, Ma C-C M, et al. Synergetic effects of graphene platelets and carbon nanotubes on the mechanical and thermal properties of epoxy composites. Carbon 2011, **49**(3): 793-803.
[196] Hu N, Karube Y, Arai M, Watanabe T, Yan C, Li Y, et al. Investigation on sensitivity of a polymer/carbon nanotube composite strain sensor. Carbon 2010, **48**(3): 680-7.
[197] Zhang R, Baxendale M, Peijs T. Universal resistivity-strain dependence of carbon nanotube/polymer composites. Physical Review B 2007, **76**(19): 195433.
[198] Dichiara A, Yuan J-K, Yao S-H, Sylvestre A, Bai J. Chemical Vapor Deposition Synthesis of Carbon Nanotube-Graphene Nanosheet Hybrids and Their Application in Polymer Composites. Journal of nanoscience and nanotechnology 2012, **12**(9): 6935-40.
[199] Rafiee M A, Rafiee J, Wang Z, Song H, Yu Z-Z, Koratkar N. Enhanced mechanical properties of nanocomposites at low graphene content. Acs Nano 2009, **3**(12): 3884-90.
[200] Wu Y-P, Jia Q-X, Yu D-S, Zhang L-Q. Modeling Young's modulus of rubber–clay nanocomposites using composite theories. Polymer Testing 2004, **23**(8): 903-9.
[201] Praveen S, Chattopadhyay P, Albert P, Dalvi V, Chakraborty B, Chattopadhyay S.

Synergistic effect of carbon black and nanoclay fillers in styrene butadiene rubber matrix: development of dual structure. Composites Part A: Applied Science and Manufacturing 2009, **40**(3): 309-16.

[202] Das A, Kasaliwal G R, Jurk R, Boldt R, Fischer D, Stöckelhuber K W, et al. Rubber composites based on graphene nano platelets, expanded graphite, carbon nanotubes and their combination: A comparative study. Composites Science and Technology 2012.

[203] Song Y S, Youn J R. Influence of dispersion states of carbon nanotubes on physical properties of epoxy nanocomposites. Carbon 2005, **43**(7): 1378-85.

[204] Park M, Kim H, Youngblood J P. Strain-dependent electrical resistance of multi-walled carbon nanotube/polymer composite films. Nanotechnology 2008, **19**(5): 055705.

[205] Li W, Yuan J, Dichiara A, Lin Y, Bai J. The use of vertically aligned carbon nanotubes grown on SiC for *in situ* sensing of elastic and plastic deformation in electrically percolative epoxy composites. Carbon 2012.

[206] Lim S-H, Dasari A, Wang G-T, Yu Z-Z, Mai Y-W, Yuan Q, et al. Impact fracture behaviour of nylon 6-based ternary nanocomposites. Composites Part B: Engineering 2010, **41**(1): 67-75.

[207] d'Almeida J, Monteiro S. The effect of the resin/hardener ratio on the compressive behavior of an epoxy system. Polymer testing 1996, **15**(4): 329-39.

[208] Bagheri R, Marouf B, Pearson R. Rubber-toughened epoxies: A critical review. Journal of Macromolecular Science®, Part C: Polymer Reviews 2009, **49**(3): 201-25.

[209] Li G, Li P, Zhang C, Yu Y, Liu H, Zhang S, et al. Inhomogeneous toughening of carbon fiber/epoxy composite using electrospun polysulfone nanofibrous membranes by in situ phase separation. Composites Science and Technology 2008, **68**(3): 987-94.

[210] Li W, Dichiara A, Bai J. Carbon nanotube-graphene nanoplatelet hybrids as high-performance multifunctional reinforcements in epoxy composites. Composites Science and Technology 2012.

[211] Hussain M, Nakahira A, Niihara K. Mechanical property improvement of carbon fiber reinforced epoxy composites by Al_2O_3 filler dispersion. Materials Letters 1996, **26**(3): 185-91.

[212] Soykasap Ö. Analysis of plain-weave composites. Mechanics of Composite Materials 2011, **47**(2): 161-76.

[213] Hussain SA, Reddy BS, Reddy VN. Prediction of elactic properties of FRP composite lamina for longitudinal loading. Journal of Engineering and Applied Sciences 2008, **3**(6): 71-5.

Publications

1. **W. Li**, J. Yuan, A. Dichiara, J. Bai. The use of vertically aligned carbon nanotubes grown on SiC for *in situ* sensing of elastic and plastic deformation in electrically percolative epoxy composites. ***Carbon***, 2012, 50, 4298-301.
2. **W. Li**, A. Dichiara, J. Bai. Carbon nanotube-graphene nanoplatelet hybrids as high-performance multifunctional reinforcements in epoxy composites. ***Composites Science and Technology***, 2013, 74, 221-7.
3. **W. Li**, D. He, J. Bai. The influence of hybrid structure on the self-sensing and mechanical properties of carbon nanotube-microparticle reinforced epoxy composites. ***Composites Part A*** (being in press).
4. J. Zha, **W. Li**, R. Liao, J. Bai, Z.M. Dang. High performance hybrid carbon fillers/ binary-polymer nanocomposites with remarkable enhanced positive temperature coefficient effect of Resistance. ***Journal of Materials Chemistry***, 2013, 1, 843.
5. Z.M. Dang, **W. Li**, H. Xu. Origin of remarkable positive temperature coefficient effect in the modified carbon black and carbon fiber cofillled polymer composites. ***Journal of Applied Physics***, 2009, 106, 024913.
6. J. Zha, Y. Zhu, **W. Li**, J. Bai, Z.M. Dang. Low dielectric permittivity and high thermal conductivity silicone rubber composites with micro-nano-sized particles. ***Applied Physics Letter***, 2012, 101, 062905.
7. J. Zha, K. Shehzad, **W. Li**, Z.M. Dang. The effect of aspect ratio on the piezoresistive behavior of the multiwalled carbon nanotubes/thermoplastic elastomer nanocomposites. ***Journal of Applied Physics***, 2013, 113, 014102.